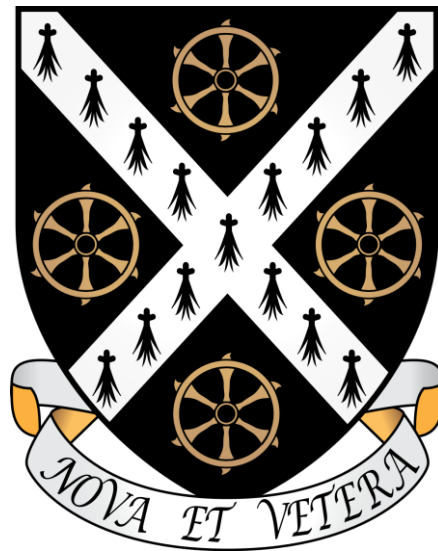


# **An Exploration of Regulatory T Cells in Transplantation: Cell Therapy Development and Immune Monitoring**



**Alaa Ibrahim Alzhrani**

St Catherine College

& Nuffield Department of Surgical Sciences,

University of Oxford

Supervisors: Dr. Joanna Hester & Dr. Fadi Issa

Thesis submitted for DPhil in Surgical Sciences in Michaelmas Term  
2021

## Abstract

### An Exploration of Regulatory T Cells in Transplantation: Cell Therapy Development and Immune Monitoring

Alaa Alzhrani, St Catherine College & Nuffield Department of Surgical Sciences, University of Oxford, DPhil in Surgical Sciences.

Regulatory T cells (Tregs) are powerful modulators of immune function, and are of increasing interest as an adoptive cellular therapy for the treatment of transplant rejection. In a number of early clinical trials, polyclonal Treg therapy has demonstrated efficacy in maintaining graft function. However, optimal Treg immunotherapy should employ alloantigen-reactive, rather than polyclonally-reactive Tregs to ensure specificity against transplant alloresponses. In the first part of this study, a method was developed to expand functional human alloantigen-reactive Tregs (arTregs). These arTregs have enhanced *in vitro* suppressive function and harbour more potent allospecific inhibition in comparison to polyclonally-expanded Tregs. An in-depth characterisation of arTregs is presented, providing a detailed immunophenotypic analysis. In the second part of this study, the phenotypical changes in peripheral immune cells in renal transplant patients receiving Treg therapy were assessed over time using standardised flow and mass cytometry panels. Immunophenotyping provided insights into the immune status of transplant recipients after Treg infusion. In the Treg therapy group, a distinct B cell signature of elevated transitional B cell numbers was identified. Mass cytometric characterisation of the peripheral Treg compartment in patients receiving Tregs identified an enrichment of Treg functional markers with notable changes in the expression of chemokine receptors on peripheral Tregs. In the final part of this study, cellular infiltrates in protocol renal biopsies of recipients who received Treg therapy were examined by spatial profiling and compared to rejection biopsies. This identified a unique signature of B cells, Tregs, and apoptotic regulators in the biopsies from Treg-treated patients. Further analysis revealed interesting differences between the cellular infiltrates in FOXP3<sup>hi</sup> segments from cells therapy compared with rejection such as enrichment in regulatory molecules and anti-inflammatory proteins. The findings presented in this thesis demonstrate the phenotypical and molecular processes associated with stable renal allograft in patients receiving Treg therapy, which in turn may assist in understanding the mechanisms of therapeutic immune regulation and the optimal timing for immunosuppression minimisation.

## Acknowledgment

During my DPhil journey, I have been very fortunate to be surrounded by supportive people, I would like to express my sincere gratitude to my supervisors Dr. Joanna Hester and Dr. Fadi Issa. Joanna trained and taught me about research and good laboratory practice during my first year with immense knowledge, patience, and kindness, then during the years, she was always close to answering questions, giving advice, and encouraging me to take new challenges for research related to my DPhil project. Fadi, for his advice, encouragement, and insightful comments, that motivate me to widen my research from various perspectives. Without their precious support, it would not be possible to conduct this research.

Besides my supervisors, my sincere thanks also go to the Saudi Arabian Cultural Bureau in London and King Abdul-aziz University in Saudi Arabia for their generous fund and for always keeping track of my research.

Other members of the TRIG, have all played a part in this project. Monica Dolton solved administrative, organisational and grant-related letters or questions in the most efficient manner. TWO Study team, Professor Kathryn Wood, Dr. Paul Harden, Dr. Matthew Brook, Dr. Matthew Bottomley, Dr. Amy Cross, Dr. Victoria Flossmann, Dr. Chenyu Wong, Miss Jasmina Kuburic and Cosmo Tullar for their help and assistance during the TWO Study trial. The departmental facility have been managed brilliantly by Jessica Doondeea and Adam Lambert. My colleagues in level 5 were great supporters and it has been extremely helpful to discuss experiences and get suggestions.

Aside from TRIG lab, I would like to thank Dr. Paul Harden, Professor Jagdeep Nanchahal, Professor Susan Fuggle, and Dr. Stephen Preston, my examiners for Transfer of Status and Confirmation of Status for the helpful discussion. I am also grateful to Dr. David Ahern at the Kennedy Institute of Rheumatology for running the samples on mass cytometry and for answering my endless questions.

Finally, I would like to express my deepest gratitude to my parents, Ibrahem and Hanaa, and my siblings, Mohammed, Hadeel, Aouf, and Hawazin for their unconditional love and support. There are no words that can express my thanks to my friends Hind Merhi and Dr.Sarah Alhumoud for their kindness and support during the difficult time.

## Abbreviations

#	Number of cells
<b>7-AAD</b>	7-aminoactinomycin D
<b>Ab</b>	Antibody
<b>ADCC</b>	Antibody-mediated cellular cytotoxicity
<b>AIRE</b>	Autoimmune regulator
<b>AKT</b>	Protein kinase B
<b>Allo moiDCs</b>	Allogeneic monocytes derived immature dendritic cells
<b>AMP</b>	Adenosine monophosphate
<b>APC</b>	Antigen presenting cell
<b>arTreg</b>	Alloantigen reactive regulatory T cell
<b>ATP</b>	Adenosine triphosphate
<b>BCR</b>	B-cell receptor
<b>BCL-2</b>	B-cell lymphoma 2
<b>Breg</b>	Regulatory B cells
<b>cAMP</b>	Cyclic adenosine monophosphate
<b>CAR</b>	Chimeric antigen receptor
<b>CCL</b>	Chemokine ligands
<b>CCR</b>	Chemokine receptors
<b>CD</b>	Cluster of differentiation
<b>CD127</b>	Interleukin-7 receptor- $\alpha$
<b>CD25</b>	Interleukin-2 receptor alpha chain
<b>CMV</b>	Cytomegalovirus
<b>CTL</b>	Cytotoxic T lymphocytes
<b>CTLA-4 (CD152)</b>	Cytotoxic T lymphocyte-associated antigen 4
<b>CXCR</b>	CXC chemokine receptors
<b>CyTOF</b>	Cytometry by Time Of Flight
<b>DAMP</b>	Damage-associated molecular patterns
<b>DC</b>	Dendritic cells
<b>DNA</b>	Deoxyribonucleic acid
<b>DSA</b>	Donor-specific antibodies
<b>DSP</b>	Digital Spatial Profiling
<b>EAE</b>	Experimental autoimmune encephalomyelitis
<b>EBV</b>	Epstein-Barr virus
<b>EDTA</b>	Ethylenediaminetetraacetic acid
<b>ENTPD1 (CD39)</b>	Ectonucleoside triphosphate diphosphohydrolase-1
<b>FACS</b>	Fluorescence-activated cell sorting
<b>FCS</b>	Fetal-calf serum
<b>FFPE</b>	Formalin-fixed paraffin-embedded
<b>FITC</b>	Fluorescein isothiocyanate
<b>FMO</b>	Fluorescence minus one
<b>FOXP3</b>	Forkhead box P3
<b>GATA-3</b>	GATA-binding protein 3
<b>GITR</b>	Glucocorticoid-Induced TNFR-related protein
<b>GM-CSF</b>	Granulocyte-macrophage colony-stimulating factor
<b>GMP</b>	Good Manufacturing Practice
<b>GvHD</b>	Graft-versus-host disease

<b>GZMB</b>	Granzyme B
<b>HLA</b>	Human leukocyte antigen
<b>ICOS</b>	Inducible T-cell costimulator
<b>iDC</b>	Immature dendritic cell
<b>IDO</b>	Indoleamine 2,3-dioxygenase
<b>IF</b>	Immunofluorescent images
<b>IFN</b>	Interferon
<b>Ig</b>	Immunoglobulin
<b>IKZF</b>	Ikaros zinc finger transcription factor
<b>IL</b>	Interleukin
<b>Ir</b>	Irridium isotopes
<b>IRF4</b>	Interferon Regulatory Factor 4
<b>iTreg</b>	Induced regulatory T
<b>LN</b>	Lymph node
<b>mAb</b>	Monoclonal antibody
<b>MACS</b>	Magnetic-activated cell sorting
<b>MDSCs</b>	Myeloid-derived suppressor cells
<b>MFI</b>	Mean fluorescence intensity
<b>MHC</b>	Major histocompatibility complex
<b>miH</b>	Minor histocompatibility
<b>MLR</b>	Mixed lymphocyte reaction
<b>MoDCs</b>	Monocyte-derived dendritic cells
<b>Mregs</b>	Regulatory macrophages
<b>mTOR</b>	Mammalian target of rapamycin
<b>NFAT</b>	Nuclear factor of activated T-cells
<b>NF-<math>\kappa</math>B</b>	Nuclear factor kappa B
<b>NK cells</b>	Natural killer cells
<b>PAMP</b>	Pathogen-associated molecular pattern molecules
<b>PBMC</b>	Peripheral blood mononuclear cell
<b>PBS</b>	Phosphate-buffered saline
<b>PCA</b>	Principal Component Analysis
<b>PD-1</b>	Programmed Death-1
<b>PE</b>	Phycoerythrin
<b>PerCP</b>	Peridinin-Chlorophyll-Protein
<b>PFA</b>	Paraformaldehyde
<b>PI3K</b>	Phosphoinositide 3-kinase
<b>PMA</b>	Phorbol myristate acetate
<b>polyTregs</b>	Polyclonally-expanded Tregs
<b>PRR</b>	Pattern recognition receptor
<b>pTreg</b>	Peripheral Tregs
<b>PTEN</b>	Phosphatase and tensin homolog deleted on chromosome ten
<b>rhIL-2</b>	Recombinant Human Interleukin-2
<b>RNA</b>	Ribonucleic acid
<b>RNP</b>	Ribonucleoprotein
<b>ROI</b>	Region of interest
<b>SD</b>	Standard deviation
<b>SEM</b>	Standard error mean
<b>STAT</b>	Signal transducer and activator of transcription
<b>STING</b>	Stimulator of interferon genes
<b>T-bet</b>	T-box transcription factor

<b>Tconv</b>	T conventional cells
<b>TCR</b>	T cell receptor
<b>TCR-Treg</b>	TCR-transduced Treg
<b>Teff</b>	T effector cells
<b>Tfh</b>	T follicular helper cells
<b>TGF-<math>\beta</math></b>	Transforming growth factor beta
<b>Th</b>	T helper cells
<b>TIGIT</b>	T cell immunoreceptor with Ig and ITIM domains
<b>TLR</b>	Toll-like receptor
<b>TNF</b>	Tumor necrosis factor
<b>TNFRSF</b>	Tumor necrosis factor receptor superfamily
<b>Treg</b>	Regulatory T cells
<b>Tr1</b>	Type 1 regulatory cells
<b>Tresp</b>	Responder T cells
<b>TSDR</b>	Treg-specific demethylated region
<b>tSNE</b>	t-distributed stochastic neighbor embedding
<b>tTreg</b>	Thymic derived Regulatory T cells
<b>visNE</b>	Visualization stochastic neighbor embedding
<b>VISTA</b>	V-domain Ig suppressor of T cell

## Table of contents

<b>Abstract</b>	<b>I</b>
<b>Acknowledgment</b>	<b>II</b>
<b>Abbreviations</b>	<b>III</b>
<b>Table of contents</b>	<b>VI</b>
<b>Chapter 1: Introduction</b>	<b>1</b>
History of transplant immunology	1
Mechanisms of allograft rejection	4
1.1.1 The role of innate immune response in graft rejection	5
1.1.2 The role of adaptive immune response in graft rejection	7
Current clinical immunosuppressive strategies to prevent graft rejection	10
1.1.3 Immunosuppressive agents in transplantation	10
1.1.4 Strategies to induce tolerance in allogenic transplantation	11
Regulatory T cells: an overview	17
1.1.5 Development of Tregs	17
1.1.6 Identification and isolation of Tregs	18
1.1.7 Tregs suppression mechanisms	19
1.1.8 Application of Tregs as a cellular therapy	22
Alloantigen-reactive Tregs (arTregs)	23
1.1.9 Strategies to expand human arTregs <i>ex vivo</i>	24
1.1.10 TCR transgenic Tregs	27
1.1.11 CAR Tregs	27
1.1.12 Direct vs indirect allospecificity	28
1.1.13 Trials of arTregs	29
Phenotypic and molecular analysis of the peripheral blood mononuclear cell compartment and graft biopsy in advanced cellular therapy in transplantation	31
1.1.14 Immune monitoring strategies in clinical trials of cell therapy	31
1.1.15 Biomarker signature for stable graft function in renal transplantation	38
Hypothesis and aims of the project	40
1.1.16 Hypotheses	41
1.1.17 Aims	42
<b>Chapter 2: Materials and methods</b>	<b>43</b>
2.1 Isolation and in vitro culture of human leukocytes from healthy donors	43
2.1.1 Human participants/ethics	43
2.1.2 Isolation of PBMCs by density gradient centrifugation	43

2.1.3	Generation of human monocytes-derived dendritic cells (moDCs)	43
2.1.4	Human Treg flow sorting method	44
2.1.5	<i>In vitro</i> expansion of human polyclonal Tregs	44
2.1.6	<i>In vitro</i> expansion of human arTregs	45
2.1.7	CD137(4-1BB) expression time course	45
2.1.8	CD137 enrichment of <i>in vitro</i> expanded arTregs	46
2.1.9	Cryopreservation and thawing of human leukocytes	46
2.2	In vitro functional assays	46
2.2.2	CD137/CD154 assay	46
2.2.2	<i>In vitro</i> suppression assay driven by allogenic or third party immature dendritic cells (iDCs)	47
2.3	Flow cytometry analysis	48
2.3.1	Cell surface staining	48
2.3.2	Intracellular immunostaining	49
2.3.3	Intracellular cytokine staining	49
2.3.4	TCR V $\beta$ repertoire staining	49
2.4	Analysis of the immune monitoring clinical samples from the cell therapy trials (ONE Study and TWO Study)	50
2.4.1	Study design and approvals	50
2.4.2	Sampling for immune-monitoring	51
2.4.3	Staining of unfractionated blood using DuraClone antibody cocktail tubes	51
2.5	Single cell analysis by mass cytometry (CyTOF)	52
2.5.1	Cell surface staining of peripheral blood for mass cytometry	52
2.2.3	Cell surface and intracellular staining of CD4 <sup>+</sup> T cells for mass cytometry using dedicated Tregs panel	53
2.5.2	Mass cytometry analysis	53
2.6	GeoMx Digital spatial profiling (DSP)	54
2.6.1	Tissue processing	54
2.2.2	DSP analysis and visualization	54
3.3	Data analysis and statistics	55
3.4	Lists of antibodies	56
<b>Chapter 3: Generation and characterization of human <i>ex vivo</i>-expanded alloantigen-reactive Tregs</b>		<b>62</b>
3.1	Introduction	62
3.2	Hypotheses	63
3.3	Results	63

3.3.1. Generation of allogeneic human immature monocyte-derived dendritic cells (imDCs) for stimulation and expansion of arTregs	63
3.3.2. CD137 expression on human Tregs is rapidly and transiently upregulated after allogeneic stimulation	66
3.3.3. Treg expansion using polyclonal or alloantigen stimulation	67
3.3.4. CD137 expression defines a population of potent alloantigen-reactive Tregs	69
3.3.5. Expanded alloantigen-reactive Tregs maintain expression of Treg functional markers	71
3.3.6. Alloantigen-reactive Tregs are more suppressive than polyclonally expanded Tregs and demonstrate enhanced specific antigen reactivity	73
3.3.7. Alloantigen-reactive Tregs produce fewer inflammatory cytokines in comparison to polyclonally-expanded Tregs	76
3.3.8. TCR repertoire analysis of alloantigen-reactive Tregs reveals restriction to several TCR beta families	77
3.3.9. Expression of CD137 and CD154 discriminates between activated Tregs and conventional T cells <i>ex vivo</i>	79
3.4 Discussion	82
<b>Chapter 4: Cellular and phenotypical analysis of the peripheral immune cell compartment following Treg therapy in renal transplantation</b>	<b>84</b>
5.2 Introduction	84
5.3 Hypotheses	86
Hypothesis-1: Immunophenotyping will provide insights into the immune status of transplant recipients receiving Treg cellular therapy.	86
Hypothesis-2: The ability to evaluate multiple antigens concomitantly using mass cytometry (CyTOF) allows for unbiased detection of specific clusters of Tregs. Appreciating how these clusters behave after treatment with a cellular therapy will offer an insight into the immune phenotype.	86
5.4 Phenotypical analysis of the peripheral immune cell compartment in TWO Study participants by flow cytometry	86
5.4.1 Study design and participants	86
5.4.2 Specimens and panels	86
5.4.3 Results	87
5.5 Phenotypical analysis of the peripheral immune cell compartment in renal transplant recipients by mass cytometry (CyTOF)	107
5.5.1 Specimens and CyTOF panel	107
5.5.2 Results	109
5.6 Phenotypical analysis of peripheral Treg compartment by mass cytometry (CyTOF)	123
5.6.1 Study design and participants	123

5.6.2 Specimens and CyTOF panel	123
5.6.3 Results	124
5.7 Discussion	132
<b>Chapter 5: Spatial protein profiling of leukocyte infiltrate in renal biopsies after cellular therapy</b>	<b>136</b>
5.1 Introduction	136
5.2 Hypothesis	137
5.3 Results	138
5.3.1. Overview of GeoMx DSP workflow and ROI selection	138
5.3.2. Proteins are differentially expressed in cell therapy versus rejection regions	140
5.3.3. Protein analysis identifies B cells, Tregs and apoptotic regulators in renal biopsies from Treg-treated recipients	142
5.3.4. Unsupervised hierarchical clustering identifies distinct protein signatures of rejection and cell therapy	144
5.3.5. Protein profiling of FOXP3 <sup>+</sup> segments reveals distinct protein signatures compared to CD4 <sup>+</sup> FOXP3 <sup>neg</sup> segments within cell therapy and rejection tissues	146
5.3.6. Proteins are differentially expressed in FOXP3 <sup>hi</sup> versus FOXP3 <sup>low/neg</sup> segments	150
5.4 Discussion	152
<b>Chapter 6: General discussion, limitations and future directions</b>	<b>155</b>
<b>References</b>	<b>163</b>
<b>Publications</b>	<b>200</b>

## Chapter 1: Introduction

### History of transplant immunology

Organ transplantation has achieved remarkable success over the last five decades and remains the most successful treatment for end-stage organ failure. Around 4761 patients received transplant in the UK in the last year (2019/2020).<sup>1</sup> The most common transplanted organ is the kidney, followed by the liver and pancreas.<sup>1</sup> Kidney transplantation has been shown to reduce mortality and improve quality of life for most patients when compared with dialysis.<sup>2</sup>

The cornea was the first successful transplanted tissue in humans, performed by Eduard Zirm in 1906.<sup>3</sup> Subsequently, Alexis Carrel invented the vascular suture technique; this technique paved the way for organ transplantation to become a reality several years later.<sup>4</sup> After several failed transplantation attempts in both animals and humans, Joseph Murray and colleagues finally performed the first successful human kidney transplant in 1954.<sup>5</sup> Notably, the success behind these two transplantation cases (cornea and kidney) was a result of bypassing the alloimmune response, since the eyes are considered an immune-privileged organ,<sup>3</sup> and the kidney transplant was between two identical twins, making rejection unlikely.<sup>5</sup>

In the early 1940s, Peter Medawar, widely regarded as the “father of transplantation”, together with colleagues, observed in a rabbit model who received both allogeneic and autologous skin grafts, the allogeneic skin grafts were rapidly lost whereas autologous skin grafts were maintained, and the second attempt at allogeneic skin grafts from the same donor resulted in accelerated loss of the grafts.<sup>6, 7</sup> This faster and more pronounced immune response following re-exposure to the same antigen is widely known nowadays as a “secondary immune response”. A further series of experiments by Billingham, Brent, and Medawar revealed the “acquired immunological tolerance” phenomenon, whereby immunological tolerance could be induced by exposing the recipients to the donor cells during the foetal period.<sup>8</sup> This hypothesis was inspired by Ray Owen’s studies reporting the presence of two types of erythrocytes in the blood of dizygotic cattle twins, whereby each twin had its

erythrocytes and cells that were acquired from the other twin through a shared placenta.<sup>9</sup> Owen emphasised that the twins must have exchanged the erythrocytes or their progenitors during the foetal stage and that the cells were maintained as the calves grew up. Indeed, the absence of an immune response to the foreign erythrocytes in Owen's study was a clear example of the immunological tolerance phenomenon. This led Burnet and Fenner to determine that the exposure to genetically different cells early in life would not trigger the immune response.<sup>10</sup> These findings were fundamental for future advances in clinical transplantation.

in 1955, John Main and Richmond Prehn showed in an experimental model that attenuating the immune system through irradiation allowed chimerism to be induced by inoculating donor-derived bone marrow.<sup>11</sup> Skin grafts were then maintained if they came from the same bone marrow donor. This encouraged Murray's team, in 1958, to use the Main-Prehn strategy in kidney transplant patients. They bypassed the genetic barrier of human organ rejection and reported the first successful kidney transplant in non-identical twins, as they found that the irradiation strategy without the total chimerism was sufficient to slow down organ rejection in humans.<sup>12</sup> However, the off-target side effects of total body irradiation carry a high risk of infection and mortality. Ultimately, total body irradiation was replaced by immunosuppressive treatments in the 1970s, which made transplantation a feasible procedure.

Although tissue matching was proposed previously by Alexis Carrel and studied in experimental models by George Snell and Peter Gorer, it failed to emerge as a reality for human transplants<sup>13</sup> until 1958, when Jean Dausset discovered the first human leukocyte antigens (HLA), which is a gene complex encoding the major histocompatibility complex (MHC), and was identified as a leading target of the alloimmune response toward the graft.<sup>14</sup> Currently, the application of histocompatibility matching along with the use of immunosuppressive agents and improvement in tissue and organ preservation methods have made it possible to successfully engraft most types of organs in the human. The one-year transplant survival in the UK has exceeded 90% for most types of organs.<sup>15</sup> However, serious limitations exist, as most of these transplanted organs failed within the first 20 years following transplantation as a result of rejection and the toxicity of life-long global pharmacological

immunosuppression.<sup>16, 17</sup> This problem is exacerbated by the shortage of available human organs along with the higher risk of rejection in the second transplant. Therefore, the investigation of therapeutic strategies that promote graft survival without overly suppressing the immune system is of great importance.

In 1971, Gershon and Kondo described a specialised subset of T cells that can inhibit alloimmune responses.<sup>18</sup> Further studies by Bruce Hall and Shimon Sakaguchi determine these T suppressor cells as CD4<sup>+</sup>CD25<sup>+</sup> T cells,<sup>19, 20</sup> currently widely known as regulatory T cells (Tregs), which are thoroughly described in Section 1.3. Indeed, the discovery of Treg biology and function led to substantial interest in their therapeutic use as a cellular therapy for tolerance induction in transplantation. The balance between the inflammatory and regulatory immune response toward allografts can determine the long-term outcome of a transplanted organ. Regulation of the alloimmune response can extend transplant survival and therefore ensure success of transplantation.

## Mechanisms of allograft rejection

Allograft rejection is caused by a complex series of interactions between innate and adaptive immune responses. While innate immune responses act as the first line of immunological defence by providing a rapid and non-specific response, the adaptive immune response plays a significant role by providing a specific and potent response against donor-derived peptides. Although the innate immune response is rarely able to reject an allograft in the absence of adaptive immunity, it might initiate and amplify the adaptive immune response through the pro-inflammatory signals from monocytes, macrophages, and natural killer (NK) cells.<sup>21, 22</sup> The recognition of allogeneic peptides by the innate cells is required to activate optimal T cell responses toward the allogeneic transplant.<sup>23</sup>

The alloantigens that trigger the host immune responses toward the allograft are both major and minor histocompatibility antigens. The major histocompatibility complex (MHC), named Human Leukocyte Antigen (HLA), consists of class I (HLA-A, HLA-B, HLA-C) and class II (HLA-DR, HLA-DP, HLA-DQ) molecules. The function of MHC molecules is to present foreign antigens to T cells. The T cell receptor (TCR) expressed on the surface of the T cells interacts with the donor MHC-peptide complex expressed by antigen-presenting cells (APCs). CD4<sup>+</sup> T cells, usually associated with helper functions, recognise peptides presented by MHC class II molecules. In contrast, CD8<sup>+</sup> T cells, usually associated with cytotoxic functions, will exercise their effector function only if they are interacting with peptides presented by MHC class I molecules. HLA is a highly polymorphic molecule and represents a leading target of the alloimmune response toward the graft. Therefore, HLA matching between recipients and donors is essential for a successful transplant outcome and can reduce the risk of allograft rejection. However, rejection might still occur even in recipients of transplants from HLA-identical siblings as a result of mismatched minor histocompatibility antigen (miHs), such as HA-1, LRH1, ACC-1, and ACC-2.<sup>24, 25</sup> There is also growing evidence of the presence of non-HLA antigens, including Angiotensin 1 receptor (anti-AT1R), Perlecan, and Collagen V, which can contribute to allograft rejection.<sup>26</sup> Allograft destruction is carried out by antibodies produced by plasma cells and cytotoxic molecules produced by CD8<sup>+</sup> T cells and NK cells, in addition to other molecules. In contrast, transplantation can also activate and generate CD4<sup>+</sup> CD25<sup>+</sup>

FOXP3<sup>+</sup> regulatory T cells, which may regulate the allograft response by a wide array of molecular mechanisms (discussed in detail in Section 1.4.3).

### 1.1.1 The role of innate immune response in graft rejection

Several factors can stimulate the innate immune response toward tissue injury and affect the graft condition, including the surgical procedure to retrieve and re-implant the graft, ischaemia reperfusion injury (IRI), infection, coagulation, and other types of tissue damage.<sup>27</sup> Cells of the innate immune system express pattern recognition receptors (PRRs) such as Toll-like receptors (TLRs), Nod-like receptors (NLRs), and Retonic acid-inducible gene I (RIG-I)-like receptors. TLRs are integral membrane glycoproteins expressed either on the external surface of the cell membrane or on endosomes; they are expressed by macrophages, NK cells, B cells, DCs, endothelial cells, and organ parenchymal cells.<sup>28, 29</sup> TLRs are specialised in the recognition of certain molecules expressed by pathogens (Pathogen Associated Molecular Patterns; PAMPs) or by cells undergoing physiological stress (Damage Associated Molecular Patterns; DAMPs). The engagement of either PAMPs or DAMPs with TLRs permits the immune system to clear infected cells and damaged tissue but can contribute to graft rejection. When the TLRs sense and engage with PAMPs or DAMPs, they activate an intracellular cascade of kinases that lead to the production of transcription factors such as AP1, NF- $\kappa$ B, and IRF3. The activation of these factors regulates the transcription of many pro-inflammatory genes, including pro-inflammatory cytokines, chemokines, and costimulatory molecules. The production of pro-inflammatory molecules by activated leukocytes can trigger the migration of other leukocytes into the graft and promote graft damage.<sup>27</sup> Moreover, the graft damage that might occur during ischemia contributes to the production of reactive oxygen species (ROS) by endothelial cells and lead to platelets aggregation and to increased expression of adhesion molecules, including P-selectin, E-selectin and ICAM-1, by endothelial cells.<sup>30</sup> These molecules can activate and trigger the migration of macrophages, neutrophils, and other leukocytes into the graft, where they contribute to graft damage and subsequently activate the adaptive immune response (Figure 1).

Besides these cellular receptors, innate immunity also includes humoral components such as complement. The complement system consists of more than 30 proteins and three distinct activation pathways, the classical, alternative, and mannose-binding lectin (MBL) pathway. In

IRI, the MBL pathway can be activated by renal tissue-expressed lectins.<sup>31, 32</sup> Following activation, the release of C5a and C3a plays a critical role in organ damage and activates adaptive immunity.<sup>33, 34</sup>

Research continues to improve strategies of organ preservation that aim to enhance the organ condition and reduce DAMP production, including the development of new technologies for organ reperfusion, complement inhibitors, gene therapy, and stem cell therapy.<sup>35, 36, 37</sup> Nevertheless, challenges remain for the prevention of tissue stress and damage created by the surgical procedure and ischemic reperfusion injury.

NK cells are a major cell type in the innate immune system. These cells are programmed to recognise and kill cells that lack self-MHC class I molecules or cells that present a foreign antigen by MHC class I molecules, making them relevant during an allogeneic response to the allograft.<sup>38</sup> Following activation, NK cells cause tissue damage in a perforin- and granzyme-dependent manner and augment the adaptive immune response through IFN- $\gamma$  secretion. In addition, NK cells express the surface Fc gamma receptor (FC $\gamma$ R), which can recognise the Fc portion on several IgG subclasses and mediate antibody-dependent cellular cytotoxicity.<sup>39</sup>

Other innate lymphoid cells might also play a role in alloresponses following solid organ transplantation. NKT cells are a subset of lymphocytes that shares phenotypic and functional characteristics with NK cells. This subset can recognise glycolipids presented by the MHC class I-like molecule, CD1d. Their role in allograft responses has yet to be clarified, with evidence of both their detrimental and tolerogenic roles in the transplantation context.<sup>40, 41</sup> The innate lymphoid cells including ILC1, ILC2, and ILC3, are lymphocytes that lack specific antigen receptors.<sup>42, 43</sup> They have a diverse function with evidence of promoting host defence against infection and tissue repairs.<sup>44</sup> These cells can be activated by microbial compounds, stress responses, and the inflammatory environment around the tissues. Recent studies suggested a major role for ILCs in allograft responses.<sup>45, 46, 47</sup> In addition,  $\gamma\delta$  T cells are a subpopulation of lymphocytes expressing T-cell receptors (TCRs) composed of transmembrane  $\gamma$  and  $\delta$  chains. The specific contribution of  $\gamma\delta$  T cells towards allografts has yet to be elucidated, with evidence of both their detrimental and tolerogenic roles in several settings.<sup>48, 49</sup> Furthermore, mucosal-associated invariant T (MAIT) cells are innate-like T cells that recognise bacterial metabolites bound to the MHC class I-related molecule (MR1). The

depletion of MAIT cells has been reported during liver,<sup>51</sup> and kidney disease,<sup>52</sup> indicating their role in the host defence against bacterial infections. The MAIT cells might play a role during allogeneic responses, however, their specific contribution remains to be investigated.

### 1.1.2 The role of adaptive immune response in graft rejection

The interaction of innate and adaptive immunity mainly occurs through antigen presentation, which can be done by professional APCs including B cells, macrophages, and dendritic cells (DCs). Alloantigen recognition is initiated through three main pathways: direct, indirect, and semi-direct.<sup>53, 54</sup> A direct alloresponse occurs when host T cells recognise allogeneic donor APCs presenting allogeneic MHC-peptide complexes.<sup>55</sup> Indirect alloresponses involve the presentation of processed donor-derived peptides by host APCs via their own MHC to host T cells. Semi-direct presentation occurs when host T cells capture intact allogeneic MHC-peptide complexes presented by host APCs.<sup>56</sup> The role of direct recognition dominates early after transplantation and can lead to a vigorous immune response. However, the limited lifespan of allogeneic APCs within the transplanted graft results in a limited time frame for this pathway to occur. Indirect presentation has been suggested to be the major pathway underlying chronic transplant rejection.<sup>57, 58</sup> Recently, studies in the mouse model have demonstrated that donor MHCs can exist on the surface of host APCs, and these known as "cross-dressed" APCs, which can present the allogeneic MHC molecules directly to host T cells.<sup>59, 60</sup> Hughes et al. highlighted the role of cross-dressed host DCs in experimental transplant models.<sup>61</sup> Semi-direct allorecognition was detected to stimulate the early alloresponses in secondary lymphoid organs and in the graft itself, indicating their role to mediate acute rejection within the first weeks post-transplantation. The studies above suggest a critical role of semi-direct allorecognition in driving acute T cell activation following transplantation. Figure 1 illustrates the mechanisms of allograft rejection.

The activation of T cells by professional APCs requires cell-to-cell contact leading to an immunological synapse, with activation through TCR and suitable costimulatory signals including cytokines to ensure the optimal delivery of signals for T cell activation and proliferation. Although costimulatory molecules and cytokines are not antigen-specific, these signals are important for the allograft response. Cytokines can influence the differentiation of

CD4<sup>+</sup> T cells into specific T cell subsets including Th1, Th2, Th17, Th9, T follicular helpers, and Tregs. Each of these cells has distinct transcriptional factors with a distinct effector function that permits a specific immune response toward different pathologies.<sup>62, 63, 64</sup> For instance, when IL-12, is produced by DCs, this cytokine activates the JAK/STAT pathway on the naive CD4<sup>+</sup> T cells and leads to IFN- $\gamma$  production. IFN- $\gamma$  activates the STAT1 pathway, resulting in the skewing of naïve CD4<sup>+</sup> T cells toward the Th1 lineage and the upregulation of the transcriptional factor T-bet.<sup>65</sup> On the other hand, the expression of costimulatory and coinhibitory receptors and cytokines might limit T cell response and induce an exhaustion state in both CD4<sup>+</sup> and CD8<sup>+</sup> T cell subsets<sup>66, 67</sup>.

B cells play a significant role in mediating alloresponses and promote graft rejection through the production of high-affinity antibodies to the donor-derived peptides. The binding of antibodies to the graft endothelium can trigger phagocytosis and initiate antibody-dependent cellular toxicity (ADCC).<sup>68, 69</sup> In addition, the complement system can be activated through antigen-antibody complex results in complement-mediated cytolysis.<sup>70</sup> Moreover, B cells act as professional APCs; when CD4<sup>+</sup> T cells recognise donor-derived peptide presented by B cells through MHC class II molecules, this results in alloreactive T cell activation, in which activated T cells provide costimulatory signals to B cells through CD40-CD40L to further activate and differentiate B cells. In addition, activated CD4<sup>+</sup> T cells will secrete pro-inflammatory cytokines such as IL-6, IFN- $\gamma$ , and TNF- $\alpha$ . These cytokines recruit other leukocytes, including NK cells, eosinophils, and macrophages, which may induce cell apoptosis through cytotoxic mechanisms including perforin, granzyme-B, and cytokines.<sup>70</sup>

Patients who have donor-reactive antibodies at the time of transplantation can develop hyperacute rejection as a result of complement system activation after graft reperfusion.<sup>71</sup> However, several strategies are currently used to reduce antibody-mediated rejection and improve graft survival, including the identification of highly sensitized patients, improving desensitization protocols, monitoring de novo donor-specific antibodies (DSAs), and performing protocol biopsies.<sup>72, 73</sup> B cells not only contribute to allograft rejection but also have a role in inducing tolerance; a subset of B cells that can exhibit immune-regulatory properties, known as B regulatory cells (Bregs), have been described in several studies.<sup>74, 75, 76</sup> These cells can modulate the immune response by directly inhibiting alloreactive T cells

through the production of the inhibitory cytokine IL-10 and may promote graft tolerance through induction of Tregs.

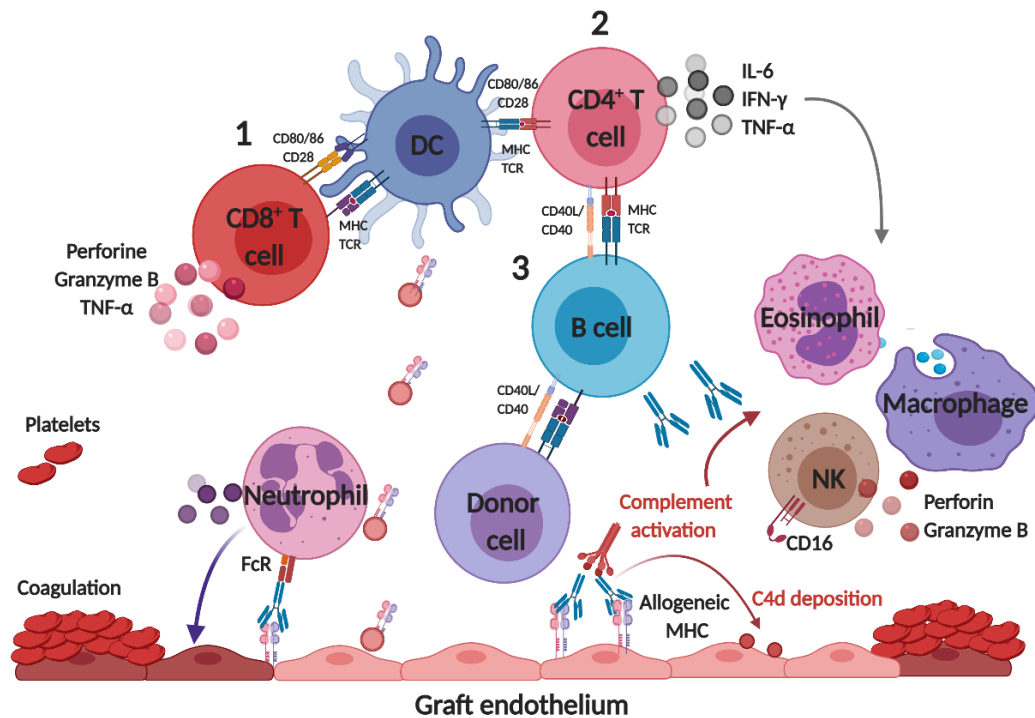


**Figure 1: Mechanisms of allograft rejection.**

1. CD8<sup>+</sup> cytotoxic T cells recognise donor-derived peptides presented on MHC class I molecules by APCs. Then activated CD8<sup>+</sup> T cells migrate to the graft and kill target cells by apoptosis through the release of the cytotoxic granules perforin and granzyme B.
2. CD4<sup>+</sup> helper T cells recognise donor-derived peptides presented on MHC class II molecules by APCs. Additional co-stimulatory signals and cytokines are also provided by activated DCs. CD4<sup>+</sup> helper T cells secrete pro-inflammatory cytokines such as IL-6, IFN-γ, and TNF-α, which activate macrophages and eosinophils, causing graft damage.
3. B cells recognise donor-derived peptides presented on MHC class I molecules of donor cells or bind to unprocessed alloantigens in an MHC-independent manner. CD4<sup>+</sup> helper T cells activate B cells, activated B cells produce antibodies. These antibodies bind to the graft and induce antibody-dependent cellular toxicity (ADCC) and activate the complement system, causing graft damage.

APC, antigen presenting cells; DC, dendritic cell; MHC, major histocompatibility complex; TCR, T-cell receptor; FcR, Fc receptor; TNF-α, Tumor Necrosis Factor alpha; IFN-γ, Interferon gamma.

## Current clinical immunosuppressive strategies to prevent graft rejection

### 1.1.3 Immunosuppressive agents in transplantation

Currently, the main strategy for suppressing alloimmune responses and avoiding organ rejection in solid organ transplantation is the use of pharmacological immunosuppression, which includes induction and maintenance agents. The goal of induction therapy is to induce strong immunosuppression for the short-term to reduce the risk of acute rejection, which might occur within three months following the transplant. Several immunosuppressive drugs are used for induction purposes, including anti-thymocyte globulin (ATG), CD52 antibodies (Alemtuzumab), and IL-2 receptor antagonists (such as basiliximab and daclizumab). Following alemtuzumab induction, an elevation in Treg and Breg frequencies has been reported in renal transplant patients; these results suggest that lymphocyte depletion with alemtuzumab might shift the *in vivo* balance toward a tolerogenic state.<sup>77, 78</sup>

For the maintenance of immunosuppression, a combination of immunosuppressants is widely used. For example, renal transplant patients are usually treated with the anti-proliferative drug mycophenolate mofetil (MMF) combined with drugs that inhibit T cell activation, such as calcineurin inhibitors (tacrolimus or cyclosporin A) or mammalian target of rapamycin (mTOR) inhibitors. In addition, other agents including T-cell costimulation blockers are also used to inhibit the T cell proliferation.<sup>79</sup> Notably, immunosuppressive regimens vary based on the transplanted organ and the transplant centre's protocol.

These immunosuppressive regimens contribute to significant morbidity and mortality arising from their off-target effects, which include life-threatening infection, cardiovascular disease, metabolic disorders, and malignancy.<sup>80, 81</sup> Moreover, immunosuppression itself may be directly toxic to the graft and therefore contribute to poor long-term outcomes. Additionally, while life-long global pharmacological immunosuppression has greatly reduced episodes of acute graft rejection leading to considerable success in short-term allograft outcomes, improvement is still necessary to avoid chronic allograft dysfunction. Therefore, there has been significant attention in the past few decades from the transplant community on developing novel therapeutic strategies to facilitate the minimisation or even cessation of pharmaceutical immunosuppression. In particular, the focus has been on the use of cellular

therapy, which could naturally and specifically regulate the alloimmune response and promote tolerance.

#### **1.1.4 Strategies to induce tolerance in allogenic transplantation**

A number of experimental and preclinical studies have provided convincing evidence that transplantation tolerance induction is feasible. Tolerance in organ transplant recipients is defined as stable graft function in patients receiving no immunosuppression for more than one year. Induction of tolerance in experimental models can be achieved by mediating central tolerance through induction of chimerism or intrathymic injection of alloantigens, and peripheral tolerance through modulation of T cell responses by costimulatory blockade or cellular therapy.

Another strategy for tolerance induction is through combined kidney and hematopoietic stem cell transplantation into conditioned recipients. This strategy provides evidence that operational tolerance can be achieved in humans by mixed chimerism, defined as a state wherein donor and recipient leukocytes coexist. A study in patients with end-stage renal disease has reported that tolerance was achieved through a transient chimeric state in HLA-mismatched renal transplant.<sup>82</sup> Another study, confirmed that tolerance was achieved through a permanent mixed chimeric state in HLA-matched renal transplant patients.<sup>83</sup> However, the risk of graft versus host disease (GVHD) development in both full chimerism and permanent chimerism states along with the toxicity related to the use of myeloablative and nonmyeloablative therapy has limited the clinical application of this approach.<sup>84, 85</sup> Studies in animal models have confirmed that intrathymic administration of alloantigens together with peripheral leukocyte depletion leads to induction of tolerance.<sup>86, 87</sup> However, concerns about the feasibility and safety of such a strategy limits its translation to the clinic.<sup>88</sup>

The discovery of therapeutic agents targeting costimulatory molecules has made it possible to control the peripheral alloresponse and mediate long-term graft survival. Engagement of the costimulatory molecule CD28 expressed by T cells with CD80/CD86 expressed by APCs at the time of allorecognition leads to alloreactive T cell activation and proliferation. CTLA-4 (Cytotoxic T-Lymphocyte Associated Protein 4) (CD152), a co-inhibitory receptor that binds to

CD80/CD86 with higher affinity than CD28 and therefore prevents the CD28 co-stimulation to T cells and inhibits their activation. The costimulatory blockade therapy CTLA-4 Ig (Belatacept) has been tested in two large randomised, phase III trials in renal transplant recipients and showed efficacy in preventing graft rejection in comparison to cyclosporine.<sup>89</sup> Therefore, it was approved by the FDA as an immunosuppressive treatment in renal transplant patients.<sup>90</sup> Despite this success, some limitations on belatacept treatment still exist, including the high risk of developing cellular-mediated rejection.

An alternative strategy is through blocking the CD40/CD154 (CD40 Ligand) co-stimulation pathway, which has shown encouraging results in nonhuman primate transplant models when used as monotherapy or together with CD28 antagonism.<sup>91</sup> Although administration of anti-CD154 antibodies in humans results in a higher incidence of thrombotic complications, research continues to modify and evaluate the optimal blocking CD40 antibodies.<sup>92</sup>

The blockade of the ICOS-ICOSL co-stimulation pathway has been also proposed as a therapeutic strategy. ICOS is expressed by activated T cells and therefore it was hypothesised that blocking ICOS-ICOSL might control some activated resistant T cell subsets.<sup>93</sup> In a mouse model, ICOS-ICOSL blockade combined with a CD28 antagonist prevented allograft rejection. However, it failed to mediate renal graft survival when it was tested in a non-human primate (NHP) model.<sup>94</sup> In contrast, blockade of the OX40-OX40L pathway has demonstrated interesting results. OX40 is also expressed by activated T cells. In the NHP model, the administration of an anti-CD40L antibody along with belatacept prolongs graft survival.<sup>95</sup> The result of this study together with safety results from a phase II clinical trial testing OX40L antibody in asthmatic patients<sup>96</sup> make OX40-OX40L blockade an attractive approach in transplantation.

Another promising therapeutic strategy is cellular therapy, which could naturally and specifically regulate the alloimmune response and promote tolerance. Various regulatory cells, including regulatory T cells, type 1 regulatory cells (Tr1), regulatory macrophages (Mregs), myeloid-derived suppressor cells (MDSCs), and tolerogenic dendritic cells (DCs), are being explored for their modulation of the immune response in several immune pathologies including organ transplantation.<sup>97, 98, 99</sup> The ONE Study, a multicentre phase I/IIa clinical trial, assessed the safety of infusing regulatory cells including Treg, Tr1 cells, (Mregs) and

tolerogenic (DCs) in renal transplant patients.<sup>100</sup> Table 1 summarises regulatory cell subtypes and their phenotypes. Among these, the canonical CD4<sup>+</sup> Tregs are the best understood, and the focus in this project is given to this population. In a number of preclinical and early clinical trials, polyclonally-expanded Tregs (polyTregs) have demonstrated efficacy in inducing graft tolerance. However, attention is turning to alloantigen-reactive Tregs (arTregs), which may exhibit an enhanced capacity to suppress alloresponses with less potential for 'off-target' immunosuppression.

**Table 1: Regulatory cell populations**

Cell population	Phenotype (human)	Regulatory mechanisms	Trial ID	Setting	Ref
<b>CD4<sup>+</sup> Tregs</b>	CD4 <sup>+</sup> CD25 <sup>hi</sup> CD127 <sup>low</sup> FOXP3 <sup>+</sup> CD45RA <sup>+</sup> (resting) or CD45RO <sup>+</sup> (activated)	See Section 1.4.3	See Section 1.5.5. Table 3	GVHD	101, 102, 103
				Solid organ transplantation	104, 105
				Autoimmunity	106, 107, 108, 109
<b>Tr1 cells</b>	CD4 <sup>+</sup> FOXP3 <sup>-</sup> CD49b <sup>+</sup> LAG3 <sup>+</sup> CD45RO <sup>+</sup>	<ul style="list-style-type: none"> <li>• IL-10 secretion</li> </ul>	ALT-TEN trial, RN: IS/11/6172/830 9/8391	GVHD	110
<b>CD8<sup>+</sup> Tregs</b>	CD8 <sup>+</sup> CD25 <sup>-</sup> CD28 <sup>-</sup> or CD8 <sup>+</sup> FOXP3 <sup>+</sup> CCR 7 <sup>+</sup> CD39 <sup>+</sup>	<ul style="list-style-type: none"> <li>• Inhibition of T cell proliferation through expression of CTLA-4 and TGF-<math>\beta</math></li> <li>• Modulation of APC activation and secretion of IL-10</li> </ul>			111
<b>CD4<sup>-</sup> CD8<sup>-</sup> T cells</b>	CD25 <sup>low</sup> CD28 <sup>low</sup> CTLA-4 <sup>-</sup> CD38 <sup>low</sup>	<ul style="list-style-type: none"> <li>• Inhibition of T cell proliferation</li> <li>• Inhibition of APC-mediated T cell activation</li> </ul>			112
<b>T follicular regulatory cells (T<sub>FR</sub>)</b>	CD4 <sup>+</sup> CXCR5 <sup>+</sup> PD-1 <sup>+</sup> FOXP3 <sup>+</sup>	<ul style="list-style-type: none"> <li>• Regulating TFH cells</li> <li>• Preventing the development of autoreactive B cells</li> </ul>			113
<b>NK T cells</b>	CD3 <sup>+</sup> TCR(V $\alpha$ 24J $\alpha$ 18 <sup>+</sup> V $\beta$ 11 <sup>+</sup> )	<ul style="list-style-type: none"> <li>• Secretion of regulatory cytokines IL-10</li> <li>• Cytokine mediated-induction of Treg and tolerogenic DCs</li> </ul>			114, 115
<b>Y<math>\delta</math> T cells</b>	CD3 <sup>+</sup> TCR(Y $\delta$ )	<ul style="list-style-type: none"> <li>• Secretion of regulatory cytokines (IL-10 and TGF-<math>\beta</math>)</li> <li>• Expression of inhibitory molecules (PDL-1 and CTLA-4)</li> </ul>			48, 116

<b>Regulatory B cells (Bregs)</b>	CD19 <sup>+</sup> CD20 <sup>+</sup> CD24 <sup>hi</sup> CD27 <sup>-</sup> CD38 <sup>hi</sup> IgD <sup>hi</sup> IgM <sup>hi</sup>	<ul style="list-style-type: none"> <li>• Secretion of inhibitory cytokines (IL-10, TGF-<math>\beta</math>, IL-35)</li> <li>• Induction of Tregs</li> <li>• Inhibit the secretion of IFN-<math>\gamma</math></li> <li>• Reduce accumulation of NK cells</li> </ul>			117, 118
<b>Regulatory macrophages</b>	No stable, specific markers are yet defined; CD14 <sup>-/low</sup> CD16 <sup>-</sup> CD64 <sup>+</sup> CD80 <sup>-/low</sup> CD86 <sup>+</sup> CD163 <sup>-/low</sup> HLA-DR <sup>+</sup> TLR2 <sup>-</sup>	<ul style="list-style-type: none"> <li>• IL-10 secretion</li> <li>• Inhibition of T cells proliferation</li> <li>• Induction of Tregs</li> </ul>	NCT02085629*	Living donor renal transplantation	119, 120
<b>Tolerogenic DCs</b>	MHCII <sup>low</sup> CD86 <sup>low</sup> CD80 <sup>low</sup> CD40 <sup>low</sup>	<ul style="list-style-type: none"> <li>• Expression of inhibitory molecules (PDL-1, FasL, IDO)</li> <li>• Secretion of inhibitory cytokines (IL-10, TGF-<math>\beta</math>,</li> <li>• Induction of Tregs</li> <li>• Induction of T cells unresponsiveness</li> </ul>	NCT02252055*	Living donor renal transplantation	121
			NCT00445913*	Type 1 diabetes	122
			NCT00396812*	Rheumatoid arthritis	123
			NCT01352858*		124
			2007-003469-42** NCT02622763*	Crohn disease	125
			NCT02283671* NCT02618902*	Multiple sclerosis	126
<b>Mesenchymal stromal cells (MSCs)</b>	CD34 <sup>-</sup> CD45 <sup>-</sup> CD73 <sup>+</sup> CD90 <sup>+</sup> CD105 <sup>+</sup> HLA-DR <sup>-</sup> ,CD11b <sup>-</sup> or CD14 <sup>-</sup> , CD19 <sup>-</sup> or CD79 $\alpha$ <sup>-</sup>	<ul style="list-style-type: none"> <li>• Induction of Tregs</li> <li>• Modulation of APC activation</li> <li>• Promote differentiation of macrophages into M2 macrophages</li> <li>• Control of memory CD8 function</li> <li>• Secretion of cytokines, chemokines, growth factors and extracellular vesicles</li> <li>• Activation of (IDO) production by phagocytes</li> </ul>	NCT00658073*	Renal transplantation	127, 128, 129, 130, 131
			NCT00752479*		
			NCT00734396*		
			2009-017795-25**	Liver transplantation	
			NCT01429038*	Liver or renal transplantation	
			NCT01663116*	Rheumatoid arthritis	132
NCT02923375*	GVHD	133			

				Small bowel transplantation	134, 135
				Lung transplantation	136, 137
<b>Myeloid-derived suppressor cells (MDSCs)</b>	<p>All subsets: CD11b<sup>+</sup> CD33<sup>+</sup> CD34<sup>+</sup>HLA-DR<sup>-</sup> /low</p> <p>Granulocyte-like MDSC subset: CD15<sup>+</sup>CD33<sup>+</sup>HLA-DR<sup>-</sup>/low</p> <p>Monocyte-like MDSC subset: CD14<sup>+</sup>CD33<sup>+</sup>HLA-DR<sup>-</sup>/low</p>	<ul style="list-style-type: none"> <li>• Nitric oxide and Arg-1 dependent inhibition of T cells, B cells and NK cells</li> <li>• Inhibition of T cells through production of ROS and peroxynitrite</li> <li>• Induction of Treg</li> <li>• Secretion of IL-10</li> <li>• Inhibition of DC maturation by HO-1</li> </ul>			138, 139, 140

**Table 1: Regulatory immune cell populations.** Clinicaltrials.gov\* and EudraCT\*\*were searched for the clinical trials. RN: Registration number; DC, dendritic cell; FOXP3, forkhead box P3; GVHD, graft-versus-host-disease; MDSC, myeloid-derived suppressor cell; MHC-II, MHC class II; TReg, regulatory T; T<sub>FR</sub>, T follicular regulatory cells; NK, natural killer; Arg-1, arginase-1; ROS, reactive oxygen species; IDO, indoleamine 2,3-dioxygenase.

## Regulatory T cells: an overview

### 1.1.5 Development of Tregs

Tregs are generated both in the thymus (tTregs), as a separate lineage from CD4<sup>+</sup> T cells, and extrathymically in the periphery by induction of FOXP3 expression in naïve CD4<sup>+</sup>FOXP3<sup>neg</sup> T cells (pTregs). Both tTregs and pTregs are crucial for the maintenance of immune homeostasis.<sup>141</sup> In the thymus, T cells are checked for their reactivity to self-peptides in a process known as thymic selection. T cells progenitors expressing TCR with high affinity to self-peptides presented by medullary thymic epithelial cells (mTEC) are selected as tTreg precursor, while those expressing TCR with low affinity to self-peptides are selected as T conventional cells.<sup>142</sup> The Treg progenitor express CD25, then FOXP3 expression is induced upon TCR stimulation, CD28 co-stimulation, and cytokine signalling triggered by IL-2. The strength and duration of TCR signalling has been shown to play a critical role in Tregs development.<sup>143, 144</sup> In addition, Xuguang et al. have demonstrated the requirement of costimulatory signal CD28 for effective Treg thymic development even if the TCR are engaged with high affinity to the peptides.<sup>145</sup>

In the periphery, (pTregs) arise from naïve CD4<sup>+</sup> cells and contribute to the homeostasis of the peripheral immune compartment. pTregs are generated under various conditions such as the presence of regulatory cytokines (TGF- $\beta$ ) and indoleamine 2,3-dioxygenase (IDO), which are secreted by tolerogenic DCs. Moreover, the presence of vitamin A metabolite (retinoic acid) can also promote the conversion of naïve T cells into pTregs.<sup>146</sup>

The *in vitro* generated Tregs (termed induced Tregs (iTregs)), can arise from naïve CD4<sup>+</sup> cells through co-culturing the CD4<sup>+</sup> cells with TGF- $\beta$ , IL-2 along with TCR stimulation.<sup>147</sup> Studies have also reported the development of iTreg cells *in vivo* in a tolerogenic setting and during inflammation.<sup>148</sup> The iTregs do not recapitulate the phenotypical and molecular features of peripheral Tregs. For example, iTregs demonstrated less FOXP3 expression stability and suppressive potency compared to the pTregs. However, studies are ongoing to generate induced Tregs with a stabilise FOXP3 expression.<sup>149</sup>

Some phenotypic markers were initially reported as a marker to distinguish thymic-derived Tregs from those peripherally induced from the naïve T cells, including the Ikaros family member Helios, and the semaphorin receptor neuropilin-1 (Nrp1).<sup>150</sup> However, later studies demonstrated that Helios may act as a marker to identify a subset of Tregs with potent suppressive activity that cannot be used to discriminate a thymic Treg subset<sup>151</sup> — similarly to the Nrp1, which does not seem to identify thymic Treg clones.<sup>152</sup>

### 1.1.6 Identification and isolation of Tregs

Tregs are heterogeneous in terms of surface marker expression and the question of which population would serve as an optimal cell product for adoptive transfer is a subject of ongoing debate. CD25 (the  $\alpha$ -subunit of the IL-2 receptor complex) is expressed at high levels on Tregs and can be utilised as an identification marker. However, activated effector T cells and in particular naïve T cells, which have a strict requirement for IL-2 for initial clonal expansion and differentiation, can also express CD25.<sup>153</sup>

The role of the transcription factor FOXP3 (Forkhead-BOX-Protein P3) in regulating the immune response in mice and humans was identified in 2001.<sup>154</sup> The identification of mutation of *Foxp3* in scurfy mice that develop severe autoimmune diseases demonstrated the critical role of *FOXP3* in maintaining immune homeostasis.<sup>154</sup> Similarly, a mutation in human *FOXP3* leads to the development of IPEX syndrome (Immunodysregulation Polyendocrinopathy Enteropathy X-linked).<sup>155, 156</sup> Further studies by Khattri et al. on scurfy mice linked *FOXP3* expression with Treg activity and phenotype.<sup>157</sup> Subsequent work demonstrated that stable *FOXP3* expression is required for Treg function.<sup>158, 159, 160, 161</sup> The *FOXP3* gene contains three conserved noncoding sequences (CNS1, CNS2, and CNS3), and a promoter region with binding sites for transcription factors including *NFAT*, *c-Rel*, and *STAT5*.<sup>162</sup> Demethylation of the CNSs permits the binding of transcription factors that control *FOXP3* expression during different stages of Tregs development. CNS3 appears to have a role in *FOXP3* expression, possibly by opening the *FOXP3* gene locus. A demethylated CNS1 is required for *FOXP3* expression in peripheral Tregs but is not necessary during thymic-Treg development. Stable *FOXP3* expression relies on CNS2 within the *Foxp3* gene locus, termed the Treg-Specific Demethylated Region (TSDR). The TSDR is highly methylated in conventional

T cells and induced Tregs, whilst it is demethylated in thymically-derived Tregs.<sup>163, 164, 165</sup> Both TSDR demethylation and *FOXP3* expression are required for thymic Treg lineage commitment.

Isolating Tregs for the therapeutic application can only be undertaken using cell surface markers, and therefore *FOXP3* and the methylation status of the TSDR cannot be used to isolate Tregs in this setting. Surface expression of CD127 (the  $\alpha$ -chain of the IL-7 Receptor) on CD4<sup>+</sup>CD25<sup>hi</sup> cells inversely correlates with *FOXP3* expression and assists in distinguishing Tregs from T effector cells. Thus, the inclusion of CD127 together with CD4 and CD25 facilitates the isolation of Tregs at relatively high purity, as confirmed using intracellular markers and functional testing.<sup>166, 167, 168</sup>

Despite providing refinement in the identification of Tregs, studies indicate that *ex vivo* expanded CD4<sup>+</sup>CD25<sup>+</sup>CD127<sup>low</sup> Tregs are heterogeneous and contain subpopulations of Tregs with different properties. For example, CD4<sup>+</sup>CD25<sup>+</sup>CD127<sup>low</sup>CD45RA<sup>+</sup> refers to a subpopulation of Tregs with a stable TSDR status, higher *FOXP3* expression, and greater suppressive function after *ex vivo* expansion in comparison to CD45RA<sup>-</sup> subpopulations.<sup>169, 170</sup>

Using these cell surface markers, magnetic bead-based isolation of Tregs has largely been the choice for several reported protocols.<sup>171, 172, 173</sup> Beads can be produced to 'Good Manufacturing Practice' (GMP) standards and allow the depletion of CD8<sup>+</sup> and CD19<sup>+</sup> cells and enrichment of CD25<sup>+</sup> cells.<sup>174</sup> As an alternative strategy, fluorescence-activated cell sorting (FACS) offers superior purity compared to magnetic bead-enriched Tregs, as well as the possibility of selecting specific cell populations based on their expression levels of cell surface molecules such as CD25 and CD127. A number of proprietary GMP-compliant FACS-based sorting processes exist and are being assessed for the production of clinical therapeutics, but are not yet accepted by some regulatory agencies.

### 1.1.7 Tregs suppression mechanisms

Discoveries in basic research have enabled the identification of multiple mechanisms by which Tregs regulate immune responses. These include the release of regulatory cytokines and molecules, the disruption of effector cell metabolism, the modulation of dendritic cells (DCs) maturation or function, and production of cytolytic mediators.<sup>175</sup> Figure 2 illustrates the suppressive mechanisms of human Tregs and their effects on various leukocytes.

One of the main mechanisms of Treg-mediated suppression is through the production of inhibitory cytokines, including interleukin (IL)-10, TGF- $\beta$ , and IL-35. These cytokines are involved in the direct suppression of effector cells and indirect suppression through inhibition of DC maturation.<sup>176</sup> Moreover, these regulatory cytokines play a role in infectious tolerance not only through conversion of T effector cells into T cells with regulatory phenotype and function,<sup>177</sup> but also through inducing B regulatory cells from B cells and promoting macrophage differentiation toward Mregs.<sup>178</sup>

Tregs may disturb the metabolic function of effector cells through the expression of CD39 and CD73. These ectoenzymes lead to degradation of ATP to adenosine and AMP. Adenosine can directly bind to the A2a receptor on T effector cells and inhibit their activation, and can also inhibit the maturation of DCs.<sup>179</sup> Another potent mechanism is through inhibitory cell surface signalling, such as through the cytotoxic T-lymphocytes antigen 4 (CTLA-4). Tregs may prevent the activation of effector T cells either through downregulating the B7 costimulatory molecules CD80 and CD86 on antigen-presenting cells (APC) in a CTLA-4-dependent manner or by the direct binding of CTLA-4 to CD80 and CD86 on naïve T cells.<sup>176</sup> Other co-inhibitory molecules are found on the cell surface of Tregs, including T cell Ig and ITIM domain (TIGIT) and lymphocyte-activation gene 3 (LAG-3): these molecules may suppress the T cell activation through DC modulation.<sup>176</sup> Moreover, multiple studies have demonstrated that Tregs may possibly regulate other cells of the innate immune system, such as NK cells, neutrophils, and type 2 innate lymphoid cells (ILC2).<sup>180</sup>

In addition, Tregs may induce T cell apoptosis in a granzyme-B-dependent manner and induce cytolysis of other cells, including B cells and NK cells, in a perforin- and granzyme-B dependent manner.<sup>181, 182</sup> Recent data suggest that Tregs may be able to inhibit T effector function through the release of extracellular vesicles including exosomes.<sup>183</sup>

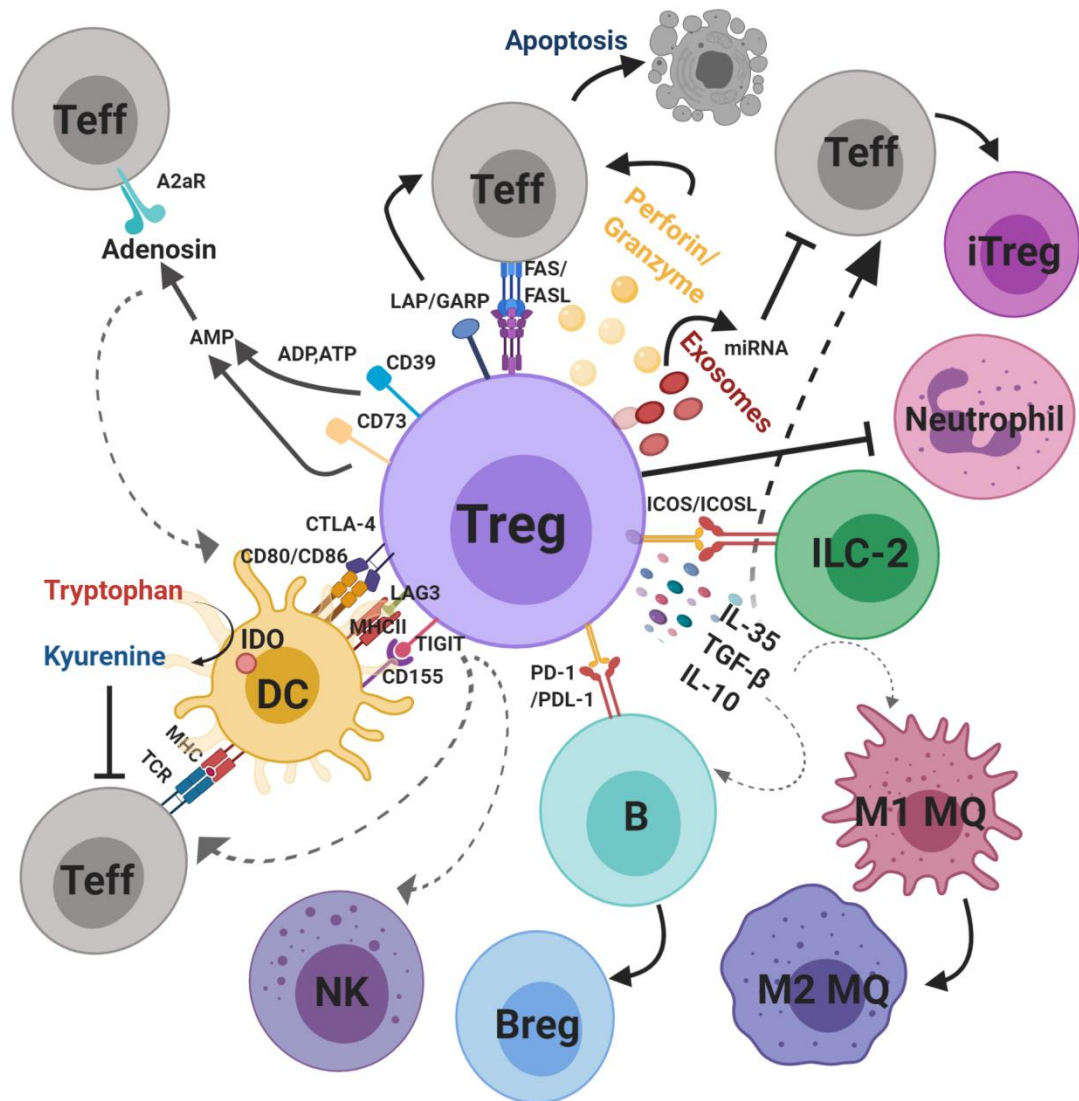


**Figure 2: Treg suppressive mechanisms.** Solid arrows indicate direct inhibition of target cells or direct induction, while dashed arrows indicate another possible target of a specified inhibitory molecule. Treg, regulatory T cell; iTreg, inducible regulatory T cell; DC, dendritic cell; Teff, T effector cell; Breg, B regulatory cell; ILC-2, type 2 innate lymphoid cell; M1 MQ, pro-inflammatory macrophage; M2 MQ, anti-inflammatory macrophage; IDO, Indoleamine 2,3-dioxygenase; MHC, major histocompatibility complex; TCR, T-cell receptor; CTLA-4, cytotoxic T-lymphocyte-associated protein 4; LAG3, Lymphocyte-activation gene 3; TIGIT, T cell Ig and ITIM domain; PD-1, Programmed cell death-1; PDL-1, Programmed death-ligand 1; ICOS, Inducible T-cell costimulator; FAS, cell death surface receptor; LAP, latency-associated peptide; GARP, glycoprotein A repetitions predominant; ATP, adenosine triphosphate; ADP, Adenosine diphosphate; AMP, Adenosine monophosphate; A2aR, adenosine A2a receptor.

### 1.1.8 Application of Tregs as a cellular therapy

Treg therapy now centres around two main methods: (I) the direct *in vivo* expansion of endogenous Tregs, and (II) the *ex vivo* expansion of Tregs. The only immunosuppressant consistently demonstrated to potentiate *in vivo* Treg expansion and survival is rapamycin.<sup>184, 185</sup> Hester et al. demonstrated the adjuvant effect of low-dose rapamycin in enhancing Tregs activity to inhibit transplant arteriosclerosis in a humanised mouse model.<sup>185</sup> However, poor patient tolerance of rapamycin has led to a search for alternative strategies to expand *in vivo* Tregs. For instance, low dose IL-2 has shown efficacy in restoring Tregs numbers without concurrent expansion of effector T cell populations in patients with GVHD.<sup>186, 187</sup> In experimental model, Pilat et al. demonstrated that low dose of IL-2 complex along with rapamycin and blockade of pro-inflammatory cytokine IL-6 prolonged survival of skin allograft, without need to immunosuppression.<sup>188</sup> However, a phase IV clinical trial using low dose IL-2 in liver transplant patients was terminated due to safety concerns (the LITE Trial [NCT02949492]). Improved IL-2 therapies might be possible using the anti-IL-2 complex with higher selectivity for Tregs than autoreactive effector T cells,<sup>189</sup> or by engineering IL-2 molecules so the modified IL-2 can selectively signal to Tregs.<sup>190</sup> Indeed, further research is needed in experimental models and later in clinics to validate the safety of anti-IL-2 complex or IL-2 modification therapies in transplantation. Furthermore, IL-33 has shown efficacy in driving the production of mouse Tregs with enhanced suppressive activity in experimental skin transplant model.<sup>191</sup> This study suggests an alternative approach for *in vivo* Tregs expansion.

Alternatively, cell therapy may be performed by adoptive transfer of *ex vivo* expanded Tregs, which has several advantages over *in vivo* cell manipulation. Tregs are closely related to T effector cells, meaning that precisely targeting Tregs and not T conventional cells can be difficult. In addition, *ex vivo* expansion of Tregs provides an opportunity to manipulate them by the selection of more efficient cell populations,<sup>192</sup> or by improving their suppressive properties using exogenous treatments or genetic modification technologies.

The low precursor frequency of Tregs in the peripheral blood means that cells require extensive *ex vivo* expansion in order to obtain enough yield for clinical application. This extensive expansion may impact Tregs' suppressive function and increase the cost of cell

therapy. Protocols for *ex vivo* expansion according to good manufacturing practice (GMP) have been reported, which results in a good yield.<sup>193, 194, 195, 196</sup> However the presence of contaminant T effector cells in the final cell product or conversion of Tregs into pathogenic T effector cells continues to be of concern. Thus new strategies are needed to enhance the purity and efficacy of *ex vivo*-expanded Tregs.

A number of supplements can promote the *ex vivo* expansion of highly suppressive Tregs. For example, the addition of all-*trans* retinoic acid (ATRA), vitamin D, and TGF- $\beta$  during Treg culture<sup>197, 198</sup> has been shown to stimulate the induction of induced Tregs (iTregs) from CD4<sup>+</sup> naive T cells and enhance the suppressive capacity of Tregs. However, it is still unknown if the immunomodulatory effects of these supplements on Tregs will persist long-term.

Recent advances in genetic modification technologies have opened the possibility to safely improve the potential therapeutic of Tregs. Recently, Eskandari et al. proposed a new methodology to improve the Tregs adoptive therapy through engineering Tregs with TCR signalling-responsive IL-2 nanogels.<sup>199</sup> Both murine and human nanogel-modified Tregs carrying an IL-2 cargo showed enhanced performance in suppressing alloimmunity in murine and humanised mouse allotransplantation models compared to non-modified Tregs. This proposed methodology may hold promise for the future of Tregs therapy, especially since the nanogel can be conjugated to antigen-reactive Tregs instead of polyTregs.

Another important approach to expand Tregs with enhanced efficacy is through the generation of non-gene modified antigen-reactive Tregs (arTregs), which will be discussed in detail in the next section.

### **Alloantigen-reactive Tregs (arTregs)**

*Ex vivo* expansion of freshly isolated Tregs from peripheral blood is generally performed by stimulation of magnetic-bead-isolated or flow-sorted cells with anti-CD3/anti-CD28 beads in the presence of recombinant human IL-2 with rapamycin.<sup>200</sup> This leads to non-specific TCR stimulation and proliferation of polyclonally-reactive Tregs (polyTregs). This approach is able to generate significant numbers of CD4<sup>+</sup>FOXP3<sup>+</sup> cells with a purity that is often improved to over 80% with the use of rapamycin to reduce T effector contaminant proliferation.<sup>200</sup> However, several theoretical drawbacks exist with polyTregs therapy, including the potential

for indiscriminate immune suppression.<sup>103</sup> In addition, animal studies suggest that high numbers of polyTregs (1:1 to 1:5 Treg to Teff) are required in order to achieve tolerance.<sup>201</sup> The use of an enriched population of arTregs may overcome these problems as these cells offer targeted regulation of a specific undesired immune response. In *in vitro* suppression studies, arTregs are 5- to 25-fold more potent at suppressing effector T cells in co-culture than polyTregs.<sup>171, 202, 203</sup>

In humanised mouse models, the adoptive transfer of *ex vivo*-expanded human polyTregs can prevent skin, vessel, and islet allograft rejection.<sup>204, 205, 206, 207</sup> However, arTregs produced through the co-culture of Tregs with allogeneic DCs or B cells are more effective than polyTregs at preventing human skin allograft rejection and may demonstrate superior migration and accumulation in the allograft.<sup>208, 209, 210, 211</sup> These Tregs migrate to and accumulate in the allograft, an effect that may contribute to their superior suppressive function. Using a different manufacturing process with allogeneic B cells instead of DCs as a stimulator, human arTregs infused at a 1:5 ratio of Tregs to responders are able to prevent skin allograft rejection, whereas polyTregs fail to be protective at this ratio.<sup>211</sup> These results suggest that infusion of alloantigen-reactive Tregs may facilitate a reduction in the total cell number needed for therapeutic efficacy.

### 1.1.9 Strategies to expand human arTregs *ex vivo*

In healthy individuals, Tregs represent approximately 5-10% of the CD4<sup>+</sup> T cell population,<sup>212, 213, 214</sup> of which only 5-10% are alloantigen-reactive.<sup>215, 216</sup> This low precursor frequency means that cells require extensive *ex vivo* expansion to obtain enough numbers for clinical application. Stimulator populations for arTreg production include peripheral blood mononuclear cells (PBMCs),<sup>171</sup> dendritic cells (DCs),<sup>217</sup> or B cells.<sup>218, 219</sup> Table 2 summarises the current approaches used in expanding human arTregs.

Peter et al. demonstrated that irradiated donor-derived PBMCs used as stimulators for Tregs sorted by FACS yield a low expansion rate over a two-week period, although interestingly this expansion improves when Tregs were isolated using magnetic beads (cliniMACS) instead.<sup>171</sup> This suggests that residual antibody binding may subsequently impair Treg expansion. The activation of Tregs requires cell-to-cell contact leading to an immunological synapse, with activation through the TCR and suitable costimulatory signals.<sup>173</sup> Therefore, most protocols

rely on the use of purified B cells or DCs as professional APCs to ensure optimal delivery of signals for Treg activation and proliferation.

The use of B cells for Treg allostimulation requires a preliminary B cell expansion and activation step. As B cells need a CD40/CD40L co-stimulatory signal to proliferate, CD40L-expressing fibroblasts have been used as feeder cells to expand B cells. Immortalised B cell lines from HLA-matched donors have been used to offer a direct expansion of alloantigen Tregs from a readily available allogeneic B cell bank.<sup>220</sup> However, this bank may not cover all HLA-donor/recipient combinations and also has the potential for cellular contamination in the final cell product. Soluble 4-trimer CD40L fusion proteins may represent an alternative to feeder cells and appear to be efficacious in generating arTregs.<sup>172</sup> Recently, B cells were successfully expanded using a soluble 4-trimer CD40L fusion protein as a replacement for CD40 feeder cells. This molecule contains four CD40L trimers per molecule and has been found to be more effective at activating B cells than single CD40L trimers.<sup>221</sup> ArTregs generated by this protocol expanded up to 20-fold with no cellular contamination reported in the final product.<sup>222</sup>

DCs provide potent allo-stimulatory signals to expand Tregs with a low risk of persistence within the culture, especially when irradiated. Tregs selected using magnetic beads and primed twice by allogeneic monocyte-derived DCs (mDCs) cultured with rapamycin, IL-2 and IL-15 have been shown to be functional both *in vitro* and *in vivo*, controlling GVHD in a mouse model.<sup>173</sup> These arTregs expand eight-fold and display a fully demethylated TSDR with high expression of FOXP3 and Helios. The most efficient method for generating arTregs remains unclear, with no studies to date directly comparing expansion using alternative stimulatory cell populations from the same donor. This would provide a useful comparison in terms of the cellular phenotype and suppressive capability of expanded arTregs.

**Table 2: Approaches for *ex vivo* expansion of human alloantigen-reactive Tregs**

Starting population	Stimulator	Ratio	Growth factors	Expansion duration	Expansion fold	Reference
CD4 <sup>+</sup> CD25 <sup>+</sup> Treg isolated by magnetic beads	Donor derived PBMCs	4:1 PBMCs: Tregs	rhIL-2 +rh IL-15	20 days	780	<sup>171</sup>
CD4 <sup>+</sup> CD25 <sup>+</sup> CD127 <sup>-</sup> Treg isolated by magnetic beads	UltraCD40L-activated donor B cells	1:1 B cells: Tregs	rhIL-2+TGF- $\beta$ +Sirolimus SRL-7days only	28 days	~20	<sup>172</sup>
CD4 <sup>+</sup> CD25 <sup>+</sup> CD127 <sup>-</sup> Treg isolated by FACS	CD40L-activated donor B cells	4:1 B cells: Tregs	rhIL-2	16 days	50-300	<sup>218</sup>
CD4 <sup>+</sup> CD25 <sup>+</sup> Treg isolated by magnetic beads	Allogeneic mature DCs	1:10 mDCs: Tregs	rhIL-2 +rh IL-15+Rapamycin	21 days	8.3	<sup>173</sup>
CD4 <sup>+</sup> CD25 <sup>+</sup> CD127 <sup>-</sup> Treg isolated by FACS	Blood or dermal donor-derived mature CD1c <sup>+</sup> DCs	Not reported	rhIL-2	4-6 weeks	Mean numbers ~2.8x10 <sup>7</sup>	<sup>223</sup>
CD4 <sup>+</sup> CD25 <sup>+</sup> Treg isolated by magnetic beads	CD40L-expanded B cell lines	10:1 B cells: Tregs	rhIL-2	2-3 weeks	80-120	<sup>220</sup>
CD4 <sup>+</sup> CD25 <sup>+</sup> CD127 <sup>-</sup> Treg isolated by magnetic beads	Allogeneic monocyte-derived DCs	1:10 DCs: Tregs	rhIL-2 +rh IL-15+ Rapamycin	12 days	8	<sup>224</sup>

APC, antigen presenting cell; DC, dendritic cell; PBMC, peripheral blood mononuclear cell; Treg, regulatory T cell; rh, recombinant human.

### 1.1.10 TCR transgenic Tregs

The recent success of specific T-cell receptor (TCR) gene therapy in the cancer setting offers the opportunity to redirect the Treg specificity as desired through TCR transgenesis. Brusko et al. reported a methodology to generate human transgenic Tregs with a class I-specific TCR in which they recognise melanoma antigen tyrosinase.<sup>225</sup> This study demonstrated that the viral transduction of a specific TCR into *in vitro* expanded CD4<sup>+</sup>CD25<sup>+</sup>CD127<sup>-</sup>CD45RA<sup>+</sup>Tregs could enrich their specificity, therefore generating antigen-specific Tregs. These TCR Tregs maintained a high expression of FOXP3 after *in vitro* expansion. Moreover, these cells suppressed antigen-specific effector T cell activity both *in vitro* and in a mouse tumour model more effectively than poly-expanded Tregs.

Another study by Kim et al. reported the generation of engineered antigen-specific Tregs which were created by the transduction of TCR from T cell clones obtained from patients with hemophilia A into *in vitro* expanded human Tregs.<sup>226</sup> These engineered Factor VIII-specific Tregs suppressed the proliferation of FVIII-specific T cells in both *in vitro* and in a humanised hemophilia A mouse model. However, there are several potential risks associated with the use of TCR transgenic Tregs, including the risk of lentiviral or retroviral vector-related toxicity following the infusion of TCR Tregs, in addition, to the risk of toxicity that may result from mispairing with endogenous TCR.<sup>227</sup> Therefore a long-term safety assessment is necessary before TCR Tregs can be used clinically.

### 1.1.11 CAR Tregs

Recent advances in chimeric antigen receptor (CAR) technologies have opened the possibility of being able to redirect the specificity of human Tregs as desired.<sup>225, 228</sup> CAR Tregs have shown promise in early experimental models in transplantation<sup>229, 230, 231</sup> and autoimmunity.<sup>232, 233</sup> CAR Tregs specific for MHC-I molecules are superior to polyTregs at preventing xenogeneic GVHD and skin graft rejection in humanised mouse models.<sup>229, 230</sup> However, there are some differences between CAR Tregs and arTregs and challenges that it must be highlighted. CAR Tregs are produced using a viral vector, in contrast to arTregs which are produced using a simple method of co-culture with donor antigen. Therefore, the safety of CAR Tregs in solid organ transplantation needs to be confirmed, as clinical experience of the adoptive transfer

of CAR T cells directed against tumour antigens shows that it can result in adverse effects related to cytokine storms and cytotoxicity.<sup>234, 235</sup>

CAR Tregs are able to inhibit direct allorecognition and consequently acute cellular rejection,<sup>229, 231</sup> but their effect on the indirect allorecognition and humoral responses remain to be investigated. For instance, Levings et al. investigated CAR efficacy at regulating *in vivo* memory responses and found that CAR Tregs were unable to regulate memory T or B cell responses in pre-sensitised mice.<sup>236</sup> Furthermore, alloreactivity may be driven by a broad array of antigens, and therefore a specificity toward several peptides might be preferable in the generated antigen-reactive Tregs. Notably, the assessment of the T cell receptor repertoire of arTregs revealed that they respond to several clones.<sup>172</sup> This wider clonality allows arTregs to react with multiple donor antigens, unlike CAR Tregs, which are very restrictive in their responsiveness to a single antigen.

The exhaustion of CAR Tregs is another concern. Some studies indicate that CAR T cells incorporating the CD28 costimulatory domain have limited *in vivo* expansion and anti-tumour efficacy, which is avoided with the 4-1BB costimulatory domain.<sup>237</sup> For CAR Tregs, studies used second-generation CAR Tregs with a CD28 domain and demonstrated suppressive efficacy.<sup>238, 239</sup> Research is still ongoing to determine the optimal CAR-encoded costimulatory signals and specificity,<sup>240</sup> to reduce immunogenicity,<sup>241</sup> and to improve CAR Tregs manufacturing frameworks.<sup>242</sup> A phase I clinical trial of autologous CAR Tregs directed against HLA-A2 is now ongoing (NCT04817774). These CAR Tregs can be administered to HLA-A2-negative recipients of an HLA-A2-positive living donor renal transplant. This study aims to assess the safety and tolerability of these CAR Tregs in patients undergoing living donor renal transplantation.

### 1.1.12 Direct vs indirect allospecificity

It is also important to note experimental evidence suggesting that indirect presentation is the major pathway underlying chronic transplant rejection;<sup>57, 58</sup> thus attention is now turning to arTregs populations with indirect allospecificity to regulate this response.

Indirect allospecificity can be enriched in Tregs through repetitive stimulation with autologous DCs pulsed with donor peptides. Generated arTregs are able to suppress both the indirect and direct alloresponse of naïve CD4<sup>+</sup>CD25<sup>-</sup> T cells *in vitro*.<sup>243</sup> Another approach used in murine

models to generate Tregs with indirect allospecificity is through TCR transduction.<sup>244, 245</sup> In one example, the TCR specific to the H-2K<sup>d</sup> peptide presented by an MHC class II molecule (H2A<sup>b</sup>) was retrovirally transduced into Tregs. These TCR-transduced Tregs (TCR-Tregs) which indirectly recognise allogeneic MHC class II molecules induced long-term survival of MHC-mismatched heart grafts.<sup>245</sup> Moreover, TCR-Tregs with indirect allospecificity showed superiority in inducing graft tolerance in comparison to Tregs with direct allospecificity. This indicates that arTregs with indirect allospecificity might be more potent than direct Tregs. However, the major drawback of transgenic TCR-Tregs is the concern of mispairing with endogenous TCRs which could lead to off-target reactivity.

### 1.1.13 Trials of arTregs

So far only a single clinical trial, in a liver transplantation setting, has tested the adoptive transfer of *ex vivo* arTregs, examining 10 adult liver transplant recipients.<sup>246</sup> The arTregs were generated using irradiated donor peripheral blood lymphocytes cocultured with unselected recipient splenocytes in the presence of anti-CD80/86 monoclonal antibodies. The protocol generated CD4<sup>+</sup>CD127<sup>low</sup>FOXP3<sup>+</sup> Tregs with a relatively low purity within the CD4<sup>+</sup> population averaging less than 25%. The infused cell product was heterogeneous, with expanded CD19<sup>+</sup> and CD8<sup>+</sup> cells also infused. Participants underwent a regimen of splenectomy and cyclophosphamide administration before Treg infusion. Acute rejection upon per-protocol weaning of immunosuppression was shown to be limited to participants with a history of autoimmune liver disease, with the remaining participants all demonstrating stable graft function up to three years after drug withdrawal. *In vitro* functional assays indicated that PBMCs from many participants demonstrated reduced proliferative activity in response to allo-stimulation to a greater degree than seen with third-party stimulation, even after drug withdrawal. Unfortunately, the immunological picture did not clearly correspond to the clinical one, with a degree of allo-specific hyporesponsiveness seen even in participants who developed acute rejection. However, there are several limitations in this study including the lack of a prospectively recruited control arm and the small number of patients with a limited follow-up period. In addition, the protocol used to generate *ex vivo* arTregs resulted in low-purity Tregs. Nevertheless, a number of early-phase clinical trials of arTregs and polyTregs in the setting of solid organ transplantation are currently ongoing and will report in the coming years (Table 3).

**Table 3: Ongoing trials of polyclonal and alloreactive Tregs.**

Trial ID	Phase	Tregs	Dose	Design	Setting	n (Treg arm)	Start Date	Primary Completion Date	Status
<b>NCT04661254*</b>	N/A	PolyTregs	Not specified	Open label, randomised	Living donor renal and liver transplantation	4	December 2020	April 2021	Not yet recruiting
<b>NCT03654040*</b>	I/IIa	arTregs	100- 500 x 10 <sup>6</sup> -30-100 <sup>6</sup> cells (single dose)	Open label	Living donor liver transplantation	9	January 2021	April 2027	Not yet recruiting
<b>NCT03284242*</b>	N/A	PolyTregs	Not specified	Open label	Renal transplantation with everolimus immunosuppression	12	March 2019	March 2021	Recruiting
<b>NCT03943238*</b>	I	Not specified	25 x10 <sup>5</sup> cells (single dose)	Non-randomised	Living donor renal transplantation, with donor BM infusion	22	February 2020	August 2024	Recruiting
<b>NCT03577431*</b>	I/IIa	arTregs	2.5 - 125 x 10 <sup>6</sup> cells (single dose)	Non-randomised	Liver transplantation, with subsequent immunosuppression withdrawal	9	March 2019	March 2025	Recruiting
<b>NCT02474199*</b>	I/IIa	arTregs	400 x 10 <sup>6</sup> cells (single dose)	Non-randomised	Living donor liver transplantation, with subsequent immunosuppression withdrawal	14	June 2016	December 2019	completed
<b>NCT03867617* 2018-003142-16**</b>	I/IIa	Not specified	10 x 10 <sup>6</sup> cells (single dose)	Non-randomised	Renal transplantation, with donor BM infusion & tocilizumab	12	August 2019	April 2023	Recruiting
<b>NCT02711826*</b>	I/IIa	PolyTregs	>300 x 10 <sup>6</sup> cells (single dose)	Open label, randomised	Renal transplantation with subclinical inflammation on protocol biopsy >5m post transplant	30	May 2016	October 2021	Recruiting
<b>2017-001421-41**</b>	IIb	PolyTregs	5-10 x 10 <sup>6</sup> cells/kg (single dose)	Open label, randomised	Living donor renal transplant with immunosuppression minimisation	68	Feb 2018	Feb 2022	Recruiting

**Table 3: Ongoing trials of polyclonal and alloreactive Tregs.** Clinicaltrials.gov\* and EudraCT\*\* were searched using the keywords “regulatory T cells” or “Tregs” in the disease area “transplantation”. Results were filtered by studies with status “ongoing”, “recruiting”, “active, not yet recruiting” and “enrolling by invitation”. Search date: 15 December 2020

## Phenotypic and molecular analysis of the peripheral blood mononuclear cell compartment and graft biopsy in advanced cellular therapy in transplantation

### 1.1.14 Immune monitoring strategies in clinical trials of cell therapy

Immune monitoring can be defined as an approach to assess the immune response by measuring cellular, molecular, and functional changes that correlate with the immune system. There has been a strong interest from transplant researchers in developing and validating assays that provide in-depth information about the efficacy of cellular therapy in solid organ transplantation. These assays have several advantages, as they provide insight about the immunological status of transplant recipients and measure alloreactivity response at multiple time-points post-transplantation, thus allowing physicians to assess the safety of withdrawing or even minimising the immunosuppressant drugs, and to determine not only the safety but also the efficacy of cellular therapy.

Clinical studies with cellular therapy in a transplantation setting aim to perform immune monitoring assays during the follow-up period for the enrolled participants. The ONE Study consortium, which works to assess the potential of infusing different regulatory cells in renal transplant recipients and compare their immunological effects between closely related trials,<sup>100, 247</sup> designed a standardised immune monitoring assay for all the participating centres to ensure that results from one trial can be accurately and fairly compared to those in other trials.

Currently, several technologies are available for immune monitoring in the cellular therapy context including (I) the use of multiparameter flow cytometry and mass cytometry (CyTOF) to assess the phenotypical changes in peripheral immune cell compartments following the cell therapy; (II) the use of multiplexed probe-based RNA analysis, bulk sequencing, and single cell sequencing to investigate the transcriptional changes in the peripheral blood mononuclear cells and matched renal biopsies; (III) viral testing by PCR to determine susceptibility for viral infection (CMV, EBK, and BK virus); (IV) assays to examine cytokines and metabolites in the serum of transplanted recipients; and (V) an *in vitro* functional assay to assess the enrichment

of antigen reactive T cells. Our group has recently commenced recruitment for the TWO Study in the UK, which is a single-centre phase IIb randomised trial of expanded polyclonal autologous Tregs in renal transplantation. The aim of the TWO Study is to assess the ability of Tregs to facilitate immunosuppression reduction in living donor kidney recipients. Various immune monitoring techniques are used in the study aiming to understand alterations in the immune cells of patients receiving Treg therapy (Figure 3). The following sections describe in more detail flow cytometry and mass cytometry (CyTOF), quantification of arTregs and T conventional cells through CD137/CD154 assays, and spatial transcriptomic technologies.

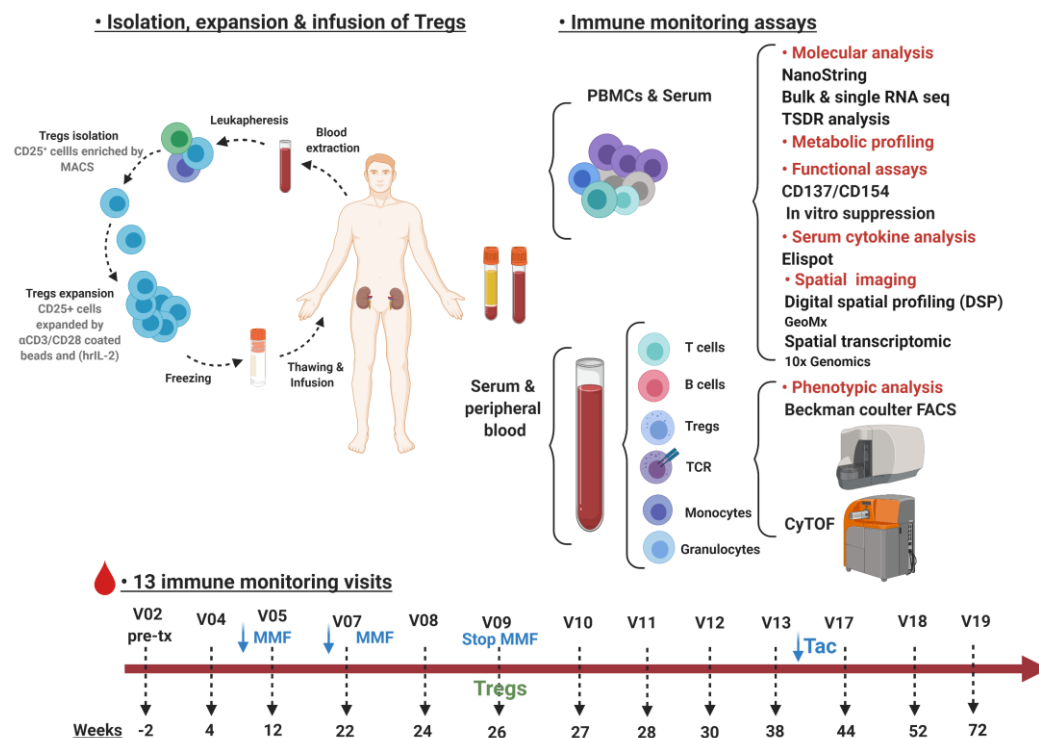


**Figure 3: Overview of immune monitoring techniques in the TWO Study trial.** Peripheral blood and serum samples are obtained from renal transplant patients during the 13 immune monitoring visits. These visits start at two weeks pre-transplantation and end at 72 weeks post-transplantation. Peripheral blood mononuclear cells (PBMCs) are isolated from the blood and cryopreserved for later analysis. Immune monitoring of transplanted patients combines several assays including molecular analysis, metabolic profiling, functional assays, serum cytokine analysis, spatial profiling, and phenotypical analysis. The phenotypical analysis covers a wide range of immune cells populations including T cells, B cells, Tregs, monocytes and granulocytes acquired by flow cytometry and mass cytometry (CyTOF). Tregs, T regulatory cells; TCR, T cell repertoire analysis; TSDR, Treg-specific demethylated region; Elispot, enzyme-linked immunospot.

### 1.1.14.1 Flow cytometry and mass cytometry (CyTOF)

For many years, immune monitoring has relied on conventional flow cytometry (FACS) to analyse and study phenotypical changes in leukocytes and their relationship to pathologies. FACS can analyse around several parameters in parallel and provide rapid assessment of the target populations. This technology has been used to investigate the efficacy of cell therapy in a number of clinical trials by measuring the cells frequency and number at different time-points pre- and post-transplantation.

In a study in renal transplant recipients receiving polyTregs, FACS was used as a key assessment method for immunophenotyping of recipients after Tregs infusion.<sup>248</sup> An elevation in CD4<sup>+</sup>CD25<sup>hi</sup>CD127<sup>-</sup>FOXP3<sup>+</sup> cells was seen for the remainder of the follow-up period (one year) post-infusion. This elevation was not seen in the control group receiving the same immunosuppressive protocol. Another study used FACS, to measure the changes in the phenotype of leukocytes among type 1 diabetic patients treated with Tregs.<sup>109</sup> An increase in the percentage of CCR7<sup>+</sup> Tregs was reported and continued to remain elevated for over three months after cell infusion compared to the pre-infusion time-point. There was also a significant decrease in CD56<sup>hi</sup>CD16<sup>lo</sup> natural killer (NK) cells early after polyTreg infusion in all the participants.

Recently, Sawitzki et al. reported the findings of the ONE Study clinical trials (seven non-randomised, single-arm, phase 1/2A trials) in renal transplant recipients receiving different regulatory cells, in which standardised multiparameter FACS analysis of various immune cell subsets was employed for immune monitoring of participants in cell therapy and in reference group.<sup>105</sup> A significant increase in the absolute numbers of CD8<sup>+</sup>CD45RA<sup>+</sup>CCR7<sup>-</sup> and CD8<sup>+</sup>CD57<sup>+</sup> chronically activated T cells were observed in patients in the reference group trials but not in patients in the cell therapy trials. They also found a normalisation of marginal zone-like B-cell numbers and a significant reduction of CD14<sup>high</sup>CD16<sup>+</sup> monocytes only in patients in the cell therapy trials. In addition, Roemhild et al. reported their immunophenotyping monitoring by FACS of patients receiving Treg therapy compared to control group.<sup>249</sup> An elevation in Treg proportions in the peripheral blood was observed for eight weeks after infusion; this phenomenon was not seen in the control group. Additionally, fewer activated

HLA-DR<sup>+</sup> CD4<sup>+</sup> conventional T cells together with fewer CD56<sup>high</sup> NK cells were seen in Treg-treated patients compared to the reference group.

Although several clinical trials have employed FACS as a potential technology for immunophenotyping, the relatively low number of parameters that can be analysed simultaneously results in a limited analysis. To examine several cells simultaneously by FACS, several panels need to be designed, which means more clinical materials (for example: peripheral blood or PBMCs) are needed. The development of mass cytometry or cytometry by time-of-flight (CyTOF) has opened the possibility to increase the parameters, therefore allowing for a comprehensive analysis of a wide array of immune populations. Moreover, this high dimensional technology allows for in-depth examination of peripheral blood leukocytes from small sample quantities. The designed antibody panels can be selected to cover cellular and intracellular markers to identify immune cell lineages and define their activation or maturation stages. Table 4 compares the main features of conventional FACS and CyTOF.

To date, few studies have employed CyTOF for deep immunophenotyping of multiple immune cell subsets in transplantation. Fribourg et al. monitored the phenotypic changes of PBMCs from 26 renal transplant recipients over 6 months post-transplantation using CyTOF.<sup>250</sup> The unbiased cluster analysis revealed an increase in PD-1<sup>+</sup>CD57<sup>-</sup> expression in both CD4<sup>+</sup> and CD8<sup>+</sup> T cells. Their findings suggest that exhausted T cells correlate with improved allograft function. Recently, Kowli et al. analysed the phenotypic changes in the peripheral blood of renal transplant recipients compared to age-matched healthy donors over 6 months using CyTOF.<sup>251</sup> An elevation of CD57<sup>+</sup>CD8<sup>+</sup> T cells together with an increase of granzyme B and CD107a expression in CD8<sup>+</sup> T cells and CD56<sup>hi</sup> NK cells were observed only in renal transplant patients. This analysis of Tregs by CyTOF demonstrated a decrease in the IL-10 production in renal transplant patients compared to healthy donors.

**Table 4: Comparison of flow cytometry and (CyTOF) mass cytometry**

Aspect	Flow cytometry	Mass cytometry (CyTOF)
<b>Type of antibody</b>	Antibodies conjugated to fluorescent probes	Antibodies conjugated to stable metal isotope probes
<b>Number of parameters</b>	Depends on the machine, a range of 8- 30 markers per cell	Up to 40 markers per cell
<b>Source of nonspecific signal</b>	<ul style="list-style-type: none"> <li>• Spectral overlap (5-100%)</li> <li>• Autofluorescence</li> <li>• Fluorophore degradation</li> </ul>	<ul style="list-style-type: none"> <li>• Spectral overlap (&gt;2%)</li> <li>• Metal oxidation</li> <li>• Metal isotopes impurity</li> </ul>
<b>Minimum cells needed at start of protocol</b>	1x10 <sup>5</sup> cells	50000 cells
<b>Number of cells acquired per second</b>	(500–40,000 cells/s)	(50–1,000 cells/s)
<b>Cell state after measurement</b>	Cells can be sorted by cell sorter for functional assays	Cells are destroyed during ionization
<b>Data analysis methods</b>	Manual analysis by Flowjo™ and FACSDiva	Manual and automated analysis by Cytobank software
<b>Single cell events gating</b>	Forward versus side scatter (FSC vs SSC)	DNA intercalator labelled to iridium isotopes ( <sup>191</sup> Ir and <sup>193</sup> Ir)
<b>Advantages/disadvantages of analysis methods</b>	<ul style="list-style-type: none"> <li>• Subjective</li> <li>• Discovery of new population is difficult</li> </ul>	<ul style="list-style-type: none"> <li>• Unbiased</li> <li>• Considers multiple dimensions at a time</li> <li>• Easier identification of novel populations</li> <li>• More consistent and reproducible</li> </ul>

CyTOF; Cytometry by time of flight. Ref <sup>252, 253, 254</sup>

### 1.1.14.2 Quantification of alloantigen reactive Tregs and T conventional cells through CD137/CD154 assay

CD137 (4-1BB) is a member of the tumour necrosis factor receptor family (TNFR). This co-stimulatory molecule is expressed on activated CD4<sup>+</sup> and CD8<sup>+</sup> T cells following an antigen encounter.<sup>255, 256</sup> Schoenbrunn et al. demonstrated that CD137 is a very suitable activation marker for CD4<sup>+</sup> CD25<sup>+</sup> FOXP3<sup>+</sup> human Tregs, which is upregulated rapidly following short stimulation (16-24 hours).<sup>257</sup> This upregulation, allows the detection of *in vivo* development of alloantigen-reactive Tregs.

CD154 (CD40L) is a member of the TNF superfamily. It is expressed by CD4<sup>+</sup> naïve and memory T cells, and by a subset of CD8<sup>+</sup> T cells after stimulation.<sup>258, 259</sup> It has been shown that engagement of CD154 with its receptor on antigen-presenting cells (APCs) or B cells in both cases results in expansion and activation of antigen-specific T cells.<sup>259, 260, 261</sup> In the liver transplantation setting, the proportion of alloreactive CD8<sup>+</sup> memory T cells was assessed in recipients receiving Tregs therapy through CD154 expression.<sup>262</sup> A trend towards a reduction in CD154 upregulation in memory CD8<sup>+</sup> T cells upon stimulation with donor PBMCs was reported in recipients receiving 4.5 x10<sup>6</sup> Treg/kg. This trend was not seen in those receiving a lower dose of Treg (1x10<sup>6</sup> Treg/kg), or in response to third-party PBMC or CMV antigens. CD154 is therefore a specific marker of activated T cells. Hence, the use of CD137 in conjunction with CD154 may help strike a balance between antigen-reactive Tregs and effector T cells. The use of this analysis in TWO Study patients will help to determine the impact of Tregs infusion on the activated T cells and whether these patients develop alloantigen-reactive Tregs after cellular therapy infusion.

### 1.1.14.3 GeoMx Digital Spatial Profiling (DSP)

In several studies, standard immunohistochemistry (IHC) and immunofluorescence have been used to identify types of cells present in fixed tissue (biopsy) samples.<sup>263, 264</sup> However, these techniques offer limited information about cellular function or gene and protein signatures in respect to their spatial location. NanoString GeoMx is a novel technology that provides morphological context with a high profiling of proteins and gene expressions using

oligonucleotide tags.<sup>265, 266</sup> These tags are attached to antibodies and RNA probes through a light-sensitive linker. A photocleaving light is projected onto the tissue sample to release photocleavable oligonucleotides within specific regions of interest covering up to 5,000 cells and 22,000 transcripts. These features make the DSP technology well-suited to the discovery of single biomarkers or proteins or the development of genes signatures where target localisation is important.

The DSP platform has been widely used in the field of cancer immunotherapy. Jeyasekharan et al. used this technology to study the immune microenvironment of patients with diffuse large B-cell lymphoma who received chemotherapy.<sup>267</sup> Using a panel of 36 immune markers, they found that tumour infiltration by M2 macrophages that express CD163 and CD68 had a significant negative impact on prognosis. This result suggests the need for treatments targeting tumour-infiltrating macrophages. Toki et al. used this technology to identify biomarkers associated with response to immunotherapy in melanoma.<sup>268</sup> They searched for biomarkers in a cohort of 60 immunotherapy-treated melanoma patients by measuring 44 immune markers in macrophages (CD68), leukocytes (CD45), and tumour compartments. They found that CD3 and CD8 expressions within the macrophage compartment were associated with better outcomes in immunotherapy-treated melanoma patients, while no clinical significance was found for CD8 expression within the CD45<sup>+</sup> compartment. This finding represents a potential new finding that needs further validation, as it suggests that CD8 close to macrophages is more important than total CD8 T cells. Another notable finding was that PD-L1 expression in macrophages, but not in melanocytes, demonstrated an association with a better response to immunotherapy.

In another example, Merritt et al. described the capability of GeoMx technology in analysing colorectal tumour tissue.<sup>269</sup> Two regions of tumour tissue were selected to assess their proteins expression, tumour cells (TC) and the tumour microenvironment (TM). The analysis revealed two distinct expression profiles with a strong enrichment of immune markers within the TM compared to TC. This enrichment of immune markers likely indicates a high prevalence of immune infiltrates within the TM. They also used GeoMx to characterise macrophages (MQ) and regions near to MQ in the inflammatory bowel disease (IBD) tissue. To identify regions containing concentrated MQ populations, they stained six different IBD tissue samples for MQ (CD68), T cells (CD3), epithelium (PanCK), and nuclei, along with the cocktail of 44 oligo-

conjugated antibodies. The profiling of MQ in IBD showed that some samples had higher expression of markers of wound healing such as CD163 and B7-H3, while other samples had higher expression of CD11c. They also identified three distinct clusters of leukocytes on the basis of proximity to MQ-enriched regions in all tissue samples; these unique clusters might participate in the dysregulated immune response of IBD. GeoMx therefore presents a potentially useful technique for analysing transplant biopsies in greater depth.

### 1.1.15 Biomarker signature for stable graft function in renal transplantation

As stated by the National Institutes of Health (NIH) Biomarker Definition Working Group, a biomarker is “a characteristic that is objectively measured and evaluated as an indicator of normal biological processes, pathogenic responses, or pharmacological responses to a therapeutic intervention”.<sup>270, 271</sup>

To date, renal function after transplantation is evaluated by measuring serum creatinine level and examining a renal biopsy using the Banff criteria,<sup>272, 273</sup> which is considered the gold standard in transplant evaluation. However, both approaches have several limitations including that elevation in serum creatinine level is not specific to the type of graft injury, and an alteration in the level might indicate acute rejection, renal artery stenosis, chronic allograft injury, or calcineurin inhibitor toxicity.<sup>274, 275</sup> Similarly, renal biopsies are invasive and cannot be performed serially. Moreover, there is a problem of subjective variation in the evaluation of biopsies by histopathologists. Therefore, advancing non-invasive, reliable, and predictive biomarkers that could help transplant clinicians to estimate the risk of graft rejection and predict graft outcomes for the transplant recipients would have potential clinical value.<sup>275</sup> These biomarkers may allow early intervention in acute rejection, and minimise the immunosuppressant drugs in a tolerogenic state, therefore reducing the risks of morbidity and promoting long-term allograft survival. These non-invasive biomarkers can be found in the peripheral blood, serum, and urine of transplant recipients,<sup>276, 277</sup> and may include gene expression, leukocyte phenotype markers, chemokines and cytokines, microRNAs, and donor-specific antibodies (DSA).

One of the earliest studies identifying the molecular signature of tolerance in the peripheral blood of renal transplant recipients was reported as part of collaborative work between a group in France (University of Nantes) and the USA (Stanford University).<sup>278</sup> In this study, they identified a set of 33 genes that could distinguish operationally tolerant renal transplant recipients from patients with allograft rejection. A downregulation of co-stimulatory signals and memory T cell allo-responses along with upregulation of many of TGF- $\beta$  regulated genes was observed in tolerant patients compared to patients with graft rejection. Another study examined cell phenotypes and transcriptional patterns in the peripheral blood of tolerant transplant patients and chronic rejection patients.<sup>279</sup> They observed a reduction in CD4<sup>+</sup>CD25<sup>hi</sup> FOXP3 transcript in chronic rejection patients in comparison to tolerant patients. Sagoo et al. searched for a tolerance signature in renal recipients with operational tolerance.<sup>280</sup> Less activated CD4<sup>+</sup> T cells were reported in the peripheral blood of tolerant transplant recipients compared to recipients undergoing chronic rejection. In addition, elevated numbers of naive and transitional B cells were observed in the peripheral blood of tolerant participants compared with those receiving immunosuppression.<sup>280, 281</sup> These results revealed an unexpected association of B cells with immune tolerance.

Other biomarkers for renal graft function include the chemokines CXCL9 and CXCL10.<sup>282</sup> These chemokines are secreted by endothelial cells and can bind to CXCR3 on the surface of activated T cells, therefore recruiting T cells to the site of inflammation.<sup>283</sup> Rabant and colleagues showed that elevated levels of urinary CXCL9 was a strong predictor of T cells-mediated rejection (TCMR), while elevation in CXCL10 showed a better performance in predicting antibody-mediated rejection (ABMR) within the first year post-transplantation.<sup>284</sup> This study suggests that low chemokine levels predict immunological tolerance.

A panel of genes and chemokines (Granzyme B, Perforin, Fas-ligand, FOXP3, CXCL10) in the peripheral blood and urine of renal transplant recipients was identified as a potential biomarker for acute rejection.<sup>285, 286, 287</sup> However, alteration in a single gene has some limitations including the lack of sensitivity and specificity. Sarwal's group developed the kSORT test (kidney solid organ response test) to assess acute rejection in renal transplant patients.<sup>288</sup> They identified 17 genes, including IFNGR1 and GZMK, to distinguish acute rejection from non-acute rejection in both adult and paediatric renal transplant recipients. This test was able to predict the acute rejection three months before the detection in renal biopsies in 64% of cases

at the time of stable graft function. However, the validation of the KSORT test has yet to be determined. Recently, Christakoudi et al. identified seven genes signatures, including IFNG, IP-10, ITGA4, MARCH8, RORc, SEMA7A, and WDR40A, which were associated with cellular-mediated rejection.<sup>289</sup> These genes were elevated in the peripheral blood before histological diagnosis and decreased after immunosuppression treatment. However, further studies are needed to assess the specificity and sensitivity of the identified biomarker.

### Hypothesis and aims of the project

The use of immunosuppressants has led to a significant improvement in the short-term graft survival in organ transplantation. However, the toxicity of life-long use of immunosuppressive agents and chronic graft rejection hinder long-term graft survival. Therefore, the investigation of cellular therapies that promote graft survival without over-suppressing the immune system is of great importance.

Treg therapy has shown promise in maintaining graft survival and permitting a reduction of immunosuppressive drugs in early clinical trials of solid organ transplantation. One of the strategies to using Tregs in clinical transplantation is to isolate Tregs from a prospective transplant recipient, expand them *ex vivo* polyclonally under a good manufacturing practice (GMP), and then reintroduce them in to the recipient after transplantation.<sup>290, 291</sup> The adoptive transfer of *ex vivo*-expanded Tregs may suppress the T effector cells that might otherwise cause graft rejection. Tregs may also exploit their natural suppressive mechanisms and induce a tolerogenic phenotype on other T cells, a process known as infectious tolerance.<sup>292</sup> In addition, Tregs may possibly regulate other immune cells, which can also suppress allogeneic immune responses.<sup>97, 293</sup> An understanding of alterations in the immune compartment following Tregs therapy is important. Therefore, the immune monitoring of transplant recipients receiving advanced cellular therapy might be able to determine whether the infusion of Tregs modifies the cellular makeup and activation status towards a tolerance phenotype.

While progress has been made in isolating and generating polyclonally-expanded Tregs, the theoretical risk that polyclonally-reactive Tregs may cause over-immunosuppression still remains. Alloantigen-reactive Tregs have shown the potential to induce tolerance to only

specific undesired immuneresponses. Research on Treg cellular therapy is therefore now focusing on the development of strategies to isolate and expand alloantigen-reactive Tregs.

### 1.1.16 Hypotheses

Given previous studies showing the superiority and specificity of alloantigen-reactive Tregs,<sup>294, 295, 296, 297</sup> more allo-specific Tregs are likely to be preferable in terms of both off-target effects and immunological effects. The major challenge is their low precursor frequency and the need for repeated allostimulation as well as the subsequent selection of those that are alloreactive. We therefore hypothesised that **antigen-reactive Tregs may be expanded and subsequently isolated through the use of activation markers CD137.**

Early phase trials of polyTregs have provided a solid grounding for conducting a trial of a cell therapy in transplantation.<sup>100, 248, 298</sup> However, the identification of Treg efficacy has been more challenging. Therefore, understanding the impact of Treg therapeutics *in vivo* is necessary. We therefore hypothesised that **immunophenotyping will provide an insight about the immune status of transplant recipients receiving Treg cellular therapy.**

Moreover, assessing and identifying cells present in the biopsies of renal transplant patients to understand the mechanisms of tolerance or acute and chronic rejection is important. We hypothesised that **in-depth examination of leukocytes that have infiltrated the transplant tissue by spatial profiling will provide in depth leukocyte phenotyping that facilitates the identification of mechanistic markers of the immune response.**

### 1.1.17 Aims

- To develop a simple and effective method to isolate and expand functional human arTregs (Chapter 3).
- To explore the functionality and specificity of arTregs (Chapter 3).
- To develop a method for the assessment of alloantigen-reactive Tregs. (Chapter 3).
- To implement a clinically-based flow cytometric and mass cytometry (CyTOF) protocol for assessment of the immune phenotype of peripheral leukocytes in patients receiving Treg cellular therapy (Chapter 4).
- To investigate the phenotypic and functional changes in peripheral Tregs after cellular therapy using mass cytometry (CyTOF) (Chapter 4).
- To explore the application of Digital Spatial Profiling technology in analysing cellular infiltrates in renal biopsies (Chapter 5).

## Chapter 2: Materials and methods

### 2.1 Isolation and in vitro culture of human leukocytes from healthy donors

#### 2.1.1 Human participants/ethics

Peripheral blood mononuclear cells (PBMCs) were isolated from blood cones obtained from healthy donors (NHS Blood and transplant {NHSBT} UK). Ethical approval for research using PBMCs was obtained from the Oxfordshire Research Ethics Committee (REC B), study number 07/H0605/130.

#### 2.1.2 Isolation of PBMCs by density gradient centrifugation

PBMCs were isolated from blood cones using a lymphocyte separation medium (LSM), (25-072-CV, Corning) for density gradient centrifugation at 2200rpm, at room temperature, for 30mins. Buffy coats were collected and washed with PBS buffer. Erythrocytes were lysed by incubating the PBMCs for 5mins in PharmLyse lysing buffer (BD biosciences, Franklin Lakes, NJ, USA). PBMCs were counted and subsequently used in PBMCs-based assays or cryopreserved for later use.

#### 2.1.3 Generation of human monocytes-derived dendritic cells (moDCs)

CD14<sup>+</sup> monocytes were isolated from PBMCs using MACS microbeads and columns (Magnetic Cell Separation, Miltenyi Biotec). PBMCs were incubated with CD14 microbeads (130-050-201, Miltenyi Biotec) for 15mins at 4°C, and isolated following Miltenyi protocol. CD14<sup>+</sup> enriched cells were incubated for 5 days in 6 well plates at 1x10<sup>6</sup> cells/ml in the presence of 100 U/ml IL-4 (200-4, Peprotech) and 50ng/ml GM-CSF (300-3, Peprotech) in a complete media RPMI supplemented with 10% Foetal Calf Serum (FCS) (heat-inactivated for 20 min at 56°C). Incubations were performed at 37°C, 5% CO<sub>2</sub> and > 80% humidity. After 5 days of incubation, monocytes-derived DCs (moDCs) were harvested, then cryopreserved and stored in liquid nitrogen for later use. To check their phenotypes, aliquots of cells were stained with viability dye 7-AAD (eBioscience), anti-CD11c APC (BD Biosciences), anti-CD86 PE (BD Biosciences), anti-CD83 PeCy7 (eBioscience), anti-CD80 FITC (BD Biosciences), anti-HLA-DR ECD (Beckman Coulter), anti-CD14 APC-Cy7 (BD Biosciences), and anti-CD3 eF450 (eBioscience). Cells were incubated for 20-30mins at 4°C in the dark, then washed in PBS or

FACS buffer to remove unbound antibodies. Cells were fixed in 200µl of 1% paraformaldehyde (PFA) and acquired using a BD FACS Canto II (BD Biosciences).

#### 2.1.4 Human Treg flow sorting method

PBMCs were isolated from blood cones by density gradient centrifugation using a lymphocyte separation medium (25-072-CV, Corning). CD25<sup>+</sup> cells were isolated from PBMCs by incubating PBMCs with Miltenyi CD25 microbeads (130-092-983, Miltenyi Biotec, Bergisch Gladbach, Germany), for 15mins at 4°C, cell suspension was washed and applied to Miltenyi LS column on a MACS magnet (Miltenyi), following the manufacturer's protocol. CD25<sup>+</sup> cells were stained with 7-aminoactinomycin D (7AAD) viability dye (00-6993, eBioscience), anti-CD4 PE-eFluor 647 (eBioscience), anti-CD25 PE-Cy7 (BD Biosciences), anti-CD127 PE (BD Biosciences) and anti-CD8 APC-Cy7(BD Biosciences). Cells were incubated for 30mins at 4°C, then washed in MACS buffer to remove unbound antibodies. Cells were resuspended in complete RPMI, and filtered using sterile green filter (BD). Then, CD4<sup>+</sup>CD25<sup>+</sup>CD127<sup>low</sup> Treg cells were FACS-sorted from CD25<sup>+</sup>-enriched PBMCs by BD FACSAria II cell sorter (BD). Cells were sorted to greater than 94% purity and subsequently expanded *in vitro* either polyclonally or by allo-stimulation.

#### 2.1.5 *In vitro* expansion of human polyclonal Tregs

The Treg expansion was performed according to established protocols<sup>299</sup>. Sorted Tregs (1x10<sup>5</sup> Treg/well) were cultured with Dynabeads Human T-activator anti-CD3/anti-CD28 beads (11132D, Thermo Fisher Scientific, MA, USA) at a cell-to-bead ratio of 1:3 in expansion medium. Expansion medium consisted of RPMI 1640 media (R0883, Sigma-Aldrich Co Ltd) supplemented with 100U/ml penicillin and 10mg/ml streptomycin (P4333, Sigma-Aldrich), L-glutamine (G7513, Sigma-Aldrich), sodium pyruvate (11360-070, Sigma-Aldrich), 10% of human pooled serum (S-101, Life Science Production) heat-inactivated for 20mins at 56°C, and Recombinant human IL-2 (rhIL-2) (Proleukin, Novartis Pharmaceuticals, Frimley, UK) was added to the medium at a concentration of 1000U/ml. Every two days cultures were split and a fresh medium was added. On day 7 or 8 Tregs were collected, beads were removed, and cells were counted and re-stimulated with beads at 1:1 Tregs to beads ratio. Every two days cultures were split and a fresh medium was added if necessary. On day 14 cultures were collected, beads were removed and cells were counted then rested for 48hrs in complete media supplemented with 200U/ml of rhIL-2. After resting, expanded cells were harvested,

counted and cryopreserved for later use.

### **2.1.6 *In vitro* expansion of human arTregs**

Sorted Tregs ( $1 \times 10^5$  Treg/well) were resuspended in 100  $\mu$ l in 10% of human serum expansion medium with 1000U/ml of rhIL-2 and cultured with irradiated allo immature DCs (iDCs) at 4:1 Treg:iDCs ratio in a round-bottomed 96-well plate (giving  $1 \times 10^5$  Tregs +  $2.5 \times 10^4$  allo-DCs per well). Cell cultures were examined daily. On day 4 or 5 cells were split and fed with irradiated allo-iDCs (primary stimulator) at the same ratio used before. If the cells proliferated rapidly, cells were split every day and topped up with medium containing rhIL-2, and cells were fed with allogeneic iDCs only when needed. If the cells proliferated slowly, cells were split every second day. On day 10, cells were collected, counted, and resuspended to give a final concentration of  $0.5 \times 10^6$  cells/500  $\mu$ l. Cells were plated in a 24-well plate and re-stimulated with irradiated allo-iDCs (4:1 ratio). Expansion medium was adjusted to have 1ml/well. Cells continued to be split when needed. On day 15, Treg culture was collected, counted, and restimulated polyclonally with Dynabeads Human T-activator anti-CD3/anti-CD28 beads (11132D, Thermo Fisher Scientific, MA, USA) at 1:1 bead:cell ratio. Cells were split and the medium was added when needed. On day 21, cultures were collected, beads were removed, and cells were counted and rested for 48hrs in the presence of 200U/ml of rhIL-2. After resting, expanded cells were harvested, counted and cryopreserved for later use.

### **2.1.7 CD137(4-1BB) expression time course**

After allo-stimulation of expanded Tregs, aliquots of cells were stained with viability dye 7-AAD (eBioscience), anti-CD137 PE (BD Biosciences), and anti-CD4 PE-Cy7 (BD Biosciences), on days 4, 5, 6, 8 and 11 of culture. The expression of CD137 by Tregs was analysed by flow cytometry.

### 2.1.8 CD137 enrichment of *in vitro* expanded arTregs

On day 6, after allostimulation of Tregs, CD137<sup>+</sup> cells were isolated from the culture and stained with anti-CD137 PE, followed by incubation with anti-PE Microbeads (Miltenyi Biotec). Cells were enriched according to the beads manufacturer's protocol. CD137<sup>+</sup> Tregs and CD137<sup>neg</sup> Tregs were cultured in a 96-well plate in the expansion medium with 1000U/ml of rhIL-2 and restimulated with irradiated allogeneic iDCs, from the same donor used in the first week of Tregs expansion (primary stimulator) at 4:1 Treg:iDCs ratio. Every three days cells were split and allo-iDCs were added if necessary. On day 14, CD137<sup>+</sup> Tregs and CD137<sup>neg</sup> were collected, counted and restimulated polyclonally with Dynabeads Human T-activator anti-CD3/anti-CD28 beads at a bead:cell ratio of 1:1. On day 21, cultures were collected, beads were removed, and cells were counted and rested for 48hrs in the presence of 200U/ml of rhIL-2. After resting, cells were harvested, counted and cryopreserved for later use.

### 2.1.9 Cryopreservation and thawing of human leukocytes

Cells were resuspended in a freezing medium composed of 45% RPMI, 45% Foetal Calf Serum(FCS), 10% DMSO at 50-100x10<sup>6</sup>cell/mL for PBMCs or 2-10x10<sup>6</sup>/mL for Tregs. Cells were frozen in 2ml cryovials as 500µl aliquots in freezing boxes at -80°C for 48 hours, before being transferred to liquid nitrogen (-160°) for long-term storage. For thawing cells, frozen vials were transferred to -80°C for at least one hour before thawing at 37°C. Thawed cells were immediately washed in 10ml RPMI, added dropwise.

## 2.2 In vitro functional assays

### 2.2.2 CD137/CD154 assay

To examine the expression of CD137 and CD154 by Tregs and T conventional cells, 2µL of FcR binding inhibitor (BD Bioscience) was added to 10<sup>7</sup> PBMCs. Cells were incubated for 15mins at 4-8°C, then washed in MACS buffer. Cells were centrifuged at 300xg for 10mins and resuspended in MACS buffer. CD4<sup>+</sup> T cells were isolated from PBMCs of Donor (A) using MACS CD4 microbeads (Cat:130-045-101, Miltenyi Biotec) following the Miltenyi protocol. CD19<sup>+</sup> cells were isolated from PBMCs of donor (B) using MACS CD19 microbeads (Cat:130-050-301,

Miltenyi Biotec) following the Miltenyi protocol. The purity of isolated CD4<sup>+</sup> T cells and CD19<sup>+</sup> cells was checked by BD FACS Canto II, and was found to be over 95%. CD4<sup>+</sup> T cells were plated at  $2 \times 10^5$  with  $2 \times 10^5$  of CD19<sup>+</sup> cells in a 96-well plate in a complete media. Anti-CD40 (BioXCell, Clone:G28.5, Cat:BE0189) and anti-CD28 (BD Biosciences, Cat:555725) were added to the cultures. Then cells were incubated at 37°C for 16 hours. CD4<sup>+</sup> T cells were cultured alone as a negative control. CD4<sup>+</sup> T cells were cultured with autologous CD4<sup>neg</sup> T cells and stimulated by SEB (Superantigen, Sigma:S-4881), and were used as a positive control. All experimental conditions were performed in 3-4 replicates. After incubation, cells were collected, washed, and stained with anti-CD4 PE-Cy7 (BD Biosciences), anti-CD3 APC-H7 (BD Biosciences), anti-FOXP3 Alexa-Fluor488 (eBiosciences), anti-Helios Alexa-Fluor647 (Biolegend), anti-CD19 PE-CF594 (BD Biosciences), anti-CD137 PE (BD Biosciences) and anti-CD154 Brilliant-Violet421 (Biolegend). Cells were incubated for 20-30mins at 4°C in the dark, then washed in PBS or FACS buffer to remove unbound antibodies. Cells were fixed in 200µl of 1% paraformaldehyde (PFA), acquired using a BD FACS Canto II (BD Biosciences), and analysed using FlowJo software. For this assay leukocytes were cultured in complete medium, composed of RPMI 1640 media (R0883, Sigma-Aldrich Co Ltd) supplemented with 100U/ml penicillin and 10mg/ml streptomycin (P4333, Sigma-Aldrich), L-glutamine (G7513, Sigma-Aldrich) and 10% Foetal Calf Serum (FCS) (heat-inactivated for 20mins at 56°C).

### **2.2.2 *In vitro* suppression assay driven by allogenic or third party immature dendritic cells (iDCs)**

To assess Tregs' suppressive capacity, autologous PBMCs (responders) were plated at  $1 \times 10^5$  with  $2 \times 10^4$  irradiated allogeneic iDCs, from the same donor used in the Tregs expansion (primary stimulator) or irrelevant third party stimulator and co-cultured with a decreasing number of Tregs in a 96-well sterile cell culture plate. Cells were incubated for 7 days; incubation was performed at 37°C, 5% CO<sub>2</sub> and > 80% humidity. Responders cultured alone were used as a negative control for proliferation. Responders cultured with allogeneic iDCs were used as a positive control for proliferation. <sup>3</sup>H-thymidine (Perkin Elmer) was added for the last 16-18 hours of the 7 days of incubation. 18-24 hours later, plates were harvested with a Skatron cell harvester onto labelled filter paper (PerkinElmer). The filter paper was allowed to dry in a drying oven for 2 hours at 60°C before being placed into a laminated cover with scintillation buffer and the thymidine incorporation into proliferating cells was measured

using a beta-scintillation counter (BD). All experimental conditions were done in 4-6 replications. Results were obtained from the beta-plate counter as cpm (counts per minute) and normalized to the positive control, with positive control values set up as maximum (100%) proliferation and all other values re-calculated accordingly. Cpm values over 10,000 for positive control were required to classify the test as passing quality control for proliferation. The <sup>3</sup>H-thymidine assay was selected to assess Tregs' suppressive capacity as it has been demonstrated enhanced sensitivity in detecting cell proliferation over VPD-based cell proliferation assay using FACS.

### **2.3. Flow cytometry analysis**

Flow cytometric data were acquired using BD FACSAria II or BD canto II (BD Biosciences, UK) and analysed using FlowJo software (FlowJo Enterprise, USA). Automated flow cytometry calibration was performed before all assays to ensure that the beads' mean fluorescence intensity falls within the correct target range for each laser in the instrument. Colour compensation was performed to eliminate the spectral overlap or spill over. A live-dead dye 7-AAD (eBioscience) was used to limit the analysis to live cells and exclude dead cells from the analysis. All fluorochrome-coupled mAbs used in this project are listed in Table 2-2.

#### **2.3.1 Cell surface staining**

Cells were washed using PBS or FACS buffer, then plated onto 96-well v-bottomed plates at  $1 \times 10^5$  cells per well. Then, appropriate fluorochrome-conjugated Ab mAbs were added to the cells and incubated for 20-30mins at 4°C in the dark. Cells were washed in PBS or FACS buffer to remove unbound antibodies. All washes were performed by adding PBS or FACS buffer to each well and centrifuging samples at 1500rpm for 5mins at 4°C, then tipping off the supernatant. After washing, cells were fixed in 200µl of 1% paraformaldehyde (PFA) before flow cytometry analysis in a FACS Canto II instrument (BD). The viability dye 7-AAD (eBioscience) was used in all flow cytometry assays to determine the live population. Unstained and fluorescence minus one (FMO) controls were used as a control to permit accurate gating of positive and negative populations during flow cytometry analysis.

### 2.3.2 Intracellular immunostaining

Cells were stained for the surface markers as described above. Cells were fixed and permeabilised using FixPerm FOXP3 staining buffer (eBiosciences, UK, 00-5523-00) for 1 hour or overnight at 4°C following manufacturer's guidelines. Cells were washed twice with Perm buffer (eBiosciences, UK, 00-5523-00). 2% mouse or rat serum (eBioscience) was added to the cells for 15mins at 4°C. Cells were stained with antibodies at 1-2µL per well or appropriate fluorescence minus one (FMO) control and washed out after 45mins incubation at 4°C in the dark. Cells were subsequently washed and fixed in 1%PFA as for cell surface staining (section 2.3.1)

### 2.3.3 Intracellular cytokine staining

Frozen poly-expanded Tregs and arTregs were thawed and stimulated with Dynabeads Human T-activator anti-CD3/anti-CD28 beads at a cell-to-bead ratio of 1:1 in expansion medium with 1000U/ml rhIL-2 for 3-4 days. After stimulation, expanded polyTregs and arTregs were collected, beads were removed, and cells were stimulated with 100 ng/ml phorbol myristate acetate (PMA) (P1585, Sigma Aldrich), 1µg/ml Ionomycin (1063, Sigma Aldrich), and 1µl/ml Golgi protein inhibitor (55029, BD Biosciences or 00-4505-51, eBioscience) for 5 hours at 37°C. Cells were washed, stained, and permeabilised using FOXP3 staining kit (eBioscience) as described in section 2.3.2. Cells were stained with IL-17 PE and IFN-γ FITC (eBioscience) for 45mins at 4°C in the dark. Cells were then washed and resuspended in 1%PFA. The expression of IL-17 and IFN-γ were assessed by flow cytometry.

### 2.3.4 TCR Vβ repertoire staining

T cell receptor diversity of alloantigen and poly-expanded Tregs was assessed at the Vβ level by flow cytometry using the IOTest Beta Mark TCR Vβ Repertoire kit (Beckman Coulter, PN IM3497). The kit consists of fluorochrome conjugated monoclonal antibodies that identify the following TCR-Vβ chains: Vβ1, Vβ2, Vβ3, Vβ4, Vβ5.1, Vβ5.2, Vβ5.3, Vβ7.1, Vβ7.2, Vβ8, Vβ9, Vβ11, Vβ12, Vβ13.1, Vβ13.2, Vβ13.6, Vβ14, Vβ16, Vβ17, Vβ18, Vβ20, Vβ21.3, Vβ22, Vβ23.

These 24 V $\beta$  chains cover 70% of the T-lymphocyte TCR-V $\beta$  repertoire in a normal individual. Expanded arTregs and polyTregs were washed by FACS buffer, then plated onto 96-well v-bottomed plates at  $1 \times 10^5$  cells per well. Cells were stained with viability dye 7-AAD (eBioscience), anti-CD4 PE-Cy7, and eight V $\beta$  antibody cocktails according to manufacturer's instructions. Cells were washed in FACS buffer and resuspended in 200 $\mu$ l of 1%PFA. The frequency of each of the targeted V $\beta$  specificities was assessed by BD Canto II (BD Biosciences, UK) and analysed using FlowJo software.

## **2.4. Analysis of the immune monitoring clinical samples from the cell therapy trials (ONE Study and TWO Study)**

### **2.4.1 Study design and approvals**

The ONE Study (REC ref: 13/SC/0568, Eudract number 2013-002099-42) and The TWO Study (REC ref: 18/SC/0054, Eudract number 2017-001421-41) were both approved by the South Central – Oxford A Research Ethics Committee. All procedures followed were in accordance with the ethical standards of the responsible committee on human experimentation. Informed consent was obtained for all subjects. Majority of assays were performed using the TWO Study samples; Treg panel CyTOF staining and Digital Spatial Profiling of kidney biopsies were performed on samples from the ONE Study. Briefly, the ONE Study was a multicentre, international study investigating immunoregulatory cell-based therapies in living donor kidney transplantation. The UK part (Oxford and London) of the study investigated autologous regulatory T cell product (1-10 million cells/kg) infused 5 days post renal transplantation, with treatment with prednisolone, mycophenolate mofetil, and tacrolimus.<sup>300</sup> The TWO Study is a single centre randomised-controlled phase II trial of autologous poly-expanded Tregs in renal transplant patients. Living donor renal transplant recipients are randomised either to the cell therapy arm or to standard of care immunosuppression. A schematic of the clinical protocol is shown in (Chapter 4, Figure 4.1). Immunosuppression used included the use of induction antibody therapy in the form of alemtuzumab (Campath). Recipients enrolled in the cell therapy arm received autologous polyTregs (infused at 6 months post-transplantation) in conjunction with tacrolimus as a maintenance immunosuppression. Recipients enrolled in the control arm received MMF and Tacrolimus. The follow-up in the trial is scheduled for 78 weeks post-transplantation. PBMC samples from the TWO study have been analysed by flow

cytometry (see Chapter 2.4.3) and CyTOF (see Chapter 2.5.1) for composition of the immune cell populations. Beads enriched CD4<sup>+</sup> T cells from the ONE Study have been analysed for Treg-focused CyTOF panel to assess Treg subpopulations in vivo (see Chapter 2.5.2); kidney biopsies from the ONE Study have been analysed by the Digital Spatial Profiling (GeoMx, NanoString) to access cellular composition of the graft immune infiltrates (see Chapter 2.6).

#### **2.4.2 Sampling for immune-monitoring**

Peripheral blood was collected from eligible patients in Oxford Transplant Centre, Churchill Hospital, Oxford (UK) following the ethical guidelines. Blood samples were collected in sodium-EDTA vacutainer tubes. The collected products were sent to our lab, TRIG lab (Transplantation Research and Immunology Group), for immediate immune-phenotyping staining and analysis.

#### **2.4.3 Staining of unfractionated blood using DuraClone antibody cocktail tubes**

Fresh blood was stained for various markers in tubes containing dry or liquid antibodies cocktails (DuraClone panels, Beckman Coulter). DuraClone panels are designed to include markers for T cell subsets, B cell subsets, Tregs, monocytes. Additionally, a custom panel to detect T follicular helper cells (Tfh) has been designed. Table 2-3 shows the list of markers in each panel. 50 or 100 µl of fresh blood was added into each of the following tubes: Basic, IM TCR, IM T cell subset, IM Treg and IM B cell tube. The surface and intracellular staining were performed according to the manufacturer's protocols. Cell pellets were suspended in PBS containing IO fixation solution. The frequency of leukocytes was assessed by Navios flow cytometer (Beckman Coulter) and analysed using Kaluza 1.2 software (Beckman Coulter).

**Table 0-1: TWO Study Monitoring visits decoded with time**

V02	V04	V05	V07	V08	V09	V10	V11	V12	V13	V17	V18	V19
Pre-transplant	Weeks post transplant											
2-4	4	12	22	24	26	27	28	30	38	44	52	72

## 2.5. Single cell analysis by mass cytometry (CyTOF)

All surface and intracellular antibodies and their heavy metal conjugates used in this project are listed in Tables 2-4 and 2-5.

### 2.5.1 Cell surface staining of peripheral blood for mass cytometry

All buffers, reagents and antibodies labelled with metal-tag which used in this section were purchased from Fluidigm, unless otherwise stated. Heparin sodium salt was diluted as a 10 KU/ml stock in PBS and stored at 4°C. Then 10µL of 10KU/ml heparin was added to 600µL of whole blood to block Fc receptors of cells. This was followed by incubation with a surface marker staining cocktail for 30mins at 4°C. Erythrocytes were lysed by incubating the stained blood in 2ml of Gibco™ ACK Lysing buffer for 2-3mins at room temperature. Cells were washed by Maxpar cell staining buffer several times to remove unbound antibodies. Cells were fixed in 1.6% formaldehyde solution. After fixation, cells were cryopreserved in a freezing medium composed of 45% FSC, 45% RPMI, and 10% DMSO for 48 hours at -80°C, then transferred to liquid nitrogen for a later run. For CyTOF data acquisition, samples were transferred frozen to the Mass Cytometry Facility at the Kennedy Institute of Rheumatology to be acquired on a third-generation Helios mass cytometer (Fluidigm). Samples were thawed and cells were washed twice in MaxPar staining buffer and stored in 1 ml of MaxPar Fix and Perm Buffer containing 125 nM MaxPar Intercalator-Ir (<sup>191</sup>Ir and <sup>193</sup>Ir) at 4°C. After 12 hours, cells were

washed in MaxPar staining buffer and re-suspended in MaxPar water containing 10% EQ™ four element calibration beads, followed by acquisition on third-generation Helios mass cytometer (Fluidigm). Acquired raw FCS files were normalised with the preloaded normaliser algorithm on CyTOF software version 6.7. Normalized CyTOF FCS files were analysed using Cytobank 6.2 (Cytobank, Inc) to manually gate different populations. To minimise the batch effect, samples were stained, cryopreserved then thawed and acquired by CyTOF in one or two batches over two sequential days. CyTOF data acquisition was performed by Dr David Ahern at the Kennedy Institute, University of Oxford. In this study, the CyTOF was adjusted to run the lysed whole blood samples at rate 250 events/sec.

### **2.2.3 Cell surface and intracellular staining of CD4<sup>+</sup> T cells for mass cytometry using dedicated Tregs panel**

Peripheral blood mononuclear cells (PBMCs) were isolated and cryopreserved from ONE Study (six renal transplant patients) who received a single dose of up to  $10 \times 10^6$ /kg autologous polyclonally-expanded Tregs shortly after transplantation, followed by standard maintenance immunosuppression. PBMCs were collected at three different time-points (V01, pre-transplantation; V03, 2 weeks post-transplantation; and V10, 60 weeks post-transplantation). CD4<sup>+</sup> cells were isolated by MACS and multiplexed for processing by cytometry time of flight mass spectrometry (CyTOF). Cell staining and CyTOF data acquisition were performed by Dr David Ahern at the Kennedy Institute, University of Oxford. The phenotype and composition of peripheral Tregs were examined using a dedicated 36-antigen panel (Table 2-5).

### **2.5.2 Mass cytometry analysis**

FCS files from CyTOF were normalised with calibration beads by Helios software. Then manual gating of FCS files was performed using the Cytobank platform. Calibration beads and cell aggregates were excluded through the manual gating, then the population of interest was gated and exported in a new FCS file. CD45<sup>+</sup> CD66b<sup>+/-</sup> populations were used for visualization stochastic neighbour embedding algorithm (viSNE) analysis using default settings and all markers were selected to visualize their phenotypic expression. FCS files of CD45<sup>+</sup> CD66b<sup>+/-</sup>

populations were exported from Cytobank and submitted to the “cytofkit” R package to generate Rphenograph. Resulting clusters were imported back into Cytobank for further examination and detection of spurious clusters. All the markers (CD markers, chemokines, and transcription factors) were used for the generation of viSNE maps. Heatmaps were performed by the Cytobank platform to show the median expression of individual cellular markers expressed in all clusters identified previously by Rphenograph. The statistical differences of marker expressions were analysed in GraphPad Prism software using the unpaired test.  $p < 0.05$  was considered significant.

## **2.6. GeoMx Digital spatial profiling (DSP)**

All antibodies used in this project are listed in Tables 2-5.

### **2.6.1 Tissue processing**

Kidney Biopsies obtained from three patients from ONE Study, and two patients with confirmed rejection from biobank. Kidney tissues were obtained at 9 months post transplantation. Tissue were fixed in formalin then paraffin-embedded. The (FFPE) tissue sections on slides were sent to NanoString technologies, Seattle, USA to perform the technique. A schematic of the DSP technique is shown in (Chapter 5, Figure 5.1). FFPE tissue sections on slides were stained with four-colour fluorescence of CD4 , CD3 , FOXP3, nuclei, and a mix of 43 oligo-conjugated antibodies. Tissue sections were loaded into the GeoMx platform and scanned for immunofluorescence signals. The regions of interest (ROIs) that represented a spectrum of immune composition were selected by a nephrologist, Dr Matthew Brook, for detailed proteins profiling.

### **2.2.2 DSP analysis, optimisation and visualization**

Quality control and initial data exploration was conducted using GeoMx DSP analysis suite. The assay included a set of six positive (POS-A to POS-F) and six negative (NEG-A to NEG-F) hybridization control probes to measure hybridization efficiency, and ensure the quality of the performed assay. Geomean probes combined to generate a single (post biological probe QC) expression value per protein target per ROIs. Digital counts from barcodes corresponding to

protein probes were first normalized to internal spike-in controls (ERCC) to account for system variation. The Histone (H3) and (S6) ribosomal protein were included in the panel as housekeeper proteins. The normalised housekeeping counts were calculated by multiplying the ERCC count with normalization factor of housekeeping proteins. The normalised housekeeping counts were used for the clustered heatmaps and principal component analysis which were created in Qlucore Omics Explorer version 3.7. The Qlucore normalize the housekeeping counts and scaled the data from -2 to 2 to generate the heatmap. The exact P value was mentioned in the figure legend of each analysis. To compare the expression level of proteins between cell therapy and rejection across the sampled regions we used house keeping count normalized by CD3 counts to effectively compare the proteins' expression between the different regions. For volcano plots, The p-value, fold change, negative log<sub>10</sub> p-value and log<sub>10</sub> fold change of proteins in rejection and cell therapy were calculated by R Studio using the ggplot2 package <sup>301</sup>, and graphs were performed in Prism version 8.0.2.

### 3.3 Data analysis and statistics

Graphs were produced and statistical analysis was performed using Graph Prism software version 7 or 8 (GraphPad Software, San Diego, CA, USA). Statistical analysis was determined as indicated in the figure legends. (SD) standard deviation is represented in the graphs with data from multiple donors, when each data point displays the data of one donor, or in graphs showing replicate samples from one representative donor. The standard error of mean (SEM) is used in graphs with data from multiple donors, with each data point showing the average of replicates for each donor. Functional assays were set up with at least three replicates for each condition or sample. Unpaired tests were used to compare between cell populations, paired tests were used when comparing a specific cell population over time and p values under 0.05 were considered significant.

### 3.4 Lists of antibodies

All antibodies for flow cytometry are reactive against human antigens, unless otherwise stated.

*Table 0-2: Flow cytometry antibodies*

Antigen	Fluorochrome	Clone	Species of origin	Supplier	Catalog number
4-1BB	PE	4B4-1	mouse	BD Biosciences	555956
CD154	BV 421	24-31	mouse	Biolegend	310823
FOXP3	FITC	PCH101	rat	eBioscience	11-4776
Helios	Alexa Fluor 647	22F6	hamster	Biolegend	137218
CD19	PE-CF594	HIB19	mouse	BD Biosciences	562294
CD4	PE-Cy7	SK3	mouse	BD Biosciences	557852
CD3	APC-Cy7	SK7	mouse	BD Biosciences	560176
CD3	eFluor 450	OKT3	mouse	eBioscience	48-0037
CD14	APC-Cy7	M $\phi$ P9	mouse	BD Biosciences	557831
HLA-DR	ECD	Immu-357	mouse	Beckman Coulter	IM3636
CD83	PE-Cy7	HB15e	mouse	eBiosciences	25-0839
CD86	PE	2331	mouse	BD Biosciences	555858
CD80	FITC	L307.4	mouse	BD Biosciences	557226
CD11c	APC	B-ly6	mouse	BD Biosciences	559877

<b>CD4</b>	PeFluor 610	RPA-T4	mouse	eBioscience	61-0049-42
<b>CD25</b>	PE-Cy7	M-A251	mouse	BD Biosciences	557741
<b>CD25</b>	APC-Cy7	M-A251	mouse	BD Biosciences	557753
<b>CD127</b>	PE	HIL-7R-M21	mouse	BD Biosciences	557938
<b>CD8</b>	APC-Cy7	SK1	mouse	BD Biosciences	557834
<b>ICOS</b>	FITC	ISA-3	mouse	eBioscience	11-9948
<b>PD-1</b>	FITC	EH12.2H7	mouse	Biolegend	329904
<b>CTLA-4</b>	PE	BN13	mouse	BD Biosciences	555853
<b>CD39</b>	PE	eBioA1	mouse	eBioscience	12-0399-42
<b>Ki67</b>	Alexa Fluor 647	B56	mouse	BD Biosciences	558615
<b>TIGIT</b>	PE	MBSA43	mouse	eBioscience	12-9500
<b>CD27</b>	eFluor 450	O323	mouse	eBioscience	40-0279
<b>IL-17A</b>	PE	eBio4CAP17	mouse	eBioscience	12-7178
<b>IFN-<math>\gamma</math></b>	FITC	4S.B3	mouse	eBioscience	11-7319

**Table 0-3: Flow cytometry panels for clinical trial (TWO Study) immune phenotyping DURAcclone panels (basic phenotype, B cells, TCR, T cell subsets, Treg) and in-house design (Tfh).**

Fluorochrome	FITC	PE	EDC	PC5.5	PC7	APC	APC- AF700	APC- AF750	Pacific blue	Krome orange
<b>Basic Phenotype</b>	CD16	CD56	CD19	-	CD14	CD4	CD8	CD3	-	CD45
<b>B cell</b>	IgD	CD21	CD19	-	CD27	CD24	-	CD38	IgM	CD45
<b>TCR</b>	TCR $\gamma\delta$	TCR $\alpha\beta$	HLA- DR	-	TCR- VD1	CD4	CD8	CD3	TCR VD2	CD45
<b>T cell subsets</b>	CD45RA	CCR7	CD28	PD-1	CD27	CD4	CD8	CD3	CD57	CD45
<b>Treg</b>	CD45RA	CD25	-	CD39	CD4	FOXP3	-	CD3	Helios	CD45
<b>Tfh</b>	CD45RO	CXCR5	CXCR3	PD-1	CCR6	ICOS	CD25	CD3	FOXP3	CD45

**Table 0-4: Metal-conjugated antibodies provided in the Human Immune Monitoring Panel Kit designed by Fluidigm for CyTOF mass cytometry**

Antigen	Clone	Mass	Catalog number
CD45	(HI30)	89Y	S3089003C
CD19	(HIB19)	142Nd	S3142001C
CD127/IL-7Ra	(A019D5)	143Nd	S3143012C
CD38	(HIT2)	144Nd	S3144014C
IgD	(IA6-2)	146Nd	S3146005C
CD11c	(Bu15)	147Sm	S3147008C
CD16	(3G8)	148Nd	S3148004C
CD194/CCR4	(L291H4)	149Sm	S3149029C
CD123/IL-3R	(6H6)	151Eu	S3151001C

TCRgd	(11F2)	152Sm	S3152008C
CD185/CXCR5	(RF8B2)	153Eu	S3153020C
CD3	(UCHT1)	154Sm	S3154003C
CD45RA	(HI100)	155Gd	S3155011C
CD27	(L128)	158Gd	S3158010C
CD28	(CD28.2)	160Gd	S3160003C
CD66b	(80H3)	162Dy	S3162023C
CD183/CXCR3	(G025H7)	163Dy	S3163004C
CD161	(HP-3G10)	164Dy	S3164009C
CD45RO	(UCHL1)	165Ho	S3165011C
CD24	(ML5)	166Er	S3166007C
CD197/CCR7	(G043H7)	167Er	S3167009C
CD8	(SK1)	168Er	S3168002C
CD25	(2A3)	169Tm	S3169003C
CD20	(2H7)	171Yb	S3171012C
HLA-DR	(L243)	173Yb	S3173005C
CD4	(SK3)	174Yb	S3174004C
CD56	(NCAM16.2)	176Yb	S3176008C
CD196/CCR6	(G034E3)	141Pr	S3141003C
CD14	(M5E2)	175Lu	S3175015C

**Table 0-5: Metal-conjugated antibodies used for surface and intracellular staining of Tregs for CyTOF mass cytometry analysis**

<b>Antigen</b>	<b>Mass</b>	<b>Antigen</b>	<b>Mass</b>
CLA	176Yb	CD45RA	143Nd
ICOS	148Nd	CD95	152Sm
CCR4	158Gd	FOXP3	162Dy
GATA3	167Er	CTLA-4	171Yb
CD45	89Y	CD38	144Nd
CD127	149Sm	TIGIT	153Eu
CD7	147Sm	CD15s	163Dy
CD73	168Er	Ki-67	172Yb
CCR6	141Pr	CD4	145Nd
OX40	150Nd	CD3	154Sm
CD39	160Gd	CD161	164Dy
CD25	169Tm	CD137	173Yb
CD57	142Nd	CD8	146Nd
CD103	151Eu	CD27	155Gd
TBET	161Dy	LAG3	165Ho
HLA-DR	170Er	PD-1	174Yb
CCR7	159Tb	HELIOS	166Er
CD147	156Gd	CD71	175Lu

**Table 0-6: Oligo-conjugated antibodies panel for multiplexed digital spatial profiling (DSP) designed by NanoString**

AKT	Beta-Catenin	CD3	CD56
B7-H3	CD11c	CD44	CD66B
B7-H4 (VTCN1)	CD14	CD45	CD68
Bcl-2	CD163	CD45RO	CD8A
Beta-2-macroglobulin	CD20	VISTA	CTLA-4
CXCL9	ICOS (CD278)	Mouse IgG	PD-L1
FOXP3	IDO-1	OX40L(CD252) TXGP1	PTEN
GZMB	IFN $\gamma$	p-ATK	Rabbit IgG
Histone H3	IL-6	PanCK	S6
HLA-DR	Ki-67	PD-1	STAT3
pSTAT3	STING (TMEM173)		

## Chapter 3: Generation and characterization of human *ex vivo*-expanded alloantigen-reactive Tregs

### 3.1 Introduction

Treg immunotherapy should ideally employ alloantigen-reactive rather than polyclonal-reactive Tregs to ensure both safety and enhanced specificity. As discussed in Chapter 1 (Section 1.5), there is evidence from animal models that alloantigen-reactive Tregs (arTregs) have enhanced therapeutic potential compared to polyTregs. Research into strategies to isolate and expand human arTregs is ongoing. The major challenges to be overcome are the low frequency of their precursors, the need for repeated allostimulation and the subsequent selection of those that are alloreactive.

There is no definitive method for determining which cells within Treg pools are alloreactive. However, some have proposed the use of Treg-specific activation markers for the selection and identification of antigen-reactive Tregs in MLR cultures. A number of Treg-specific or Treg-associated activation markers have been described, including LAP,<sup>302</sup> GARP,<sup>303, 304</sup> CD27,<sup>305</sup> CD69 and CD71,<sup>203</sup> and CD137.<sup>257</sup> CD137 (4-1BB) is a member of the tumor necrosis factor receptor family (TNFR).<sup>257</sup> Wolf et al. demonstrated that up-regulation of CD137 on CD8<sup>+</sup> T cells following an antigen encounter permits identification and isolation of antigen-specific CD8<sup>+</sup> T cells from *in vitro* culture.<sup>255</sup> In addition, Schoenbrunn et al., reported that CD137 is a suitable marker for identification of human CD4<sup>+</sup>CD25<sup>+</sup>Foxp3<sup>+</sup> Helios<sup>+</sup> Tregs following allostimulation, enabling direct access to arTregs in the cell culture.<sup>306</sup>

In a similar manner, CD154 (CD40L), a member of the TNF superfamily, serves as a marker for activated CD4<sup>+</sup> and CD8<sup>+</sup> T cells after stimulation.<sup>259, 260</sup> Quantification of memory CD8<sup>+</sup> T cells that express CD154 was assessed to evaluate the *in vivo* impact of Treg infusion on allospecific immune responses in liver transplant patients.<sup>307</sup>

In this chapter, we looked to develop a simple method for the generation and expansion of *ex vivo* human arTregs. The first aim was to examine the suppressive potential of CD137-enriched arTregs and non-enriched arTregs compared to those of polyTregs. The second aim was to study the characteristics of *ex vivo*-generated arTregs, including their phenotype and specificity, and compare them with the characteristics of polyclonal-expanded Tregs. The third aim was to develop a technique to simultaneously measure the *in vivo* presence of alloantigen-reactive Tregs and conventional T cells through the expression of CD137 and CD154. Such a technique could then be used to analyse peripheral blood samples from patients receiving Treg cell therapy to determine whether these patients develop alloantigen-reactive Tregs after cellular therapy infusion.

## 3.2 Hypotheses

**Hypothesis-1:** The isolation, generation and expansion of alloantigen-reactive Tregs is feasible.

**Hypothesis-2:** The activation markers CD137 and CD154 can discriminate between *in vivo*-activated Tregs and conventional T cells.

## 3.3 Results

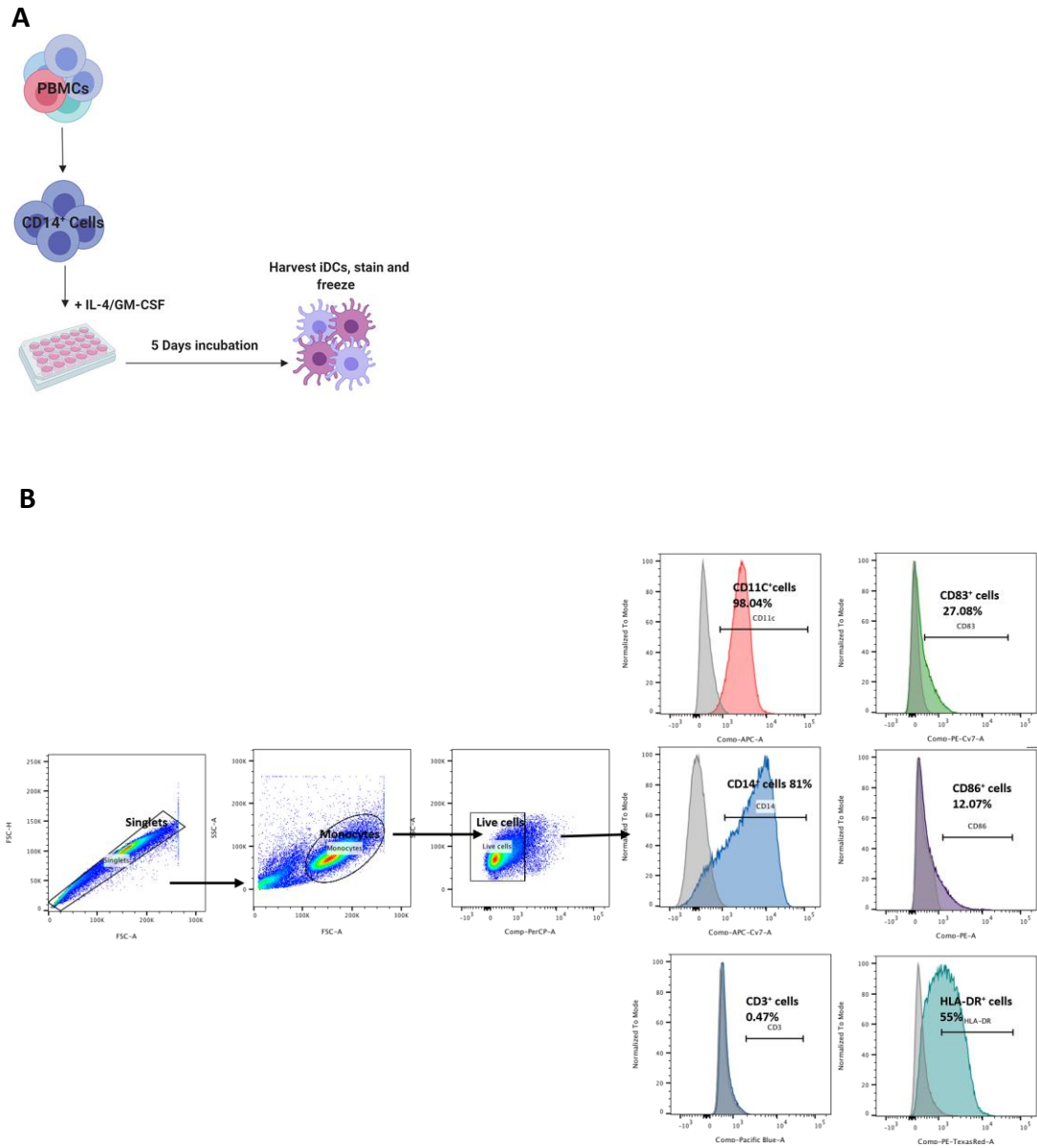
### 3.3.1. Generation of allogeneic human immature monocyte-derived dendritic cells (imDCs) for stimulation and expansion of arTregs

As discussed in Chapter 1 (Section 1.5.1), stimulators for arTreg production include PBMCs,<sup>171</sup> B cells<sup>202</sup> and DCs<sup>308</sup>. Here, imDCs were used to stimulate and expand arTregs given that the isolation and generation of allogeneic imDCs is feasible and can be translated into a GMP process. imDCs were generated by incubating CD14<sup>+</sup> mononuclear cells with IL-4 and granulocyte macrophage colony stimulating factor (GM-CSF) for 5 days, as illustrated in Figure 3.1A. After incubation, the imDCs were harvested and their phenotype was assessed. Surface expression of CD11c, CD14 and activation marker HLA-DR was analysed using flow cytometry, along with that of the costimulatory markers CD80, CD86 and CD83 on the generated imDCs. The phenotypic profile of generated immature DCs was CD11c<sup>high</sup> CD14<sup>+</sup>CD3<sup>neg</sup>CD80<sup>int-</sup>

# Chapter 3: Generation and characterization of human ex vivo-expanded alloantigen-reactive Tregs

$lowCD86^{int-low}CD83^{int-low}HLA-DR^+$  (Figure 3.1C). These imDCs were irradiated prior to use to prevent cellular contamination of the final Treg product.

**Figure 3.1**



C

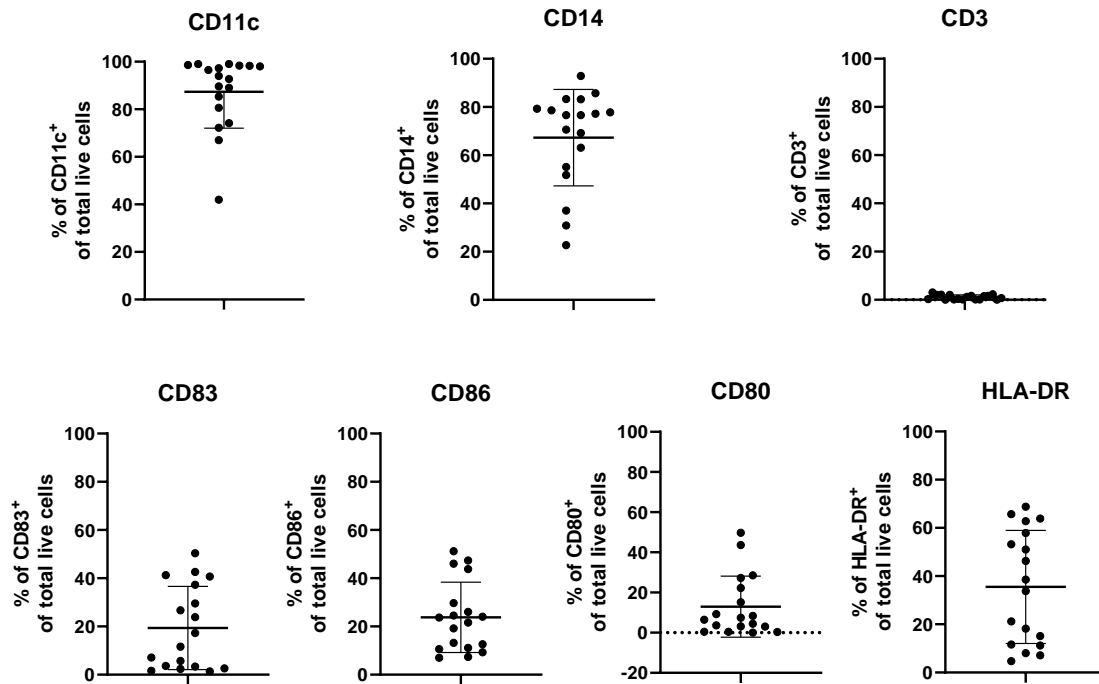


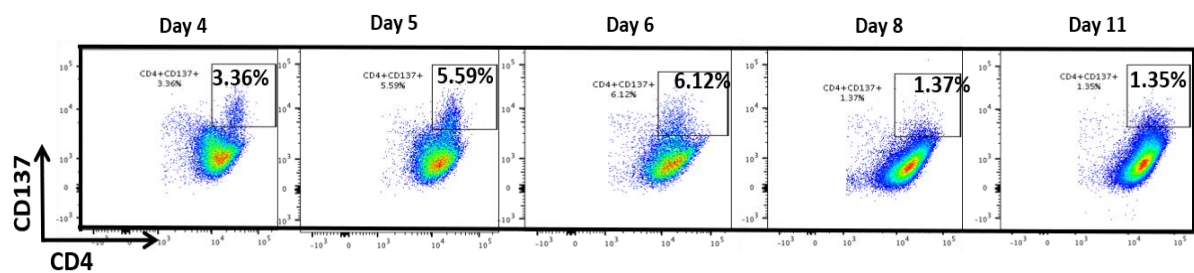
**Figure 3.1: Generation of immature monocyte-derived dendritic cells (imDCs) and phenotypic analysis. (A)** Schematic of the experimental design for isolating and generating allogeneic imDCs. **(B)** An example of a gating strategy used to assess the phenotypes of generated imDCs including FMOs (gray histograms). **(C)** The percentages of CD11c, CD14, CD3, CD83, CD86, CD80 and HLA-DR expression, analysed using flow cytometry. Error bars represent mean with SD. Data representative of six independent experiments, 18 donors in total, are shown.

### 3.3.2. CD137 expression on human Tregs is rapidly and transiently upregulated after allogeneic stimulation

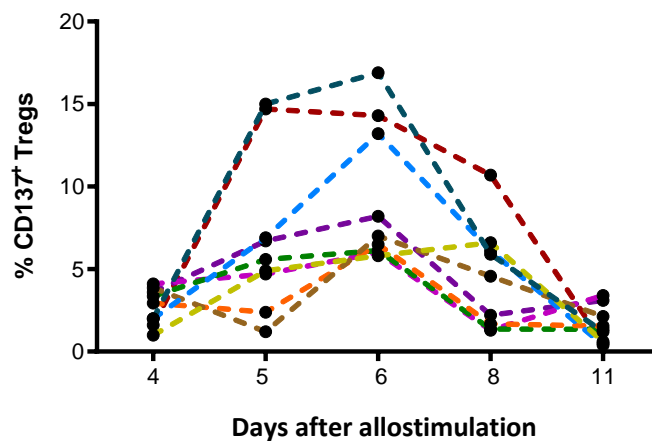
To isolate arTregs based on CD137 expression, CD4<sup>+</sup>CD25<sup>+</sup>CD127<sup>low</sup> Treg cells were flow sorted from peripheral blood of healthy donors and stimulated with irradiated allogeneic imDCs. The kinetics of CD137 expression on Tregs was monitored over 11 days after allogeneic stimulation (Figure 3.2A). CD137 expression peaked on day 6, when Tregs were stimulated with allogeneic imDCs (Figure 3.2A and B). Therefore, day 6 after allostimulation was chosen as an optimal time for CD137-assisted enrichment of arTregs.

Figure 3.2

A



B



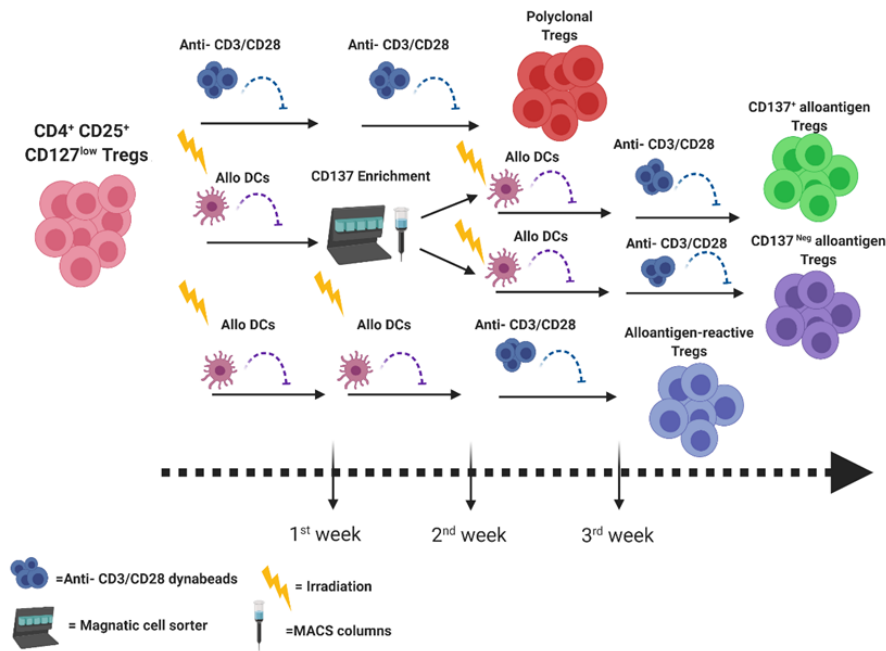
**Figure 3.2: CD137 expression upon allostimulation of Tregs.** Freshly isolated CD4<sup>+</sup>CD25<sup>+</sup>CD127<sup>low</sup> Tregs were stimulated with irradiated allogeneic imDCs at a Treg-to-imDC ratio of 4:1. Tregs were assessed for CD137 expression using flow cytometry for several days after allostimulation. **(A)** Representative FACS plots generated using samples from one donor. **(B)** Analysis of samples from several independent donors (n = 9).

### 3.3.3. Treg expansion using polyclonal or alloantigen stimulation

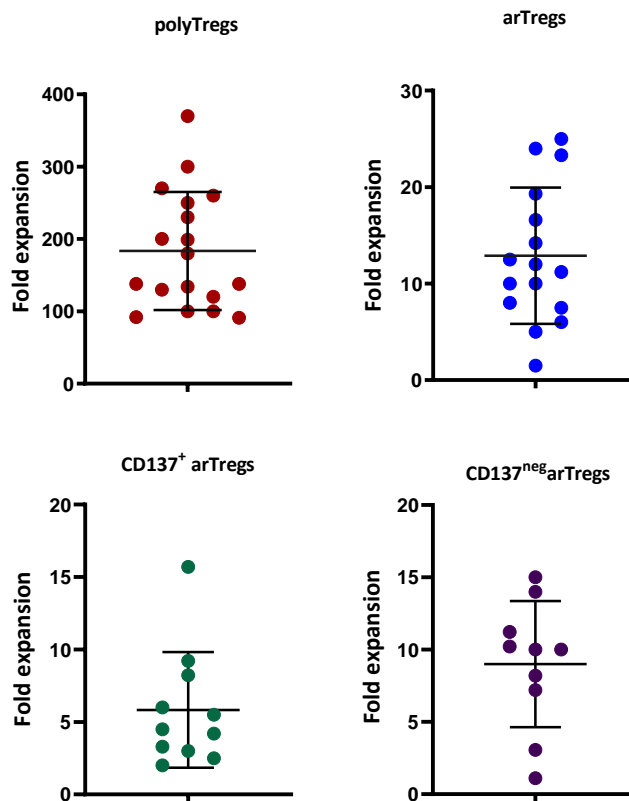
Next, we expanded Tregs using polyclonal or alloantigen-driven methods. For polyclonal Treg expansion, CD4<sup>+</sup>CD25<sup>+</sup>CD127<sup>low</sup> cells were sorted and expanded using an established protocol with  $\alpha$ CD3/ $\alpha$ CD28-coated beads and 1,000 U/ml recombinant human IL-2 for 2 weeks.<sup>185</sup> For alloantigen-reactive Treg expansion, cells were stimulated with irradiated imDCs (Treg to imDC ratio of 4:1). These cells were then enriched for CD137 and further expanded, while others were expanded without enrichment. These CD137<sup>+</sup> arTregs, non-enriched arTregs and CD137<sup>neg</sup> arTregs were divided and re-stimulated with alloantigen several times during expansion. This was followed by stimulation with  $\alpha$ CD3/ $\alpha$ CD28-coated beads for the last round of expansion, as detailed in Figure 3.3A. The extent of Treg expansion was highly variable among the different donors. As expected, polyclonal Tregs expanded 100–300-fold when stimulated with two rounds of  $\alpha$ CD3/ $\alpha$ CD28-coated beads, while arTregs with no enrichment expanded 5–25-fold with three rounds of stimulation. CD137<sup>+</sup> arTregs expanded only 2–10-fold and CD137<sup>neg</sup> arTregs expanded 4–15-fold with three rounds of stimulation (Figure 3.3A). These data highlight the challenge of obtaining high yields of arTregs for clinical application.

Figure 3.3

A



B



**Figure 3.3: Treg expansion using polyclonal or alloantigen stimulation. (A)** Experimental schematic for *in vitro* expansion of polyclonal Tregs, CD137<sup>+</sup> arTregs, CD137<sup>neg</sup> arTregs and non-enriched arTregs. PolyTregs were stimulated with  $\alpha$ CD3/ $\alpha$ CD28-coated beads and 1,000 U/ml recombinant human IL-2 for 2 weeks. Non-enriched arTregs, CD137<sup>+</sup> arTregs and CD137<sup>neg</sup> arTregs were stimulated with allogeneic irradiated imDCs at a Treg to imDC ratio of 4:1 for 2 weeks, followed by one week of bead-stimulated expansion **(B)** Extent of expansion of *in vitro*-cultured polyTregs (red), non-enriched arTregs (blue), CD137<sup>+</sup> arTregs (green) and CD137<sup>neg</sup> arTregs (purple) after the expansion period. Data from six independent experiments using samples from 10–18 donors are shown. Error bars represent mean with SD

#### 3.3.4. CD137 expression defines a population of potent alloantigen-reactive Tregs

The functional potency of expanded CD137<sup>+</sup> arTregs was then assessed. CD137<sup>+</sup> arTregs were compared with polyclonally-expanded Tregs and alloantigen-reactive Tregs that were either non-enriched, or CD137<sup>neg</sup> arTregs. Autologous PBMCs (responders) were stimulated with irradiated allogeneic iDCs, from the same donor used in the Tregs expansion (primary stimulator) and co-cultured with a decreasing number of Tregs. Responders cultured alone were used as a negative control for proliferation. Responders cultured with allogeneic iDCs were used as a positive control for proliferation. Cells were incubated for 7 days, then assessed for cell proliferation by thymidine incorporation assay. As shown in Figure 3.4A, non-enriched arTregs (*blue*) suppressed responder cell proliferation potently in comparison with polyclonal Tregs (*red*). Moreover, CD137<sup>+</sup> arTregs (*green*) were significantly more suppressive than CD137<sup>neg</sup> Tregs (*purple*) (Figure 3.4B)<sup>309</sup>. These data highlight the usefulness of CD137<sup>+</sup> as an additional marker of Tregs produced using alloantigen stimulation.

Figure 3.4

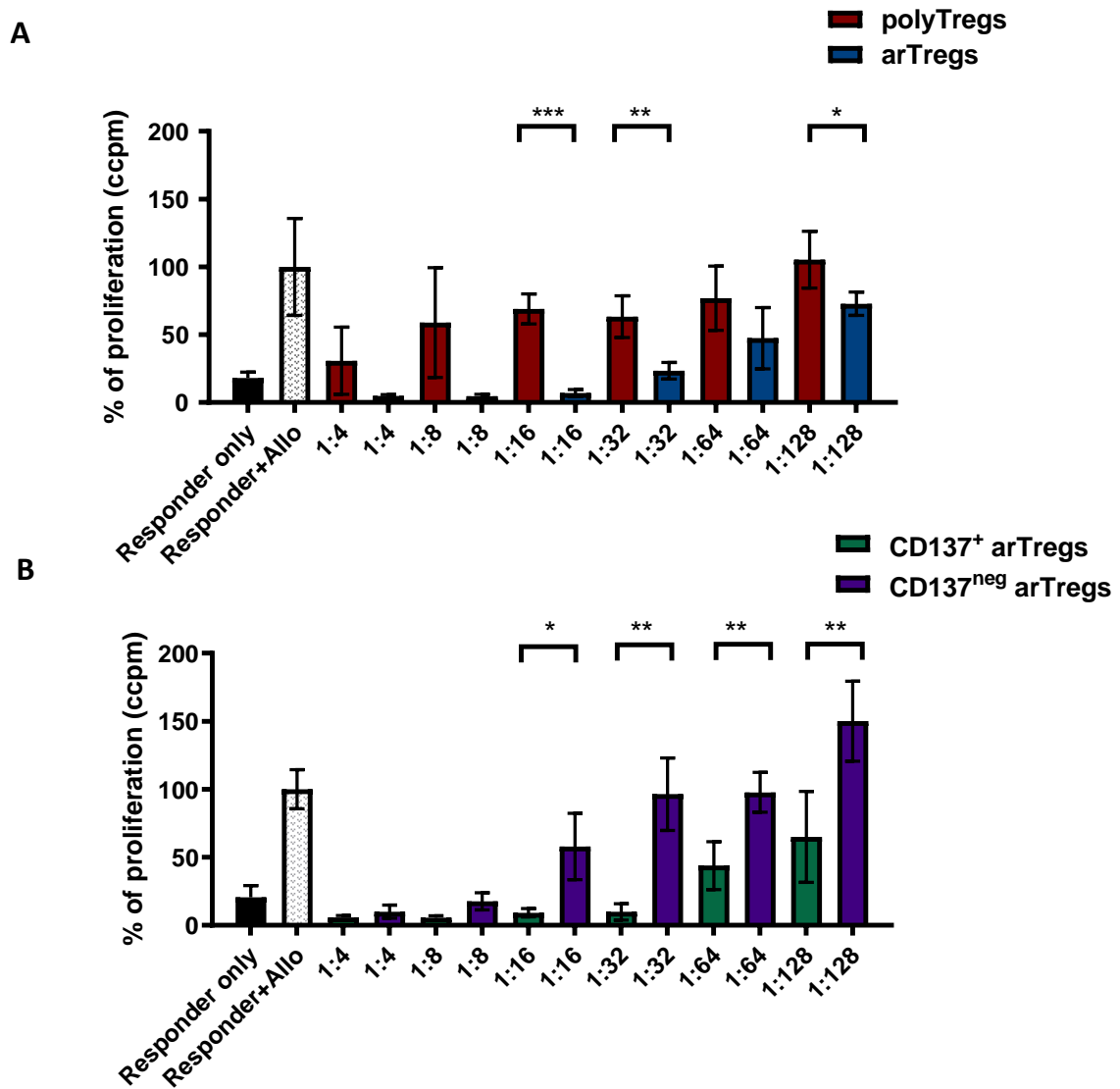


**Figure 3.4: CD137<sup>+</sup> alloantigen-expanded Tregs (green) are more suppressive than polyclonal Tregs (red), non-enriched arTregs (blue) and CD137<sup>neg</sup> alloantigen-expanded Tregs (purple).** Suppression assays were performed using <sup>3</sup>H-thymidine incorporation; responder cells were stimulated with allogeneic imDCs from the same donor as used for Treg allo-expansion. Polyclonal, non-enriched, expanded CD137<sup>+</sup> and CD137<sup>neg</sup> Tregs were titrated into the culture. Responders alone were used as a negative control. Responders with alloantigen were used as a positive control. Six days later, thymidine was added to the culture and after 16 hours of incubation, cells were harvested. Data are represented as mean +/-SD. Statistical analysis was performed using unpaired t-tests (\*p<0.05, \*\*p<0.01, \*\*\*p<0.001). Representative data from one of five donors are shown.

### 3.3.5. Expanded alloantigen-reactive Tregs maintain expression of Treg functional markers

Tregs express high levels of FOXP3, which is indispensable for their suppressive function. However, Hoffmann et al. reported that CD4<sup>+</sup>CD25<sup>+</sup>CD127<sup>low</sup> Tregs display decreased levels of FOXP3 expression after repetitive T-cell receptor (TCR) stimulation. Here, FOXP3 expression in CD137<sup>+</sup>arTregs, non-enriched and CD137<sup>neg</sup> arTregs subsets as well as polyTregs was assessed using flow cytometry. It was found that the enriched CD137<sup>+</sup> arTregs (*green*), non-enriched arTregs (*blue*), CD137<sup>neg</sup> arTregs subset (*purple*) and polyTregs (*red*) expressed high levels of FOXP3 (Figure 3.5B).

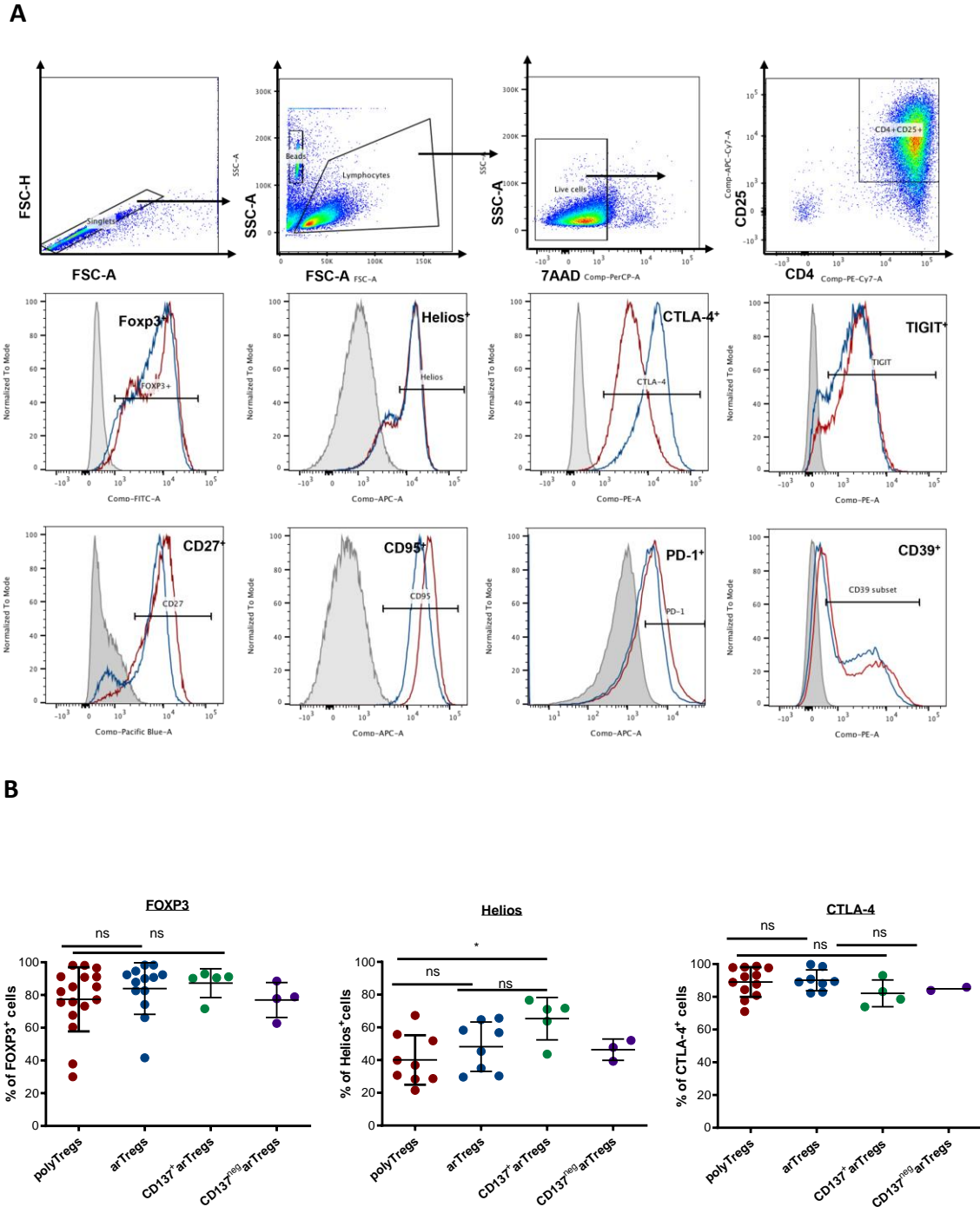
Helios was initially used as a marker to distinguish between thymic-derived Tregs (tTreg) and peripheral Tregs (pTregs).<sup>310</sup> However, later studies demonstrated that the tTreg compartment contains both Helios<sup>+</sup> and Helios<sup>neg</sup> Treg subsets.<sup>152, 311, 312</sup> Furthermore, studies using experimental models found that specific deletion of Helios from Tregs led to a delayed onset of autoimmune disease, which was associated with defects in Treg function.<sup>313, 314, 315</sup> Thus, Helios may act as a marker for stable Tregs. Interestingly, CD137<sup>+</sup> arTregs contained a higher frequency of Helios<sup>+</sup> cells after expansion compared to polyclonal Tregs (Figure 3.5B).

Cytotoxic T-lymphocytes-associated protein 4 (CTLA-4) is a coinhibitory molecule expressed by T cells, including CD4<sup>+</sup>FOXP3<sup>+</sup> Tregs.<sup>316</sup> CTLA-4 prevents the CD28-mediated activation of T cells by directly binding to CD80 and CD86 on naïve T cells or downregulating CD80 and CD86 on APCs.<sup>317, 318</sup> Studies demonstrated that specific blockade of CTLA-4 on Tregs leads to the onset of autoimmune diseases in experimental models, highlighting the requirement of CTLA-4 expression for Treg suppressive function.<sup>316, 319</sup> Here, CTLA-4 expression was found to be high in polyTregs as well as in arTregs subsets (Figure 3.5B). Expression of the co-stimulatory molecule CD27 was also assessed. This is a marker found in highly suppressive Treg subsets.<sup>192</sup> No significant differences were found in the CD27 expression between the arTregs and polyTregs (Figure 3.5C). In addition, the death receptor CD95 (Fas) showed no significant differences between arTregs and polyTregs. The co-inhibitory molecule TIGIT, a marker found on Tregs that specifically control Th1 and Th17 responses,<sup>320</sup> showed no significant differences between the arTregs and polyTregs. The CD39 and PD-1 also showed no significant differences between the arTregs and polyTregs (Figure 3.5C). Taken together, this phenotypic analysis indicates that both CD137<sup>+</sup> arTregs and non-enriched arTregs maintain the expression of

Chapter 3: Generation and characterization of human ex vivo-expanded alloantigen-reactive Tregs

specific and functional Treg markers after expansion. However, the sample size is small, and it would be valuable to validate the findings in more donors.

Figure 3.5



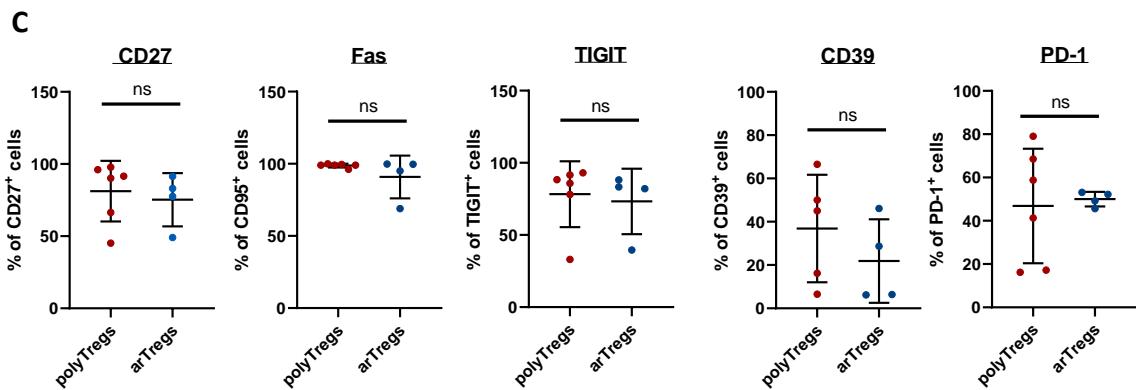


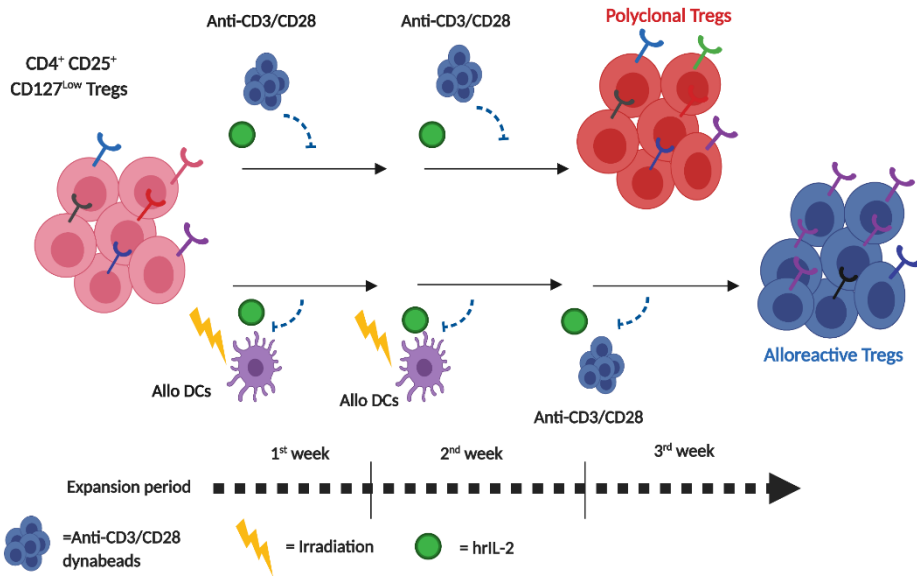
**Figure 3.5: Expression of cell surface molecules in polyTregs and arTregs by flow cytometry.** (A) An example of a gating strategy used to assess the phenotypes of polyTregs (red histogram), arTregs (blue histogram) and FMOs (gray histogram). (B) Expression of FOXP3, Helios and CTLA-4 in polyTregs (red), non-enriched arTregs (blue), CD137<sup>+</sup> arTregs (green) and CD137<sup>neg</sup> arTregs (purple). Dots represent individual blood donors and error bars represent mean with SD, One-way ANOVA with Tukey's was used for multiple comparisons, \*p<0.05, ns = not significant. (C) Expression of CD27, CD95 (Fas), TIGIT, CD39 and PD-1 in polyTregs (red) and non-enriched arTregs (blue). Statistical significance was assessed by unpaired t-test. ns = not significant.

### 3.3.6. Alloantigen-reactive Tregs are more suppressive than polyclonally expanded Tregs and demonstrate enhanced specific antigen reactivity

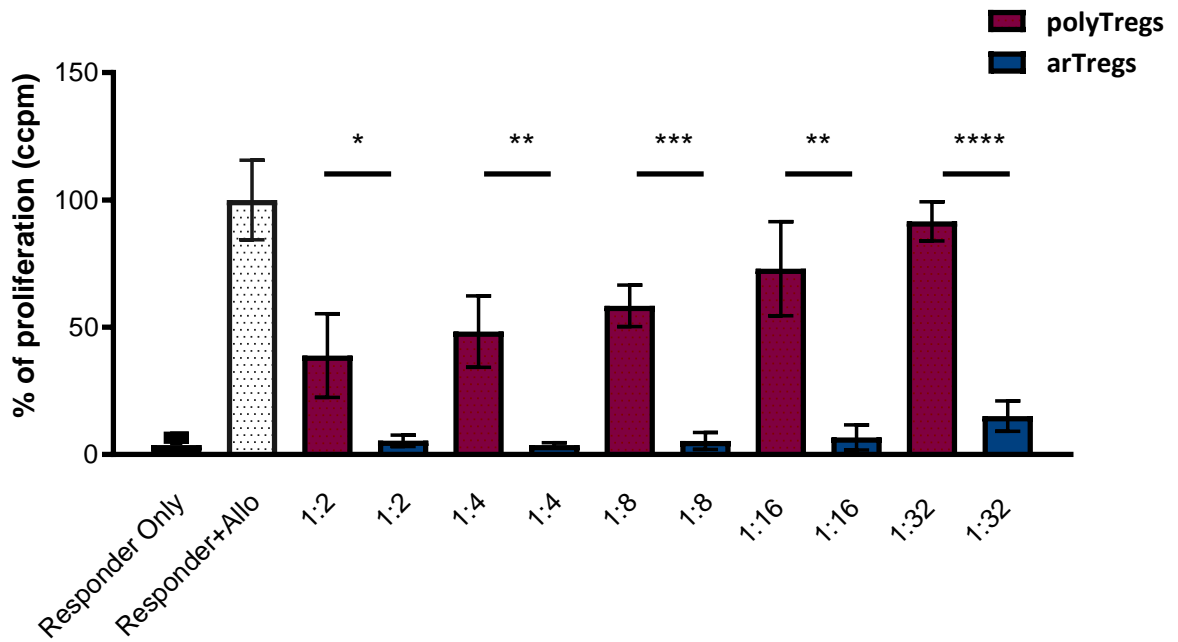
Although CD137 is a good marker for enriching alloantigen-activated Tregs, the yield using this technique is very low, making it unsuitable for clinical translation. Therefore, we aimed to expand non-enriched arTregs and study their functionality. For expansion, CD4<sup>+</sup>CD25<sup>+</sup>CD127<sup>lo</sup> Tregs were flow sorted and expanded either polyclonally (with anti-CD3/CD28 beads) for 2 weeks or by alloantigen stimulation (with irradiated allogeneic imDCs) for 2 weeks, followed by a week-long expansion with anti-CD3/CD28 beads as shown in Figure 3.6A. These expanded arTregs demonstrated a significant suppression of responder cell proliferation compared with polyclonal Tregs (Figure 3.6B). Moreover, arTregs demonstrated a much higher suppressive capacity at lower cell ratios, with more than 50% suppression preserved even at the lowest tested ratio of 1:32, whereas polyTregs started losing 50% suppression at 1:4 ratio. (Figure 3.6B). Donor specificity of the expanded arTregs was then examined and compared to arTreg suppression against other third-party stimulators. Responder PBMCs, which were autologous to the Tregs, were stimulated with irradiated imDCs from either the primary stimulator used in the generation of arTregs or a third-party irrelevant stimulator in the presence of expanded arTregs. Notably, arTregs were able to mediate specific suppression of autologous T effector proliferation in response to a primary stimulator more than irrelevant third-party stimulators (Figure 3.6C), demonstrating the antigen specificity of the expanded arTregs.

Figure 3.6

A



B



C

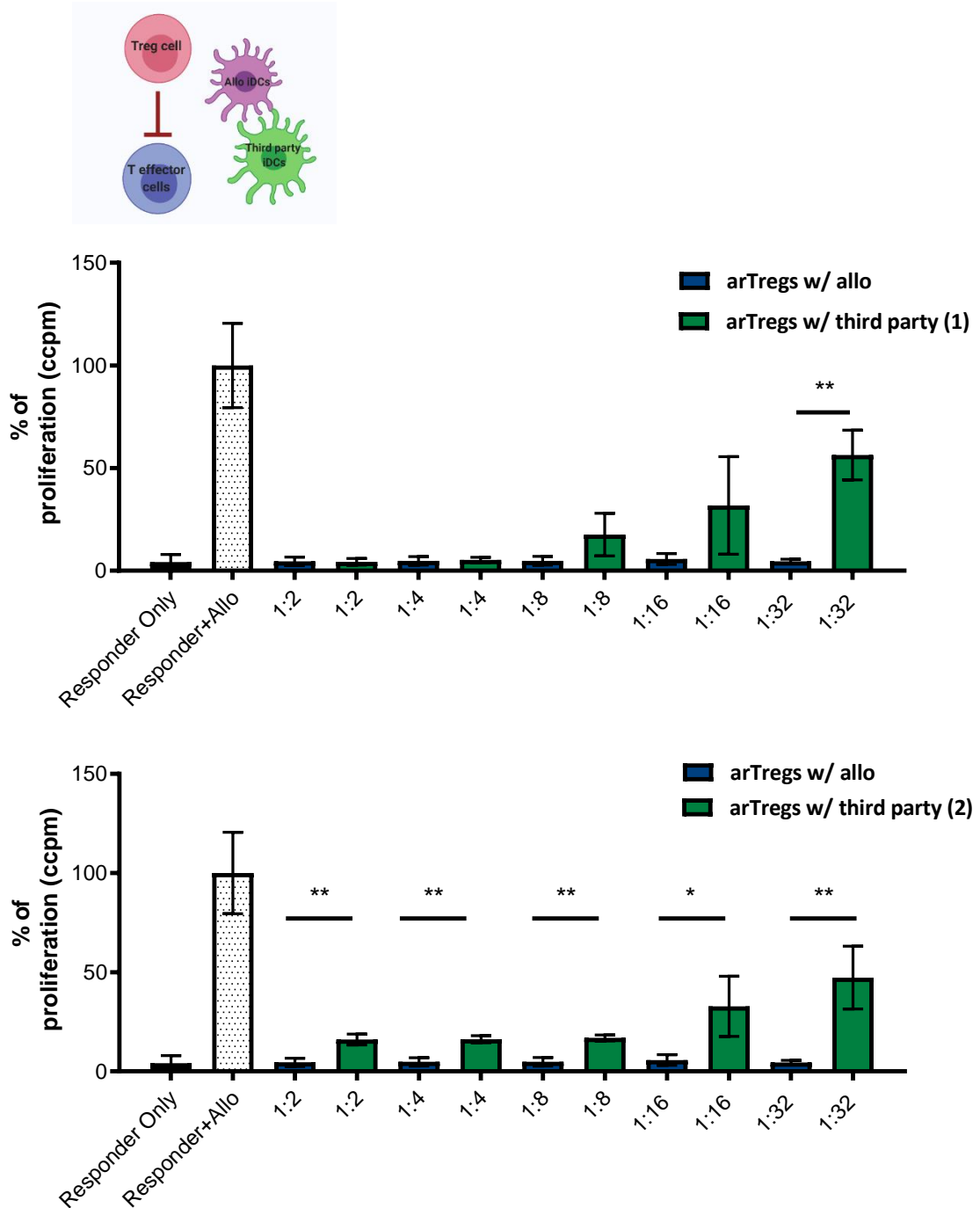


**Figure 3.6: Alloantigen-reactive Tregs are more suppressive than polyclonally expanded Tregs and demonstrate enhanced reactivity towards specific allogeneic donor cells. (A)** Schematic of experimental *in vitro* expansion of polyclonal- and alloantigen-expanded Tregs. **(B)** Suppression assays were performed using <sup>3</sup>H-thymidine incorporation; responder cells were stimulated with irradiated allogeneic iDCs. Representative data from one assay is shown. Polyclonal- and alloantigen-expanded Tregs were titrated into the culture. Responders alone were used as a negative control. Responders with alloantigen were used as a positive control. Six days later, thymidine was added to the culture and after 16 hours of incubation, cells were harvested. Data are represented as mean +/-SD. Statistical analysis was performed using unpaired t-tests (\*p<0.05, \*\*p<0.01, \*\*\*p<0.001). Representative data from one donor out of five is shown. **(C)** Suppression assays were performed using <sup>3</sup>H-thymidine incorporation; responder cells were stimulated with irradiated specific allogeneic iDCs or two different third-party irradiated imDCs (1 and 2). Data are represented as mean +/- SD. Statistical analysis was performed using unpaired t-tests (\*p<0.05, \*\*p<0.01, \*\*\*p<0.001). Data representative of three Treg donors, data from one donor are shown.

### 3.3.7. Alloantigen-reactive Tregs produce fewer inflammatory cytokines in comparison to polyclonally-expanded Tregs

Next, measurement of the levels of the inflammatory cytokines IL-17 and IFN- $\gamma$  in arTregs and polyclonally expanded Tregs was performed. After 2 weeks of expansion of polyTregs and 3 weeks of expansion of arTregs, the cells were rested for 2 days. Then polyTregs and arTregs were restimulated polyclonally with anti-CD3/CD28-coated beads (1 bead:5 cells) and rhIL-2 (250 U/ml) for 72 hours. Levels of intracellular IL-17 and IFN- $\gamma$  expression were measured by flow cytometry following Treg restimulation with PMA and ionomycin in the presence of a Golgi protein transport inhibitor. arTregs were found to produce lower level of intracellular IL-17 compared with polyclonally-expanded Tregs (Figure 3.7B). These preliminary results showed a trend of fewer proinflammatory cytokines produced by arTregs compared to polyTregs. However, the sample size is small, and it would be valuable to validate the findings in more donors.

Figure 3.7

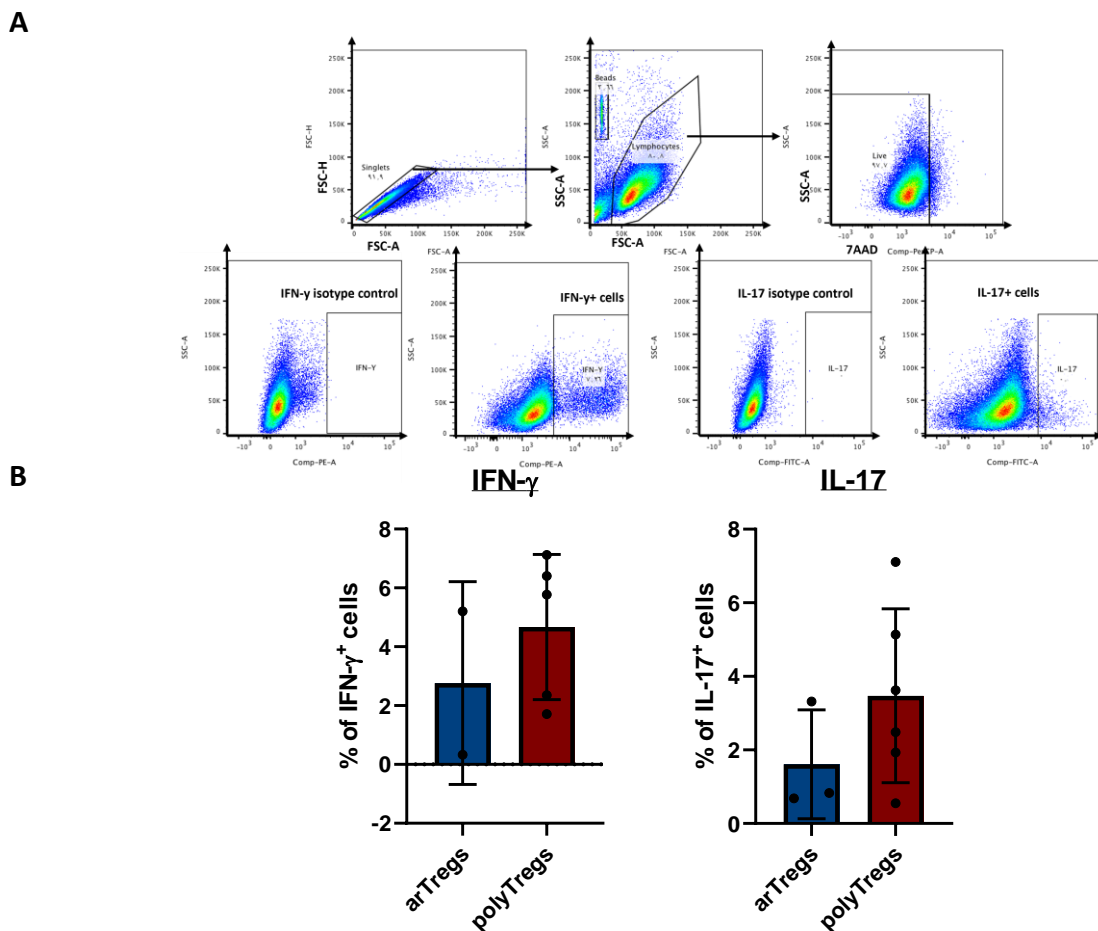


**Figure 3.7: arTregs (blue) and polyclonally expanded Tregs (red) express distinct proinflammatory cytokines.** (A) An example of a gating strategy used to assess the IL-17<sup>+</sup>,IFN- $\gamma$ <sup>+</sup> cells and isotype controls. (B) Percentage of IL-17<sup>+</sup> and IFN- $\gamma$ <sup>+</sup> cells analysed by intracellular cytokine staining in alloantigen-expanded Tregs (blue) and polyclonally expanded Tregs (red). Tregs were restimulated with phorbol myristate acetate (PMA) (100 ng/ml) and ionomycin (1  $\mu$ g/ml) in the presence of a Golgi protein inhibitor. Analysis was performed using flow cytometry. Dots represent individual donors and error bars represent mean with SD.

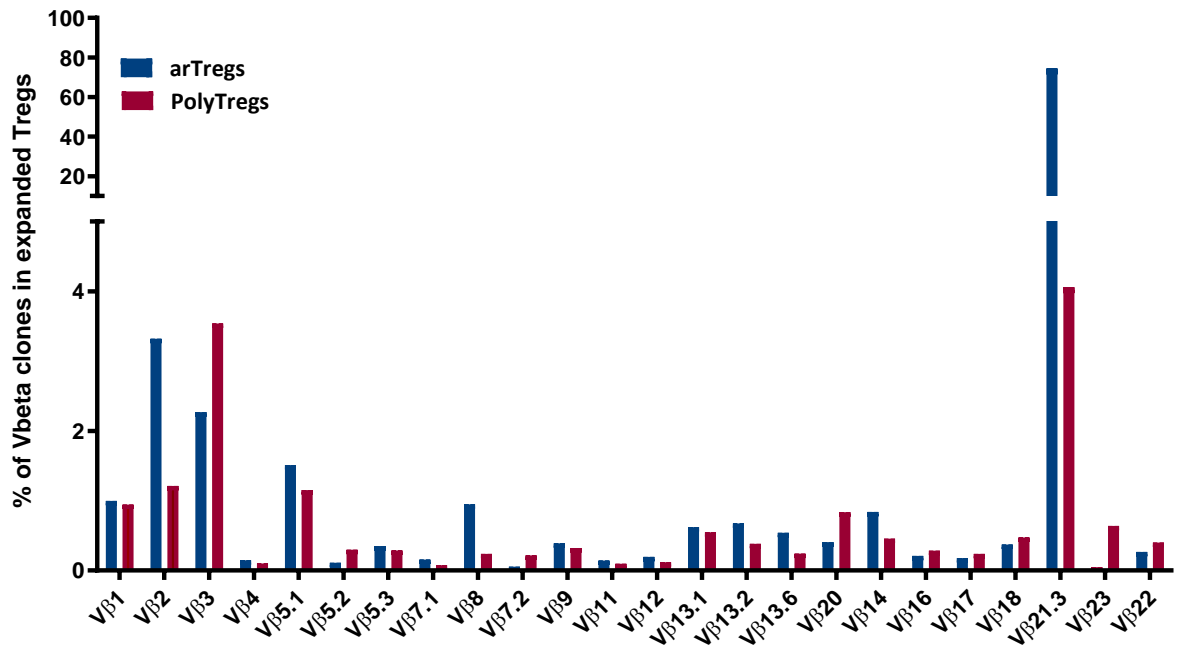
### 3.3.8. TCR repertoire analysis of alloantigen-reactive Tregs reveals restriction to several TCR beta families

The TCR is a heterodimer composed of  $\alpha$  and  $\beta$  (or  $\gamma$  and  $\delta$ ) chains located on the surface of T cells. It recognises the MHC-peptide complex presented by APCs, which leads to T-cell activation and proliferation. The TCR is formed by random recombination of TCR gene segments termed variable (V), diversity (D) and joining (J) segments.<sup>321</sup> This random recombination leads to the diversity of the TCR repertoire. The V segment of the  $\beta$  chain contains three highly diverse loops, termed complementarity determining regions (CDR1, CDR2 and CDR3), that make direct contact with the antigen. The CDR3 is encoded by the region spanning the V and J or the V, D and J segments—unlike CDR1 and CDR2, which are encoded within the V gene segment portion of the V region gene. Therefore, CDR3 is more diverse than CDR1 and CDR2.<sup>322</sup>

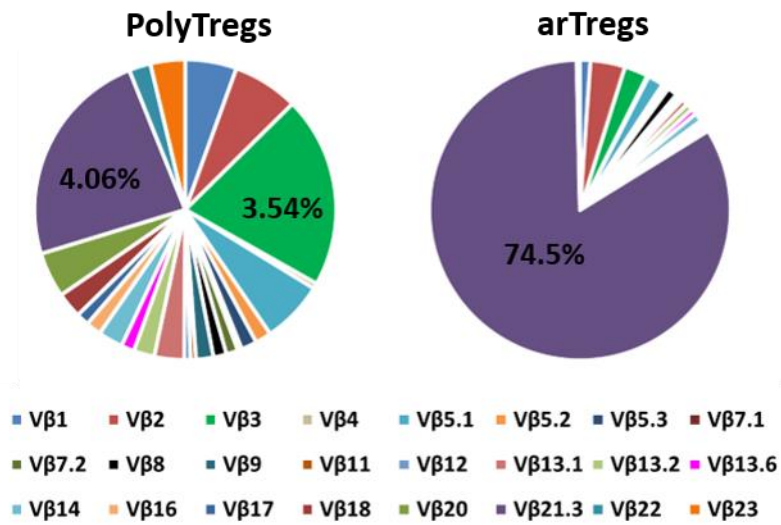
Analysis of TCR V $\beta$  will help to elucidate the repertoire narrowing that might occur when arTregs are stimulated with alloantigen. Therefore, the TCR V $\beta$  of arTregs and polyTregs was profiled at the end of the expansion period by immunophenotyping 24 distinct V $\beta$  chain families. These families cover approximately 70% of the human TCR V $\beta$  repertoire in normal individuals. As shown in Figures 3.8 A and B, polyTregs were found to express all 24 V $\beta$  chains, indicating clonal diversity in their TCR repertoire. The frequencies of V $\beta$ 3 and V $\beta$  21.3 segments were higher than other segments, representing around 3.54% and 4.06% of polyTregs, respectively. In contrast, arTregs showed an oligoclonal expansion of the V $\beta$  21.3 TCR family, representing around 74.5% of their TCR repertoire, in contrast with a low frequency of the other V $\beta$  chains. The exact frequencies of TCR V $\beta$  segments detected in the expanded polyTregs and arTregs are listed in Figure 3.8C. Taken together, TCR repertoire analysis results demonstrated narrowing of the repertoire to several clones in arTregs.

Figure 3.8

A



B



C

Vβ type	PolyTregs	ArTregs	Vβ type	PolyTregs	ArTregs
Vβ1	0.944	0.996	Vβ12	0.117	0.196
Vβ2	1.21	3.32	Vβ13.1	0.547	0.622
Vβ3	3.54	2.27	Vβ13.2	0.383	0.673
Vβ4	0.099	0.147	Vβ13.6	0.241	0.538
Vβ5.1	1.15	1.51	Vβ14	0.457	0.838
Vβ5.2	0.296	0.111	Vβ16	0.282	0.208
Vβ5.3	0.287	0.35	Vβ17	0.236	0.177
Vβ7.1	0.0769	0.156	Vβ18	0.472	0.371
Vβ7.2	0.217	0.0551	Vβ20	0.836	0.405
Vβ8	0.239	0.949	Vβ21.3	4.06	74.5
Vβ9	0.321	0.389	Vβ22	0.4	0.265
Vβ11	0.098	0.143	Vβ23	0.639	0.046

**Figure 3.8: The TCR repertoire analysis of alloantigen- and polyclonally-expanded Tregs.** PolyTregs and arTregs were analysed for Vβ profile using flow cytometry and a IOTest Beta Mark TCR Vβ Repertoire Kit. **(A)** The frequencies of Vβ families in the expanded polyTregs (*red*) and arTregs (*blue*). **(B)** Pie charts illustrating the diverse distribution of TCR clonotypes in the expanded polyTregs and arTregs. **(C)** Exact values (%) of the 24 TCR Vβ families detected in the expanded polyTregs and arTregs. Data representative of one donor.

### 3.3.9. Expression of CD137 and CD154 discriminates between activated Tregs and conventional T cells ex vivo

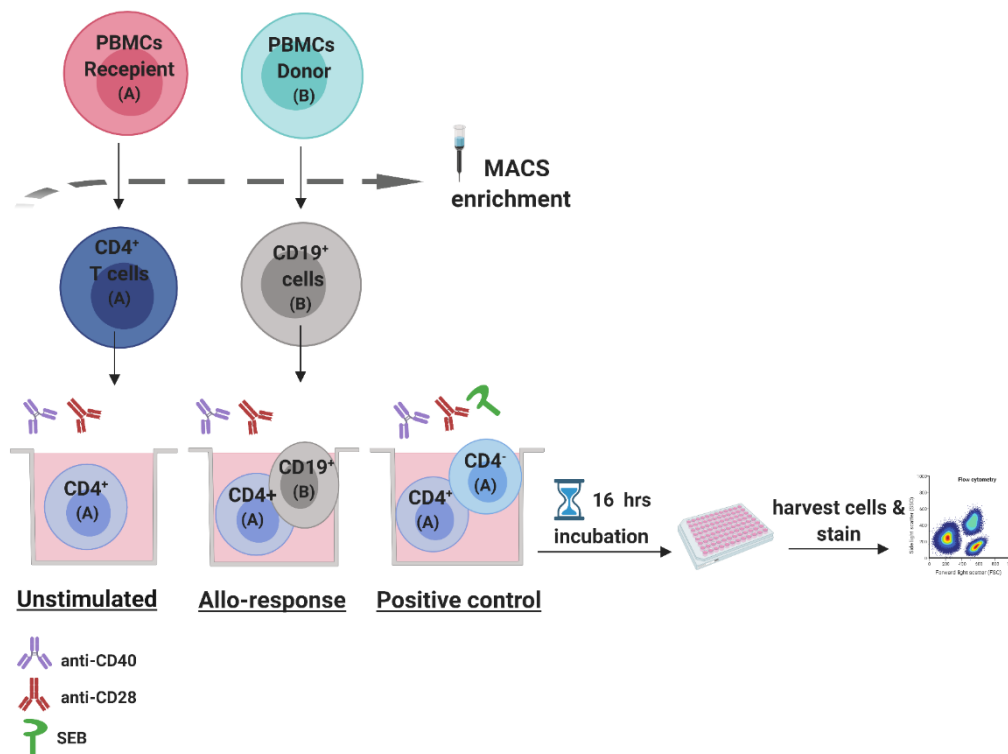
Development of donor-specific hypo-responsiveness is a specific defining feature of tolerance. A study in liver transplantation by Sanchez-Fueyo et al. examined the impact of Treg infusion on alloreactive T cell responses in recipient PBMCs after infusion; here there was a reduction in CD154 upregulation in memory CD8<sup>+</sup> T cells after allostimulation only in recipients who received 4.5 x 10<sup>6</sup> Treg/kg.<sup>307</sup> This suggests development of hypo-responsiveness after Treg infusion. It is also important to measure *in vivo* alloreactive Tregs, along with alloreactive T cells, after Treg infusion. Given that CD137 was found to be upregulated rapidly after allogeneic stimulation and selecting CD137 positive Tregs results in potent arTregs, it was hypothesised that CD137/CD154 differential expression can define the *in vivo* arTregs and conventional alloantigen-reactive T cells (arTcons).

### Chapter 3: Generation and characterization of human ex vivo-expanded alloantigen-reactive Tregs

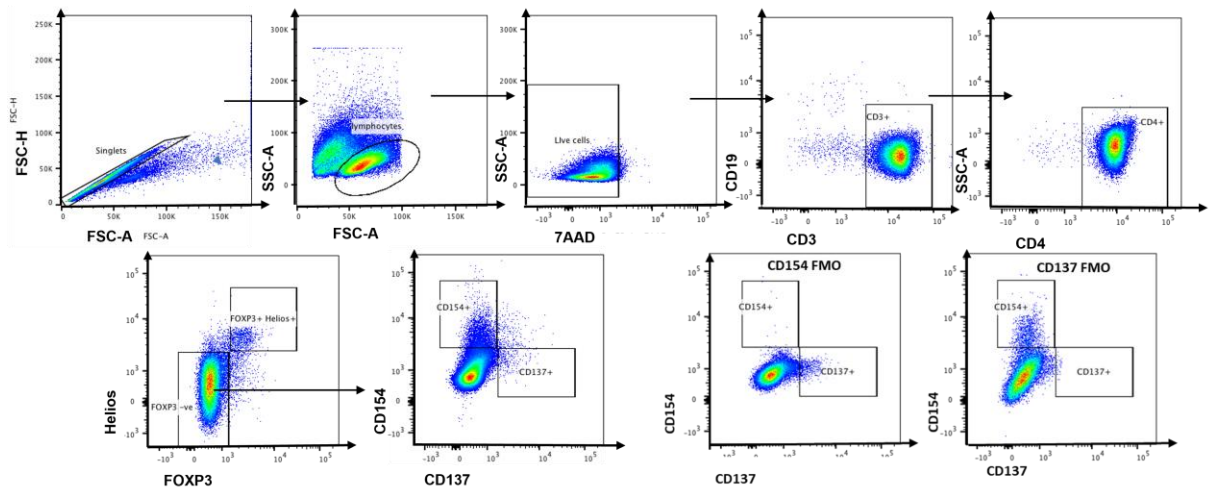
To examine the expression of CD137 and CD154 on Tregs and Tcons, CD4<sup>+</sup> T cells were stimulated with donor CD19<sup>+</sup> cells as shown in Figure 3.9.A. Unstimulated CD4<sup>+</sup> T cells were used as a negative control. Stimulated CD4<sup>+</sup> with autologous CD4<sup>neg</sup> T cells were used as a positive control. After 16 hours of incubation, it was possible to differentiate between CD137<sup>neg</sup> CD154<sup>+</sup> Tcons and CD137<sup>+</sup> CD154<sup>neg</sup> Treg cells. Almost all CD137<sup>+</sup> cells were detected within the FOXP3<sup>+</sup> Helios<sup>+</sup> population (Tregs) and were completely absent from the FOXP3<sup>neg</sup> subset (Tcons) (Figure 3.9.C). By contrast, the levels of CD154<sup>+</sup> cells were higher among FOXP3<sup>neg</sup> cells compared with FOXP3<sup>+</sup> Helios<sup>+</sup> cells (Figure 3.9.D). These data indicate that the identification of activated Tregs and Tcons is feasible based on the expression of CD137 versus CD154.

**Figure 3.9**

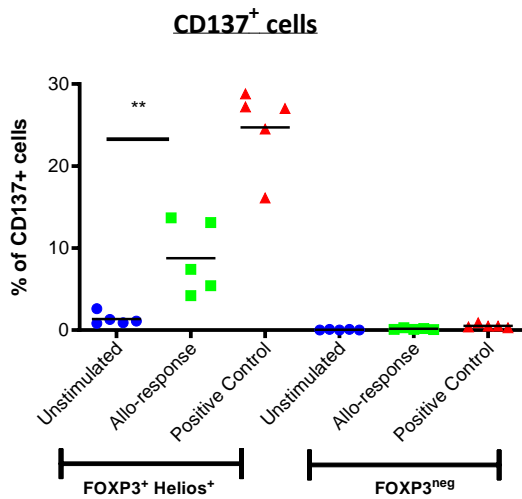
**A**



**B**



**C**



**D**

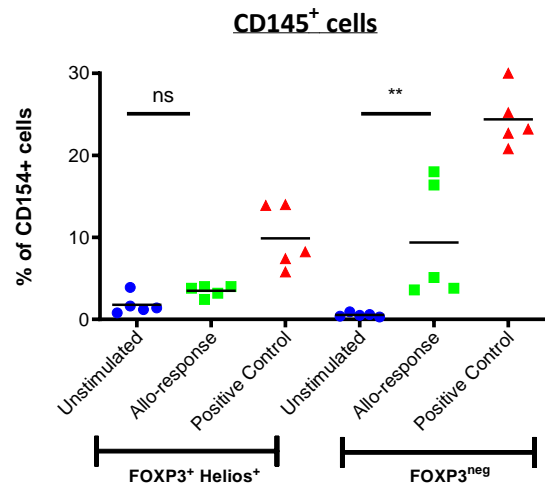


**Figure 3.9. CD137<sup>+</sup> T cells were mainly detected within the FOXP3<sup>+</sup> Helios<sup>+</sup> population, while CD154<sup>+</sup> T cells were mainly found within the FOXP3<sup>neg</sup> population. (A)** Schematic of the experimental design of the CD137/CD154 assay. **(B)** An example of a gating strategy followed to identify CD137<sup>+</sup> cells and CD154<sup>+</sup> cells from FOXP3<sup>neg</sup> population and FMOs. **(C)** Percentages of CD137<sup>+</sup> T cells gated on FOXP3<sup>+</sup>Helios<sup>+</sup> (Treg) and on FOXP3<sup>neg</sup> subsets. **(D)** Percentages of CD154<sup>+</sup> T cells gated on FOXP3<sup>+</sup>Helios<sup>+</sup> (Treg) and on FOXP3<sup>neg</sup> subsets. CD4<sup>+</sup> T cells were used as a negative control. CD4<sup>+</sup> and CD4<sup>neg</sup> T cells from the recipient, stimulated with superantigen Staphylococcal enterotoxin B (SEB), was used as a positive control. Expression of CD137 and CD154 was analysed using flow cytometry. Statistical significance was assessed by Mann-Whitney test, \*\*p= 0.0079, ns = not significant. Data representative of two independent experiments, five donors in total, each point represents an independent donor.

### 3.4 Discussion

Polyclonally reactive Treg cellular therapy is making clear progress in trials for the treatment of autoimmunity and transplant rejection. However, optimal Treg immunotherapy should employ alloantigen-reactive rather than polyclonally reactive Tregs to ensure both safety and enhanced specificity. Therefore, the aims of this project were to identify methods for the detection of arTregs in patients and to develop a technique for the isolation and expansion of these cells for therapy.

Studies have proposed the use of Treg-specific activation markers for the selection and identification of potent arTregs. For example, enriched CD27<sup>+</sup> arTregs were ten times more suppressive than CD27<sup>neg</sup> arTregs in *in vitro* suppression assays.<sup>305</sup> Here, it was found that CD137 upregulated rapidly in Tregs, with levels peaking on day 6, indicating that it has the potential to be used to select arTregs from *ex vivo* culture. Based on this, flow-sorted Tregs were cultured *ex vivo* with allogeneic irradiated imDCs. They were then enriched according to CD137 expression on day 6 after allostimulation, and further expanded with a combination of alloantigen stimulation and polyclonal anti-CD3/anti-CD28 bead stimulation to increase overall yield.

The stability and potency of arTregs are vital considerations in the development of Treg expansion protocols. In terms of suppressive capacity, CD137<sup>+</sup> enriched arTregs are superior to CD137<sup>neg</sup> arTregs, non-CD137 enriched arTregs or polyclonally expanded Tregs. This enhanced potency may compensate for the lower final yield of cells at the end of the expansion process. However, challenges remain in the feasibility of generating high yields of enriched arTregs at a scale that is practical for clinical use. We therefore focused on the non-CD137 enriched arTregs population which had a better expansion yield and demonstrated significantly greater inhibition of cell proliferation than polyclonal Tregs. This is in line with previous studies, which showed that arTregs are more potent at suppressing effector T cells in co-culture than polyTregs.<sup>171, 294, 295</sup> Additionally, it has been reported that arTregs have superior *in vitro* suppressive function in mixed lymphocyte reaction against primary stimulator than third-party stimulator.<sup>171, 222, 295</sup> Here, arTregs were very effective in mediating specific suppression towards the primary stimulator, but less towards a third-party stimulator. It is therefore conceivable that these cells, when used *in vivo*, would provide high levels of

therapeutic suppression compared to polyclonal Tregs, but without the potential detrimental effects. The TCR assessment of arTregs showed restriction to several TCR V $\beta$  families, suggesting an oligoclonal expansion. Roemhild et al, monitored the TCR repertoire of infused polyTregs at different time points post renal transplantation and compared them with the corresponding pre-infused Treg cell product.<sup>249</sup> The TCR repertoire assessment of Treg products revealed *in vivo* shift toward an oligoclonal pattern, suggesting an *in vivo* expansion of alloantigen responsive Tregs. It has been suggested that *in vivo* expansion of arTregs is linked to tolerance induction post-transplantation in organ transplant patients.<sup>323</sup>

Sánchez Fueyo et al, measured alloreactive Tconv responses after Treg infusion in liver transplant patients through quantifying the number of CD8<sup>+</sup> CD45RO<sup>+</sup> cells that express CD154 after *ex vivo* stimulation with surrogate donor PBMCs.<sup>307</sup> They observed a gradual decrease in the CD154 expression on memory CD8 T cells in recipients who received 4.5x10<sup>6</sup> Tregs/kg, suggesting development of alloreactive hypo-responsiveness after Tregs infusion. Here we developed and optimised CD137/ CD154 assay. This assay can be used in clinical studies investigating tolerogenic therapies, including the currently ongoing Treg cell therapy trial, the TWO Study to determine whether cellular therapy with regulatory cells results in the increase in prevalence of arTregs and/or decrease in antigen reactive T cells.

In conclusion, the data presented in this chapter demonstrate that the *ex vivo* isolation and expansion of human arTregs is feasible. This finding might prove useful in the clinical application of Tregs, aiming at the development of tolerance to only specific undesired immune responses.

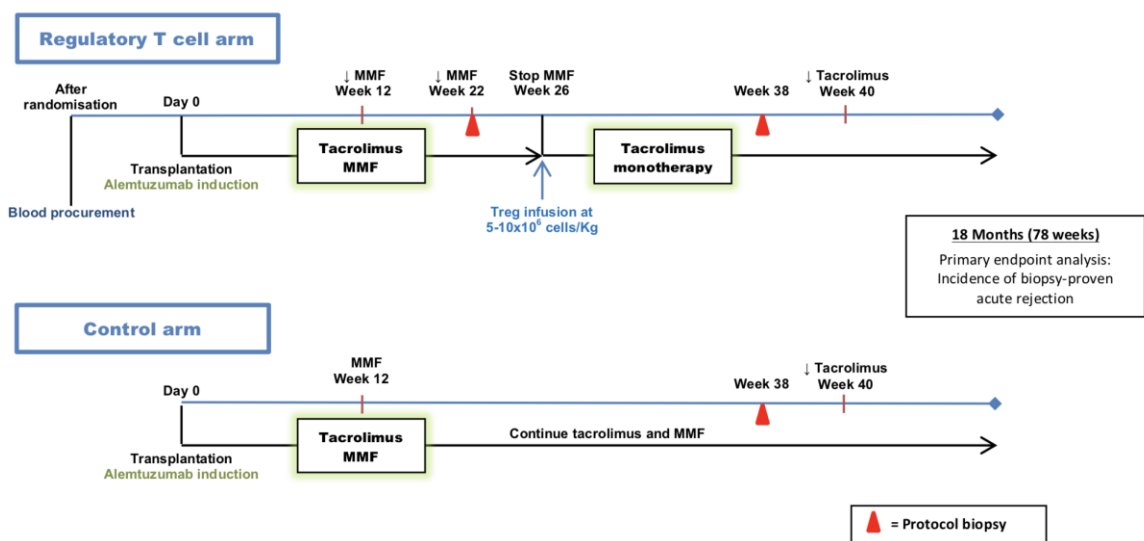
## Chapter 4: Cellular and phenotypical analysis of the peripheral immune cell compartment following Treg therapy in renal transplantation

### 4.1 Introduction

After three decades of preclinical research into Treg biology, we are beginning to see the progression of Treg therapy through clinical trials. Early phase trials of polyclonally-expanded Tregs provided evidence of the feasibility and safety of Treg therapy in transplantation.<sup>105, 248, 324</sup> However, determining the efficacy of Treg therapy has been more challenging due to difficulties in observing clinical outcomes over short follow up periods. The monitoring of renal transplant recipients receiving Treg therapy allows an in-depth analysis of the phenotypic and functional changes in immune cells, which may in turn help facilitate an understanding of the impact of Treg infusion.

Our group recently commenced recruitment to the TWO Study, which is a single-centre, phase IIb, randomised clinical trial of polyclonally expanded Tregs in renal transplantation. This study aims to compare the efficacy of autologous Treg therapy used in conjunction with tacrolimus to the standard of care immunosuppression (mycophenolate mofetil (MMF) and tacrolimus) in preventing acute biopsy-proven rejection in renal transplant recipients. A schematic of the trial protocol is shown below:

Figure 4.1



## Chapter 4: Cellular and phenotypical analysis of the peripheral immune cell compartment following Treg therapy in renal transplantation

**Figure 4.1: Diagrammatic representation of the immunosuppressive regimen for renal transplant recipients in TWO Study (protocol A).** Living donor renal transplant recipients are randomised either to the Regulatory T cell arm or control arm. Immunosuppression used included the use of induction antibody therapy in the form of alemtuzumab (Campath). Recipients enrolled in the Regulatory T cell arm received autologous polyTregs (infused at 6 months post-transplantation) in conjunction with tacrolimus as a maintenance immunosuppression. Recipients enrolled in the control arm received MMF and Tacrolimus. The follow-up in the trial is scheduled for 78 weeks post-transplantation.

An understanding of the alterations in immune phenotype of patients enrolled in the TWO Study is important for the assessment of the *in vivo* effect of Tregs on other immune cells and their fate after infusion. In this chapter, we profiled the peripheral blood immune phenotype of seven enrolled participants pre-transplantation to provide both a baseline assessment and an assessment at regular intervals post-transplantation, including post-Treg infusion. We compared the phenotypic changes in the peripheral immune cells of 3 living kidney transplant recipients who received polyclonal-expanded Treg therapy with 4 control transplant patients who received standard immunosuppression.

To examine the phenotypic changes in peripheral leukocytes in the enrolled participants, we employed (I) conventional flow cytometry using standardised DURAClone panels from Beckmann Coulter and examined the potential of (II) the high-dimensional technology cytometry time of flight (CyTOF) using a dedicated 36-antigen panel. DURAClone flow cytometry panels were previously developed in collaboration with Beckmann Coulter to profile a wide range of immune cell populations, including T cells, B cells, Tregs, gamma delta cells and NK subsets and their activation status (Table 2-2) with the aim to be used as an immunomonitoring tool in clinical trials. The disadvantage of the DURAClone panels is the lack of FMOs control in the panels, which might affect the analysis. The use of CyTOF has permitted an increase in the number of cellular and intracellular markers that can be measured simultaneously in cell suspensions. For data analysis, the traditional manual bivariate analysis is unlikely to be optimal for such datasets considering the large number of parameters. Therefore, a number of specialised analytical tools have been developed to facilitate the clustering analysis of multidimensional datasets, including viSNE,<sup>325</sup> PhenoGraph,<sup>326</sup> FlowSOM,<sup>327</sup> SPADE<sup>328</sup> and Citrus.<sup>329</sup> Data visualisation tools for CyTOF continue to evolve.<sup>330</sup>  
<sup>331</sup> In this project, the FlowSOM clustering algorithm, along with viSNE tools, and phenoGraph were used to analyse mass cytometry data.

## 4.2 Hypotheses

**Hypothesis-1:** Immunophenotyping will provide insights into the immune status of transplant recipients receiving Treg cellular therapy.

**Hypothesis-2:** The ability to evaluate multiple antigens concomitantly using mass cytometry (CyTOF) allows for unbiased detection of specific clusters of Tregs. Appreciating how these clusters behave after treatment with a cellular therapy will offer an insight into the immune phenotype.

## 4.3 Phenotypical analysis of the peripheral immune cell compartment in TWO

### Study participants by flow cytometry

#### 4.3.1 Study design and participants

The TWO study is a single-centre, phase IIb, randomised clinical trial of polyclonally expanded Tregs in living donor kidney transplant recipients. The trial was approved by the Health Research Authority, Oxford A research ethics committee (Reference:18/SC/0054). Recipients received alemtuzumab as an induction therapy at the time of kidney transplantation to achieve lymphodepletion. After transplantation, recipients received tacrolimus and mycophenolate-based immunosuppressive drug therapy. At week 26 post-transplantation, MMF was stopped in recipients enrolled in the cell therapy arm. Shortly after, patients received a single intravenous infusion of *ex vivo* expanded autologous polyclonal Tregs at 5–10x10<sup>6</sup> cells/kg, and subsequently maintained on tacrolimus monotherapy with an optional reduction from week 40 onwards. Patients randomised to the control arm received identical induction and initial maintenance immunosuppression but with no weaning of MMF or Treg infusion.

#### 4.3.2 Specimens and panels

Sequential peripheral blood samples were collected from **7** recipients at 13 different time points between enrolment and the end of follow-up. Blood was collected into EDTA vacutainers and run fresh in flow cytometry experiments. DuraClone antibody panels (Beckman Coulter) were used to profile T cells, B cells,  $\gamma\delta$  T cells, Tregs, NK cells and monocytes (Table 2-3 shows the list of markers in each panel). **Three** recipients from the Treg therapy

Chapter 4: Cellular and phenotypical analysis of the peripheral immune cell compartment following Treg therapy in renal transplantation arm and **four** recipients from the control arm of the trial were used for immune phenotypical analysis of the peripheral leukocyte compartment by flow cytometry.

### 4.3.3 Results

#### 4.3.3.1 Lymphocytes were depleted from the peripheral blood of renal transplant recipients after alemtuzumab induction therapy

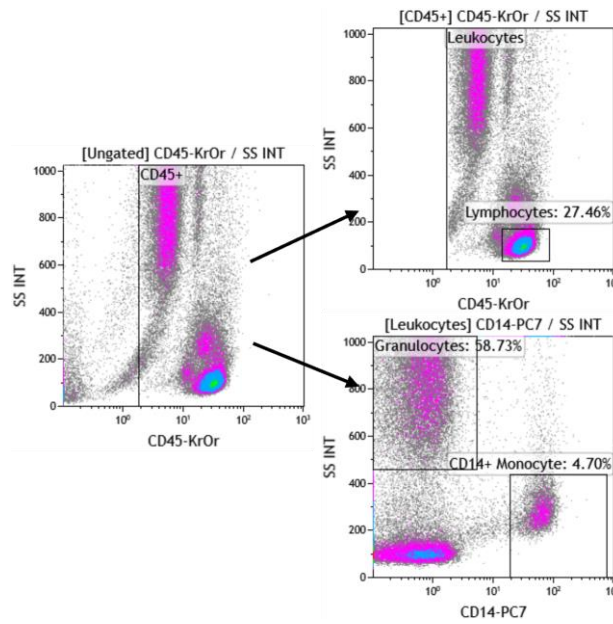
Alemtuzumab (Campath-1H) is a monoclonal antibody directed against the CD52 surface antigen. In humans, CD52 is highly expressed on T and B cells and at lower levels on NK cells, monocytes, including (moDCs),<sup>332</sup> macrophages and eosinophils. It is almost absent or expressed at very low levels on tissue-resident DCs,<sup>333</sup> neutrophils and hematopoietic stem cells.<sup>270</sup>

To examine the effect of alemtuzumab on leukocytes, we assessed changes in absolute numbers of lymphocytes, granulocytes and monocytes longitudinally in the peripheral blood of the recipients enrolled in the Treg therapy group (101, 102, 105; 3 patients) and the control group (103, 104, 106, 107; 4 patients) before transplantation and up to 72 weeks post-transplantation by flow cytometry. As expected, we observed that lymphocytes were completely depleted from the peripheral blood at 4 weeks post-transplant (V04) (Figure 4.2B). Two of the Treg-treated recipients (101 (red) and 102 (blue)) demonstrated almost complete recovery of lymphocytes at 72 weeks post-transplant (V19) (Figure 4.2B). However, granulocytes and monocytes at 4 weeks post-transplant (V04) and the following timepoints till V19 were at a level similar to that pre-transplant (V02) (Figure 4.2C and D). These data highlight that the depletion of granulocytes and monocytes by alemtuzumab was less profound and shorter-lasting than that of lymphocytes, which is likely related to their lower expression of the CD52 antigen.<sup>334,335</sup>

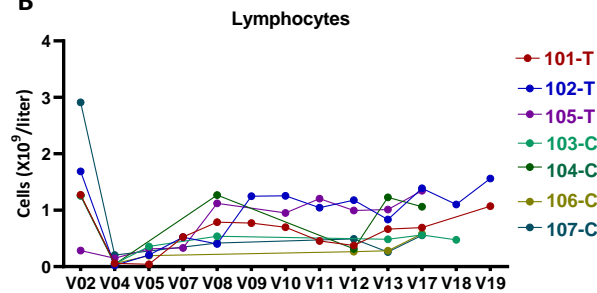
Chapter 4: Cellular and phenotypical analysis of the peripheral immune cell compartment following Treg therapy in renal transplantation

Figure 4.2

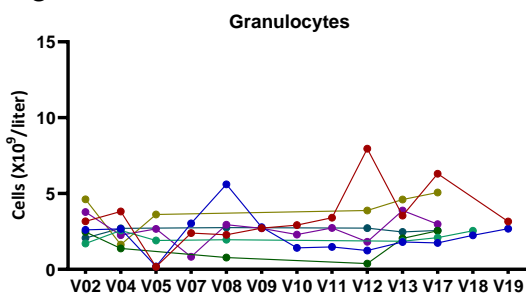
A



B



C



D

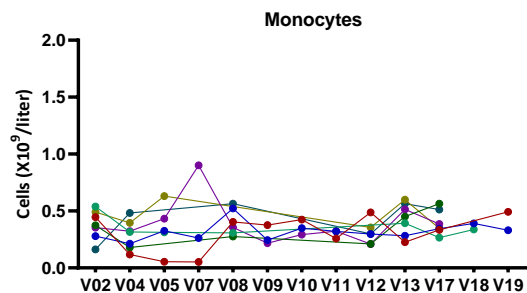


**Figure 4.2. Absolute number of lymphocytes, granulocytes and monocytes in peripheral blood of renal transplant recipients receiving Treg therapy.** Seven renal transplant recipients were treated with alemtuzumab and maintained reduced immunosuppression with mycophenolate mofetil (MMF) and tacrolimus. Three renal transplant recipients (101-T, 102-T, 105-T) received polyTregs at V09 (six months post-transplantation) and were maintained on tacrolimus, whereas four renal transplant recipients were in the control arm (103-C, 104-C, 106-C, 107-C) and were maintained on the standard of care immunosuppression. **(A)** Schematic illustration of the gating strategy for the identification of lymphocytes, granulocytes and monocytes. **(B-C-D)** Absolute numbers of lymphocytes, granulocytes and monocytes in whole blood samples collected from patients prior to transplantation (V02) and at 4 (V04), 12 (V05), 22 (V07), 24 (V08), 26 (V09), 27 (V10), 28 (V11), 30 (V12), 38 (V13), 44 (V17), 52 (V18) and 72 (V19) weeks post-transplant. Absolute numbers were calculated based on data derived from clinical laboratory reports. Data points represent individual samples and lines are specific patients.

#### 4.3.3.2 Repopulation of T cells after depletion with alemtuzumab

A key component of allograft responses is the activation and differentiation of alloreactive T cells.<sup>336, 337</sup> Alloreactive T cells can have a directly destructive effect on renal transplants and can indirectly impact other immune cells, which may damage the transplant. Previous animal model reports have shown that the depletion of host peripheral T cells together with Treg infusion synergises to promote allograft survival.<sup>338</sup>

We examined the effect of alemtuzumab on the number and proportion of total CD3<sup>+</sup> T cells in the peripheral blood of patients in the Treg therapy group (101, 102, 105) and control group (103, 104, 106, 107). As expected, there was a complete depletion of total CD3<sup>+</sup> T cells at 4 weeks post-transplant (V04) in both groups after alemtuzumab induction, after which CD3<sup>+</sup> T cells started to repopulate gradually (Figure 4.3B and C). Although no significant differences were seen in the numbers of total CD3<sup>+</sup> T cells at 44 weeks post-transplant (V17) between the Treg therapy and control groups, the numbers of T cells were slightly higher at V17 in the Treg therapy group compared to the control group (Figure 4.3D). However, the numbers of total CD3<sup>+</sup> T cells at 44 weeks post-transplant (V17) in both groups remained below the baseline level (V02) (Figure 4.3D). These data indicate that low T cell numbers persist for more than 10 months post-transplant after alemtuzumab induction therapy.

Figure 4.3

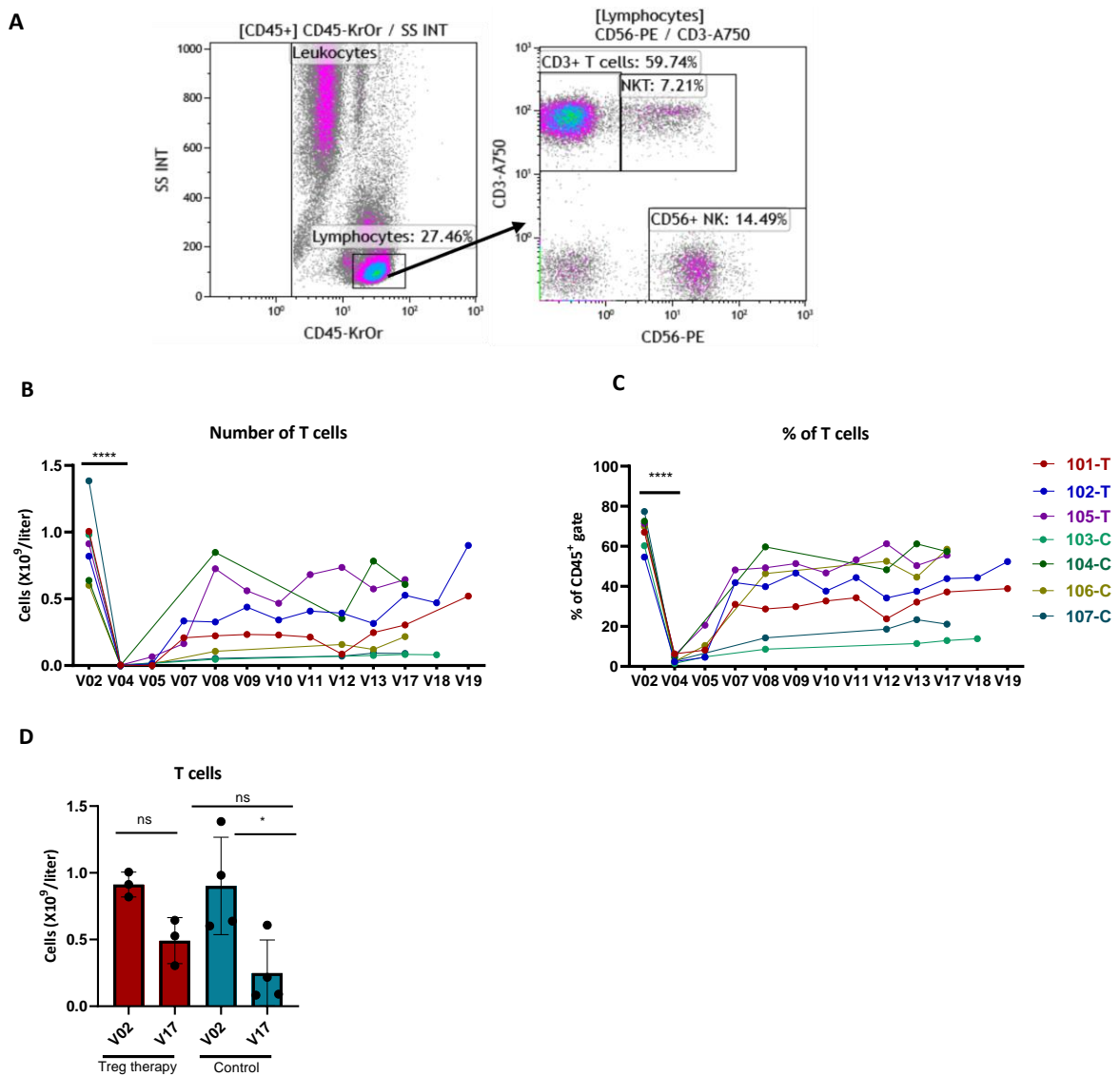


**Figure 4.3. Repopulation of T cells after *in vivo* depletion with alemtuzumab.** (A) Schematic illustration of the gating strategy for the identification of CD3<sup>+</sup> T cells. (B) Absolute numbers of T cells in whole blood samples collected from patients prior to transplantation (V02), at 4 (V04), 12 (V05), 22 (V07), 24 (V08), 26 (V09), 27 (V10), 28 (V11), 30 (V12), 38 (V13), 44 (V17), 52 (V18) and 72 (V19) weeks post-transplant. (C) The frequency (%) of CD3<sup>+</sup> T cells among CD45<sup>+</sup> leukocytes was assessed at immune-monitoring visits by flow cytometry. (D) Absolute numbers of peripheral CD3<sup>+</sup> T cells in the blood samples of the Treg therapy group ( $n = 3$ ) at V02 (pre-transplant) and V17 (week 44, post-transplant) (red) compared to the control group ( $n = 4$ ) at V02 and V17 (blue). Absolute numbers were calculated based on data derived from clinical laboratory reports. Dots represent individual samples. Statistical significance was calculated by paired *t*-test (Band C) and by one-way ANOVA with Tukey's for multiple comparisons (C), \*\*\*\* =  $p < 0.0001$ , \*  $p < 0.05$ , ns = non-significant. Data are represented as mean with SD.

#### 4.3.3.3 Assessment of CD4 and CD8 T cells and their subsets in the peripheral blood of renal transplant recipients receiving Treg therapy

Next, we investigated the effect of alemtuzumab induction therapy and Treg infusion on T cell subpopulations, including CD4<sup>+</sup> and CD8<sup>+</sup> T cells. In agreement with previous studies, alemtuzumab treatment resulted in a prolonged depletion of CD4<sup>+</sup> T cells in both groups (Figure 4.4B). A significant reduction in the number of total CD4<sup>+</sup> T cells was observed at 44 weeks post-transplant (V17) compared to baseline (V02) in the control group (Figure 4.4C). Conversely, the number of total CD8<sup>+</sup> T cells was comparable between V02 and V17 in both groups (Figure 4.4D and E). These data indicate that alemtuzumab is associated with a protracted deficiency of CD4<sup>+</sup> T cells to a greater degree than CD8<sup>+</sup> T cells. Memory T cells are generally viewed as pathogenic cells in the context of organ transplantation and are thought to accelerate graft rejection due to their robust effector functions.<sup>339, 340</sup> However, under certain circumstances, they show regulatory capacity and can downregulate immune responses.<sup>341</sup>

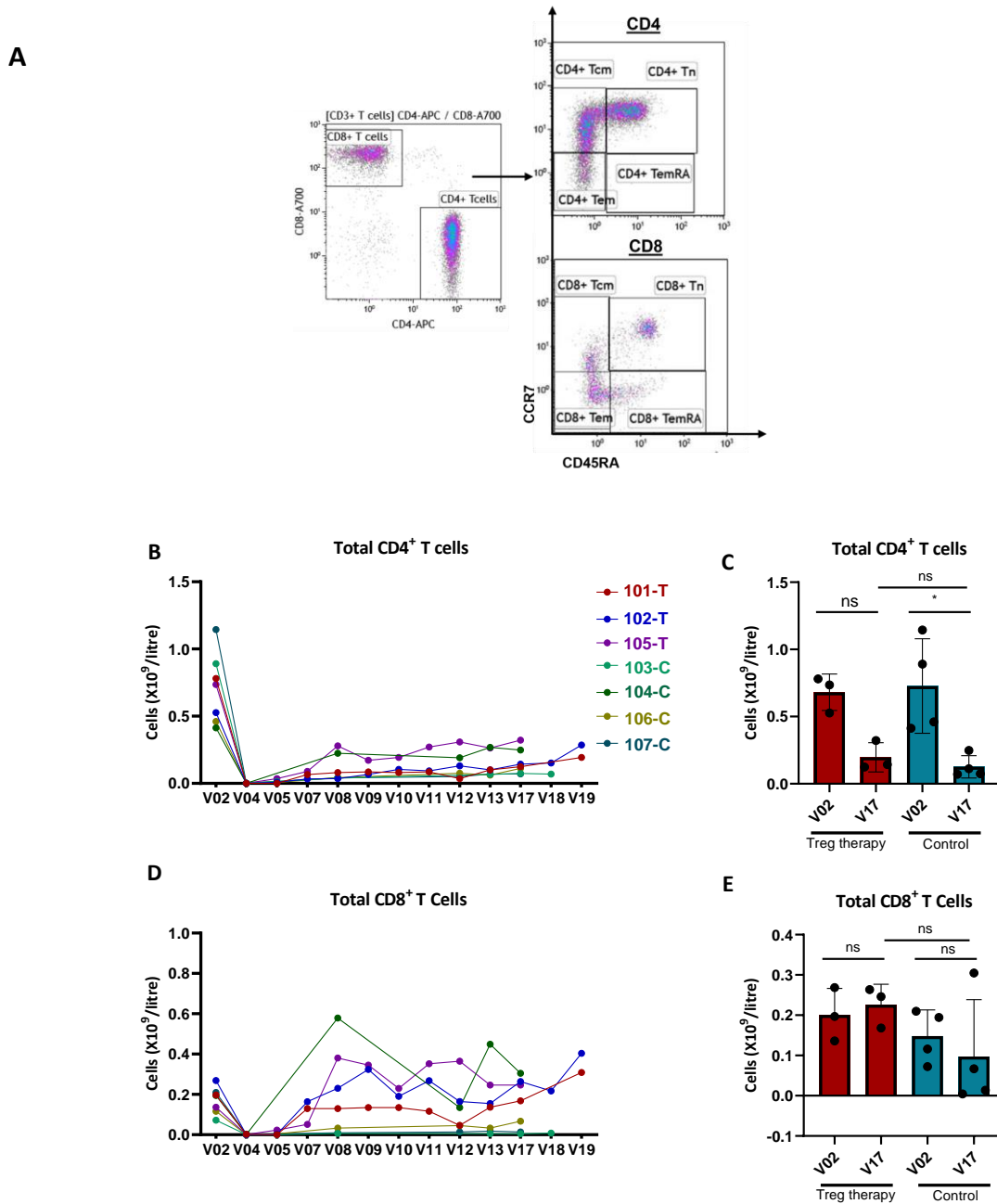
Here, we looked at the numbers of naïve (CD45RA<sup>+</sup> CCR7<sup>+</sup>), central memory (CM) (CD45RA<sup>neg</sup>CCR7<sup>+</sup>), effector memory (EM) (CD45RA<sup>neg</sup> CCR7<sup>neg</sup>), and terminally differentiated effector memory (TEMRA) (CD45RA<sup>+</sup> CCR7<sup>neg</sup>) CD4<sup>+</sup> T cells in the peripheral blood of the Treg therapy group at pre-transplant (V02) and at 44 weeks post-transplant (V17) (red) compared to the control group at V02 and V17 (blue) (Figure 4.4F). A slight reduction in the number of CM CD4<sup>+</sup> T cells and naïve CD4<sup>+</sup> T cells was observed at V17 compared to V02 in both groups. Yet, this reduction was not statistically significant. In addition, a slight reduction in the number of EM CD4<sup>+</sup> T cells was observed at V17 in the Treg therapy group when compared to V02, but was not statistically significant (Figure 4.4F).

We also assessed the numbers of naïve (CD45RA<sup>+</sup>CCR7<sup>+</sup>), CM (CD45RA<sup>neg</sup>CCR7<sup>+</sup>), EM (CD45RA<sup>neg</sup>CCR7<sup>neg</sup>), and TEMRA (CD45RA<sup>+</sup>CCR7<sup>neg</sup>) CD8<sup>+</sup> T cells in the peripheral blood of the Treg therapy group at V02 and V17 (red) compared to the control group at V02 and V17 (blue) (Figure 4.4G). There was a trend towards a reduction in the CM CD8<sup>+</sup> T cells at V17 compared to V02 in both groups, although this was not statistically significant (Figure 4.4F). In addition, the level of naïve CD8<sup>+</sup> T cells at V17 was comparable to the pre-transplant level V02 in the Treg therapy group, whereas in the control group, the level of naïve CD8<sup>+</sup> T cells was reduced at V17, but was not statistically significant (Figure 4.4G). The level of EM CD8<sup>+</sup> T cells appeared

Chapter 4: Cellular and phenotypical analysis of the peripheral immune cell compartment following Treg therapy in renal transplantation

lower at V17 compared to V02 in the Treg therapy group, but this level was not statistically significant. It was also not statistically significant when compared with V17 in the control group (Figure 4.4G). The level of TEMRA CD8<sup>+</sup> T cells appeared slightly elevated in both groups at V17 compared to V02, but was not statistically significant (Figure 4.4F). These data show that 10 months after alemtuzumab induction and Treg infusion, a recovery in CD8<sup>+</sup> T cells occurred, whereas CD4<sup>+</sup> T cells remained below the baseline level.

**Figure 4.4**



Chapter 4: Cellular and phenotypical analysis of the peripheral immune cell compartment following Treg therapy in renal transplantation

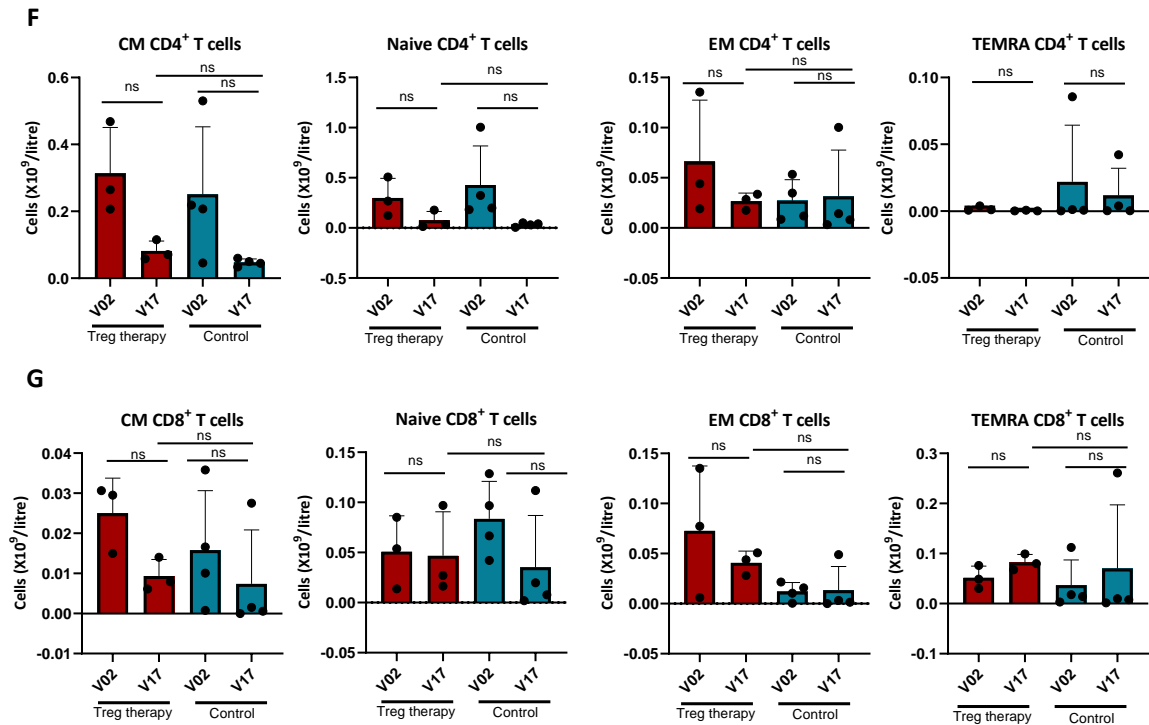


**Figure 4.4. Absolute numbers of CD4<sup>+</sup> and CD8<sup>+</sup> T cells and their subsets in the peripheral blood of renal transplant recipients over time.** (A) Schematic illustration of the gating strategy for the identification of CD4<sup>+</sup> T cells and CD8<sup>+</sup> T cells. (B–D) Absolute numbers of total CD4<sup>+</sup> T cells and CD8<sup>+</sup> T cells in whole blood samples collected from patients prior to transplantation (V02) and at 4 (V04), 12 (V05), 22 (V07), 24 (V08), 26 (V09), 27 (V10), 28 (V11), 30 (V12), 38 (V13), 44 (V17), 52 (V18) and 72 (V19) weeks post-transplant. (C–E) Absolute numbers of total CD4<sup>+</sup> T cells and CD8<sup>+</sup> T cells in the blood samples of the Treg therapy group ( $n = 3$ ) at V02 (pre-transplantation) and V17 (week 44, post-transplantation) (red) compared to the control group ( $n = 4$ ) at V02 and V17 (blue). (F) Absolute numbers of central memory (CM) CD4<sup>+</sup> T cells, naïve CD4<sup>+</sup> T cells, effector memory (EM) CD4<sup>+</sup> T cell and terminally differentiated effector memory (TEMRA) CD4<sup>+</sup> T cells in the blood samples of the Treg therapy group ( $n = 3$ ) at V02 and V17 (red) compared to the control group ( $n = 4$ ) at V02 and V17 (blue). (G) Absolute numbers of CM CD8<sup>+</sup> T cells, naïve CD8<sup>+</sup> T cells, EM CD8<sup>+</sup> T cells and TEMRA CD8<sup>+</sup> T cells in the blood samples of the Treg therapy group ( $n = 3$ ) at V02 and V17 (red) compared to the control group ( $n = 4$ ) at V02 and V17 (blue). Dots represent individual samples. Statistical significance was calculated by one-way ANOVA with Tukey's for multiple comparisons, \* $p < 0.05$ , ns = not significant. Data shown as absolute values (B and D) or mean  $\pm$  SD.

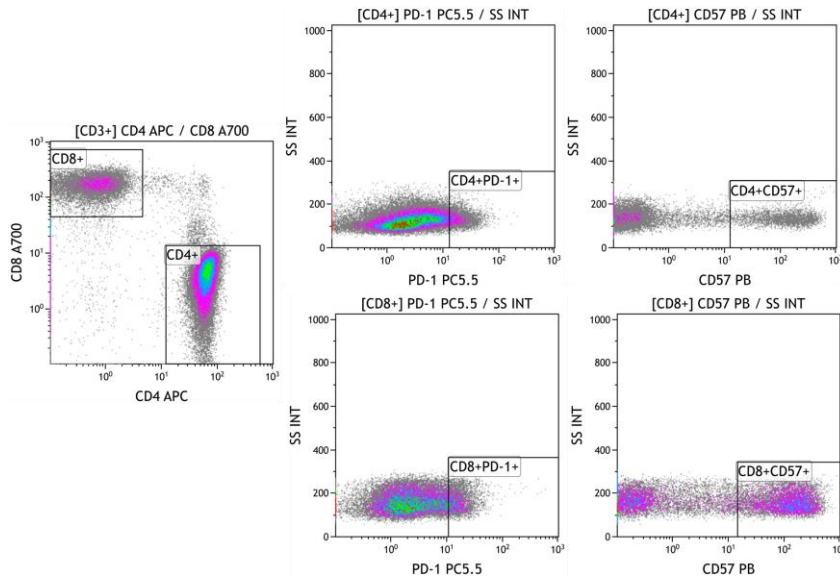
#### 4.3.3.4 Changes in PD-1 and CD57 expression among CD4 and CD8 populations over time post-transplantation

Co-stimulatory or co-inhibitory molecules are important regulators of T cell responses. Programmed death 1 (PD-1) is a co-inhibitory molecule expressed by peripheral T cells, B cells, and myeloid cells upon activation.<sup>342, 343</sup> PD-1 binds to its ligands, PD-L1 and PD-L2, to inhibit TCR signalling and prevent T cell activation. In experimental models of chronic viral infection, the upregulation of PD-1 on T cells was reported to identify exhausted T cells with reduced function.<sup>344</sup> There is evidence from experimental models to suggest that T cell exhaustion occurs in transplantation and is associated with transplant tolerance.<sup>345, 346, 347</sup> Recently, a study in renal transplant recipients reported an increase in peripheral PD-1<sup>+</sup> T cells after anti-thymocyte globulin (ATG) induction therapy in recipients with a stable graft.<sup>250</sup>

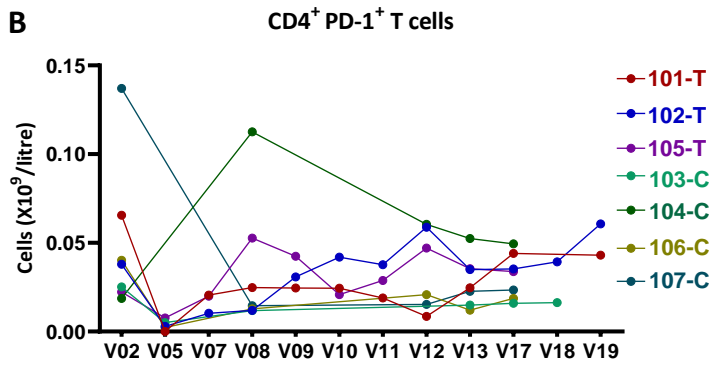
The expression of CD57, a terminally sulfated glycan carbohydrate epitope, on T cells might represent a marker of T cell senescence. In *in vitro* proliferation assays, CD57<sup>+</sup> T cells fail to proliferate after antigen-specific stimulation and show increased susceptibility to cell death through apoptosis.<sup>348</sup> Also, CD57<sup>+</sup> T cells have been demonstrated to be associated with several inflammatory diseases.<sup>349, 350</sup> In solid organ transplantation, several studies reported an elevation in the absolute count of CD57<sup>+</sup>CD8<sup>+</sup> T cell subsets without evidence of allograft rejection or viral infection.<sup>351, 352, 353</sup> CD57<sup>high</sup> CD8<sup>+</sup> T cells were also suggested to be a marker to predict the development of cutaneous squamous cell carcinoma in renal transplant. Here, we studied the expression of PD-1 and CD57 on CD4<sup>+</sup> and CD8<sup>+</sup> T cells in the peripheral blood of enrolled participants during the study period (Figure 4.5). We found that the number of CD4<sup>+</sup>PD-1<sup>+</sup> T cells and CD8<sup>+</sup>PD-1<sup>+</sup> T cells were comparable between baseline (V02) and V17 in both groups (Figure 4.5B-C-D-E). Furthermore, the level of CD57<sup>+</sup>CD8<sup>+</sup> T cells at V17 appeared slightly higher compared to the baseline (V02) in both groups, but this increase was not statistically significant (Figure 4.5G). In addition, two of the Treg-treated patients at V19 (end of observation period) had higher numbers of CD57<sup>+</sup>CD8<sup>+</sup> T cells compared to the baseline (V02) (Figure 4.5F), however V19 samples for other patients were not available at the time of writing. Taken together, these data highlight the changes of PD-1 and CD57 expression among CD4 and CD8 T cells over time post-transplantation, assessing these changes might help in identifying recipients who develop T cells exhaustion and would benefit from immune-suppression reduction.

Figure 4.5

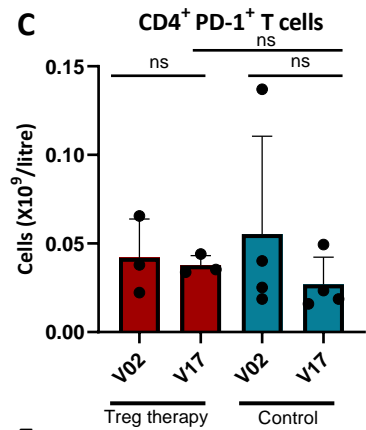
A



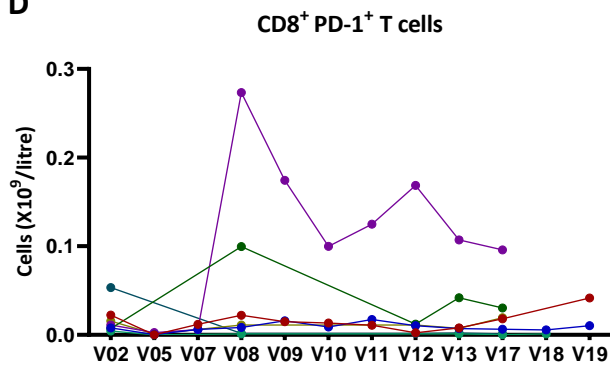
B



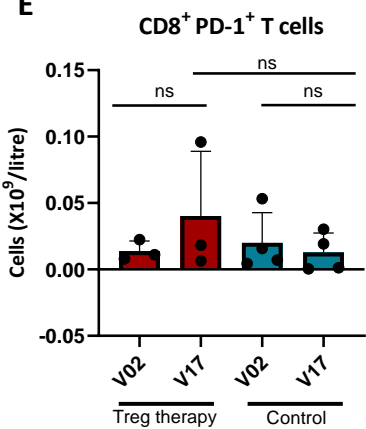
C



D



E



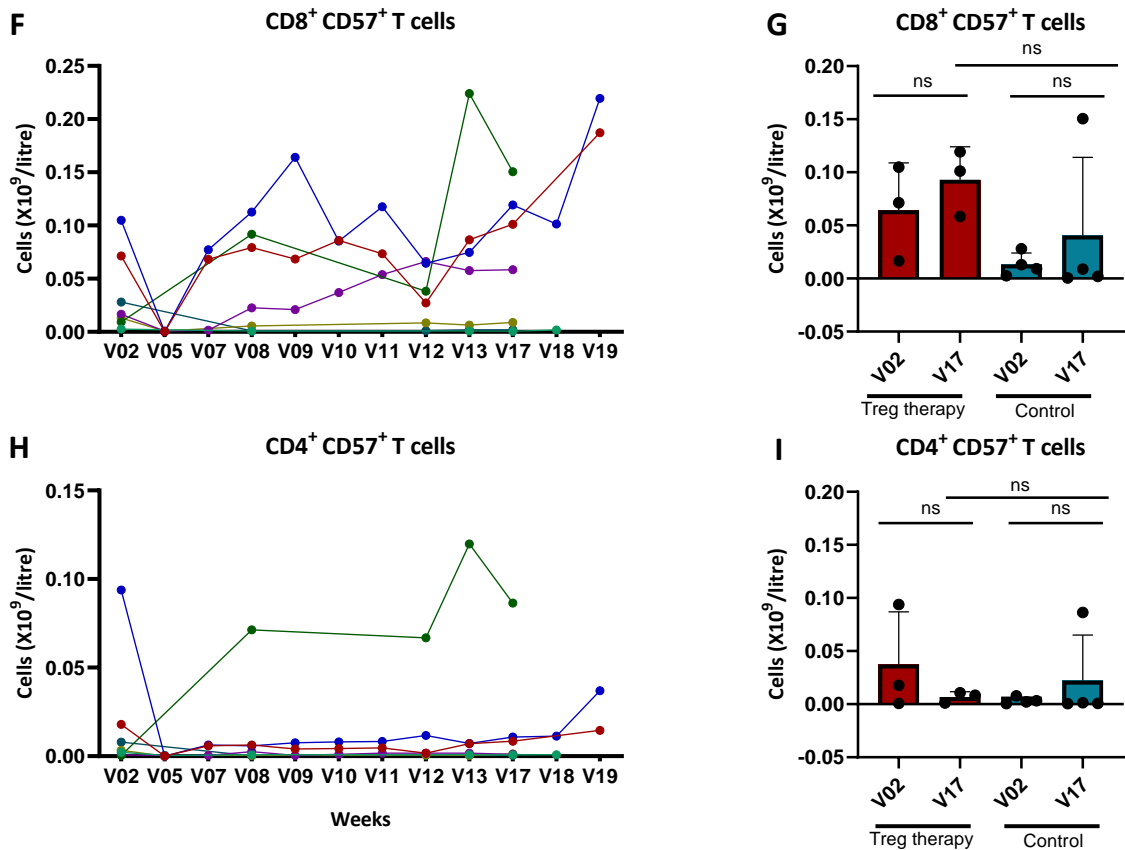


**Figure 4.5. Analysis of absolute numbers of PD-1<sup>+</sup> T cells and CD57<sup>+</sup> T cells over time.** (A) Schematic illustration of the gating strategy for the identification of CD4<sup>+</sup>PD-1<sup>+</sup> T cells, CD8<sup>+</sup>PD-1<sup>+</sup> T cells, CD8<sup>+</sup>CD57<sup>+</sup> T cells and CD4<sup>+</sup>CD57<sup>+</sup> T cells. (B-D-F-H) Absolute numbers of CD4<sup>+</sup>PD-1<sup>+</sup> T cells, CD8<sup>+</sup>PD-1<sup>+</sup> T cells, CD8<sup>+</sup>CD57<sup>+</sup> T cells and CD4<sup>+</sup>CD57<sup>+</sup> T cells in blood samples collected from patients prior to transplantation (V02) and at 4 (V04), 12 (V05), 22 (V07), 24 (V08), 26 (V09), 27 (V10), 28 (V11), 30 (V12), 38 (V13), 44 (V17), 52 (V18) and 72 (V19) weeks post-transplant. (C-E-G-I) Absolute numbers of CD4<sup>+</sup>PD-1<sup>+</sup> T cells, CD8<sup>+</sup>PD-1<sup>+</sup> T cells, CD8<sup>+</sup>CD57<sup>+</sup> T cells and CD4<sup>+</sup>CD57<sup>+</sup> T cells in the blood samples of the Treg therapy group (*n* = 3) at V02 and V17 (red) compared to the control group (*n* = 4) at V02 and V17 (blue). Dots represent individual samples. Statistical significance was calculated by one-way ANOVA with Tukey's for multiple comparisons, \**p* < 0.05, ns = not significant. Data shown as absolute values (B, D, F, H) or mean +/- SD.

#### 4.3.3.5 Phenotypical analysis of $\gamma\delta$ T cells over time post-transplantation shows a reduction in the V $\delta$ 2<sup>+</sup> $\gamma\delta$ T cell subset

$\gamma\delta$  T cells are a subpopulation of lymphocytes expressing T-cell receptors (TCRs) composed of transmembrane  $\gamma$  and  $\delta$  chains. The specific contribution of  $\gamma\delta$  T cells towards allografts has yet to be elucidated, with evidence of both their detrimental and tolerogenic roles in several settings.<sup>48</sup> In humans,  $\gamma\delta$  T cells are a heterogeneous population and can be classified by the TCR  $\delta$  chains expression into V $\delta$ 1, V $\delta$ 2 and other, less frequent V $\delta$  chains. Extensive immunophenotyping of liver transplant recipients who developed operational tolerance has revealed a significant increase in  $\gamma\delta$  T cells and a V $\delta$ 1:V $\delta$ 2 ratio of >1.<sup>49</sup> By contrast, the

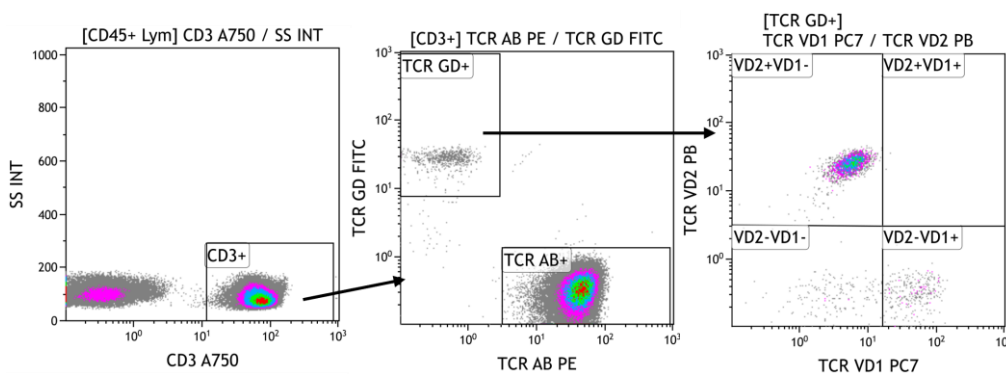
Chapter 4: Cellular and phenotypical analysis of the peripheral immune cell compartment following Treg therapy in renal transplantation

frequencies of V $\delta$ 1 and V $\delta$ 2 subsets have been analysed in the peripheral blood of liver transplant patients with stable graft function compared with those whose grafts had rejected, showing an increase in the proportion of V $\delta$ 2  $\gamma\delta$  T cells being reported during allograft rejection episodes.<sup>50</sup>

Here, we quantified the absolute numbers of peripheral blood  $\gamma\delta$  T cells in renal transplant recipients receiving Treg therapy. We observed a slight increase in the number of  $\gamma\delta$  T cells in the Treg therapy group at 44 weeks post-transplant (V17) in comparison to baseline (V02) (Figure 4.6B and C). This might indicate that Treg infusion boosts the repopulation of  $\gamma\delta$  T cells – however, this increase was not statistically significant. We also examined the numbers of the two main  $\gamma\delta$  T cell subsets, namely V $\delta$ 1<sup>+</sup> and V $\delta$ 2<sup>+</sup>, over time (Figure 4.6D and F). There was a trend toward an increase in the number of V $\delta$ 1<sup>+</sup>  $\gamma\delta$  CD3<sup>+</sup> T cells at 44 weeks post-transplant (V17) compared to baseline (V02) in both groups, although this was not statistically significant (Figure 4.6E). Conversely, we observed a reduction in the number of V $\delta$ 2<sup>+</sup>  $\gamma\delta$  T cells at 44 weeks post-transplant (V17) as compared to the baseline level (V02) in the control group, but was not statistically significant (Figure 4.6G). This suggests that repopulating  $\gamma\delta$  T cells have an alteration towards more V $\delta$ 1<sup>+</sup> and fewer V $\delta$ 2<sup>+</sup> cells, which might have a role in promoting tolerance.

**Figure 4.6**

**A**



Chapter 4: Cellular and phenotypical analysis of the peripheral immune cell compartment following Treg therapy in renal transplantation

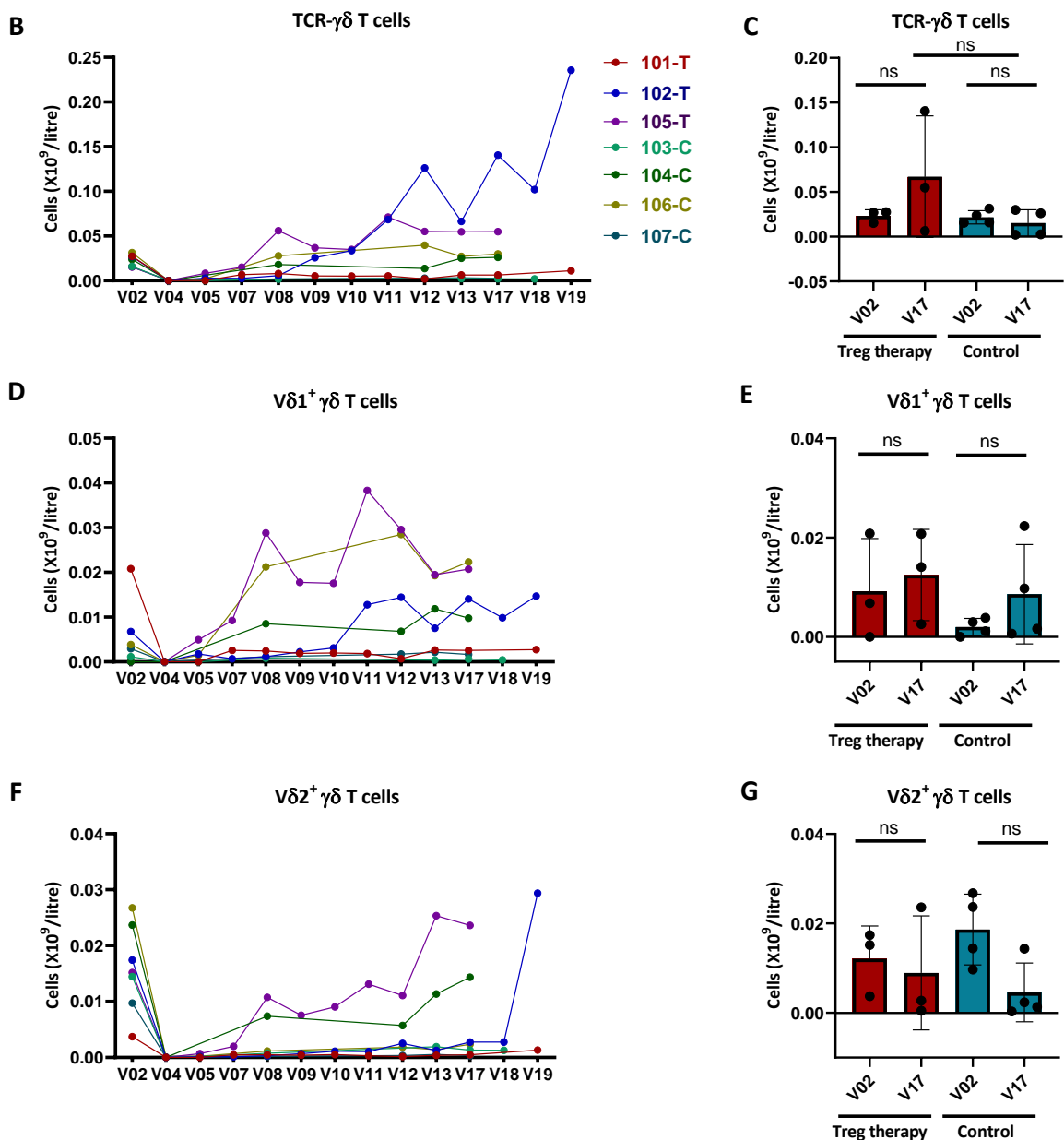


**Figure 4.6. Absolute numbers of TCR- $\gamma\delta$  T cells and their subpopulations, V $\delta 1^+$  and V $\delta 2^+$   $\gamma\delta$  T cells, in the peripheral blood of renal transplant recipients over time. (A)** Schematic illustration of the gating strategy for the identification of total  $\gamma\delta$  T cells and V $\delta 1^+$  and V $\delta 2^+$   $\gamma\delta$  T cells. **(B-D-F)** Absolute numbers of total  $\gamma\delta$  T cells and V $\delta 1^+$  and V $\delta 2^+$   $\gamma\delta$  T cells in whole blood samples collected from patients prior to transplant (V02) and at 4 (V04), 12 (V05), 22 (V07), 24 (V08), 26 (V09), 27 (V10), 28 (V11), 30 (V12), 38 (V13), 44 (V17), 52 (V18) and 72 (V19) weeks post-transplant. **(C-E-G)** Absolute numbers of total  $\gamma\delta$  T cells and V $\delta 1^+$  and V $\delta 2^+$   $\gamma\delta$  T cells in blood samples of the Treg therapy group ( $n = 3$ ) at V02 (pre-transplant) and V17 (week 44, post-transplant) (red) compared to the control group ( $n = 4$ ) at V02 and V17 (blue). Dots represent individual samples. Statistical significance was calculated by one-way ANOVA with Tukey's for multiple comparisons, ns = not significant. Data shown as absolute values (B, D, F) or mean  $\pm$  SD.

#### 4.3.3.6 Peripheral B cells repopulate rapidly and exceed baseline levels

Humoral immunity is a crucial component of the alloimmune response. It is well reported that alloantibodies produced by B cells, including the *de novo* production of donor-specific antibodies (DSAs) post-transplantation, can lead to both acute graft rejection and long-term allograft dysfunction.<sup>53</sup> In contrast, other studies have suggested that specific populations of B cells might contribute to the development of transplant tolerance and can promote allograft survival.<sup>354</sup> In one example, Louis et al. reported an elevation in the total number of peripheral B cells in operationally tolerant renal transplant recipients.<sup>279</sup> Newell et al. also demonstrated an increase in naïve and transitional B cells in operational renal recipients when compared to recipients with biopsy-proven chronic rejection.<sup>281</sup> These findings highlight the potential role of specific populations of B cells in mediating operational tolerance in renal transplant recipients.

We therefore investigated the phenotypical changes of B cells in the peripheral blood of renal transplant recipients before and at regular intervals post-transplant, as well as post-Treg infusion (Figure 4.7). Alemtuzumab induction therapy effectively depleted CD19<sup>+</sup> B cells from the peripheral blood, but the B cells started to repopulate in six out of seven donors from 12 weeks onward (V05) (Figure 4.7C). Both the proportion and the absolute number of B cells increased post-transplant as compared to pre-transplant in the Treg therapy group (Figure 4.5B-C-D). We also assessed the proportion and absolute number of transitional B cells over time, a B cell population thought to contain regulatory B cells (Figure 4.7B and E). It is noteworthy that there was a slight elevation in the absolute number of CD19<sup>+</sup>CD24<sup>hi</sup>CD38<sup>hi</sup> transitional B cells after Treg infusion (Figure 4.7F). The elevation of CD19<sup>+</sup>CD24<sup>hi</sup>CD38<sup>hi</sup> transitional B cells was higher at V17 (week 44 post-transplant), compared to V02 in the Treg therapy group. This was significant in comparison to the control group (Figure 4.7G), suggesting that Treg infusion enriches transitional B cells.

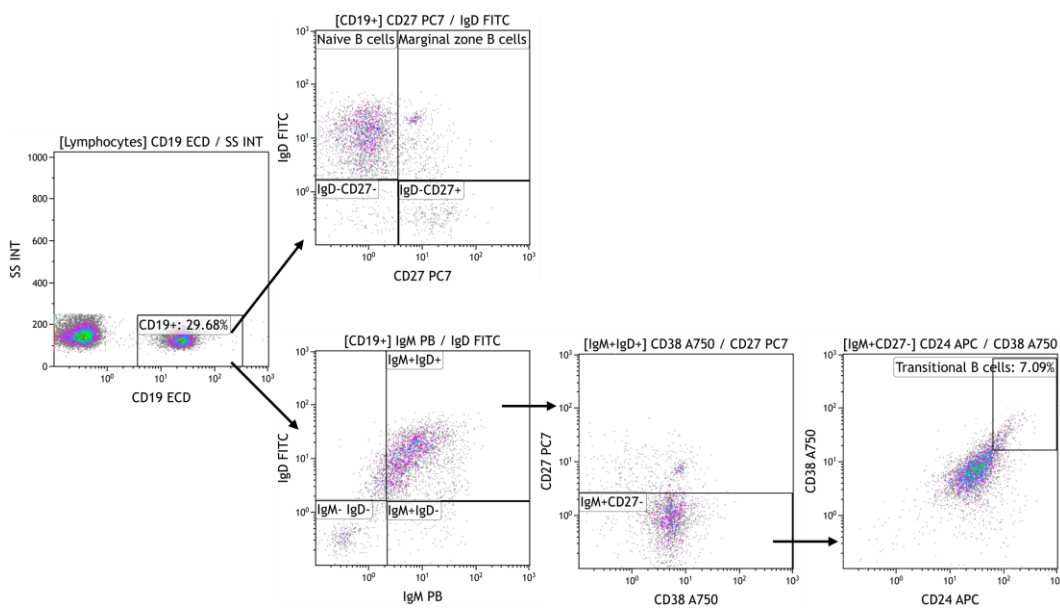
B cell differentiation stages can be identified by flow cytometry using the CD27-IgD classification scheme. We used this scheme to gate naïve B cells (IgD<sup>+</sup>CD27<sup>neg</sup>), circulating marginal zone B cells (IgD<sup>+</sup>CD27<sup>+</sup>, alternatively described as unswitched memory cells), switched memory B cells (IgD<sup>neg</sup>CD27<sup>+</sup>), and exhausted memory B cells (IgD<sup>neg</sup>CD27<sup>neg</sup>).<sup>355</sup> Following alemtuzumab treatment, the level of naïve B cells was increased at V17 when compared to pre-transplant levels (V02), especially in the Treg therapy group. Yet, this

Chapter 4: Cellular and phenotypical analysis of the peripheral immune cell compartment following Treg therapy in renal transplantation

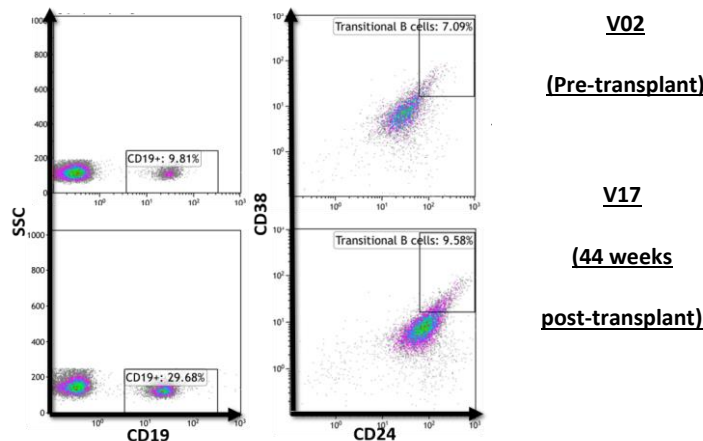
elevation was not statistically significant (Figure 4.7H). There was a shift to lower levels of memory B cells in the peripheral blood, including marginal zone B cells (IgD<sup>+</sup>CD27<sup>+</sup>) and switched memory B cells (IgD<sup>neg</sup>CD27<sup>+</sup>) in both groups at V17, compared to V02. But, this was not statistically significant (Figure 4.7I and J). The IgD<sup>neg</sup>CD27<sup>neg</sup> B cell population, which has been described as exhausted memory B cells, was slightly increased in Treg therapy group at V17 compared to pre-transplant levels (V02). Yet, this elevation was not statistically significant (Figure 4.7K). These data demonstrate the shift of B cell subsets towards more transitional B cells post-Treg infusion.

**Figure 4.7**

**A**



**B**



Chapter 4: Cellular and phenotypical analysis of the peripheral immune cell compartment following Treg therapy in renal transplantation

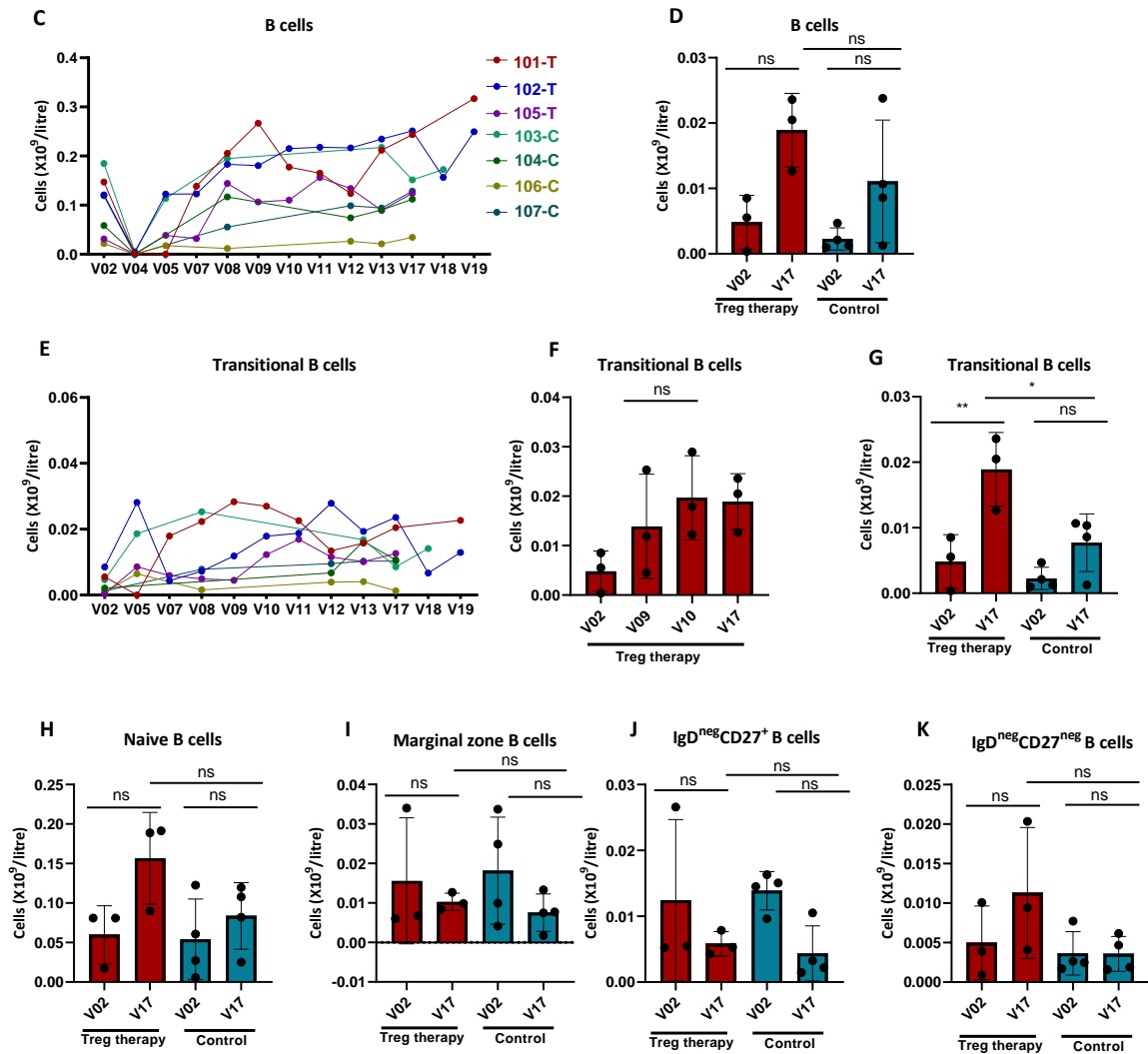


**Figure 4.7. Analysis of absolute numbers of B cells over time.** (A) Schematic illustration of the gating strategy for the identification of total B cells, and B cell subsets. (B) Example FACS plots show the percentages of CD19<sup>+</sup> and CD19<sup>+</sup>CD24<sup>hi</sup>CD38<sup>hi</sup> transitional B cells at V02 pre-transplant (top) and at V17, week 44 post-transplant (bottom) from one of the Treg-treated recipients. (C–E) Absolute numbers of total B cells and CD19<sup>+</sup>CD24<sup>hi</sup>CD38<sup>hi</sup> transitional B cells in whole blood samples collected from patients prior to transplant (V02) and at 4 (V04), 12 (V05), 22 (V07), 24 (V08), 26 (V09), 27 (V10), 28 (V11), 30 (V12), 38 (V13), 44 (V17), 52 (V18) and 72 (V19) weeks post-transplant. (D–G) Absolute numbers of total B cells and CD19<sup>+</sup>CD24<sup>hi</sup>CD38<sup>hi</sup> transitional B cells in the blood samples of the Treg therapy group ( $n = 3$ ) at V02 and V17 (red) compared to the control group ( $n = 4$ ) at V02 and V17 (blue). (F) Absolute numbers of CD24<sup>hi</sup>CD38<sup>hi</sup> transitional B cells in the blood samples of the Treg therapy group ( $n = 3$ ) prior to transplantation (V02) and at 26 (V09), 27 (V10) and 44 (V17) weeks post-transplant. (H–I–J–K) Absolute numbers of naïve B cells, marginal zone B cells, IgD<sup>neg</sup>CD27<sup>+</sup> B cells, and IgD<sup>neg</sup>CD27<sup>neg</sup> B cells in the blood samples of the Treg therapy group ( $n = 3$ ) at V02 and V17 (red) compared to the control group ( $n = 4$ ) at V02 and V17 (blue). Dots represent individual samples. Statistical significance was calculated by one-way ANOVA with Tukey's for multiple comparisons, ns = non-significant; \* $p < 0.05$ , \*\* $p < 0.01$ . Data shown as absolute values (C, E) or mean  $\pm$  SD.

#### 4.3.3.7 Alterations in the absolute numbers and frequencies of NK and NKT populations over time

NK cells play a critical role in anti-viral and anti-tumour defence.<sup>356</sup> NK cells are heterogeneous and consist of different subsets with different properties. In humans, studies have reported the presence of two main NK subsets in the peripheral blood<sup>357</sup>: (1) CD56<sup>dim</sup> NK cells, which were revealed to be more abundant and highly cytotoxic towards virally infected cells or cancer cells. These cells express Fc gamma receptor (FCγR) CD16, which can recognise the Fc portion on several IgG subclasses and mediate antibody-dependent cellular cytotoxicity. (2) CD56<sup>bright</sup> NK cells, which express a low level of CD16 and have regulatory activity.<sup>358,359</sup>

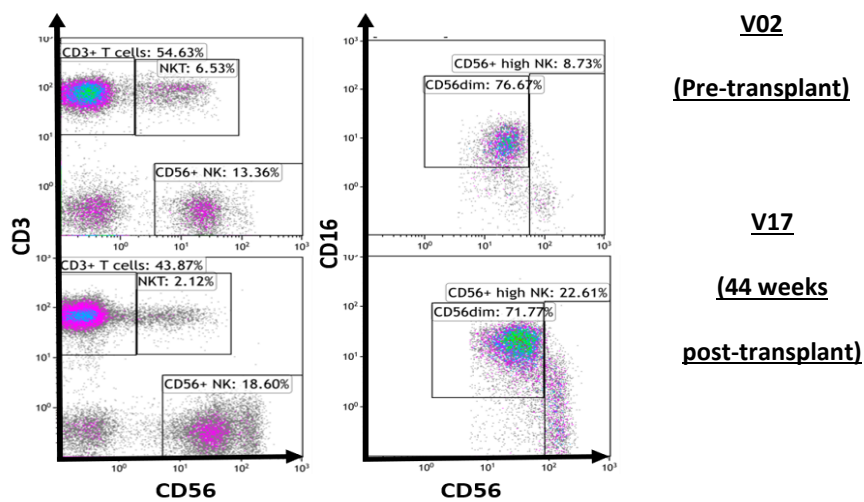
It is well established that NK cells can contribute to allograft damage.<sup>360, 361</sup> In contrast, growing evidence is now indicating that NK cells may also have a significant role in allograft tolerance.<sup>362, 363</sup> For example, studies have reported an increase of NK cells in the peripheral blood of tolerant renal and liver recipients.<sup>280, 364</sup> There is work showing that in tolerant recipients the cytotoxic CD56<sup>dim</sup> NK subset decreases, while the immunoregulatory CD56<sup>bright</sup> NK subset increases over time post-transplantation.<sup>365</sup> NKT cells are a subset of T cells that co-express NK cell surface markers and a conserved αβ TCR repertoire, which recognise glycolipid proteins presented by MHC class I-like protein CD1d.<sup>366, 367</sup> They play a critical role in several pathological states, including microbial infection,<sup>368</sup> autoimmunity,<sup>369</sup> and cancer.<sup>370</sup>

Here, we immune-monitored the peripheral CD56<sup>+</sup> NK cells and the CD56<sup>+</sup>CD3<sup>+</sup> NKT cells over time pre- and post-transplant and investigated the impact of alemtuzumab induction along with Treg infusion on the peripheral NK cell repertoire. As shown in Figures 4.8A, we found an increase in the percentage of total NK cells in the Treg therapy group post-transplantation, as compared to pre-transplantation. However, the absolute number of total NK cells was comparable at V17, compared to the baseline in both groups (Figure 4.8C). We also observed a trend towards a reduction in the percentage and absolute number of CD56<sup>+</sup>CD3<sup>+</sup> NKT cells at 44 weeks post-transplantation (V17) in comparison to pre-transplantation in both groups (Figure 4.8D and E), although this was not statistically significant. We also monitored the CD56<sup>dim</sup> and CD56<sup>bright</sup> NK cells over time post-transplant (Figure 4.8A-F-H). We found a decrease in the frequency of CD56<sup>dim</sup> NK along with an increase in CD56<sup>bright</sup> NK at V17 compared to the baseline (Figure 4.8A). However, the absolute number of CD56<sup>dim</sup> NK cells

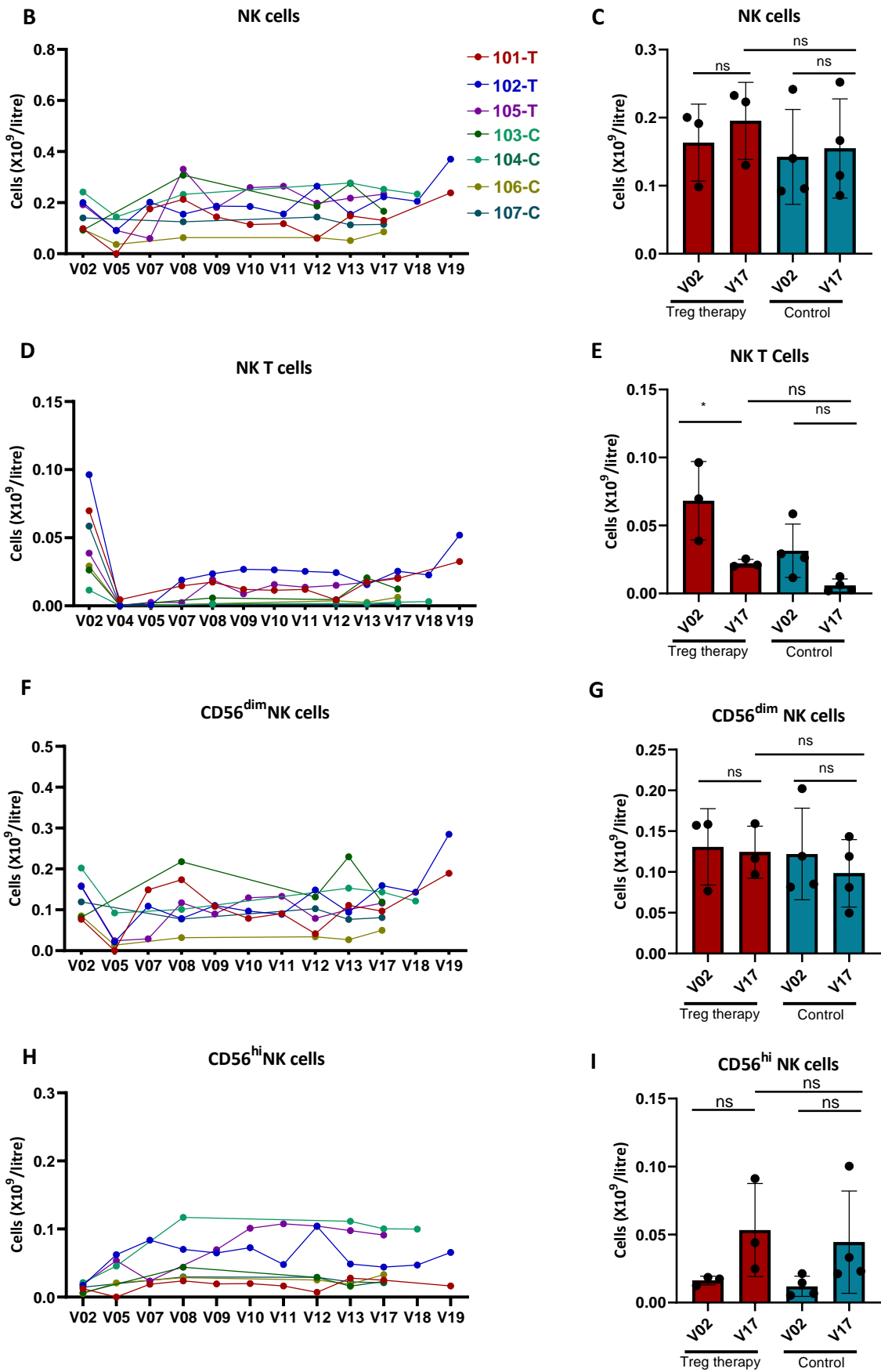
Chapter 4: Cellular and phenotypical analysis of the peripheral immune cell compartment following Treg therapy in renal transplantation was comparable between V17 and the pre-transplant level (V02) in both groups (Figure 4.8G). While, there was a trend toward an increase in the number of CD56<sup>bright</sup> NK cells in V17, compared to pre-transplant level (V02) in both groups, this increase was not statistically significant (Figure 4.8I). These data highlight the changes of NK and NKT populations over time post-transplantation.

**Figure 4.8**

**A**



Chapter 4: Cellular and phenotypical analysis of the peripheral immune cell compartment following Treg therapy in renal transplantation



## Chapter 4: Cellular and phenotypical analysis of the peripheral immune cell compartment following Treg therapy in renal transplantation

**Figure 4.8. Changes in the absolute numbers and frequencies of NK and NKT populations over time.**

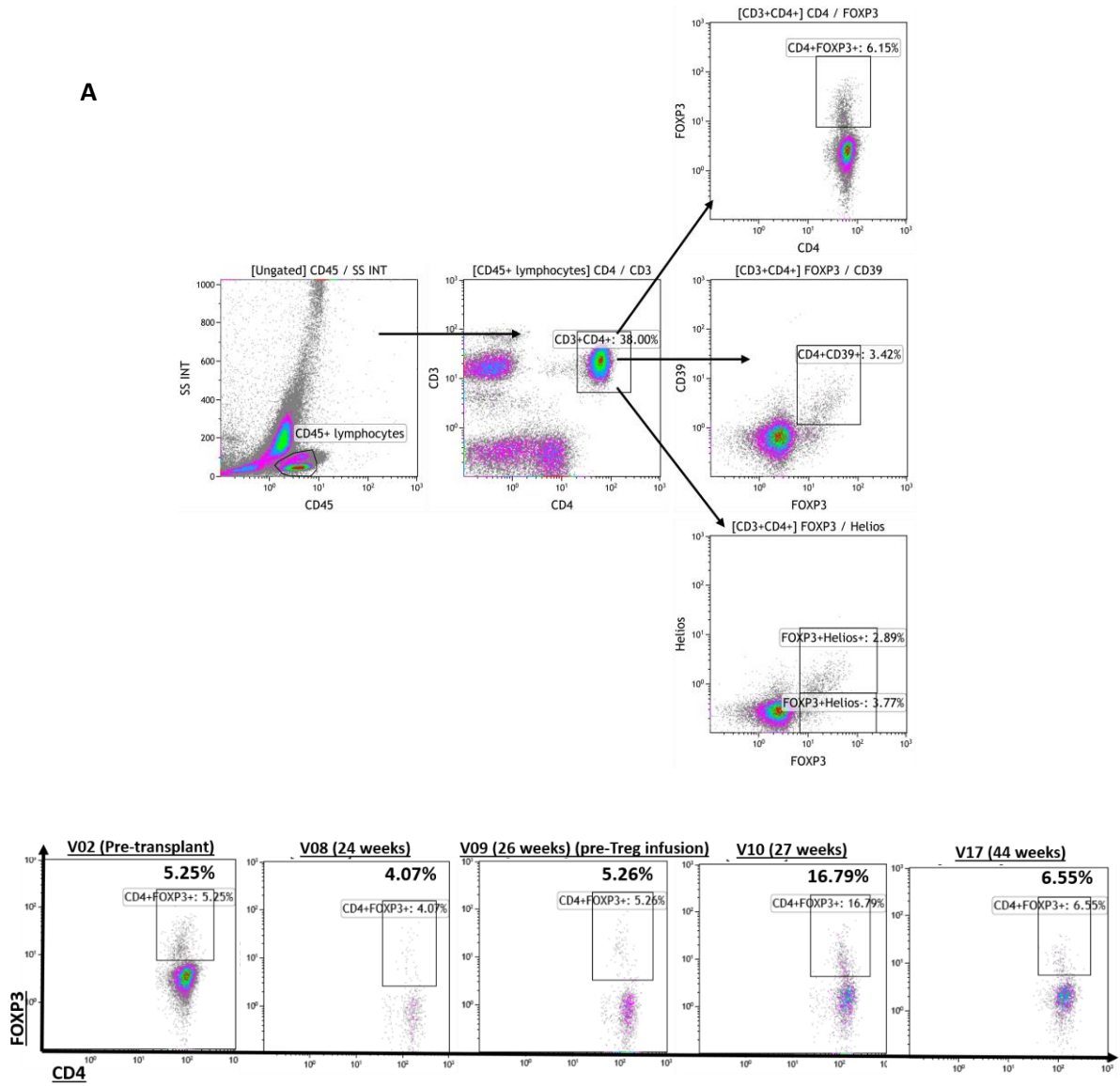
**(A)** FACS plots show the percentages of CD3, CD56<sup>+</sup>NK, CD56<sup>+</sup>CD3<sup>+</sup>NKT cells and CD56<sup>dim</sup>CD16<sup>hi</sup>NK and CD56<sup>hi</sup>CD16<sup>low</sup> NK cells at V02 pre-transplantation (top) and at V17, week 44 post-transplantation (bottom) from one of the Treg-treated recipients. **(B-D-F-H)** Absolute numbers of total NK cells, NKT cells, CD56<sup>dim</sup>CD16<sup>hi</sup>, and CD56<sup>hi</sup>CD16<sup>low</sup> NK cells in whole blood samples collected from patients prior to transplantation (V02) and at 4 (V04), 12 (V05), 22 (V07), 24 (V08), 26 (V09), 27 (V10), 28 (V11), 30 (V12), 38 (V13), 44 (V17), 52 (V18) and 72 (V19) weeks post-transplant. **(C-E-G-I)** Absolute numbers of total NK cells, NKT cells, CD56<sup>dim</sup>CD16<sup>hi</sup>, and CD56<sup>hi</sup>CD16<sup>low</sup> NK cells in the blood samples of the Treg therapy group ( $n = 3$ ) at V02 and V17 (red) compared to the control group ( $n = 4$ ) at V02 and V17 (blue). Dots represent individual samples. Statistical significance was calculated by one-way ANOVA with Tukey's for multiple comparisons, \* $p < 0.05$ , ns = not significant. Data shown as absolute values (B, D, F, H) or mean  $\pm$  SD.

### 4.3.3.8 Modest changes in peripheral Tregs after Treg infusion in renal transplant recipients

Next, we monitored peripheral Tregs (FOXP3<sup>+</sup> cells) over time. Initially, we found an increase in the frequency of FOXP3<sup>+</sup> cells at V10 (1 week post-Treg infusion), at around 9%, after which the frequency reduced over time, as demonstrated in Figure 4.9A. We also observed an increase in the number of peripheral FOXP3<sup>+</sup> Tregs after Treg infusion at V10, when compared to V09, but this increase was not statistically significant (Figure 4.9B and C). The level of FOXP3<sup>+</sup> cells at V17 was reduced in both groups, compared to pre-transplant level; this reduction was statistically significant in the control group (Figure 4.9D). In addition, the level of FOXP3<sup>+</sup> Helios<sup>+</sup> cells at V17 was reduced in both groups, compared to pre-transplant level; this reduction was not statistically significant (Figure 4.9F). We observed an increase in the frequency of FOXP3<sup>+</sup>CD39<sup>+</sup> at V10 (post-Treg infusion)(data not shown), suggesting that Treg infusion enriches the peripheral CD39<sup>+</sup> Tregs. However, there was a trend toward a decrease in the number of FOXP3<sup>+</sup>CD39<sup>+</sup> at V17, compared to baseline level (V02) in both groups, although this was not statistically significant (Figure 4.9G-H). These data highlight the changes of Treg subsets over time post-transplantation.

Chapter 4: Cellular and phenotypical analysis of the peripheral immune cell compartment following Treg therapy in renal transplantation

Figure 4.9



## Chapter 4: Cellular and phenotypical analysis of the peripheral immune cell compartment following Treg therapy in renal transplantation

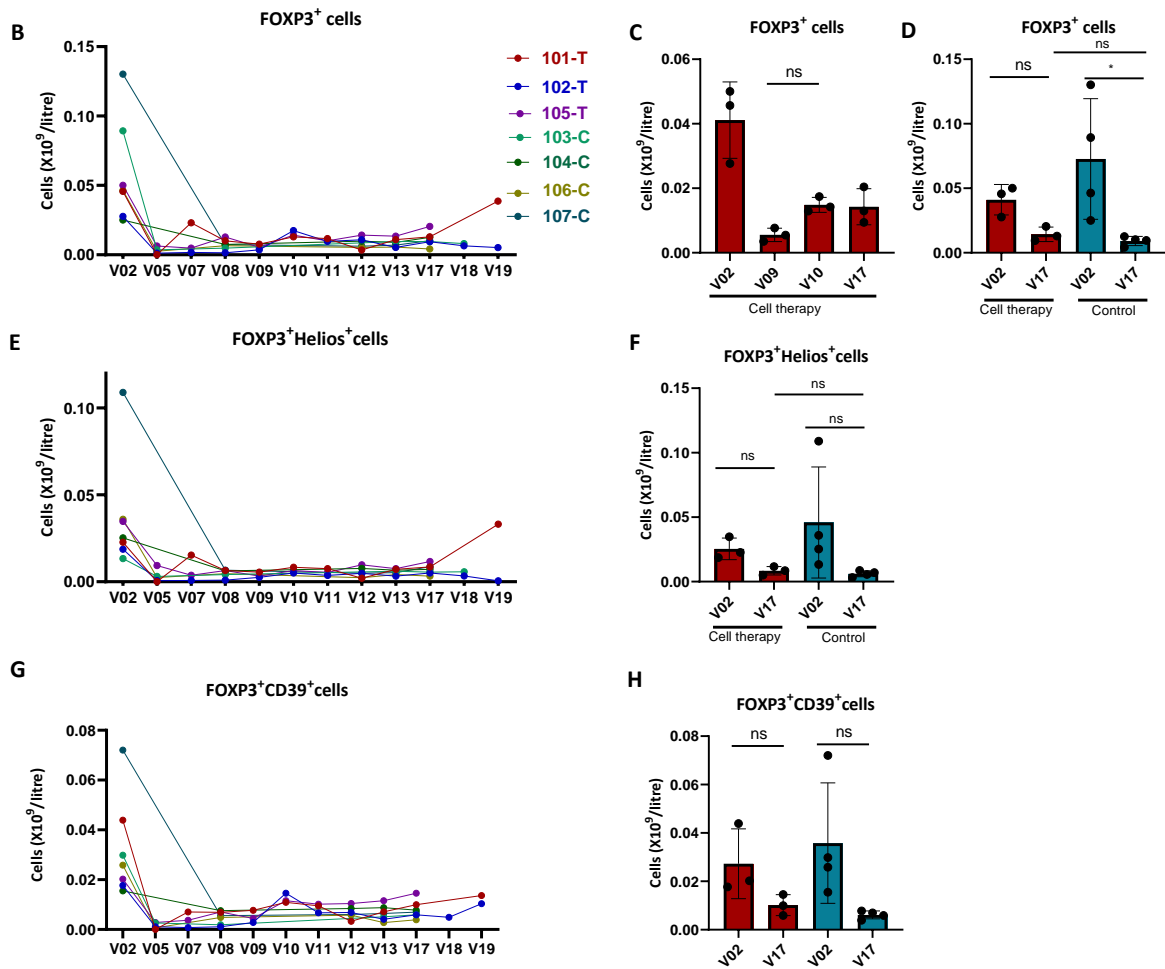


**Figure 4.9. Absolute numbers of Tregs in the peripheral blood of renal transplant recipients over time.** (A) FACS plots show the gating strategy of Tregs and the percentages of FOXP3<sup>+</sup> cells prior to transplantation (V02) and at 24 (V08), 26 (V09), 27 (V10) and 44 (V17) weeks post-transplant from one of the Treg-treated recipients. (B-E-G) Absolute numbers of FOXP3<sup>+</sup> cells, FOXP3<sup>+</sup>Helios<sup>+</sup> cells, and FOXP3<sup>+</sup>CD39<sup>+</sup> cells in the blood samples collected from patients prior to transplantation (V02) and at 12 (V05), 22 (V07), 24 (V08), 26 (V09), 27 (V10), 28 (V11), 30 (V12), 38 (V13), 44 (V17), 52 (V18) and 72 (V19) weeks post-transplant. (C) Absolute numbers of FOXP3<sup>+</sup> cells in the blood samples of the Treg therapy group ( $n = 3$ ) prior to transplantation (V02), before Treg infusion at 26 (V09), after Treg infusion 27 (V10) and at 44 (V17) weeks post-transplant. (D-F-H) Absolute numbers of FOXP3<sup>+</sup> cells, FOXP3<sup>+</sup>Helios<sup>+</sup> cells, and FOXP3<sup>+</sup>CD39<sup>+</sup> cells in the blood samples of the Treg therapy group ( $n = 3$ ) at V02 and V17 (red) compared to the control group ( $n = 4$ ) at V02 and V17 (blue). Dots represent individual samples. Statistical significance was calculated by one-way ANOVA with Tukey's for multiple comparisons, \* $p < 0.05$ , ns = not significant. Data shown as absolute values (B, E, G) or mean  $\pm$  SD.

### 4.4 Phenotypical analysis of the peripheral immune cell compartment in renal transplant recipients by mass cytometry (CyTOF)

#### 4.4.1 Specimens and CyTOF panel

Next, we explored whether using a bigger panel of 30 markers analysed by mass cytometry can have practical and scientific advantages over using flow cytometry based DuraClone

Chapter 4: Cellular and phenotypical analysis of the peripheral immune cell compartment following Treg therapy in renal transplantation

panels. Peripheral blood samples were collected from donors ( $n = 3$ ) and renal transplant recipients (enrolled in the TWO Study trial) at five different time points, including 2 weeks pre-transplant (V02-( $n = 2$ )), 24 (V08-( $n = 4$ )), 30 (V12-( $n = 4$ )), 38 (V13-( $n = 4$ )) and 72 weeks post-transplant (V19-( $n = 1$ )). Fresh blood was stained using 30 markers panel and multiplexed for processing by CyTOF. This panel, designed by Fluidigm, enables the comprehensive identification and characterisation of various immune cells within the peripheral blood of renal transplant recipients (Figure 4.10). This panel was designed to detect all major T cell subsets ( $CD4^+$  and  $CD8^+$  naïve, CM, EM, and terminal effector (TE)), regulatory T cells, NK cells, NKT cells, B cell subsets (naïve, memory and plasmablast), gamma delta ( $\gamma\delta$ ) T cells, monocytes, and DCs, in addition to granulocytes, including basophils, eosinophils and neutrophils (Table 2-4 shows the list of metal-conjugated antibodies used in this assay).

**Figure 4.10**

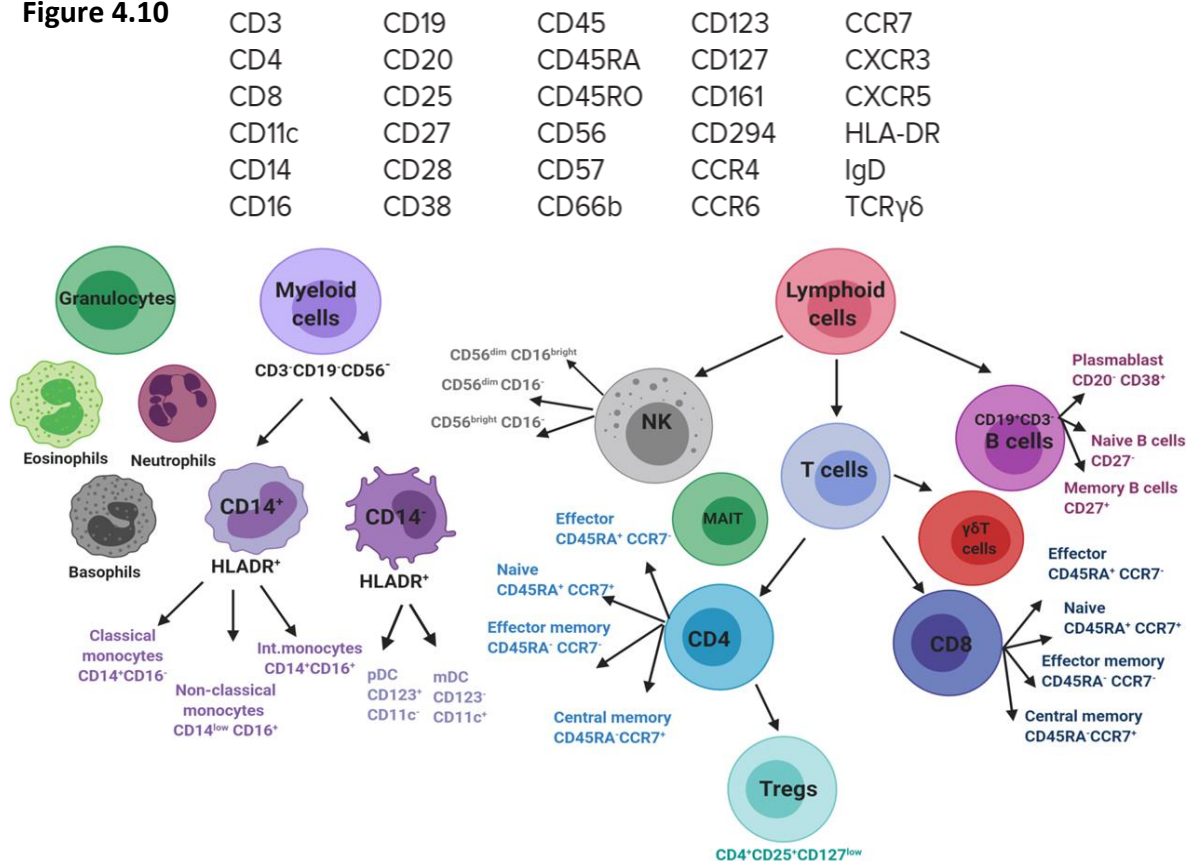


**Figure 4.10. CyTOF panel to study the phenotypical changes of leukocytes in the peripheral blood of renal transplant recipients.** The Maxpar Direct Immune Profiling Kit, designed by Fluidigm, includes 30 antibodies for the comprehensive identification and characterisation of several immune cell populations, including all major T cell subsets ( $CD4^+$  and  $CD8^+$  naïve, CM, EM and TE), regulatory T cells,  $CD4$ -mucosal-associated invariant T cells (MAIT)/natural killer T (NKT) cells, B cell subsets (naïve, memory and plasmablast), NK cells, gamma delta ( $\gamma\delta$ ) T cells, monocytes, dendritic cells (DCs) and granulocytes, including basophils, eosinophils and neutrophils.

## 4.4.2 Results

### 4.4.2.1 Manual gating strategy to identify CD45<sup>+</sup> cells for downstream automated analysis

A clean-up strategy was used to remove debris, normalisation beads, doublets and dead cells prior to cell gating using antibody targets. The Beads parameter was plotted against Time of experimental measurement (in minutes) to select the largest band of events (red-orange-yellow colouring) and to exclude the beads as demonstrated in Figure 4.11. Then, Gaussian discrimination (GD) channels (Center, Width, Offset, Residual) versus Time were used to select the largest band of events and to exclude the doublet. Next, event length, which is generated based on the time taken for the contents of an ion cloud to travel, was used to estimate the cell size, after which the intact cells were gated based on the DNA Intercalator, including <sup>191</sup>Ir and <sup>193</sup>Ir versus Time, which were used to identify nucleated (DNA-containing) cells. This was followed by manual gating of the CD45<sup>+</sup> compartment based on the CD45 vs CD66b channels for the downstream automated analysis.

Figure 4.11

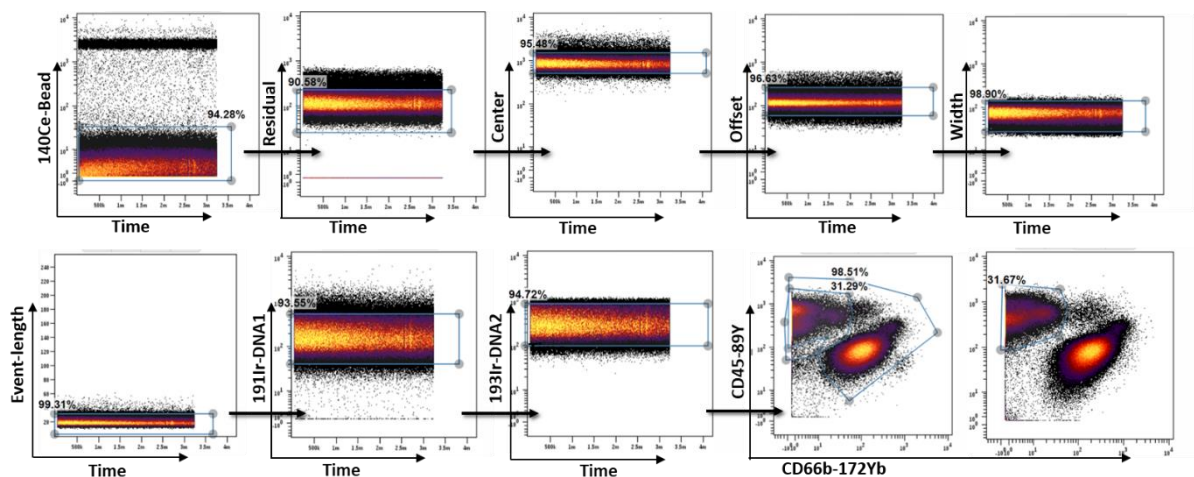


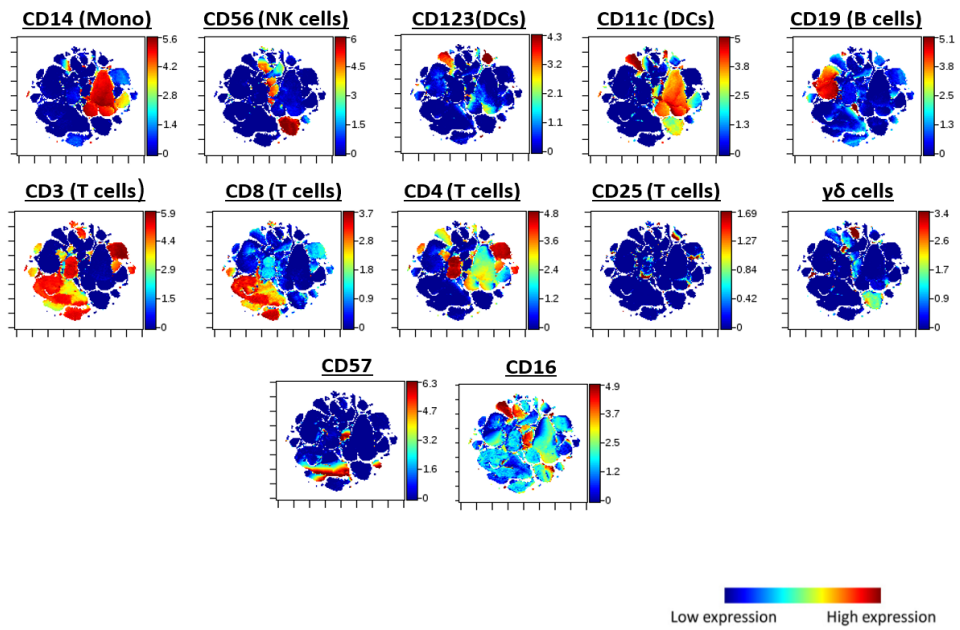
**Figure 4.11. The gating strategy for the clean-up and identification of the CD45<sup>+</sup> compartment by the Cytobank platform.** A clean-up strategy was used to remove debris, normalisation beads, doublets and dead cells. Beads versus Time of experimental measurement (in minutes) was used to gate the low-intensity events and to exclude the beads. Gaussian discrimination (GD) channels (Center, Width, Offset, Residual) versus Time were used for the clean-up method, followed by Event length versus Time, nucleated (DNA-containing) cells, <sup>191</sup>Ir versus Time, and <sup>193</sup>Ir versus Time to identify nucleated cells. A CD45 vs CD66b plot was used to gate the CD45 population manually for the downstream automated analysis.

#### 4.4.2.2 The viSNE map of the CD45 population identifies known immune cells based on the staining intensity of an indicated marker

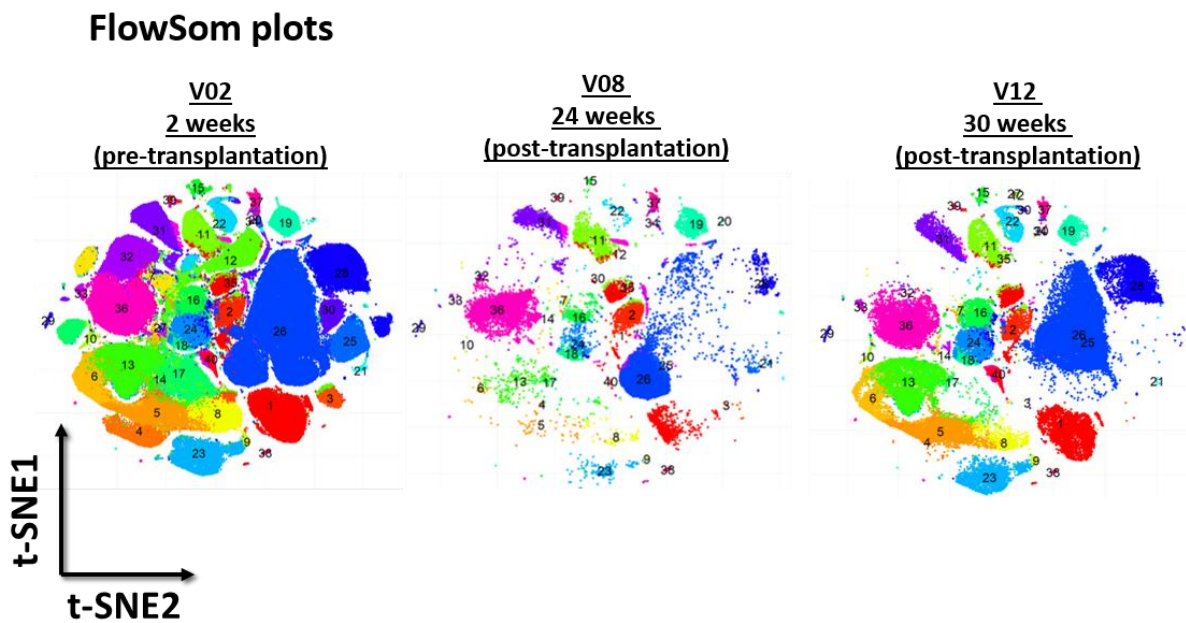
viSNE analysis allows the visualisation of high-dimensional data into a two-dimensional plot using t-distributed stochastic neighbour embedding (t-SNE) algorithms. After gating the CD45<sup>+</sup> cells manually by the Cytobank platform, we used this population for viSNE analysis to visualise the distribution of cell phenotypes. The viSNE map identifies known immune cells based on the staining intensity of an indicated marker. For example, we identified the monocytes based on the intensity of CD14 (Figure 4.12A). We also identified NK cells, DCs, B cells, T cells and  $\gamma\delta$  cells (Figure 4.12A). Before examining the viSNE data in detail, the maps were used to check antibody binding specificity and to confirm that the cellular markers expressed by different cell populations were consistent with the molecules that were expected to be expressed by particular lineages. For example, as expected, CD3<sup>+</sup> T cell islands contain both CD4<sup>+</sup> and CD8<sup>+</sup> islands; these islands were negative for monocyte marker CD14 (Figure 4.12A). Some of the CD56<sup>+</sup> NK cells expressed the NK markers CD16 and CD57, but not CD8 or CD4 (Figure 4.12A). We also used unbiased clustering analysis (FlowSom)<sup>327</sup> to assess the changes in cellular subsets within CD45<sup>+</sup> cells over time including 2 weeks pre-transplant (**V02**-( $n = 2$ )), 24 (**V08**-( $n = 4$ )), (**V13**-( $n = 4$ )). As shown in (Figure 4.12B), the FlowSom analysis identified a total of 40 phenotypically distinct clusters within the CD45 compartment. In addition, FlowSom revealed a depletion in most of the clusters after alemtuzumab induction therapy at 24 weeks post-transplant (V08), which was followed by gradual recovery at 30 weeks post-transplant (V12). The heatmap showed the expression of cellular markers expressed by the cell subsets, which was identified by the FlowSOM analysis (Figure 4.12C).

Figure 4.12

A



B



C

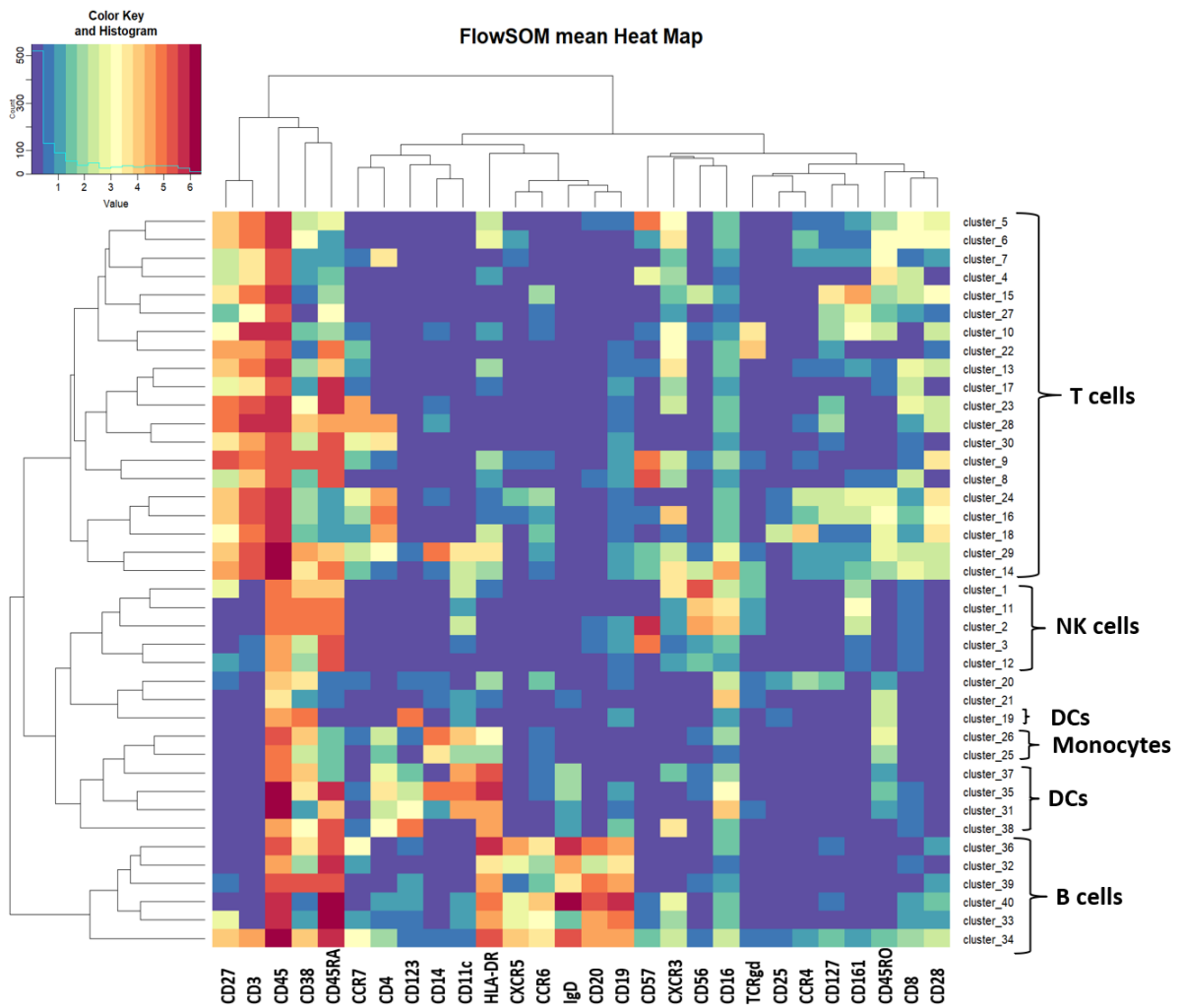


**Figure 4.12. ViSNE maps of CD45<sup>+</sup> cells are coloured according to the staining intensity of the indicated marker. (A)** Merged samples were used to generate visualisation stochastic neighbour embedding (viSNE) plots of CD45<sup>+</sup> cells depicting the expression pattern of CD14<sup>+</sup>, CD56<sup>+</sup>, CD123<sup>+</sup>, CD11c<sup>+</sup>, CD19<sup>+</sup>, CD3<sup>+</sup>, CD8<sup>+</sup>, CD4<sup>+</sup>, CD25<sup>+</sup>,  $\gamma\delta$ <sup>+</sup> T, CD57<sup>+</sup> and CD16<sup>+</sup> cells. **(B)** A FlowSOM clustering algorithm was performed on the total CD45 at 2 weeks pre-transplant (V02), 24 (V08), and 30 (V12) weeks post-transplant to assess distinct cellular subsets within the CD45 population. **(C)** Heatmap showing mean expression of the markers expressed by the cell subsets identified in **(B)**.

#### 4.4.2.3 High-dimensional clustering analysis revealed changes in the peripheral CD4<sup>+</sup> T cell subsets over time

We next examined the changes in CD4<sup>+</sup> T cell subsets post-transplant by performing FlowSOM clustering on the CD4<sup>+</sup> population using 15 cellular markers at five different time points, including 2 weeks pre-transplant (**V02**-(*n* = 2)), 24 (**V08**-(*n* = 4)), 30 (**V12**-(*n* = 4)), 38 (**V13**-(*n* = 4)) and 72 weeks post-transplant (**V19**-(*n* = 1)). FlowSOM identified 10 distinct clusters within the peripheral CD4 compartment, which revealed a high degree of heterogeneity within CD4<sup>+</sup> T cells (Figure 4.13A). We next identified these clusters using the heatmap, which showed the expression of cellular markers on each cluster (Figure 4.13B). For example, clusters #1 and #5 were identified as  $\gamma\delta$  T cell clusters because they expressed the TCR  $\gamma\delta$  marker. Clusters #7 and #9 were identified as naïve T cell clusters because they are CD45RA<sup>+</sup>CCR7<sup>+</sup> (the table in Figure 4.13D shows in detail the cellular markers expressed on each cluster). We then assessed the changes in the CD4 clusters, including naïve (CD45RA<sup>+</sup>CD45RO<sup>neg</sup> CCR7<sup>+</sup>, clusters #7 and #9), EM (CD45RA<sup>neg</sup> CD45RO<sup>+</sup> CCR7<sup>neg</sup>, cluster #10), CM (CD45RA<sup>neg</sup>CD45RO<sup>+</sup> CCR7<sup>+</sup>, cluster #8), and TEMRA (CD45RA<sup>+</sup>CCR7<sup>neg</sup>, clusters #2, #3, #4 and #6) subsets over time post-transplant, as well as the  $\gamma\delta$  CD4 T cells (clusters #1 and #5). Analysis revealed an expansion in clusters #1 and #5 post-transplant (at V08, V12 and V13), followed by reduction at V19 (Figure 4.13C and D). This observation is in agreement with the flow cytometry immune-monitoring data, which showed a slight expansion in the number of  $\gamma\delta$  T cells over-time post transplant (Figure 4.6A). Moreover, generally, there was an increase in the percentages of clusters #2, #3, #4 and #6 post-transplant (V08, V12, V13 and V19) compared to the baseline (V02) (Figure 4.13C). These clusters were identified as TEMRA CD4 clusters as they were CD45RA<sup>+</sup> and CCR7<sup>neg</sup>. Among these clusters, an interesting expansion was seen in cluster #4 at a single V19 time point, compared to V02 (Figure 4.13C). The heatmap revealed that cluster #4 was a TEMRA subset that expressed the chemokine receptor CXCR3, activation markers CD27 and CD38, and exhaustion marker CD57 (Figures 4.13B and D). It will be of interest to determine if this observation would be repeated in further patients as more patients reach the last immune monitoring time point. In addition, a clear reduction in the percentages of naïve cluster #9 was seen at all post-transplant time points, compared to V02 (Figure 4.13C). These observations are in line with flow cytometry immune-monitoring data, which showed a trend towards reduction in the absolute number of naïve CD4 subset over time post-transplant (Figure 4.4E).

Chapter 4: Cellular and phenotypical analysis of the peripheral immune cell compartment following Treg therapy in renal transplantation

Figure 4.13

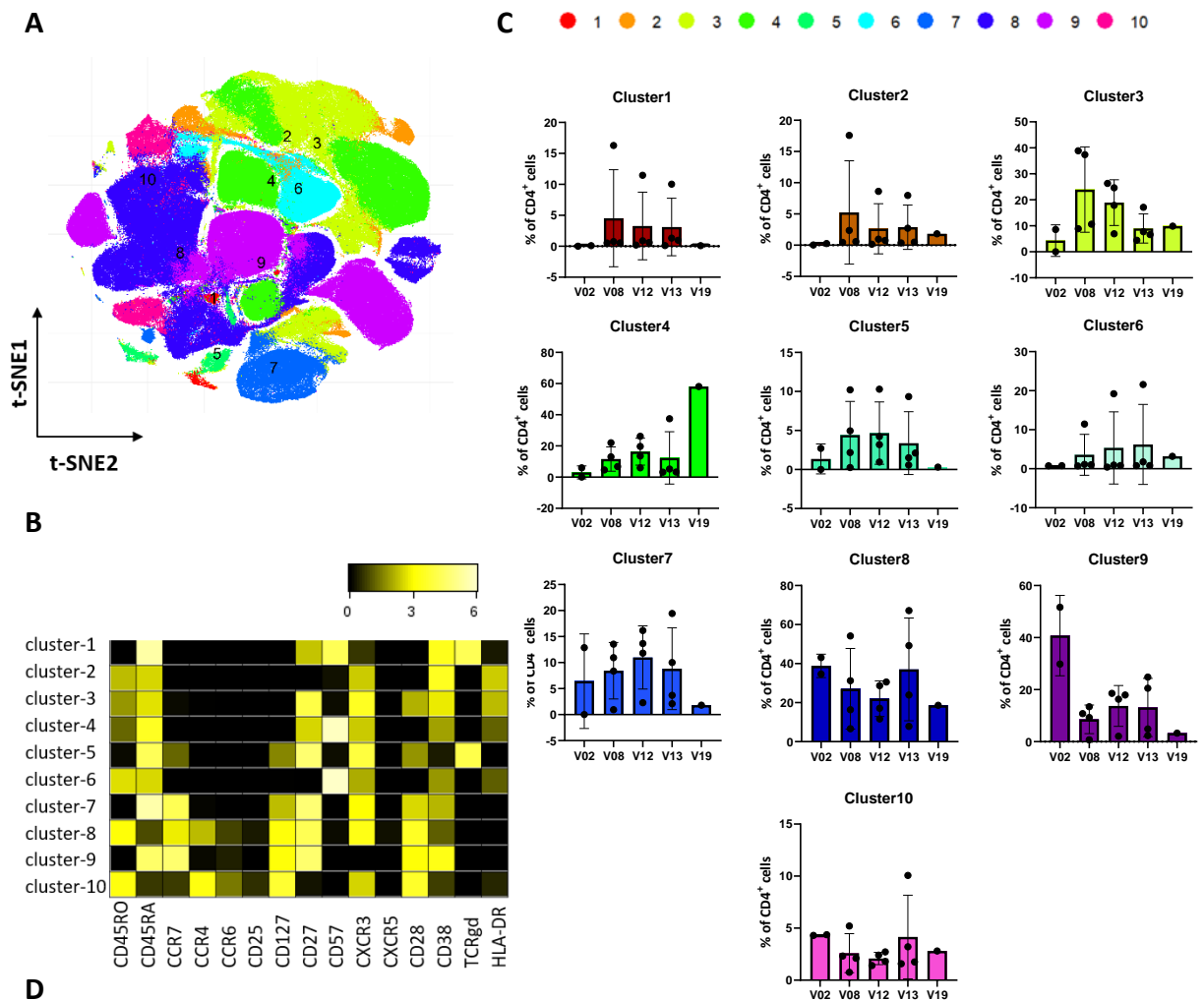


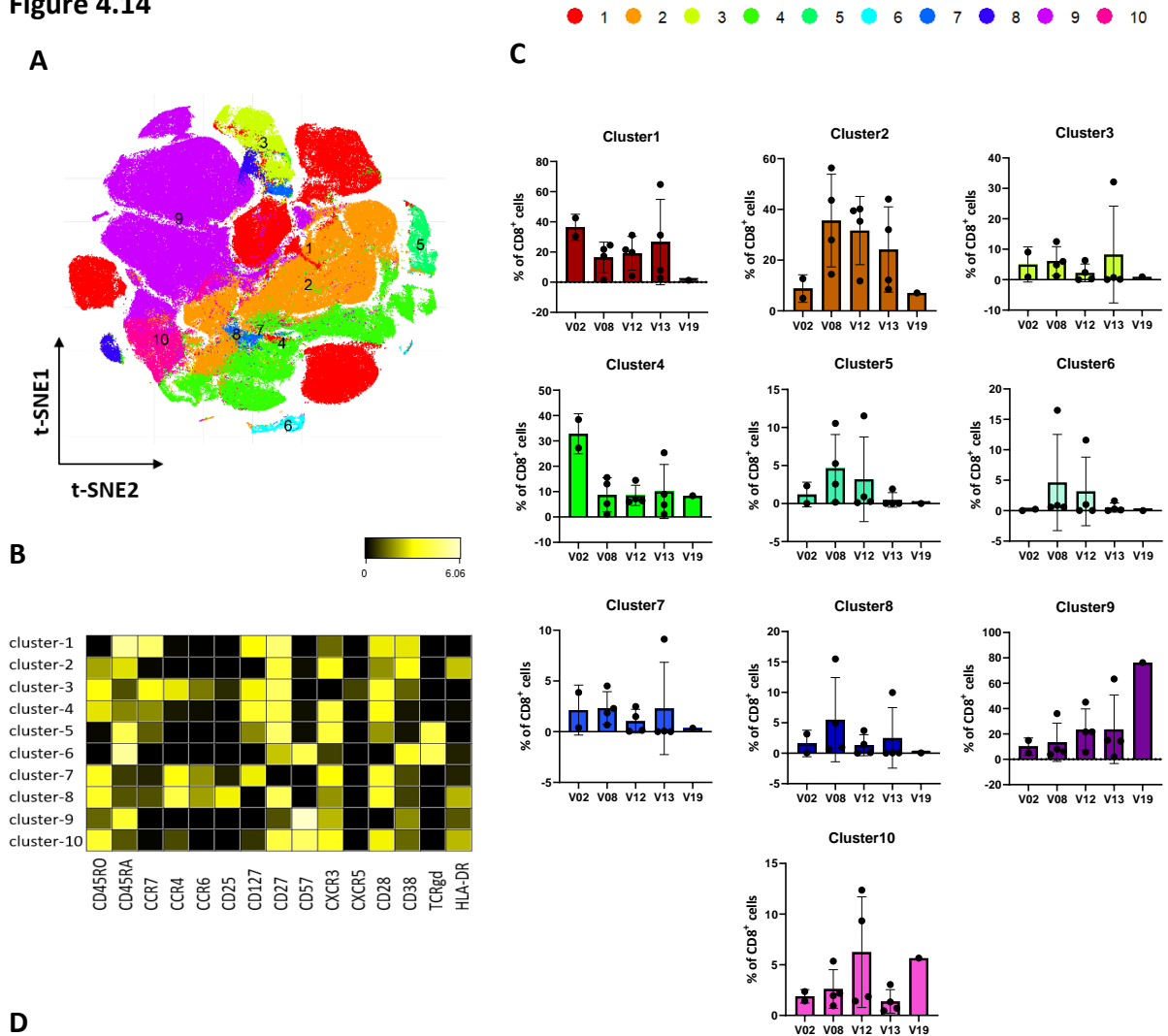
**Figure 4.13. Analysis of the peripheral CD4<sup>+</sup> compartment over time by CyTOF.** (A) Representative viSNE analysis of peripheral CD4<sup>+</sup> T cells using the FlowSOM clustering algorithm from the peripheral blood of healthy donors ( $n = 2$ ) and renal transplant recipients prior to transplantation (V02:  $n = 2$ ) and at 24 (V08:  $n = 4$ ), 30 (V12:  $n = 4$ ), 38 (V13:  $n = 4$ ) and 72 (V19:  $n = 1$ ) weeks post-transplant. (B) Heatmap showing the median expression of cellular markers expressed in the clusters identified by FlowSOM. (C) Percentages of each cluster within the CD4 compartment calculated by the FlowSOM algorithm at (V02), 24 (V08), 30 (V12), 38 (V13) and 72 (V19) weeks post-transplant. Dots represent individual samples. (D) Table shows that CD4 clusters were identified based on their cellular marker expression.

#### 4.4.2.4 High-dimensional clustering analysis revealed changes in the peripheral CD8 subsets over time

We next analysed the changes in CD8 T cell subsets over time post-transplant by performing the same unbiased clustering strategy on the CD8<sup>+</sup> compartment using 15 cellular markers at five different time points, including 2 weeks pre-transplant (V02-( $n = 2$ )), 24 (V08-( $n = 4$ )), 30 (V12-( $n = 4$ )), 38 (V13-( $n = 4$ )) and 72 weeks post-transplant (V19-( $n = 1$ )). The analysis revealed heterogeneity within the CD8 T cells manifesting in 10 distinct clusters (Figure 4.14A). These clusters were visualised on the heatmap, which showed the expression of cellular markers on each cluster (Figure 4.14B). We deconvoluted the frequencies of naïve (cluster #1), CM (cluster #3), EM (clusters #4, #7, #8 and #10) and TEMRA (clusters #2 and #9) subsets. The analysis revealed a reduction in the frequency of clusters #4 (EM) post-transplant versus the baseline (Figure 4.14C and D). We observed a defined subset of EM CD8 T cells (cluster #8) characterised by the expression of CCR4, CCR6, CD25, and CXCR3, which was reduced post-transplant compared to the baseline (Figure 4.14C and D). The analysis also revealed an increase post transplantation in the frequency of TEMRA clusters #2, and #9 (Figure 4.14C and D). These observations are in line with flow cytometry immune-monitoring data, which showed a slight increase in the absolute number of TEMRA CD8 subset in some patients over time post-transplant (Figure 4.4F).

Chapter 4: Cellular and phenotypical analysis of the peripheral immune cell compartment following Treg therapy in renal transplantation

Figure 4.14



CD8 <sup>+</sup> clusters	Markers
Cluster1-Naive	CD45RA <sup>+</sup> CCR7 <sup>+</sup> CD27 <sup>+</sup> CD28 <sup>+</sup> CD38 <sup>+</sup>
Cluster2-TEMRA	CD45RA <sup>+</sup> CCR7 <sup>neg</sup> CD27 <sup>+</sup> CXCR3 <sup>+</sup> CD38 <sup>+</sup> HLA-DR <sup>+</sup>
Cluster3-CM	CD45RA <sup>neg</sup> CD45RO <sup>+</sup> CCR7 <sup>+</sup> CCR4 <sup>+</sup> CD27 <sup>+</sup> CD28 <sup>+</sup>
Cluster4-EM	CD45RO <sup>+</sup> CD45RA <sup>low</sup> CCR7 <sup>low</sup> CD27 <sup>+</sup> CXCR3 <sup>+</sup> CD28 <sup>+</sup>
Cluster5- $\gamma\delta$ T cells	CD45RA <sup>+</sup> TCR $\gamma\delta$ <sup>+</sup> CXCR3 <sup>+</sup> CD27 <sup>+</sup> CD57 <sup>neg</sup> CD28 <sup>+</sup> CD38 <sup>neg</sup>
Cluster6- $\gamma\delta$ T cells	CD45RA <sup>+</sup> TCR $\gamma\delta$ <sup>+</sup> CXCR3 <sup>neg</sup> CD27 <sup>+</sup> CD57 <sup>+</sup> CD28 <sup>neg</sup> CD38 <sup>+</sup>
Cluster7-EM	CD45RO <sup>+</sup> CD45RA <sup>neg</sup> CCR7 <sup>neg</sup> CXCR3 <sup>+</sup> CD27 <sup>+</sup>
Cluster8-EM	CD45RO <sup>+</sup> CCR4 <sup>+</sup> CCR6 <sup>+</sup> CD25 <sup>+</sup> CD127 <sup>neg</sup> CD27 <sup>+</sup> CXCR3 <sup>+</sup> CD28 <sup>+</sup> HLA-DR <sup>+</sup>
Cluster9- TEMRA	CD45RA <sup>+</sup> CCR7 <sup>neg</sup> CD57 <sup>+</sup> CXCR3 <sup>+</sup> CD27 <sup>neg</sup>
Cluster10-EM	CD45RO <sup>+</sup> CD45RA <sup>neg</sup> CCR7 <sup>neg</sup> CD27 <sup>+</sup> CD57 <sup>+</sup> CXCR3 <sup>+</sup>

**Figure 4.14. Analysis of the peripheral CD8<sup>+</sup> compartment over time by CyTOF. (A)** Representative viSNE analysis of peripheral CD8<sup>+</sup> T cells using the FlowSOM clustering algorithm from the peripheral blood of healthy donors ( $n = 2$ ) and renal transplant recipients prior to transplantation (V02:  $n = 2$ ) and at 24 (V08:  $n = 2$ ), 30 (V12:  $n = 4$ ), 38 (V13:  $n = 4$ ) and 72 (V19:  $n = 1$ ) weeks post-transplant. **(B)** Heatmap showing the median expression of cellular markers expressed in the clusters identified by FlowSOM. **(C)** Percentages of each cluster within the CD8 compartment calculated by the FlowSOM algorithm at (V02) and at 24 (V08), 30 (V12), 38 (V13) and 72 (V19) weeks post-transplant. Dots represent individual samples. **(D)** Table shows that CD8 clusters were identified based on their cellular marker expression.

#### 4.4.2.5 Changes in peripheral B cell subsets post-transplant

We next examined changes in the B cell subsets after transplant by performing unbiased clustering on CD19<sup>+</sup> cells over time. FlowSOM analysis revealed heterogeneity within the B cells manifested by six distinct clusters (Figure 4.15A). We then identified these clusters using a heatmap, which showed the expression of cellular markers on each cluster (Figure 4.15B). We analysed the frequencies of B cell clusters over time post-transplant. The analysis revealed an increase in the frequencies of cluster #1 post-transplant compared to the baseline, with the cells in this cluster having the naïve B cell phenotype, as they were CD19<sup>+</sup> CD20<sup>+</sup> IgD<sup>+</sup> CD27<sup>neg</sup>, and they were express CCR6, CCR7, and CXCR5 (Figure 4.15B). We also observed a strong reduction in the frequencies of cluster #3, and #5 (marginal zone B cells), and cluster #4 (switched memory B cells) post-transplant compared to the baseline (Figure 4.15B). This finding suggests that the induction therapy alemtuzumab shifted the B cell compartment into a high level of naïve phenotypes. We also observed the appearance of cluster #6 post-transplant, which might be transitional B cells, as these cells were mainly CD27<sup>neg</sup> and expressed a high level of CD38. These results confirm the flow cytometry analysis of peripheral B cells, which showed an increase in the naïve B cells and an increase in transitional B cells post-transplant (Figure 4.7).

Figure 4.15

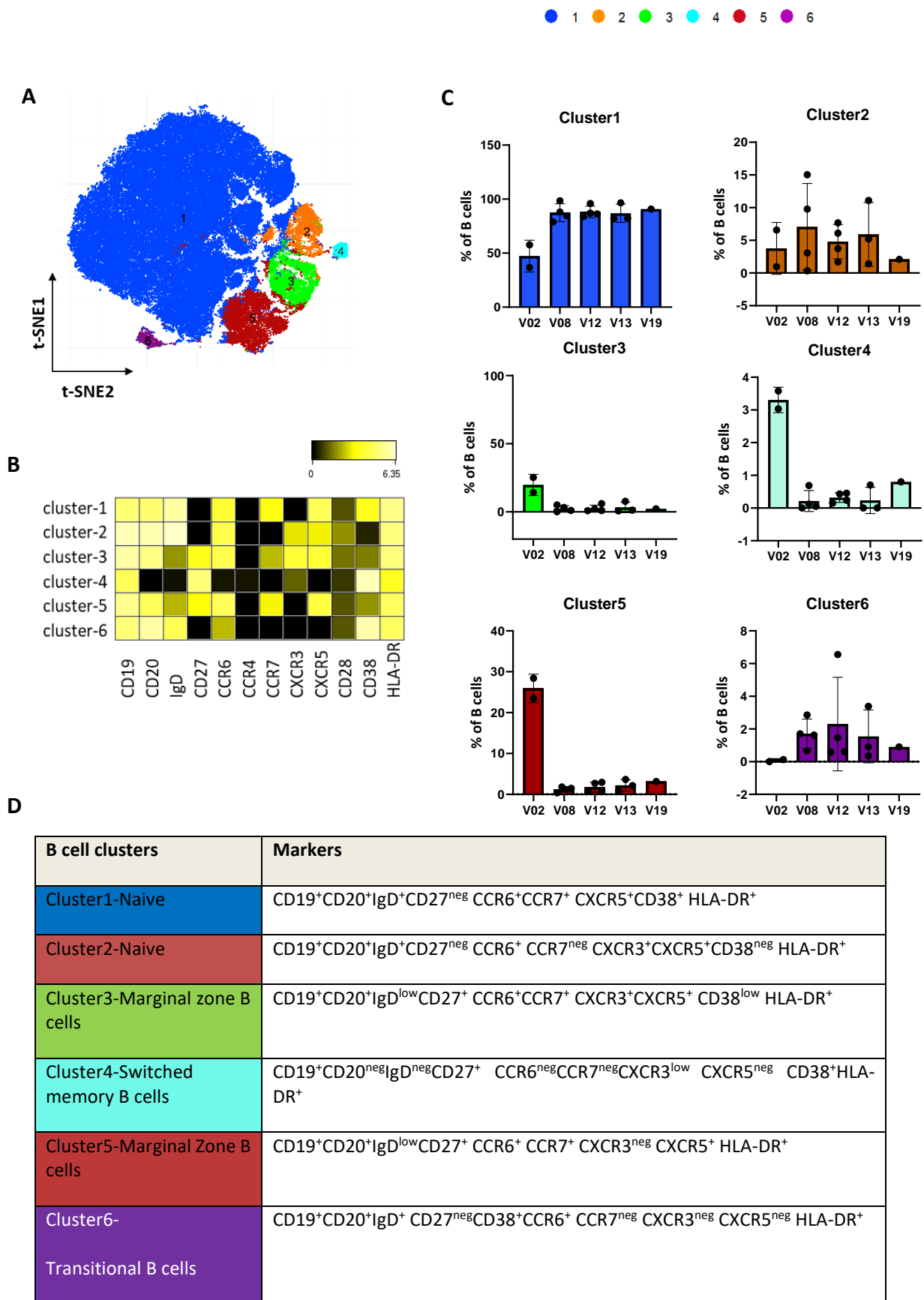


**Figure 4.15. Analysis of peripheral B cells over time by CyTOF. (A)** Representative viSNE analysis of peripheral B cells using the FlowSOM clustering algorithm from the peripheral blood of healthy donors ( $n = 2$ ) and renal transplant recipients prior to transplantation (V02:  $n = 2$ ) at 24 (V08:  $n = 4$ ), 30 (V12:  $n = 4$ ), 38 (V13:  $n = 4$ ) and 72 (V19:  $n = 1$ ) weeks post-transplant. **(B)** Heatmap showing the median expression of cellular markers expressed in the clusters identified by FlowSOM. **(C)** Percentages of each cluster within the B cell compartment calculated by the FlowSOM algorithm at (V02) and at 24 (V08), 30 (V12), 38 (V13) and 72 (V19) weeks post-transplant. Dots represent individual samples. **(D)** Table shows B cell clusters identification based on specific marker expression.

#### 4.4.2.6 Changes in peripheral NK and NKT cell subsets post-transplant

We next examined the changes in the NK and NKT subsets after transplant by performing unbiased clustering on the CD56<sup>+</sup> population. FlowSOM analysis revealed heterogeneity within the NK and NKT cells manifested by five distinct clusters (Figure 4.17A). We then identified the clusters using the heatmap, which showed the expression of cellular markers on each cluster (Figure 4.16B). We next analysed the frequencies of identified clusters over time post-transplant. We found that 4 out of 5 clusters (cluster #1 – cluster #4) were CD56<sup>dim</sup> and CD16<sup>+</sup>, and expressed a CD3 marker, thus likely belonging to the NKT cell compartment, while cells in cluster #5 were CD56<sup>bright</sup>CD16<sup>high</sup> and negative for CD3, forming the main NK cell subset (Figures 4.16 C and D).

Figure 4.16

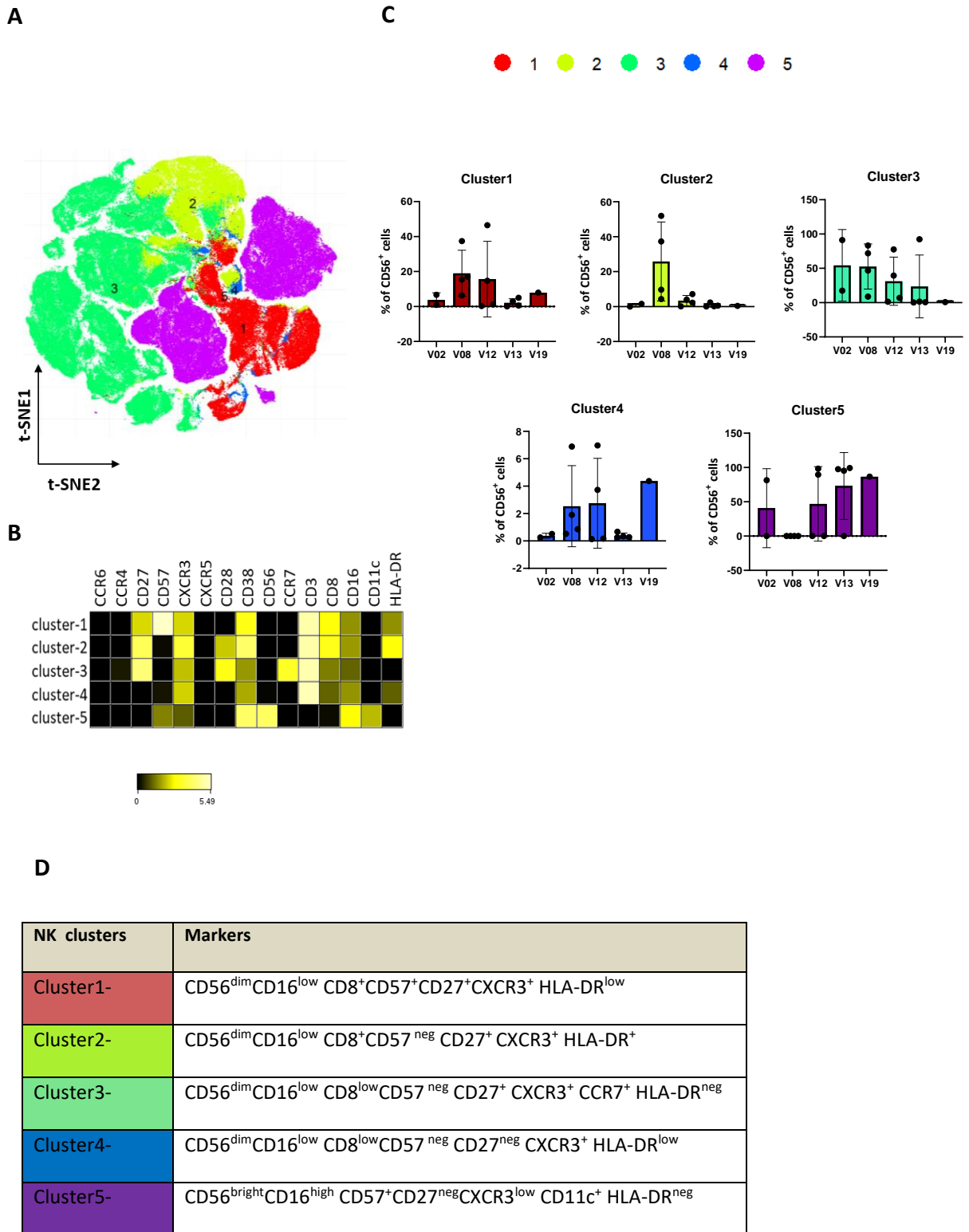


**Figure 4.16. Analysis of peripheral NK and NKT cells over time by CyTOF. (A)** Representative viSNE analysis of CD56<sup>+</sup> cells using the FlowSOM clustering algorithm from the peripheral blood of healthy donors ( $n = 2$ ) and renal transplant recipients prior to transplantation (V02:  $n = 2$ ) at 24 (V08:  $n = 4$ ), 30 (V12:  $n = 4$ ), 38 (V13:  $n = 4$ ) and 72 (V19:  $n = 1$ ) weeks post-transplant. **(B)** Heatmap showing the median expression of cellular markers expressed in the clusters identified by FlowSOM. **(C)** Percentages of each cluster within the CD56<sup>+</sup> cell compartment calculated by the FlowSOM algorithm at (V02) and at 24 (V08), 30 (V12), 38 (V13) and 72 (V19) weeks post-transplant. Dots represent individual samples. **(D)** Table shows that the NK and NKT cell clusters were identified based on their cellular marker expression.

#### 4.4.2.7 Changes in peripheral monocyte subsets post-transplant

We also examined the changes in the monocyte population over time post-transplant by performing unbiased clustering on the CD14<sup>+</sup> compartment. The FlowSOM analysis revealed heterogeneity within the monocytes manifesting in 10 distinct clusters (Figure 4.17A and B). Clusters #3, #5, #6, and #7 were excluded from the analysis as their frequencies were below 1%. We observed an increase in the frequency of cluster #9 post-transplant over the baseline, these cells were expressed CD14<sup>+</sup> and CD16<sup>int</sup>, thus likely belonging to classical monocytes subset (Figures 4.17C and D).

Figure 4.17

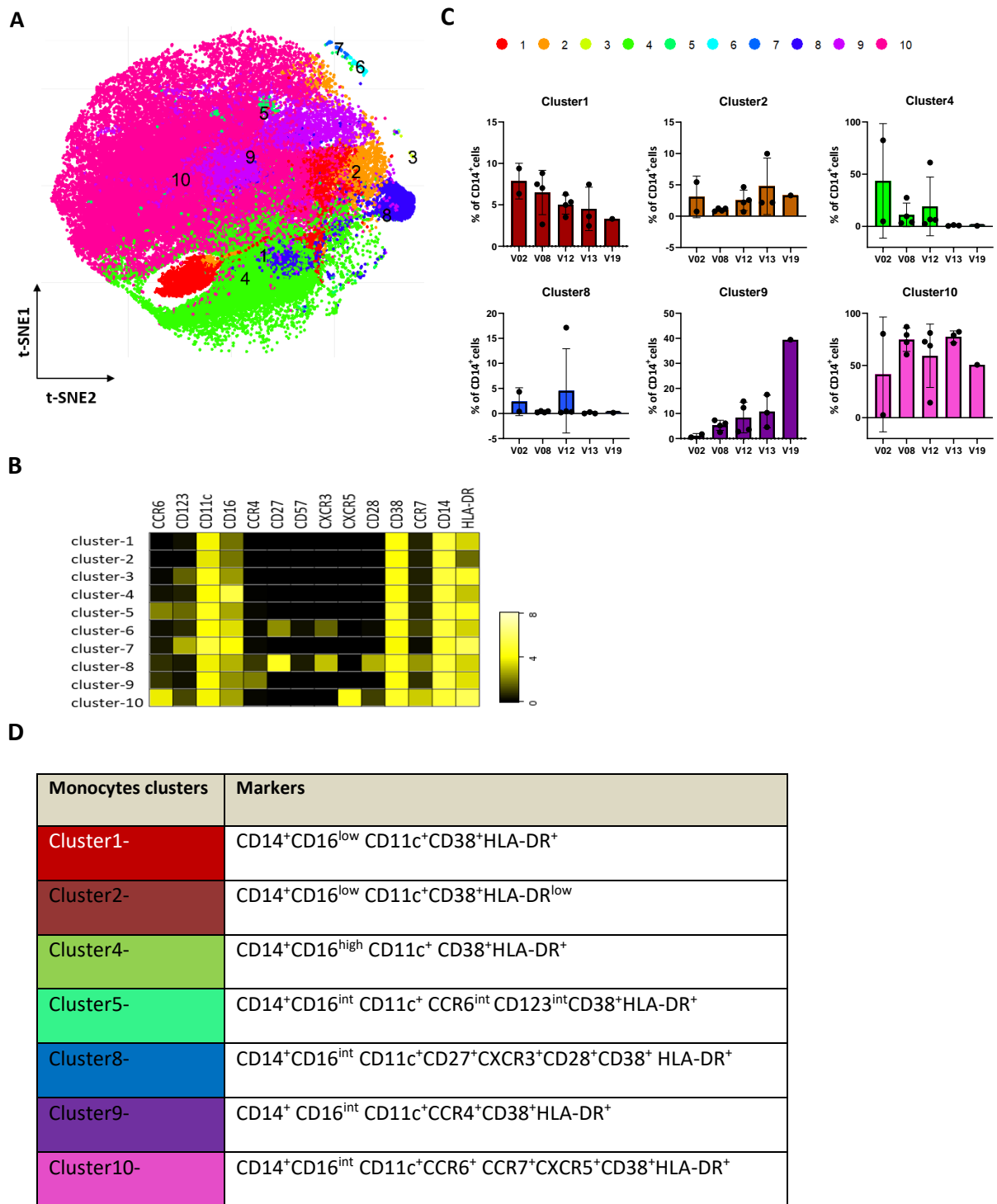


**Figure 4.17. Analysis of peripheral monocyte subsets over time by CyTOF. (A)** Representative viSNE analysis of peripheral monocytes using the FlowSOM clustering algorithm from the peripheral blood of healthy donors (n = 2) and renal transplant recipients prior to transplantation (V02: n = 2) and at 24 (V08: n = 4), 30 (V12: n = 4), 38 (V13: n = 4) and 72 (V19: n = 1) weeks post-transplant. **(B)** Heatmap showing the median expression of cellular markers expressed in the clusters identified by FlowSOM. **(C)** Percentages of each cluster within the monocyte compartment calculated by the FlowSOM algorithm at (V02), 24 (V08), 30 (V12), 38 (V13) and 72 (V19) weeks post-transplant. Dots represent individual samples. **(D)** Table showing monocyte clusters identified based on

## Chapter 4: Cellular and phenotypical analysis of the peripheral immune cell compartment following Treg therapy in renal transplantation

their specific expression. Clusters #3, #5, #6, and #7 were excluded from the analysis as their frequencies were below 1%.

### 4.5 Phenotypical analysis of peripheral Treg compartment by mass cytometry (CyTOF)

#### 4.5.1 Study design and participants

In order to further characterise the peripheral Treg compartment in patients receiving Treg cell therapy, we utilised available samples from a preliminary, small scale phase I study utilising the same cell product as the current trial. This was a phase I clinical trial of autologous polyclonal-expanded Tregs in renal transplant patients (The ONE Study (EuDra CT, No 2011-004301-24)).<sup>105</sup> The aim of this study was to assess the feasibility and safety of several immune regulatory cells using a single standardized immunosuppression regime and a reference cohort, which was used as a comparison. Patients in the control arm received basiliximab as an induction therapy followed by standard maintenance immunosuppression (tacrolimus, MMF, and a reducing dose of prednisolone), while patients in the cell therapy arm received the same standard maintenance immunosuppression drugs but without basiliximab. These patients received a single dose of up to  $10 \times 10^6$ /kg autologous polyclonal-expanded Tregs on day 5 post-transplant.

#### 4.5.2 Specimens and CyTOF panel

Peripheral blood mononuclear cells (PBMCs) were collected from six renal transplant recipients from the cell therapy arm at three different time points: pre-transplantation (**V01**:  $n = 6$ ), 2 weeks post-transplantation (**V03**:  $n = 3$ ) and 60 weeks post-transplantation (**V10**:  $n = 6$ ). These were compared to PBMCs at 60 weeks post-transplantation (**V10**:  $n = 3$ ) collected from patients in the control arm of the trial, as demonstrated in (Figure 4.18).  $CD4^+$  cells were isolated and multiplexed for processing by CyTOF. In this assay, we used a panel of 36 metal-labelled monoclonal antibodies specific for surface and intracellular markers associated with Treg function and phenotype (Table 2-5 shows the list of antibodies used in this assay).

Figure 4.18

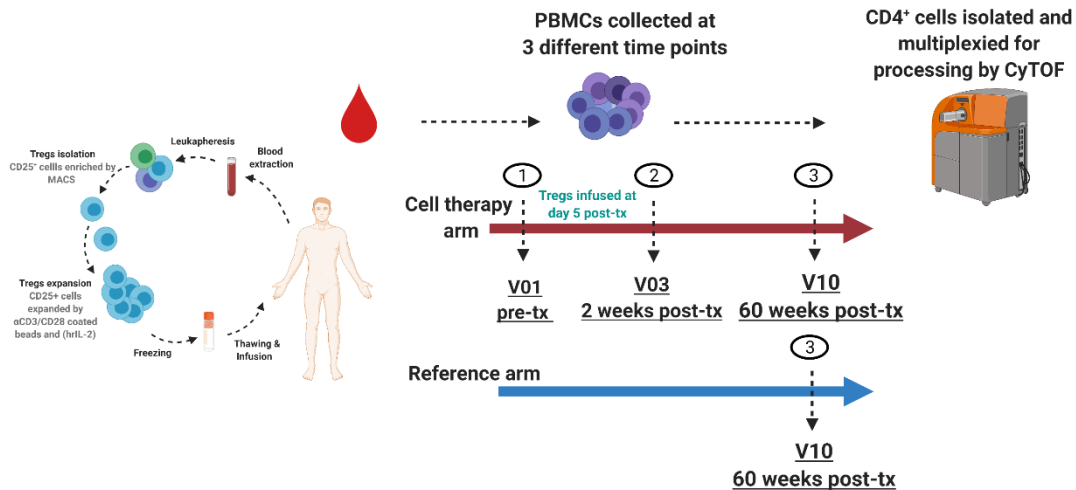


**Figure 4.18. Experimental design for phenotyping analysis of peripheral Tregs from renal transplant recipients receiving Treg therapy.** Six renal transplant patients received a single dose of up to  $10 \times 10^6$ /kg autologous polyclonally expanded Tregs shortly after transplantation followed by standard maintenance immunosuppression. PBMCs were collected at three different time points: V01, pre-transplantation; V03, 2 weeks post-transplantation; and V10, 60 weeks post-transplantation. CD4<sup>+</sup> cells were isolated and multiplexed for processing by CyTOF mass spectrometry. The phenotype and composition of peripheral Tregs were examined using a dedicated 36-antigen panel.

## 4.5.3 Results

### 4.5.3.1 Changes in peripheral blood Treg frequency after infusion of Treg therapy in renal transplant recipients

CD4<sup>+</sup> T cells and CD4<sup>+</sup>CD25<sup>+</sup>CD127<sup>low</sup> were gated manually using the Cytobank platform for downstream analysis. Then, the high-dimensional viSNE analysis was applied to the CD4 compartment to visualise the T cell clusters. CD4 viSNE maps were annotated based on the intensity of FOXP3 expression. As shown in (Figure 4.19A), Tregs were identified by the expression of FOXP3 (red) and clustered together into a distinct CD4<sup>+</sup> population. We observed changes in Treg frequency as a percentage of total CD4<sup>+</sup> T cells between V01 (4 weeks pre-transplantation) and V03 (2 weeks post-transplantation) or at V10 (60 weeks post-transplantation) (Figure 4.19A and B). However, these changes were not statistically

significant. The percentages of Tregs at V10 (60 weeks post-transplantation) were at a similar level between Treg-treated patients and control patients (Figure 4.19C).

**Figure 4.19**

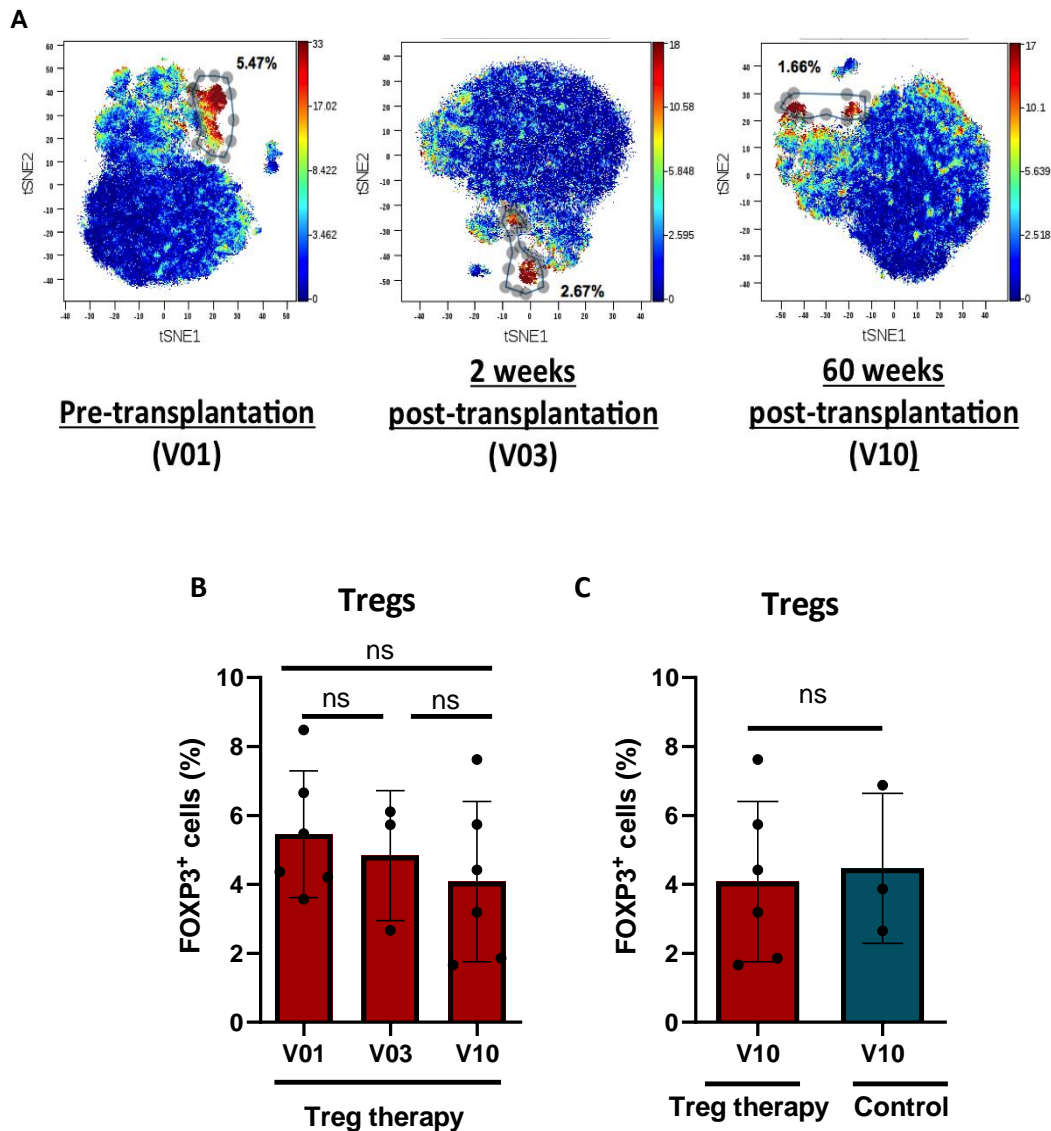


**Figure 4.19.** The frequency of Tregs (gated as FOXP3<sup>+</sup> cells) within peripheral blood CD4<sup>+</sup> T cells assessed in renal transplant recipients receiving an infusion of Treg therapy. **(A)** t-distributed stochastic neighbour embedding (t-SNE) plot of CD4<sup>+</sup> cells annotated based on the intensity of FOXP3 expression from one patient pre-transplantation (V01), and at 2 (V03) and 60 (V10) weeks post transplantation. **(B)** Changes in Treg frequency as a percentage of total CD4<sup>+</sup> T cells between V01, V03 and V10 in Treg-treated patients. one-way ANOVA with Tukey's was used for multiple comparisons. ns = non-significant **(C)** Treg frequency at V10 (60 weeks post-transplantation) in Treg-treated patients (red) and control patients (blue). Scatter dots represent individual samples. Statistical significance was analysed by unpaired *t*-tests. ns = non-significant. Data shown as mean +/- SD.

#### 4.5.3.2 Expression of Treg-related cellular markers

PhenoGraph is another automated clustering method, it can automatically optimise the number of clusters.<sup>371</sup> Therefore, it has been used here over other techniques. PhenoGraph was performed on the total Treg compartment from all samples to assess distinct cellular subsets within Tregs. Clustering analysis identified a total of 20 phenotypically distinct subsets (Figure 4.20A).

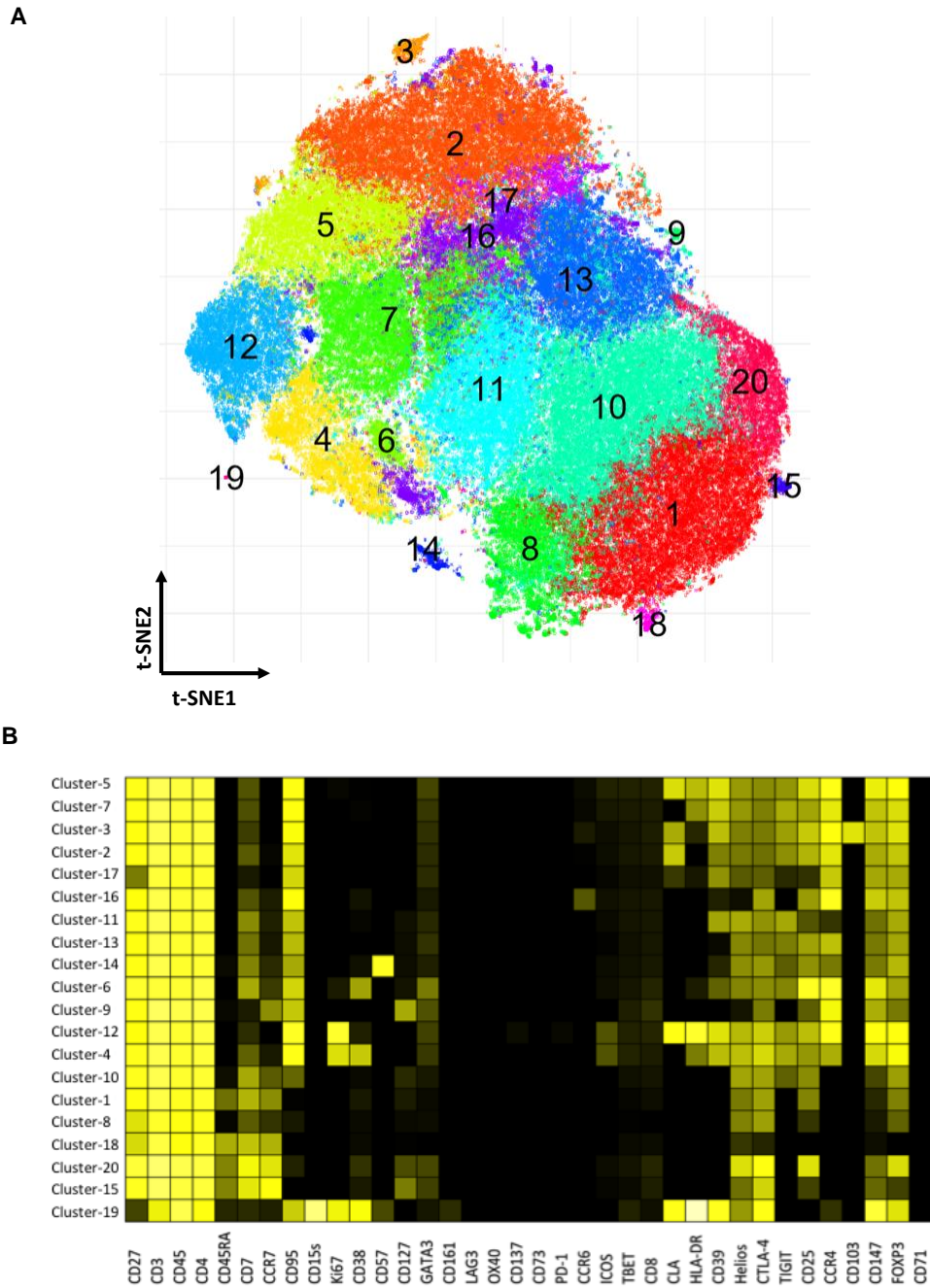
Heatmap analysis demonstrated a median expression of individual cellular markers in the 20 Treg clusters. Initially, we found a high expression of Treg functional markers, including CD25, FOXP3 and Helios, and a high expression of co-inhibitory/co-stimulatory molecules, including CTLA-4 and TIGIT (Figure 4.20B). The detailed analysis of these clusters revealed characteristics consistent with published reports. For example, reduced CD45RA expression was noted in the CD147<sup>+</sup> Treg subsets with clear gradients of FOXP3 and CTLA-4 expressions (Figure 4.20B). This is consistent with a previous report that suggested that CD147 identifies FOXP3<sup>+</sup> CTLA-4<sup>+</sup> CD45RO<sup>+</sup>-activated human Tregs.<sup>372</sup> Our analysis revealed more detailed phenotypical characteristics of CD147<sup>+</sup> Tregs, as we observed that CD147 expression correlated well with CD95<sup>+</sup> Treg subsets, Helios<sup>+</sup> Treg subsets (except clusters #9 and #16), CD27<sup>+</sup> Treg subsets, TIGIT<sup>+</sup> Treg subsets (except clusters #9 and #16), and CCR4<sup>+</sup> Treg subsets. Furthermore, high FOXP3 expression and low CD45RA expression were noted in CCR4<sup>+</sup> Treg subsets. This is similar to previous findings, which described CCR4<sup>+</sup> Tregs as an effector Tregs that expresses high levels of FOXP3 and low levels of CD45RA.<sup>373</sup> We also found that CCR4 expression correlated with CD25<sup>+</sup> Treg subsets, CD95<sup>+</sup> Treg subsets, CD27<sup>+</sup> Treg subsets, Helios<sup>+</sup> Treg subsets (except clusters #9 and #16), CTLA-4<sup>+</sup> Treg subsets, TIGIT<sup>+</sup> Treg subsets (except clusters #9 and #16), as well as CD147<sup>+</sup> Treg subsets. In addition, we found that CD39 expression correlated well with HLA-DR or CLA expression and with Treg functional markers, including FOXP3, Helios, CTLA-4, CD27 and CD95 (Figure 4.20B).

Next, we used the samples from Treg-treated patients at different time points (**V01, V03, and V10**) to generate viSNE maps. These maps were annotated based on the expression of specified parameters. The viSNE maps showed an enrichment of Treg key functional and stable markers, including Helios, CD27, CD39 and CTLA-4, over time, and the level of enrichment was comparable to that from the control group (Figure 4.20C). Interestingly, viSNE maps demonstrated that a cluster in the left side of viSNE plots (highlighted by arrows) was

Chapter 4: Cellular and phenotypical analysis of the peripheral immune cell compartment following Treg therapy in renal transplantation

diminished at the V03 time point (2 weeks post-transplant) (Figure 4.20C). This cluster was identified by PhenoGraph analysis as cluster #12 (Figure 4.20A). The phenotype of this cluster demonstrated a highly proliferative Treg subset, as it expressed KI67, ICOS, HLA-DR and CCR4 and also cutaneous lymphocyte-associated antigen (CLA) (Figure 4.20B), suggesting that this highly proliferative Treg subset could be more susceptible to immunosuppressive drugs or cells from this cluster have trafficked to the allograft. Interestingly, a recovery of this cluster was seen at 60 weeks post-transplant (Figure 4.20C). Taken together, these data demonstrated the phenotypical complexity of the Treg compartment at high resolution and suggested the enrichment of Treg key functional markers over time, as well as demonstrating intriguing specific cluster alteration early post transplantation and Treg treatment.

Figure 4.20



C

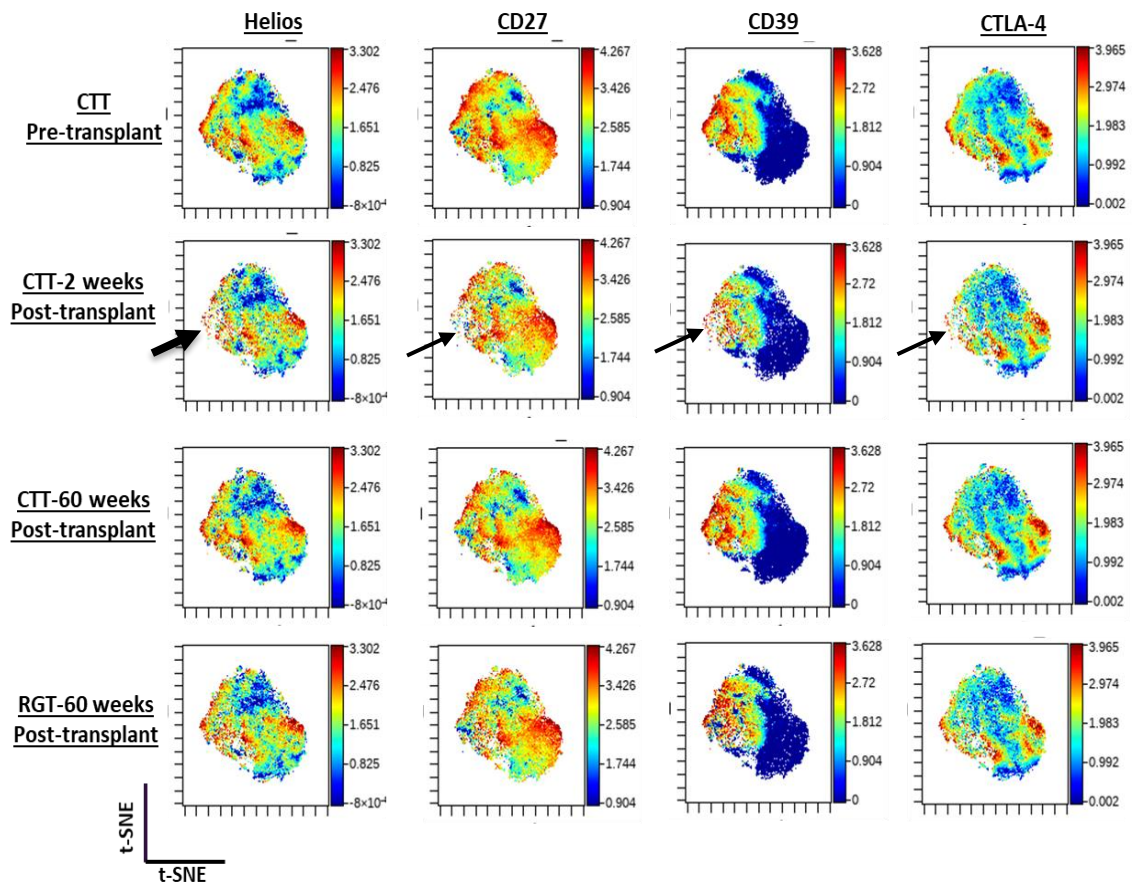


**Figure 4.20. Clustering analysis demonstrates heterogeneity within the Treg population.**

(A) A PhenoGraph clustering algorithm was performed on the total Treg compartment from all samples to assess distinct cellular subsets within Tregs. PhenoGraph was performed using the Cytokit package. (B) Heatmap analysis demonstrates a median expression of individual cellular markers expressed in the 20 Treg clusters. A high expression of Treg functional markers, including CD25, FOXP3 and Helios, and a high expression of co-inhibitory/co-stimulatory molecules, including CTLA-4, CD39 and TIGIT, corresponded with the expression of tissue homing marker CCR4. A clear gradient of CD147 expression correlated with Treg functional markers. (C) Merged samples from patients were used to generate t-SNE plots of Tregs depicting the expression pattern of analysed parameters. Clustering analysis of Tregs demonstrated high enrichment of key functional markers, including Helios and CD27. A high expression of Treg co-inhibitory/co-stimulatory molecules, including CD39 and CTLA-4. Arrows are pointing to a specific Treg cluster, which was altered at the V03 time point (2 weeks post-transplant). CTT – cell therapy transplant recipients; RGT – reference group (control) transplant recipients.

#### 4.5.3.3 Changes in the homing markers CCR7, CCR4 and CLA were observed within the Treg population

We next studied the expression of Treg markers on peripheral Tregs at V01 (4 weeks pre-transplantation) and V10 (60 weeks post-transplantation) from the six Treg-treated patients. The level of Helios expression on the peripheral Tregs was maintained at V10, compared to their level at V01 (Figure 4.21A), which is a known marker for stable Tregs.<sup>374, 375</sup> Likewise, the co-stimulatory molecule CD27 is a marker of highly suppressive Tregs,<sup>192, 376</sup> and as shown in (Figure 4.21B), the level of CD27 expression on peripheral Tregs was also comparable between V01 and V10. In addition, the expression of co-inhibitory or co-stimulatory molecules CTLA-4, CD39 and TIGIT on peripheral Tregs was also maintained at V10, in comparison to V01 (Figure 4.21C, D and E). The assessment of CD147, KI67 and HLA-DR expression revealed no difference between V01 and V10 (Figure 4.21F, G and H). However, the expression of chemokine receptors CCR4 and CLA on peripheral Tregs was significantly reduced between V01 and V10 (Figure 4.21J and K), meanwhile, CCR7 expression on peripheral Tregs was significantly increased at V10 compared to V01 (Figure 4.21I). CCR7 is a known marker of the suppressive function of Tregs.<sup>377</sup> Taken together, the phenotype analysis of peripheral Tregs over time shown no changes in the expression of Treg functional markers but some changes in the expression of chemokine receptors, particularly CCR4 and CLA, possibly resulting from the long term treatment with the immunosuppressive drugs.

Figure 4.21

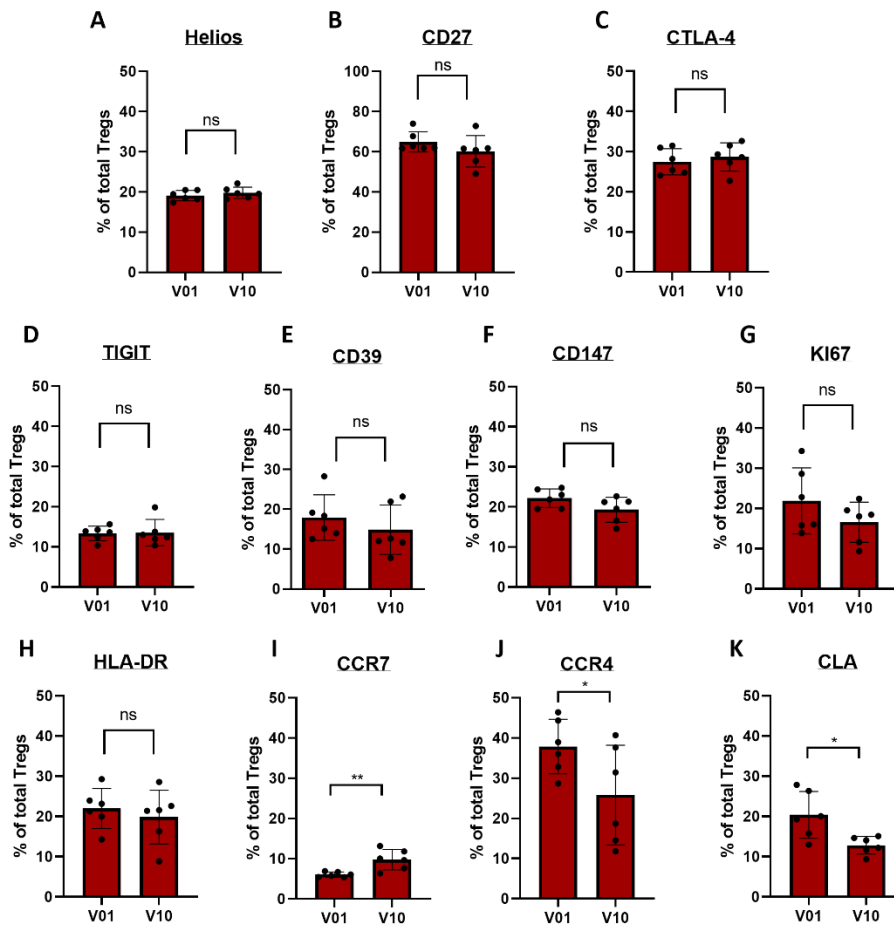


**Figure 4.21. The frequencies of Treg-associated markers within peripheral Tregs assessed in renal transplant recipients receiving an infusion of Treg therapy.** Helios, CD27, CTLA-4, TIGIT, CD39, CD147, KI67, HLA-DR, CCR7, CCR4 and CLA expression on peripheral Tregs was assessed at V01 (4 weeks pre-transplantation) and at V10 (60 weeks post-transplantation) in 6 Treg-treated patients by CyTOF. Scatter dots represent individual samples. Statistical significance was analysed by paired *t*-test. Error bars represent the mean with SD. ns = non-significant; \**p* < 0.05, \*\**p* < 0.01.

#### 4.6 Discussion

Immune monitoring through phenotypical analysis of peripheral leukocytes from renal transplant recipients receiving Treg therapy facilitated the understanding of the *in vivo* phenotypical changes of the immune compartment upon alemtuzumab induction and Treg infusion. Here we used comprehensive flow cytometry panels to profile several immune cells populations at regular intervals post-transplantation and post-Treg infusion. It has previously been shown that CD4<sup>+</sup> T cells contracted more than CD8<sup>+</sup> T cells after alemtuzumab induction.<sup>378</sup> Here, we showed that the recovery of CD4<sup>+</sup> T cells after alemtuzumab depletion was different than that of CD8<sup>+</sup> T cells. While the number of CD4<sup>+</sup> T cells remained low even at 44 weeks post-transplantation, the number of CD8<sup>+</sup> T cells returned to the pre-transplant level.

The composition of the B cell compartment has been recognised to play an important role in the graft outcome. Specifically, a distinct B cell signature has been identified in operational tolerant renal transplant recipients, including the elevation of peripheral numbers of B cells along with an elevation in the naïve and transitional B cell subsets, in comparison to recipients with stable graft function who received immunosuppressive drugs or biopsy-proven chronic rejection cases.<sup>280, 281</sup> These studies suggest that the shift toward a transitional B cell phenotype might be required for inducing tolerance. Here, we have shown that following alemtuzumab induction there was an increase in both the proportion and absolute number of B cells post-transplant, as compared to pre-transplant, especially in Treg-treated patients who were maintained on tacrolimus monotherapy. In addition, we found that the number of transitional B cells was higher at 44 weeks post-transplantation in Treg therapy group, compared to the control group. It, therefore, appears that Treg infusion enhances the *in vivo* repopulation of transitional B cells.

NK cells are a heterogeneous population and contain subsets with distinct phenotypes and functionalities.<sup>379</sup> These subsets can contribute to both allograft responses and tolerance.<sup>380</sup> Studies in tolerant renal and liver transplant patients reported an increase in the peripheral NK cells.<sup>280, 381</sup> This suggests that high NK cells post-transplant are not harmful and might contribute to graft tolerance. Here, we reported an elevation in the frequency and absolute number of total NK cells in the Treg therapy group post-transplant, as compared to pre-

#### Chapter 4: Cellular and phenotypical analysis of the peripheral immune cell compartment following Treg therapy in renal transplantation

transplant. This increase was not seen in patients in the control arm. We speculate that the cytotoxic CD56<sup>dim</sup> NK subset might decrease, while the immunoregulatory CD56<sup>bright</sup> NK subset might increase, over time post-Treg infusion. We demonstrated a trend towards this at 44 weeks post-transplantation, compared to baseline in both groups, although it was not statistically significant.

It remains to be known which induction therapy is optimal to combine with Treg therapy in transplantation. Alemtuzumab is believed to create a Treg-permissive environment with a study showing an increase in the Treg:Teff ratio in the peripheral blood of renal transplant patients receiving alemtuzumab compared with basiliximab (anti-CD25 antibody) immunosuppression.<sup>382</sup> In a Phase I clinical trial of Treg adoptive therapy into renal transplant recipients who received alemtuzumab immunosuppression. Only one out of nine patients experienced subclinical rejection, which was associated with immunosuppression non-concordance.<sup>248</sup> The 3C study aimed to assess the efficacy and safety of alemtuzumab with reduced calcineurin inhibitor compared with basiliximab with standard calcineurin inhibitor in patients receiving renal transplants.<sup>383</sup> This study showed that the rejection rate was reduced in patients receiving alemtuzumab compared with patients receiving basiliximab, however, no difference was observed in the long-term graft survival post-transplant. The coronavirus disease 2019 (COVID-19) outbreak has affected the TWO Study trial and the induction immunosuppression was modified. Patients in the control arm planned to receive basiliximab instead of alemtuzumab (Chapter 4, Figure 4.1) followed by standard maintenance immunosuppression (tacrolimus, and MMF), while patients in the cell therapy arm receive the same standard maintenance immunosuppression drugs ( tacrolimus and a reducing doses of MMF), but without basiliximab. These patients receive a single dose of autologous polyclonal-expanded Tregs on day five post-transplant. This will allow a potential subgroups analysis comparing basiliximab versus alemtuzumab (control arm), and alemtuzumab versus no induction immunosuppression (cell therapy arm).

Here, we showed that after Treg infusion, there was a modest increase in the absolute number and proportion of FOXP3<sup>+</sup> Tregs. However, the level of FOXP3<sup>+</sup> Tregs decreases at 44 weeks post-transplantation, compared to baseline in both groups. These data may be related to the use of tacrolimus, or a lack of the required survival signals. A previous study reported that low

#### Chapter 4: Cellular and phenotypical analysis of the peripheral immune cell compartment following Treg therapy in renal transplantation

doses of tacrolimus promoted the induction of peripheral Tregs compared with standard dose in kidney transplant recipients,<sup>384</sup> suggesting to minimise the tacrolimus doses.

In the mass cytometry assays, we examined the changes in the immune compartment in the renal transplant recipients over time post-transplant. When analysing the B cell population by unsupervised clustering, we observed a shift towards a more naïve phenotype post-transplant, which was also observed by our flow cytometry immune-phenotypical analysis of peripheral B cells. The enrichment of naïve B cells during the immune constitution post-transplant has previously been reported.<sup>385</sup> However, CyTOF revealed detailed features about the naïve cluster, which appeared to co-express CCR6, CCR7, and CXCR5, highlighting the advantages of a more detailed subset analysis with the CyTOF as opposed to the flow cytometry. The expression of CCR6, CCR7 and CXCR5 have been reported to play a role in the localisation of naïve B cells in the secondary lymphoid organs.<sup>386, 387</sup> In addition, CyTOF analysis of the B cell compartment revealed the appearance of a specific cluster post-transplantation, which might be transitional B cells, as these cells were expressed a high level of CD38. Here, we did not examine the differences between the control group and the Treg therapy group due to the limited availability of subject numbers. Therefore, further experiments are needed with greater subject numbers than presented in this preliminary study to reveal deep phenotypical differences between the Treg therapy group and the control group.

CytoF has previously been used to characterise the Treg compartment in liver transplant patients following autologous Treg therapy.<sup>262</sup> An attempt was made to identify expanded Tregs by comparing phenotypes of individual clusters to those examined pre-transfusion. Expanded Tregs were reported to be more homogenous and proliferative than circulating Tregs. Changes in marker expression among circulating Tregs after Treg infusion were reported and a significant increase in the expression of CD38 was found, which was no longer detected over time.<sup>262</sup> In our CyTOF analysis of peripheral Tregs from the patients enrolled in the ONE Study, there were changes in the peripheral Treg frequency over time post-transplantation. The Treg multiparameter phenotyping demonstrated high enrichment of key functional markers including FOXP3 , Helios, CD27, and CTLA-4. Furthermore, a distinctive alteration in clustering was observed, which was associated with specific post-transplantation changes. We also identified a significant increase in CCR7 expression on peripheral Tregs,

#### Chapter 4: Cellular and phenotypical analysis of the peripheral immune cell compartment following Treg therapy in renal transplantation

which is a known marker of Treg *in vivo* suppressive function and migration into the lymph node.<sup>377</sup>

In conclusion, the data presented in this chapter demonstrate that the deep cellular phenotyping of the peripheral leukocyte compartment in renal transplant recipients receiving Treg therapy provides an insight into overall systemic immune phenotype changes. While flow cytometry allows the measurement of the numbers and proportions of different immune cell subsets over time during the observation period to provide a subtle assessment in immune subset composition and numbers following the Treg therapy, multidimensional analysis using CyTOF facilitates a more in-depth and unbiased examination of peripheral blood lymphocytes phenotype changes. The ability to evaluate multiple antigens concomitantly allows for the detection of specific clusters of Tregs and other immune cells. Appreciating how these clusters behave after treatment with cellular therapy offers insight into the phenotype of tolerance, which in turn may assist in determining the optimal time for immunosuppression minimisation or help identify new therapeutic targets.

## Chapter 5: Spatial protein profiling of leukocyte infiltrate in renal biopsies after cellular therapy

### 5.1 Introduction

Standard immunohistochemistry (IHC) and immunofluorescence (IF) have been widely used to assess cellular infiltrates in fixed tissue biopsy samples.<sup>388</sup> However, these techniques offer limited information about infiltrated cell types or functions since they utilise limited numbers of fluorescence channels. The development of advanced digital spatial profiling (DSP) techniques has opened the possibility to profile the proteome and transcriptome of tissues at greater depth while retaining the context of the cells' spatial location.<sup>389, 390, 391</sup> As discussed in Chapter 1 (Section 1.6.1.3), this novel technology provides multiplex profiling of genes and proteins in specific regions within the tissue, covering up to 200 proteins and 22,000 transcripts.

Examining cellular infiltrates in renal biopsies of recipients who received Treg therapy is important, as it may help to understand the local immunological mechanisms active after cellular infusion. Chandran et al. examined the ability of Treg therapy to control inflammation in renal transplant patients with subclinical rejection on protocol biopsies, by assessing graft pathology at two weeks and six months post-infusion.<sup>392</sup> They found lower numbers of infiltrating CD8<sup>+</sup> T cells, CD20<sup>+</sup> cells (B cells) and CD68<sup>+</sup> cells (monocytes) post-infusion compared to the baseline level in two out of three patients, indicating the efficacy of cell therapy in controlling graft inflammation. However, the third patient continued to have inflammation on the follow-up biopsy. Therefore, more studies that examine the cellular infiltrates after Treg infusion will increase the knowledge about the behaviour of the infused Tregs and how they modulate the alloimmune response *in vivo*.

The enrichment of FOXP3<sup>+</sup> cells in transplanted tissue has been well documented in patients with stable graft function or patients with operational tolerance.<sup>393</sup> This finding is linked to the critical role of FOXP3<sup>+</sup> Tregs in suppressing the alloimmune responses. However, FOXP3<sup>+</sup> cells have also been detected within grafts during acute cellular rejection, likely representing activated effector T cells.<sup>394, 395, 396, 397</sup> While multiplexed IF or (single cell) RNA sequencing can provide further detail on phenotype, these techniques disregard the cells' spatial location. Spatial location is important to understand the biological process in a particular region and

their interaction with different spatial compartments through identifying the distribution of proteins and RNAs *in situ* within the tissue. Therefore, using spatial profiling techniques such as the Nanostring GeoMX DSP could provide comprehensive information about the presence and spatial localisation of leukocyte subsets within the tissue, as well as a detailed characterisation of their functional status or activation.

In this chapter, we employ spatial profiling to provide detailed protein analyses across multiple spatially discrete regions in renal biopsies from three transplant patients who received Treg therapy and two control patients with confirmed rejection. To further the analysis, we examine the FOXP3<sup>hi</sup> CD4<sup>+</sup> and FOXP3<sup>low/neg</sup> CD4<sup>+</sup> regions in both groups to assess the protein signatures of these cellular infiltrates.

## 5.2 Hypothesis

An in-depth examination of leukocytes that have infiltrated the transplanted tissue by spatial profiling will provide detailed molecular data facilitating the identification of local mechanistic markers of tolerance and rejection.

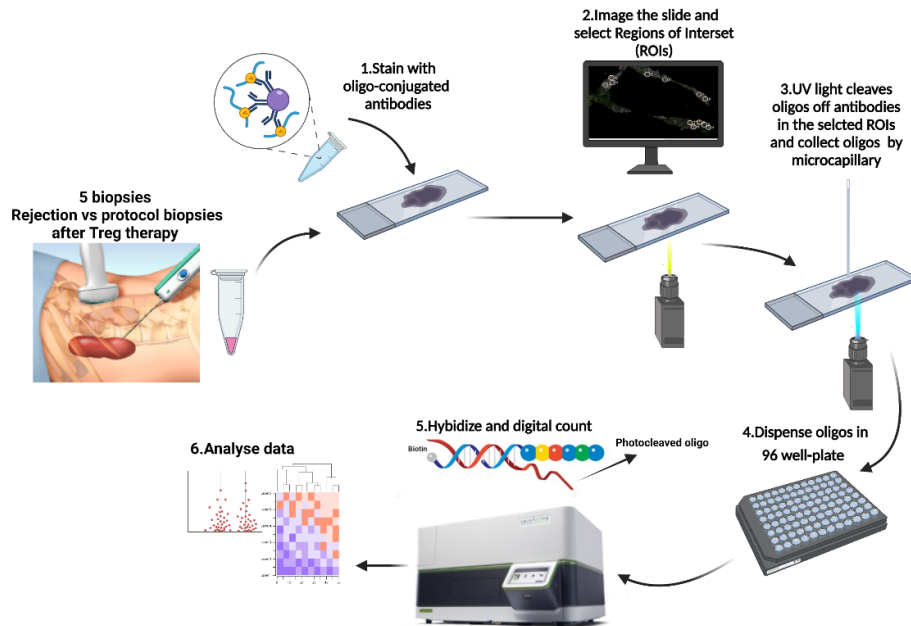
## 5.3 Results

### 5.3.1. Overview of GeoMx DSP workflow and ROI selection

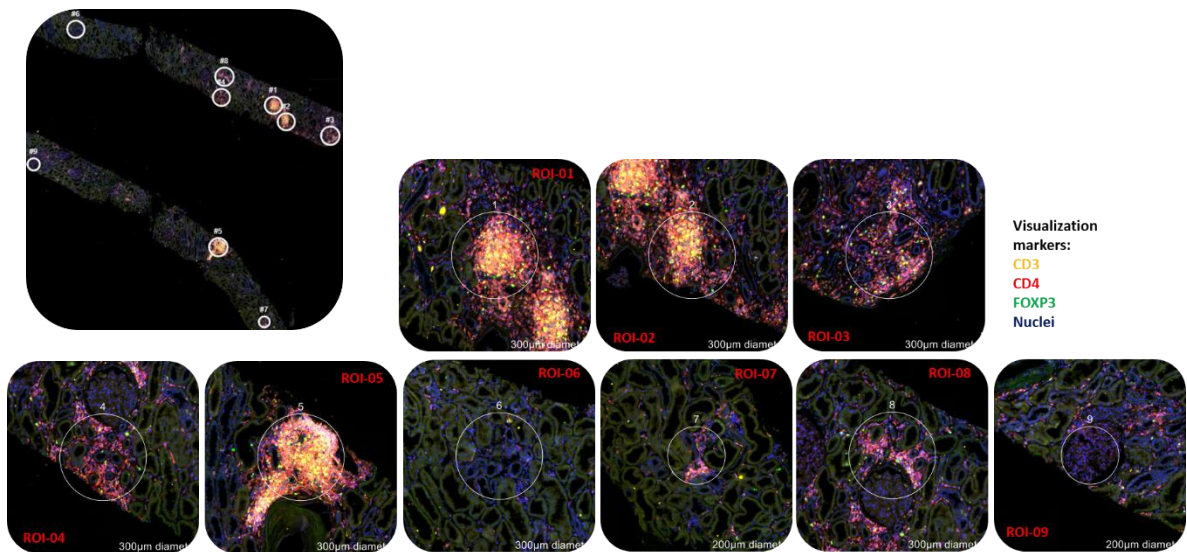
DSP combines standard immunofluorescence with tagged oligonucleotides conjugated to antibodies to allow high-plex protein expression profiling. Figure 5.1A illustrates the workflow of the GeoMx DSP technology. We assessed the cellular infiltrates in tissue biopsies from 3 transplant patients who received Treg therapy (A, B, C) and two patients with confirmed rejection (D, E), with biopsies taken at similar time points after transplantation (6-12 months). Formalin-fixed paraffin-embedded (FFPE) tissue sections on slides were stained with fluorescently-labelled antibodies against CD3, CD4, FOXP3 and a nuclear stain, which enabled the identification of T lymphocytes, CD4 T cells, Tregs and general tissue architecture (Figure 5.2 A). Based on the morphological fluorescence markers, we identified regions of interest (ROIs) that represented a spectrum of immune infiltrates for detailed proteomic profiling with a panel of 43 oligo-conjugated antibodies. Multiplexed *in situ* hybridisation then allowed quantification of the expression of 43 proteins in each ROI utilising the NanoString nCounter instrument. Counts were normalised to housekeeping proteins (Histone (H3) and ribosomal protein (S6)) to standardise the expression of proteins between the ROIs. Immunofluorescence-guided ROI selection was performed on a range of different infiltrate types in each patient (Figure 5.1 B). (Table 2-6 shows the list of antibodies used in this assay).

Figure 5.1

A



B



**Figure 5.1: Schematic diagram of the GeoMx DSP workflow. (A)** Biopsies were obtained from three renal transplant patients who received cell therapy (ONE study trial) and two patients with confirmed rejection. FFPE tissue sections on slides were stained with four-colour fluorescence of CD4 (*red*), CD3 (*yellow*), FOXP3 (*green*) and nuclei (*blue*) and a mix of 43 oligo-conjugated antibodies. Slides were scanned using the DSP instrument, and ROIs were selected based on morphological fluorescence markers. Oligos in each ROI were cleaved by UV light and then collected by microcapillary into 96-well plates. The collected oligos were hybridised and counted using the NanoString nCounter instrument. **(B)** ROIs selected from patient B demonstrating the morphology and immune infiltrate observed in each region.

### 5.3.2. Proteins are differentially expressed in cell therapy versus rejection regions

To perform an unbiased exploration of the cellular and phenotypical variations across the profiled ROIs from cell therapy and rejection tissues, we employed unsupervised clustering by principal component analysis (PCA). The ROIs from cell therapy group (*red*) formed a cluster distinct from the ROIs belonging to rejection patients (*blue*) (Figure 5.3 A). However, 3 ROIs from rejection (*blue*) were relatively closer to some ROIs from cell therapy and four ROIs from cell therapy (*red*) clustered away from the other regions, indicating that these four ROIs had a distinct protein expression signature. We then visualised the PCA by labelling ROIs of each patient, which showed some clustering of patient B away from other cell therapy patients, which in turn were separate from the rejection patients. Interestingly, differential expression analysis comparing rejection with cell therapy group across all sampled ROIs identified 15 proteins with significantly higher expression in cell therapy regions (fold change >1.5), including FOXP3, CD20, the apoptotic regulator Bcl-2, the memory marker CD45RO, the granulocyte activation marker CD66b, proteins known to be expressed by activated APCs (OX40L and HLA-DR) and pro-inflammatory cytokines (IL-6 and IFN- $\gamma$ ). In contrast, proteins that showed higher expression in rejection (n = 7, fold change > 1.5) included markers for cell proliferation (Ki67), markers related to classical monocytes and macrophages (CD14, CD68 and CD163) and proteins associated with active inflammation, including interferon (IFN) responses such as stimulator of IFN genes (STING) (Figure 5.3 C).

Figure 5.2

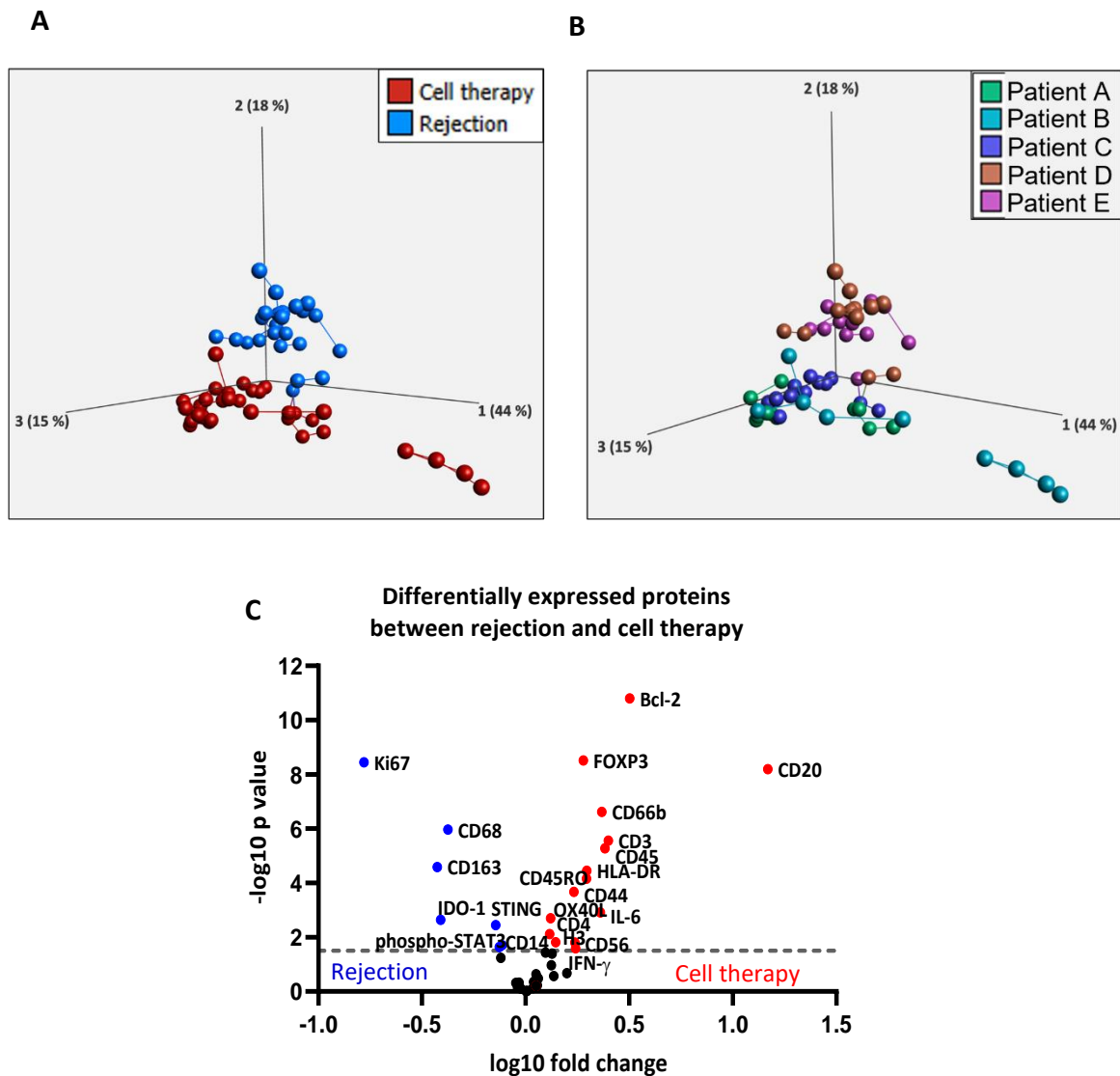


**Figure 5.2: Principal component analysis (PCA) of regions from cell therapy and rejection. (A)** (PCA) analysis of regions from cell therapy (*red*) and rejection (*blue*); each dot represents ROI. **(B)** (PCA) plot of regions from patient A (*green*), B (*light blue*), C (*purple*), D (*brown*) and E (*pink*) based on the expression of 32 proteins; each dot represents ROI. The PCA plots were performed using Qlucore Omics Explorer software. The statistical filtering of the Qlucore was applied to keep the variables (proteins) that differentiate between different regions (32 proteins out of 43 were used for the above PCA plots [ $P < 0.05$ , ANOVA]). **(C)** Volcano plot of differentially expressed proteins between rejection (*blue*) versus cell therapy (*red*). Coloured and annotated proteins have a negative  $\log_{10}$  p value (horizontal line)  $> 1.5$  with p value  $< 0.05$ . Statistical test was performed using t-test with Welch's correction and p value, fold change, negative  $\log_{10}$  p value and  $\log_{10}$  fold change of proteins between rejection and cell therapy were calculated by R Studio using the ggplot2 package, and a graph was performed in Prism version 8.0.2.

### 5.3.3. Protein analysis identifies B cells, Tregs and apoptotic regulators in renal biopsies from Treg-treated recipients

During the analysis it was clear that some ROIs contained more leukocytes than others; therefore, normalisation by CD3 counts was performed to effectively compare protein expression between the different regions. In general, CD8 showed higher counts than CD4 across all sampled ROIs (Figure 5.5 A&B). CD4 expression was found to be high in some specific ROIs from cell therapy but was not statistically significant compared to rejection (Figure 5.5 A). In contrast, CD8 expression in the ROIs of rejection biopsies appeared to be higher than that of Treg therapy, but was not statistically significant (Figure 5.5 B). Interestingly, the B cell marker CD20 showed significantly higher expression in the ROIs from cell therapy than in the ROIs from rejection patients, suggesting that the presence of CD20<sup>+</sup> B cells might play a protective role in the context of Treg therapy (Figure 5.5 C). CD45RO expression was significantly higher in the sampled ROIs from cell therapy than rejection (Figure 5.5 D).

CD14 expression was found to be high in some specific ROIs from cell therapy but was not statistically significant compared to rejection (Figure 5.5 E). Notably, CD68 and CD163 expression was higher in most of the ROIs in rejection compared to Treg therapy, suggesting that CD68<sup>+</sup> CD163<sup>+</sup> macrophages might play a role in the rejection process and that this is controlled with Treg infusion (Figure 5.5 F&G). Furthermore, some ROIs within cell therapy had enrichment of CD11c expression but were not statistically significant compared to rejection (Figure 5.5 H). Some ROIs from cell therapy displayed a notable expression of FOXP3 and the apoptotic regulator BCL-2 compared to the ROIs from the rejection group (Figure 5.5 I and J). The expression of the proliferation marker Ki67 was significantly higher within ROIs belonging to rejection compared to cell therapy patients (Figure 5.5 K). Unexpectedly, cytotoxic granzyme B (GZMB) was enriched in some ROIs from cell therapy compared to rejection (Figure 5.5 L).

Figure 5.3

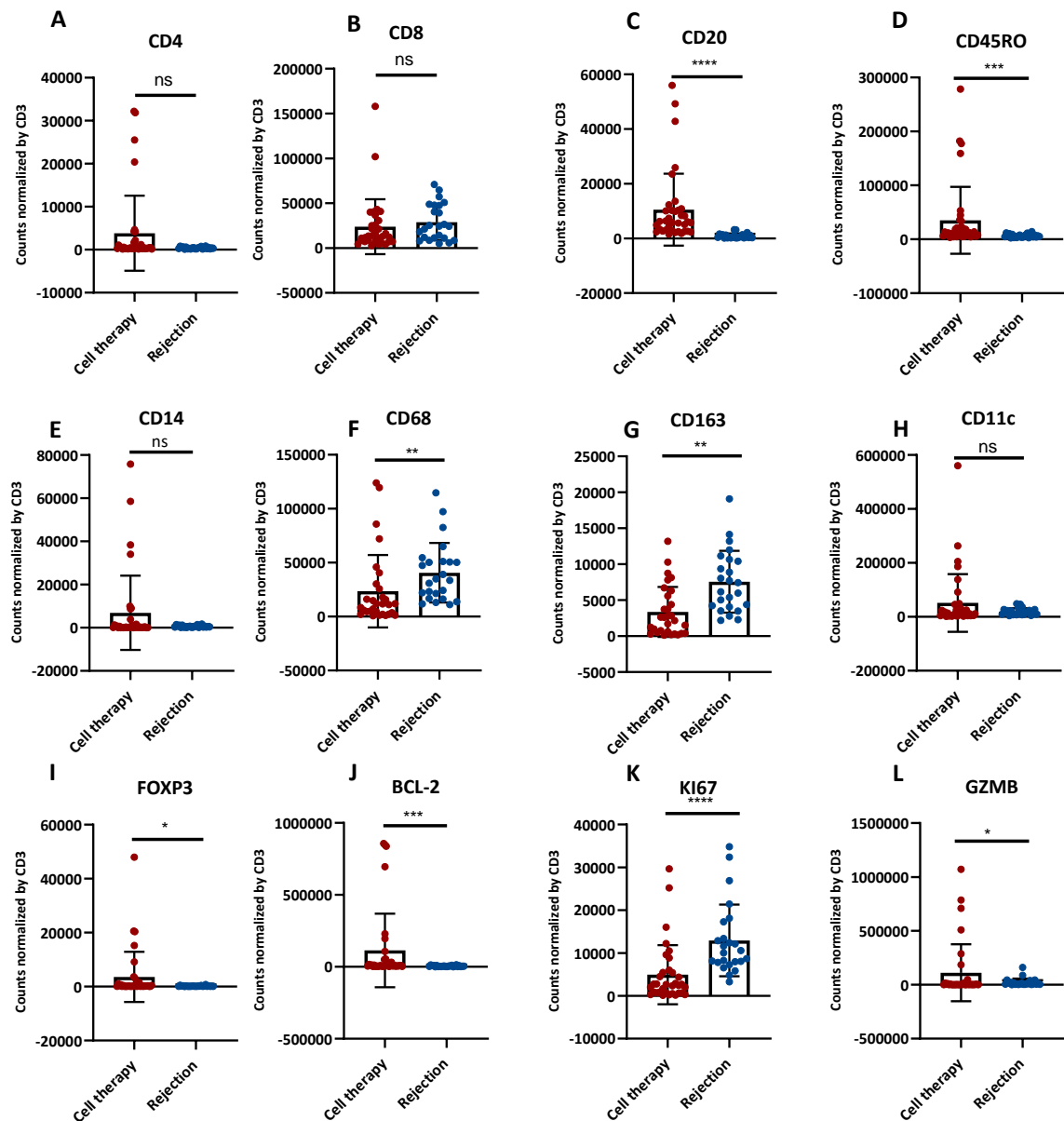


**Figure 5.3: Expression level of selected proteins across sampled areas in renal biopsies from cell therapy (red) and rejection (blue).** Analysis was performed with housekeeping counts normalised to CD3 digital signal across the sampled ROIs. The relative expression of (A) CD4, (B) CD8, (C) CD20, (D) CD45RO, (E) CD14, (F) CD68, (G) CD163, (H) CD11c, (I) FOXP3, (J) BCL-2, (K) Ki67, and (L) GZMB from cell therapy (red) and rejection (blue) tissues. Each point represents an ROI, and the line is the mean with standard deviation (SD). Statistical significance was performed using Mann–Whitney test. ns = non-significant, \*p < 0.05, \*\*p < 0.005, \*\*\*p < 0.0005, \*\*\*\*p < 0.0001.

#### 5.3.4. Unsupervised hierarchical clustering identifies distinct protein signatures of rejection and cell therapy

To better understand the variations in cellular and immune phenotypes present in the sampled ROIs, an unsupervised hierarchical clustering was performed across all the ROIs from rejection and cell therapy tissues. The analysis revealed eight groups of ROIs with distinct protein signatures (Figure 5.4). Group 1 included four ROIs from patient B (cell therapy) that showed a distinct protein signature compared to other ROIs, as these ROIs revealed higher expression of CXCL9, inhibitory signalling pathways (PD-1, PDL-1, CTLA-4), GZMB, proteins related to signalling pathways (AKT, P-AKT, PTEN, B-catenin), FOXP3, and the apoptotic regulator BCL-2 (Figure 5.4).

ROIs in Group 2 came from patient D (rejection), and were marked by high prevalence of CD8 T cells (CD8A), DCs (CD11c), costimulatory molecules (ICOS) and PD-1 (Figure 5.4). Group 3 included ROIs from patient C (cell therapy), and these ROIs showed enrichment of B cells (CD20) (Figure 5.4). Group 4 included ROIs from patients C and A (cell therapy), and these ROIs had enrichment in B cells (CD20), FOXP3 and CD45RO<sup>+</sup> cells (Figure 5.4). The ROIs in Group 5 all came from patient E (rejection), and were marked by high expression of monocytes/macrophages markers (CD68, CD163), the proliferation marker Ki67, STING and the anti-inflammatory protein IDO (Figure 5.4).

Group 6 included nine ROIs from four patients: D, A, E and C (rejection & cell therapy) (Figure 5.4). Some of these ROIs were marked by high enrichment of CXCL9, CTLA-4, GZMB, and proteins related to signalling pathways (PTEN, AKT, P-AKT,  $\beta$ -catenin). The ROIs in Group 7 all came from patient D (rejection), and showed higher prevalence of monocytes/macrophages (CD14, CD68, CD163), Ki67, STING, ICOS, PD-1, CD11c, CD8 T cells, and activated signal transducer and activator of transcription 3 (phospho-STAT3) (Figure 5.4). Finally, Group 8 included five ROIs from patient B (cell therapy), marked by high expression of FOXP3, BCL-2, HLA-DR, CD20, CD11c and ICOS (Figure 5.4).

Figure 5.4

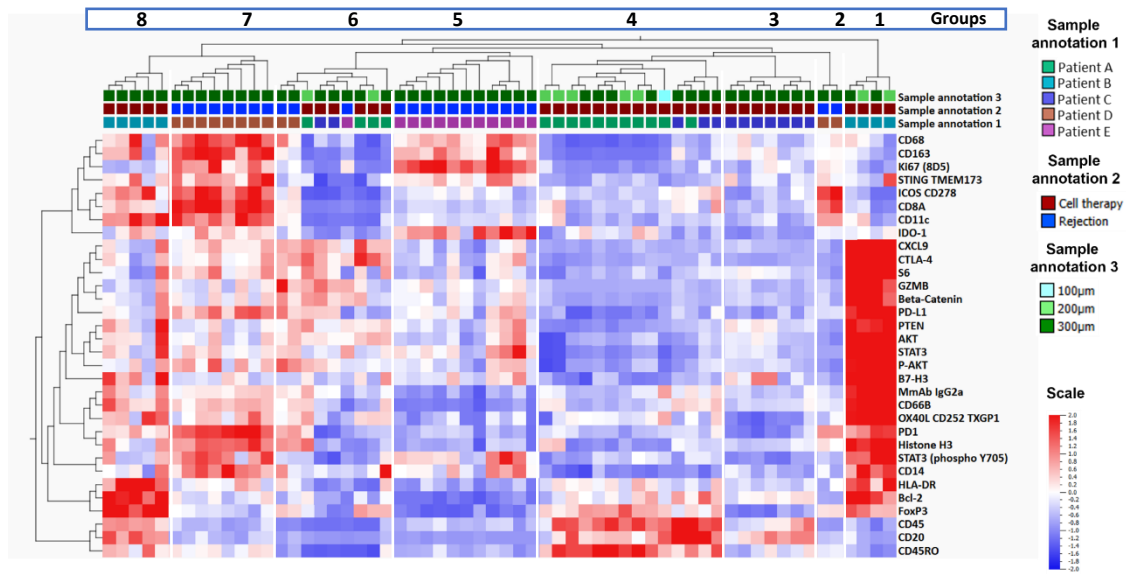


**Figure 5.4: Heatmap hierarchical clustering reveals eight spatial groups with distinct protein profiles.** The dendrograms at the top of the heatmap cluster the regions with similar protein profiles together. Red indicates high counts of the examined protein, while blue indicates low counts, on a scale from  $-2$  to  $2$ . Sample annotation 1 represents the examined patients A (*green*), B (*light blue*), C (*purple*) D (*brown*) and E (*pink*). Sample annotation 2 represents ROIs from cell therapy (*red*) and ROIs from rejection (*blue*). Sample annotation 3 represents the size of the circular ROIs  $300\ \mu\text{m}$  (*green*),  $200\ \mu\text{m}$  (*light green*) and  $100\ \mu\text{m}$  (*light blue*). The heatmap was produced using the Qlucore omics-explorer version 3.7. The statistical filtering of the Qlucore was applied to keep the variables (proteins) that differentiate between different sampled regions, 32 proteins out of 43 were used for the above Heatmap hierarchical clustering using  $P < 0.05$ , ANOVA.

### 5.3.5. Protein profiling of FOXP3<sup>+</sup> segments reveals distinct protein signatures compared to CD4<sup>+</sup>FOXP3<sup>neg</sup> segments within cell therapy and rejection tissues

Next, we gated FOXP3<sup>+</sup> and CD4<sup>+</sup>FOXP3<sup>neg</sup> areas of interest (AOIs) within the same region for detailed proteomic analysis. The gating was based on FOXP3 immunofluorescence signal, to assess the protein signatures of FOXP3<sup>+</sup> and their paired CD4<sup>+</sup>FOXP3<sup>neg</sup> segments from cell therapy and rejection tissues. The immunofluorescent images (IF) of FOXP3<sup>+</sup> AOIs demonstrated different morphology and cellular infiltrate, compared to their paired CD4<sup>+</sup>FOXP3<sup>neg</sup> AOIs (Figure 5.5 A). The sampled FOXP3<sup>+</sup> segments had high FOXP3 digital signal whereas CD4<sup>+</sup>FOXP3<sup>neg</sup> segments had no/low FOXP3 signal (Figure 5.5 B). This reassures the successful gating of FOXP3<sup>+</sup> and CD4<sup>+</sup>FOXP3<sup>neg</sup> areas of interest for detailed analysis.

We employed unsupervised clustering by principal component analysis (PCA), to examine the cellular and phenotypical variations across the profiled FOXP3<sup>+</sup> and CD4<sup>+</sup>FOXP3<sup>neg</sup> segments from cell therapy and rejection tissues (Figure 5.5 C). Generally, the clustering of AOIs was patient-dependent, for example, the AOIs from patient A (green-cell therapy) formed a cluster distinct from the remaining AOIs. Similarly, the AOIs from patient B (light-blue-cell therapy) clustered away from other AOIs. However, the AOIs from patient C (purple-cell therapy) were clustering relatively close to the AOIs belonging to patient E (pink-rejection). In addition, in the clustering analysis of only FOXP3<sup>+</sup> AOIs, AOIs from patient C (purple-cell therapy) was also closer to the AOIs belonging to patient E (pink-rejection) than to the other cell therapy AOIs (Figure 5.5 C). This might suggest that patient's C FOXP3<sup>+</sup> graft infiltrating cells have different characteristic than FOXP3<sup>+</sup> cells from other cell therapy patients.

Next, we performed an additional FOXP3 based normalisation to further stratify FOXP3 signal. As high Treg suppressive function is correlated with high FOXP3 expression, we have re-annotated AOIs as FOXP3<sup>hi</sup> and FOXP3<sup>low/neg</sup> based on the FOXP3 digital signal (Figure 5.6 A). The annotation of FOXP3<sup>hi</sup> and FOXP3<sup>low/neg</sup> AOIs was based on segment gating of FOXP3<sup>+</sup> and FOXP3<sup>neg</sup> cells by antibody fluorescence signal, followed by housekeeping normalised counts of FOXP3 (in which counts above 700 were considered FOXP3<sup>hi</sup> regions and those AOIs with FOXP3 counts less than 700 were considered FOXP3<sup>low/neg</sup>) (Figure 5.6 A). Notably, FOXP3

digital signal was higher in the FOXP3<sup>hi</sup> segments in cell therapy compared with FOXP3<sup>hi</sup> segments in rejection patients (Figure 5.6 B).

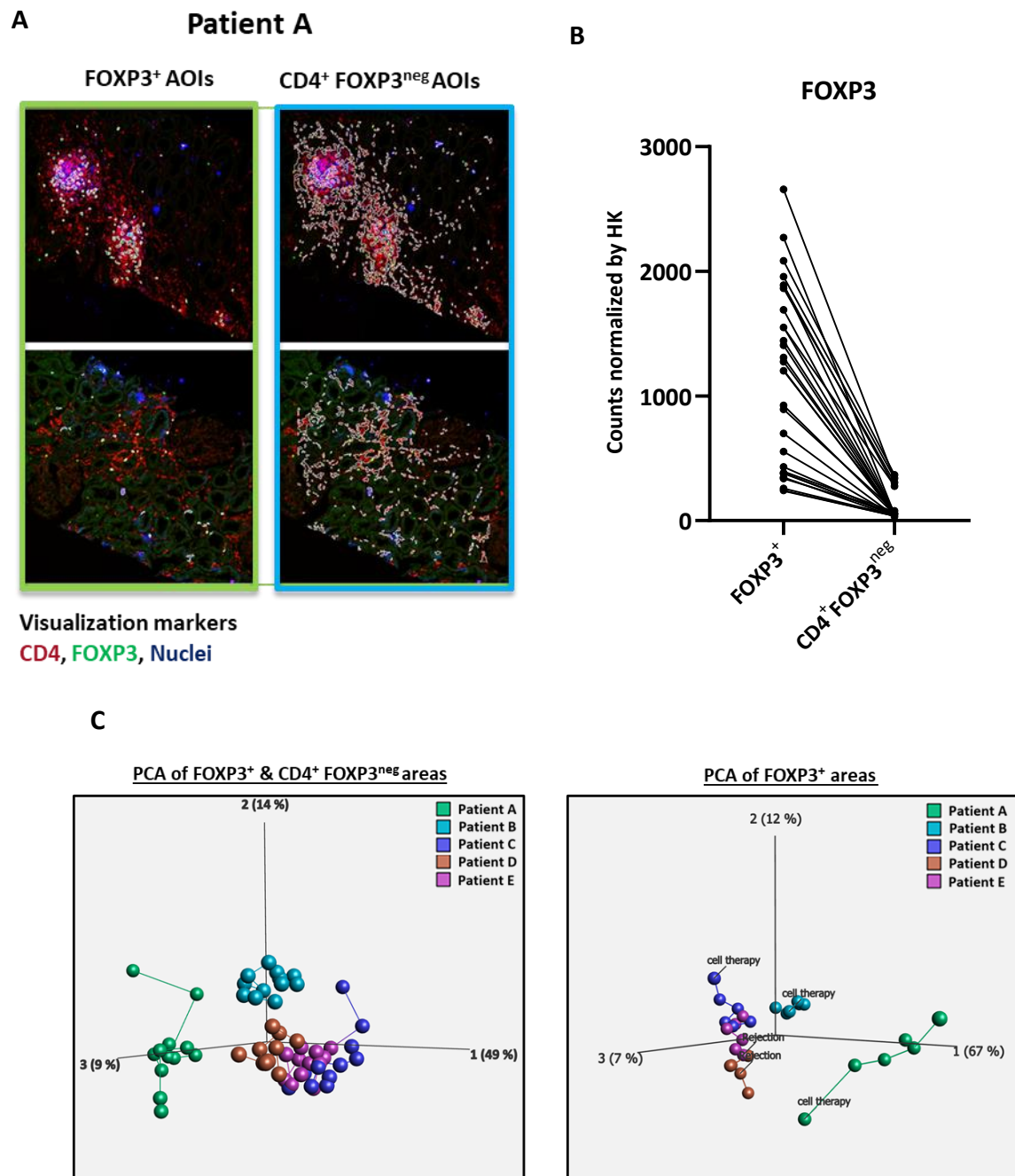
We performed unsupervised hierarchical clustering of FOXP3<sup>hi</sup> and FOXP3<sup>low/neg</sup> segments across the sampled areas from cell therapy and rejection tissues. The analysis revealed four groups of AOs with distinct protein signatures (Figure 5.6 C). Group 1 included AOs from patient D (rejection); five AOs contained FOXP3<sup>hi</sup> cells, and these FOXP3<sup>hi</sup> regions shown enrichment in inhibitory molecules (CTLA-4, PD-1) and activation molecule (ICOS)(Figure 5.6 C). Some of FOXP3<sup>hi</sup> AOs contained a high fraction of CD8, CD11c, CD56, IFN- $\gamma$ , and the cytotoxic molecule (GZMB). However, FOXP3<sup>low/neg</sup> segments contained higher CD8, CD11c, CD68, CD163, and ki67 compared to FOXP3<sup>hi</sup> regions.

Group 2 included AOs from patient C (cell therapy) and patient E (rejection). Interestingly, in patients C and E, even the AOs gated as FOXP3<sup>+</sup> based on immunofluorescence were mostly reclassified as FOXP3<sup>low/neg</sup> after the normalisation for digital FOXP3 signal. Interestingly, most of the AOs in group 2 demonstrated a relatively low protein expression when compared to AOs classified into other groups.

Group 3 included AOs from patient B (cell therapy); half of the AOs contained a high fraction of FOXP3<sup>+</sup> cells; these FOXP3<sup>hi</sup> AOs clustered together beside the FOXP3<sup>low/neg</sup> AOs, except one AO (Figure 5.6 C). All the FOXP3<sup>hi</sup> AOs (in Group 3) demonstrated enrichment in ICOS, IFN- $\gamma$ , CTLA-4, and PTEN compared to FOXP3<sup>low/neg</sup> AOs (in Group3). Conversely, FOXP3<sup>low/neg</sup> segments contained higher CD68, CD163, CD8, pan-cytokeratin, GZMB,  $\beta$ -catenin, and  $\beta$ -2-microglobulin compared to FOXP3<sup>hi</sup> segments (Figure 5.6 C).

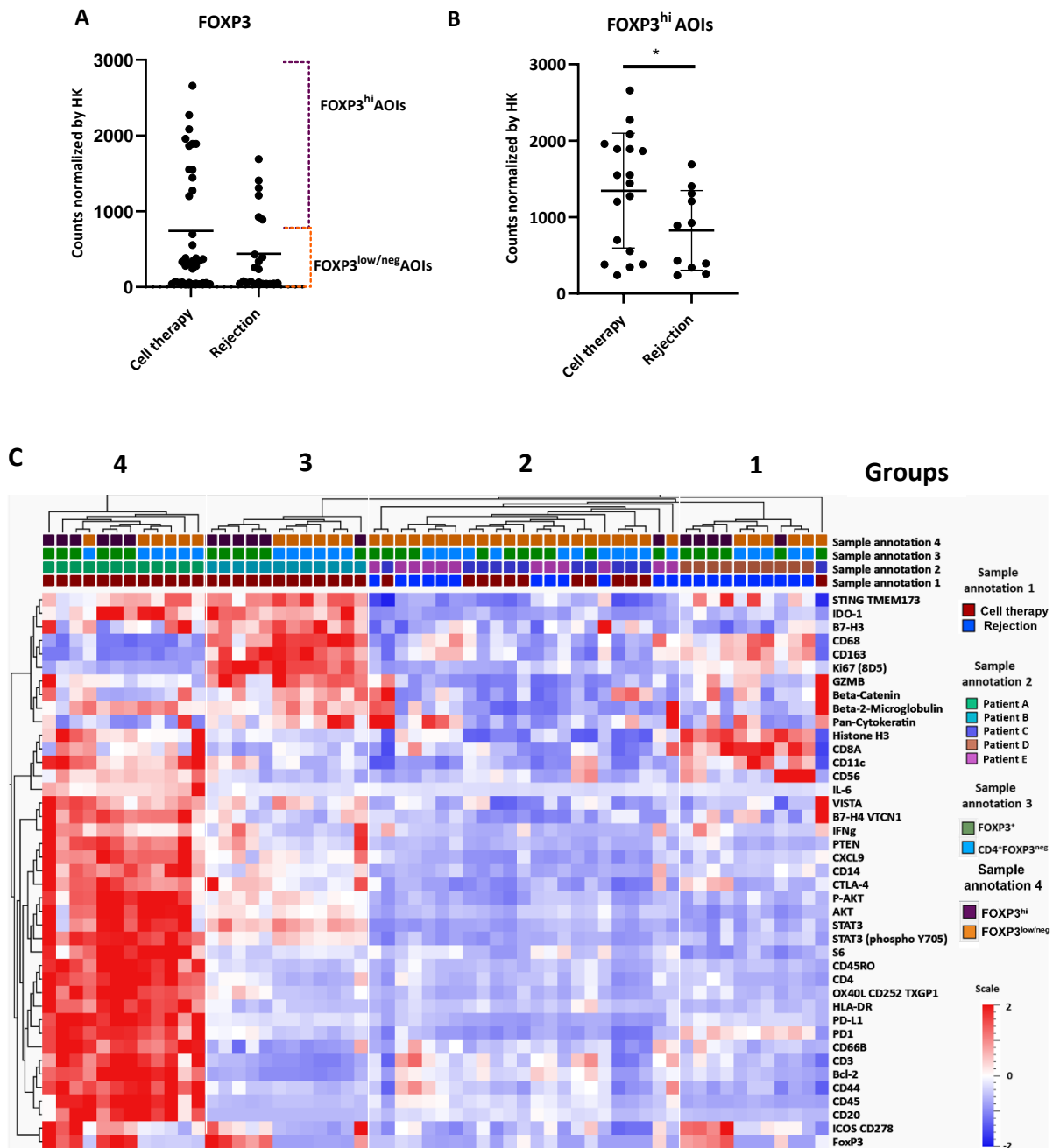
Group 4 included AOs from patient A (cell therapy), and these AOs revealed enrichment in NK cells (CD56), CD4 T cells, memory T cells (CD45RO, CD44), granulocyte markers (CD66b), DCs (CD11c), B cells (CD20), apoptotic regulator (BCL-2), alongside proteins involved in signalling cascade (STAT, P-STAT, P-AKT, PTEN) and inhibitory molecules (PD-1, PD-L1, CTLA-4). The FOXP3<sup>hi</sup> AOs demonstrated enrichment in ICOS and IFN- $\gamma$  (Figure 5.6 C).

Figure 5.5



**Figure 5.5: Protein profiling of FOXP3<sup>+</sup> and CD4<sup>+</sup>FOXP3<sup>neg</sup> segments from cell therapy and rejection patients. (A)** Immunofluorescent images (IF) of AOIs showing the morphology and immune infiltrate observed in FOXP3<sup>+</sup> and CD4<sup>+</sup>FOXP3<sup>neg</sup> segments from patient A (cell therapy), Nuclei-blue, CD4-red and FOXP3-green. **(B)** FOXP3 digital counts normalized by housekeeping proteins across the sampled FOXP3<sup>+</sup> and CD4<sup>+</sup>FOXP3<sup>neg</sup> segments from cell therapy and rejection patients. **(C)** Principal component analysis (PCA) of FOXP3<sup>+</sup> and CD4<sup>+</sup>FOXP3<sup>neg</sup> segments (left panel) or FOXP3<sup>+</sup> (right panel) segments from patient A (green), B (light blue), C (purple), D (brown), and E (pink); each dot represents area of interest. Statistical analysis performed for the above PCA to keep the variables (proteins) that differentiate between different segments using  $P < 0.05$ , ANOVA.

Figure 5.6



**Figure 5.6: Heatmap hierarchical clustering of the FOXP3<sup>+</sup> and CD4<sup>+</sup>FOXP3<sup>neg</sup> areas from cell therapy and rejection tissue. (A)** The selection of FOXP3<sup>hi</sup> and FOXP3<sup>low/neg</sup> AOIs was based on housekeeping normalised counts of FOXP3 in which counts above 700 (above the mean) were considered FOXP3<sup>hi</sup> regions and those AOIs with FOXP3 counts less than 700 (below the mean) were considered FOXP3<sup>low/neg</sup>. **(B)** FOXP3 digital signal in the FOXP3<sup>hi</sup> segments in cell therapy and rejection, line is the mean with standard deviation (SD). Statistical significance was performed using t-test, \*p < 0.05. **(C)** Unsupervised hierarchical clustering (heatmap) of the measured proteins in FOXP3<sup>+</sup> and CD4<sup>+</sup>FOXP3<sup>neg</sup> across the ROIs from rejection group. The dendrograms in the top cluster the regions that have similar protein expression pattern together. Red indicates higher counts of the examined protein, while blue indicates lower counts, on a scale from -2 to 2. Sample annotation 1 represents regions from cell therapy tissue (red) or rejection tissue (blue). Sample annotation 2 represents the examined samples 16436 (green), 19524 (light blue) and 25754 (purple). Sample annotation 3 represents AOIs of FOXP3<sup>+</sup>

(green) and CD4<sup>+</sup>FOXP3<sup>neg</sup> (blue) gated based on morphology. Sample annotation 4 represents AOs of FOXP3<sup>hi</sup> (burgundy) and FOXP3<sup>low/neg</sup> (orange) annotated based on FOXP3 digital signal. The heatmap was performed using Qlucore Omics-Explorer version 3.7.

### 5.3.6. Proteins are differentially expressed in FOXP3<sup>hi</sup> versus FOXP3<sup>low/neg</sup> segments

Differential expression analysis comparing FOXP3<sup>low/neg</sup> versus FOXP3<sup>hi</sup> across sampled AOs in cell therapy tissues identified 16 proteins with significantly higher expression in FOXP3<sup>hi</sup> segments (fold change > 1.5), including enrichment in FOXP3 and, to a lesser extent, CD4 and CD45RO, alongside an enrichment in inhibitory molecules (CTLA-4, PD-1, PDL-1), co-stimulatory molecules (ICOS, OX40L), IDO, IFN- $\gamma$ , CXCL9, proteins involved in signalling cascade (STAT, P-STAT, P-AKT, PTEN), and STING. In contrast, the proteins in FOXP3<sup>low/neg</sup> segments were all expressed below the negative log<sub>10</sub> p-value of 1.5 (Figure 5.7 A).

Conversely, differential expression analysis comparing FOXP3<sup>low/neg</sup> versus FOXP3<sup>hi</sup> across sampled AOs from rejection tissues identified only six proteins with significantly higher expression in FOXP3<sup>hi</sup> segments (fold change > 1.5), including FOXP3, ICOS, CTLA-4, IFN- $\gamma$ , and PTEN, while proteins that showed higher expression in FOXP3<sup>low/neg</sup> segments (n = 5 proteins, fold change > 1.5) were CD45, CD20, CD44 and HLA-DR (Figure 5.7 B).

Rejection was compared to cell therapy across the FOXP3<sup>hi</sup> segments, identifying 23 proteins expressed significantly higher in cell therapy segments, including proteins involved in signalling pathways (STAT, P-STAT, P-AKT, PTEN), alongside proteins involved in antigen processing and presentation ( $\beta$ 2-Microglobulin, HLA-DR), IDO, FOXP3, CD4, CD45RO, CD45, CD44, CD20, OX40L, VISTA, IL-6, CXCL9 and immune regulatory molecules (B7-H4, B7-H3). In contrast, the protein that was highly expressed in FOXP3<sup>hi</sup> rejection segments was CD8 (Figure 5.7 C).

Finally, rejection was compared to cell therapy across the FOXP3<sup>low/neg</sup> segments, and 14 proteins were expressed significantly higher in cell therapy regions, including proteins involved in signalling pathways (STAT, P-STAT, AKT, P-AKT,  $\beta$ -catenin), IDO, GZMB, OX40L, HLA-DR, CXCL9, VISTA, CTLA-4 and B7-H3. In contrast, all proteins in FOXP3<sup>low/neg</sup> rejection segments were expressed below the negative log<sub>10</sub> p-value of 1.5 (Figure 5.7 D).

Figure 5.7

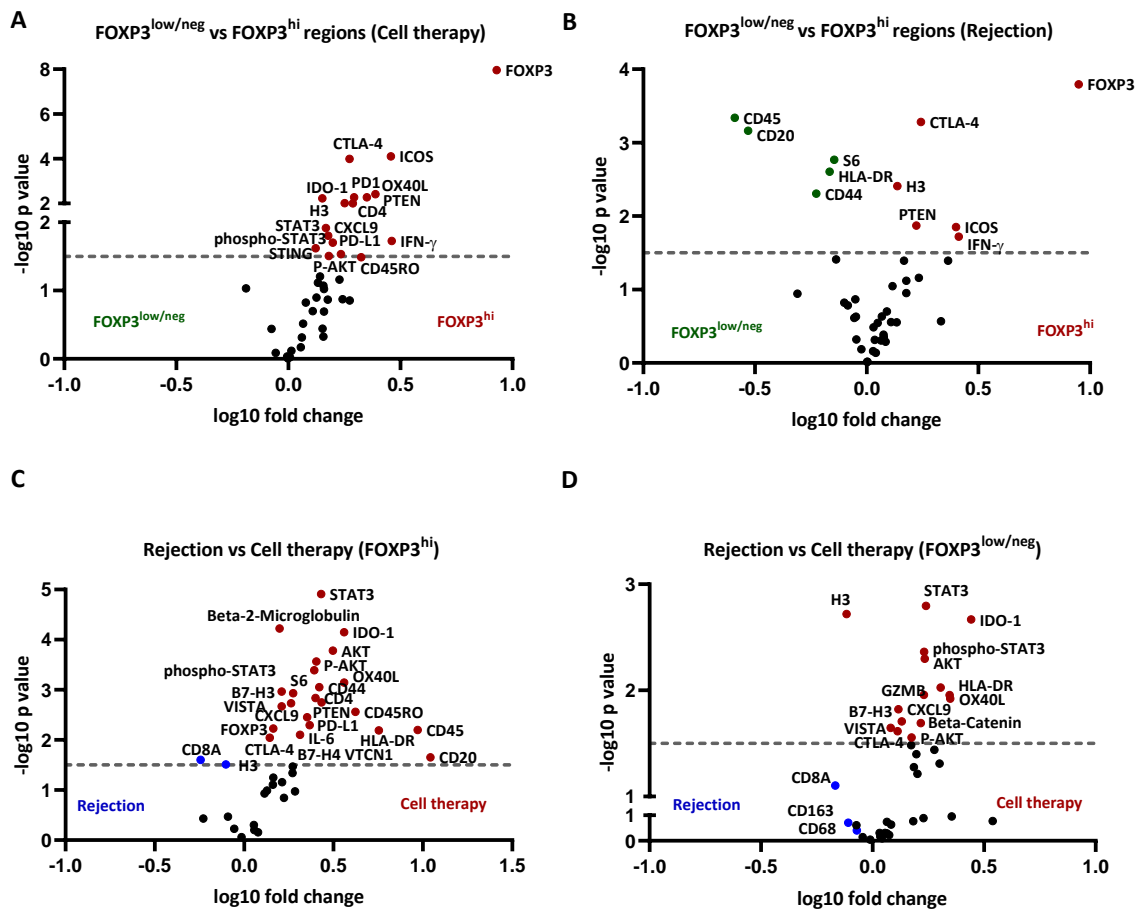


**Figure 5.7: Protein profiling of FOXP3<sup>hi</sup> and FOXP3<sup>low/neg</sup> segments from cell therapy and rejection tissue.** (A) Differentially expressed proteins in FOXP3<sup>low/neg</sup> (green) versus FOXP3<sup>hi</sup> (red) from cell therapy tissue areas. (B) Differentially expressed proteins in FOXP3<sup>low/neg</sup> (green) versus FOXP3<sup>hi</sup> (red) from rejection areas. (C) Differentially expressed proteins in rejection (blue) versus cell therapy (red) from FOXP3<sup>hi</sup> areas. (D) Differentially expressed proteins in rejection (blue) versus cell therapy (red) from FOXP3<sup>low/neg</sup> areas. Coloured and annotated proteins have a negative log<sub>10</sub> p value (horizontal line) > 1.5. Statistical test was performed using t-test with Welch's correction; p-value, fold change, negative log<sub>10</sub> p-value and log<sub>10</sub> fold change of proteins in rejection and cell therapy were calculated by R Studio using the ggplot2 package, and graphs were performed in Prism version 8.0.2.

## 5.4 Discussion

IHC and immunofluorescence techniques have been the most commonly employed approaches in the analysis of fixed tissue biopsies. However, these methods offer limited details about the phenotype of cells in specific areas. Here, digital spatial profiling of renal biopsies have revealed interesting differences between the cellular infiltrates in cell therapy treated patients as compared with rejection biopsies. By selecting specific cell-infiltrated ROIs based on immunofluorescence, we observed distinct protein signatures which may reflect overall cellular dynamic processes active within grafts after Treg therapy or rejection.

FOXP3 expression is indispensable for the suppressive function of Treg cells.<sup>398, 399</sup> The FOXP3<sup>+</sup> graft infiltrating cells were previously detected by our group by IHC analysis of renal tissue in the setting of stable graft function in patients who received Treg therapy.<sup>247</sup> However, it has been reported that Tregs, under certain inflammatory conditions, can lose FOXP3 expression, thereby becoming the so-called 'exFOXP3' Tregs and acquiring pathogenic phenotypes that contribute to the pathophysiology of several diseases.<sup>400, 401</sup> Here, we found that the FOXP3 signal was highly enriched in regions from cell therapy versus rejection patients, suggesting that infused regulatory T cells are likely homing to the allograft. We also found higher expression of the antiapoptotic protein BCL-2 in cell therapy regions compared to the rejection group. Activated human Tregs upregulated BCL-2 and were shown to have an enhanced *in vivo* function.<sup>402</sup> We found higher expression of the B cell marker CD20 in the cell therapy ROIs than in rejection ROIs, suggesting a link between infused Tregs and allograft infiltration by B cells. This parallels a previous study that reported that the presence of CD20<sup>+</sup> infiltrating cells has a protective effect on renal allograft and was unrelated to intra-graft C4d deposition or detection of donor-specific antibodies (DSA).<sup>403</sup>

IFN- $\gamma$  is a key inflammatory cytokine secreted by several cells, including CD4 (Th1) cells, CD8 T cells,  $\gamma\delta$  T cells, macrophages, NK cells and Tregs, following activation by APCs.<sup>404</sup> This cytokine is classically considered a pro-inflammatory cytokine and plays several roles in the activation of pro-inflammatory macrophages,<sup>405</sup> modulation of T cell responses, induction of MHC molecules for antigen presentation, alongside the induction of chemokines that may augment leukocyte infiltration.<sup>406</sup> However, in some circumstances, IFN- $\gamma$  plays a regulatory role and triggers the induction of Tregs and myeloid-derived suppressor cells (MDSCs).<sup>407, 408, 409, 410</sup> It also plays a crucial role in maintaining *in vivo* suppressive function of Tregs.<sup>411</sup> IFN- $\gamma$  is required

for graft survival because of its association with the prevention of early graft necrosis and thrombosis.<sup>412</sup> Our data revealed that the expression of IFN- $\gamma$  appears to be associated with cell therapy, not with rejection (Figure 5.2C). It is possible that IFN- $\gamma$  were playing immunoregulatory roles in the cell therapy regions since it is well known that, under certain conditions, this cytokines can divert their function towards a regulatory response.<sup>411</sup>

Allograft rejection is known to involve various interactions between diverse populations of immune cells.<sup>73, 413</sup> Our data revealed that rejection regions have a high expression of Ki67, indicating the presence of highly proliferative cells. The monocyte/macrophage markers CD14, CD68, and CD163 were also enriched in the rejection regions (Figure 5.2C), suggesting that macrophages may contribute to graft rejection of these patients. Early studies by Hancock and colleagues reported that macrophages represent the predominant cells that infiltrate the allograft during severe rejection episodes.<sup>414</sup> Also, an increase in the frequencies of CD68<sup>+</sup> macrophages has been associated with poor graft outcomes.<sup>415</sup> Moreover, the presence of CD68<sup>+</sup>CD163<sup>+</sup> cells was detected in the peripheral blood and tissue during renal and heart rejection.<sup>416, 417</sup> Our data also revealed enrichment in indoleamine 2,3-dioxygenase (IDO) within the rejection regions. This enzyme is produced by DCs and macrophages,<sup>418, 419</sup> and is involved in the metabolic breakdown of the amino acid tryptophan into Kynurenine. Kynurenine has a regulatory function and can convert mature DCs into tolerogenic DCs, which sequentially suppress the T effector cells, thereby promoting tolerance. However, the IDO gene contains IFN-response elements; therefore, the release of IFN type I (IFN-I) and type II (IFN-II) by activated leukocytes may induce IDO expression by monocyte-derived DCs through the downstream Jak/STAT signalling cascade.<sup>420</sup> This may explain the elevation of IDO levels and phospho-STAT3 (Tyr705) which were seen in our dataset within the rejection regions.

FOXP3<sup>+</sup> cells were detected in the tolerogenic state and rejection tissue. Here, we assessed the presence of cells with a high FOXP3 signal (denoted as FOXP3<sup>hi</sup> areas of interest) in cell therapy and rejection regions. We showed that overall the FOXP3 signal was higher within FOXP3<sup>hi</sup> segments in cell therapy compared to FOXP3<sup>hi</sup> segments in rejection group. However, patient C demonstrated less FOXP3 signal compared to patients A and B. Patient C had a biopsy sample six months before the DSP biopsy and was diagnosed with BK virus-associated nephropathy and suspected vascular rejection. This may explain the low level of FOXP3 signal

which was seen in patient C regions, with the overall protein expression patterns similar to the rejection patient (Figure 5.6C).

FOXP3<sup>hi</sup> segments from cell therapy group were compared to rejection, to determine the protein signature of FOXP3<sup>hi</sup> cells and their spatial location. We found enrichment in proteins related to signalling, including STAT and P-STAT, which are critical for Treg suppressive function.<sup>421</sup> Also, an enrichment was found in CD45RO, CD44 and B cells (CD20), suggesting a possible role for these cells in regulating alloresponse and coinciding with the enrichment of the regulatory molecules CTLA-4 and PD-1. An enrichment of anti-inflammatory IDO was found, and VISTA protein (V-domaine Ig suppressor of T cell activation), a co-inhibitory receptor for T cells and myeloid-derived antigen-presenting cells,<sup>422</sup> was found to be highly enriched in FOXP3<sup>hi</sup> segments in cell therapy regions (Figure 5.7C). It is likely that VISTA plays a regulatory role in suppressing the alloimmune response.

Lipid phosphatase (PTEN), a negative regulator of PI3K/AKT signalling, was notably enriched in FOXP3<sup>hi</sup> regions within renal tissue in cell therapy and rejection patients (Figure 5.7A and B). In a previously reported experimental model, the control of PI3K signalling through PTEN was required to maintain suppressive function and Foxp3 expression of Tregs.<sup>423</sup> Studies have reported that Tregs, but not T effector cells, maintain a high level of PTEN expression, thereby preventing the downstream activation of PI3K/AKT signalling following IL-2 stimulation while permitting further signalling through the JAK kinases and STAT transcription factors.<sup>424, 425</sup> FOXP3<sup>hi</sup> cells that are present in rejection regions are likely suppressive Tregs since they express a high level of PTEN. However, these Tregs failed to control the alloresponse, as can be observed by the enrichment of CD8 T cells, which were notably represented in the FOXP3<sup>hi</sup> regions in the rejection tissues.

In summary, the spatial resolution of GeoMx DSP allowed for an in-depth, detailed analysis of leukocyte infiltrates and provided a clearer picture of the dynamic process that occurs in the transplanted tissue after cellular therapy compared to rejection.

## Chapter 6: General discussion, limitations and future directions

Tregs are powerful modulators of immune function and are of increasing interest as an adoptive cellular therapy for the control of transplant alloresponses. Polyclonal Treg therapy has been assessed in a number of Phase I/II clinical trials in both solid organ transplantation and for the treatment or prevention of GVHD.<sup>105, 248, 300</sup> However, concerns around non-specific immune suppression and the necessity to enhance potency at lower cell doses have shifted attention to arTregs. As discussed in Chapter 1 (Section 1.5), there is good evidence from preclinical animal models that arTregs have enhanced therapeutic potential compared to polyTregs in transplantation. This project aimed to generate and characterise human *ex vivo*-expanded arTregs.

In Chapter 3, it was shown that the isolation and generation of allogeneic imDCs is feasible and that these cells can be used as stimulators for arTregs (Figure 3.1). Generated arTregs showed enhanced suppressive function compared to polyTregs (Figures 3.4 and 3.6B) and maintained the expression of specific and functional Treg markers after expansion (Figure 3.5). This indicated that imDCs provide a potent allo-stimulatory signal to expand Tregs without impacting the function and cellular phenotype of Tregs. This is in line with a previous study, which reported that Tregs primed twice with allogeneic monocyte-derived DCs were functional both *in vitro* and *in vivo*, controlling GVHD in a mouse model.<sup>426</sup> Several studies demonstrated that the use of B cells as APCs is efficient to expand human arTregs *ex vivo*.<sup>209, 427, 222</sup> However, a recent study compared the efficacy of generated arTreg populations using either B cells or mDCs as stimulators from the same donor.<sup>428</sup> The arTregs expanded by mDCs had two-fold higher expansion than arTregs-expanded by B cells, suggesting that mDCs can be valuable stimulators for the generation of arTregs for clinical use. We showed that generated imDCs express co-stimulatory molecules, including CD80, CD86 and HLA-DR, that are likely to act to stimulate and expand Tregs (Figure 3.1C). However, further studies should be performed to study the mechanism of interaction between imDCs and Tregs and determine whether imDCs express specific costimulatory molecules or cytokines needed for Treg expansion.

Although we successfully developed a technique to isolate and expand arTregs, further optimisation is needed to manufacture arTregs according to GMP standards. To comply with these standards, Tregs need to be isolated using magnetic beads (cliniMACS), which might result in initial Treg products with less purity. Therefore, it is important to assess the suppressive potency and long-term stability of expanded arTregs when Tregs are magnetically isolated and stimulated with allogeneic imDCS in the presence of IL-2 and rapamycin. GMP-compliant FACS-based sorting devices are currently being assessed for the production of clinical therapeutics and might allow for the isolation of Tregs by flow cytometry in the near future.

Although FOXP3 expression is indispensable for Treg development and function, TSDR demethylation determines the stability of FOXP3 expression.<sup>429, 430, 431</sup> Genome-wide studies have reported demethylation at other genes, including *Il2ra* (CD25), *Ctla4*, *Tnfrsf18* (GITR), *Ikzf2* (Helios) and *Ikzf4* (Eos) in thymic and peripheral Tregs but not *in vitro*-induced Tregs or conventional T cells.<sup>432</sup> In Chapter 3, we showed that expanded arTregs maintain Treg functional markers, including FOXP3 and CTLA-4 (Figure 3.5B). However, it would be valuable to assess whether these arTregs display characteristics of stable thymically-derived Tregs by examining the epigenetic status of the *FOXP3* gene and other genes from expanded arTregs and comparing them to the polyclonal Tregs. This might enable a better understanding of the functional stability and plasticity of arTregs.

Analysis of TCR clonal diversity helps to elucidate the repertoire narrowing that might occur when arTregs are stimulated with alloantigen. Mathew et al.<sup>222</sup> assessed the TCR repertoire of poly-expanded Tregs and arTregs by next-generation sequencing. The Treg receptor diversity was maintained post-expansion in the polyTreg population in contrast to arTregs, which demonstrated significant shrinkage. In Chapter 3, it was shown that TCR repertoire analysis demonstrated narrowing of the repertoire to several clones in arTregs (Figure 3.8A,B). However, this analysis was tested from one donor only, and validating the finding is crucial to ensure the narrowing of the expanded arTregs.

We showed that expanded arTregs were more potent in suppressing cell proliferation than polyclonal Tregs using an *in vitro* suppression assay (Figure 3.6B). However, assessing arTreg suppressive function *in vivo* is more physiologically relevant. Examining the ability of arTregs

to prevent human skin graft rejection using our established humanised model can provide information about the functionality and optimal doses of arTregs.<sup>204</sup> For example, Landwehr-Kenzel<sup>427</sup> demonstrated that arTregs, which were expanded with a CD40L-B cell line, were effective at promoting skin graft survival, while polyTregs failed at a ratio of 1:1 Treg to Teff in a humanised mouse model. This study suggests that arTregs can overcome the requirement of high numbers of polyTregs and improve clinical efficiency.

ArTregs were able to mediate enhanced specific suppression of cell proliferation in response to a primary stimulator compared with irrelevant third-party stimulators (Figure 3.6C). Exploring the functionality of arTregs in response to a primary stimulator versus a third-party stimulator in a humanised mouse model can provide more information about the *in vivo* specificity of arTregs. Additionally, the analysis of grafts and peripheral lymphoid tissues for the presence of a FOXP3<sup>+</sup> infiltrate can determine whether arTregs have enhanced tissue or lymphoid homing and infiltration capabilities compared to polyclonally-expanded Tregs.

The impact of immunosuppressive drugs, including tacrolimus, mycophenolate and methylprednisolone, on the therapeutic efficacy of adoptively-transferred Tregs, was previously assessed in a humanised mouse model.<sup>433</sup> The viability and proliferative capacity of Tregs were both reduced in a dose-dependent manner by these immunosuppressant drugs. The only immunosuppressant shown to potentiate Treg expansion and survival is rapamycin.<sup>185</sup> However, the 3C Study reported that rapamycin-based maintenance therapy was not effective clinically in preventing rejection and was linked with significant risks of infection compared to tacrolimus therapy.<sup>434</sup> The ability of arTregs to maintain their phenotype in strong inflammatory environments or within immunosuppressive conditions is important to consider. Therefore, investigating the stability of these cells in different inflammatory conditions (e.g., with IL-6, TNF- $\alpha$  and IL-1 $\beta$ ), along with assessing the effect of common immunosuppressive drugs used by transplant patients, might help to identify the optimally favourable environment for arTreg therapy and to select an immunosuppressive drug that does not impact the identity and functionality of these cells.

The detection of *in vivo* arTreg expansion might prospectively identify patients in whom immunosuppression can be successfully weaned. Savage et al.<sup>323</sup> assessed the role of *in vivo* expansion of arTregs in combined kidney and bone marrow transplantation (CKBMT) patients

and suggested that early expansion of arTregs was linked to tolerance induction following CKBMT. We developed the functional assay CD137/CD154 (Figure 3.9), which can be used in clinical studies, such as the TWO study, to monitor the frequency of donor-responsive Tregs and conventional CD4 T cells and to determine whether adoptive Treg therapy results in an increased prevalence of arTregs and/or developments of alloreactive conventional T cell hyperresponsiveness. The limitation of the CD137/CD154 assay is that it requires *ex vivo* manipulation of cells that may not reliably replicate what is happening *in vivo*; therefore, correlating the results with clinical outcomes might help us to know if the result of this functional assay replicates the *in vivo* immune status. In addition, CD137 and CD154 can be used to sort Tregs and conventional T cells after short stimulation of recipient PBMCs with relevant donor cells to determine the molecular profile of circulating arTregs and conventional T cells on a single-cell level in patients treated with Treg therapy.<sup>435</sup>

There are a number of considerations which will need to be addressed in future work, prior to widespread use of arTregs in clinical therapy. The motivation for the development arTregs is to reduce off-target immunosuppression. Whilst the work of Todo and colleagues does provide initial data to suggest even relatively impure cell population can be infused safely and possibly even with clinical efficacy in liver transplantation,<sup>436</sup> pre-clinical data suggests that infusion of high purity arTregs may have a much more marked effect upon alloresponses. Whether this will be linked with an altered risk of adverse effects is unclear. In theory, the use of a population of Treg reactive to alloantigen should reduce off-target immunosuppression. However, it is possible that enhanced bystander suppression due to activation of large numbers of arTregs could lead to increase of local infection or viral reactivation by viruses present within the graft, including BK virus in renal allograft.<sup>437</sup> A number of early phase clinical trial utilising arTregs in the setting of solid organ transplantation are currently ongoing and will report in the coming years.

Whilst polyTregs can be generated and stored before transplantation using recipients PBMCs, arTregs require donor stimulation and this creates a logistical challenge. Donor identity maybe known in advance in the setting of living donor transplantation allowing pre-emptive Treg generation, however, in cadaveric transplantation the donor is only identified at time of transplant. Thus the use of arTregs clinically would be limited to (I) living donor transplantation, where the donor is identified and available prior to transplant; or (II) infusion

of arTregs at a delayed timepoint after transplant, following expansion with allogeneic stimulation.

It is now more crucial than ever to elucidate the impact of Treg therapeutics *in vivo* and monitor resulting immune responses. The majority of clinical trials studying advanced cellular therapies in solid organ transplantation have used flow cytometry analysis as part of the associated immune monitoring to identify the therapeutic efficacy.<sup>105, 248, 307</sup> In Chapter 4, we used conventional flow cytometry to examine phenotypical changes in peripheral leukocytes in renal transplant patients who received Treg therapy compared to control patients. This phenotypical analysis allowed an assessment of the effect of alemtuzumab induction therapy on peripheral leukocytes and detection of cell repopulation over time post-transplantation. The conducted phenotypical analysis was performed using a small number of patients, however, the long-term follow-up of all enrolled patients might provide a potential analysis to assess the changes in the peripheral leukocytes after Tregs infusion. In addition, the data from other clinical trials worldwide can be compared to the TWO Study findings to identify the efficacy of Tregs therapy.

Treg infusion has the potential to modulate the host immune system and promote the *in vivo* expansion of regulatory immune cells. We observed an elevation in the absolute number of total B cells and naïve B cells over time post-transplantation in the Treg therapy group (Figure 4.7). Additionally, the absolute number of CD24<sup>hi</sup>CD38<sup>hi</sup> transitional B cells were slightly elevated after Treg infusion and remained high even at 44 weeks post-transplantation (Figure 4.7F). This elevation was significantly higher in the Treg therapy group than the control group (Figure 4.7G), suggesting a link between Treg infusion and expansion of transitional B cells. The elevation of peripheral naïve and transitional B cells was also reported in cases of spontaneous tolerance in renal transplantation.<sup>281, 438</sup> It has been reported that the CD24<sup>hi</sup>CD38<sup>hi</sup> transitional B cell subset contains B regulatory cells and can suppress the differentiation of Th1 cells in an IL-10-dependent manner.<sup>439</sup> Additionally, the ability of Bregs to induce or recruit Tregs has been implicated.<sup>440, 441</sup> Further studies to assess the function of CD24<sup>hi</sup>CD38<sup>hi</sup> transitional B cells and dissect their mechanisms of action in the context of Treg therapy would be valuable. The presence of infiltrated B cells along with other immune cells has been well reported during kidney chronic rejection.<sup>442, 443</sup> Likewise, the infiltrated B cells has been detected during acute cellular rejection which was associated with glucocorticoid

resistance and graft failure.<sup>444</sup> These infiltrated B cells were not associated with alloantibody production, or complement C4d deposition, but it is thought that these B cells acted as APCs and triggered T cells. However, our spatial profiling dataset showed that the B cell marker (CD20) was more highly enriched in biopsies from patients receiving cell therapy than in the rejection (Figures 5.2C and 5.3C). This is an interesting finding, and further studies are needed to investigate the role and phenotype of graft-infiltrating B cells in the context of Treg therapy.

Furthermore, extensive immunophenotyping of liver transplant recipients who developed operational tolerance has revealed a significant increase in the circulating V $\delta$ 1<sup>+</sup> T cells.<sup>49</sup> Here, repopulated  $\gamma\delta$  T cells showed a skewing towards more V $\delta$ 1<sup>+</sup> and fewer V $\delta$ 2<sup>+</sup> cells over time post-transplantation. Further analyses will be necessary to determine whether these cells are truly associated with tolerance in renal transplantation and to reveal their precise function.

We next assessed peripheral immune phenotype using a larger panel of 30 markers by CyTOF (Figure 4.10). As discussed in Chapter 1 (Section 1.6.1.1), a key advantage of CyTOF is the possibility to perform comprehensive deep immune profiling using up to 50 markers, facilitating cell type identification. CyTOF revealed detailed features about cell subsets compared to flow cytometry. For example, CyTOF detected the expansion of naïve B cells over time post-transplantation and revealed that this subset co-expresses CCR6, CCR7 and CXCR5; these chemokine receptors are required for B cells to enter lymphoid organs.<sup>445</sup> Unfortunately, the conducted CyTOF study did not examine the phenotypical changes between Treg therapy and the control arm of the trial because of the small sample size. Future work will cover this as more patients are recruited to the TWO study trial. In the future, it would also be useful to add additional markers to the panel, including markers related to Treg function, such as FOXP3 and CTLA-4, to further resolve and characterise the circulating Treg compartment. In addition, markers related to  $\gamma\delta$  T cell subsets, including V $\delta$ 1 and V $\delta$ 2, could be used to investigate the changes in these subsets over time post-transplantation and determine the impact of Treg infusion on these subsets.

Recently, there have been significant advances in spatial profiling techniques,<sup>446</sup> which allow for the extraction of spatially-resolved molecular information from tissue biopsies. In Chapter 5, we examined the leukocytes that infiltrated the transplanted tissue using GeoMx DSP with the aim of identifying local markers of tolerance and rejection. We assessed the cellular

infiltrates in tissue biopsies from three transplant patients who received Treg therapy and two patients with confirmed rejection. While this might be considered a small sample size, various ROIs were selected (from 9 to 12 regions) from each patient with diverse infiltration types. In addition, six FOXP3<sup>+</sup> and six FOXP3<sup>neg</sup> segments were selected to assess their protein signature. The protein signature of each of the rejection patients was distinct. For example, regions from Patient D showed a high prevalence of monocytes/macrophages along with CD8 T cells. In contrast, regions from Patient E showed high expression of monocytes/macrophages with less expression of CD8 T cells (Figure 5.4). These differences might indicate different stages of rejection; therefore, further analyses might provide a clearer picture of the rejection process and the associated cells.

Recently, the Banff Molecular Diagnostics Working Group suggested the Banff Human Organ Transplant (B-HOT) transcriptomic panel to reliably and reproducibly evaluate transplant-related pathological conditions.<sup>447</sup> This panel includes 758 of the most relevant genes in terms of tolerance, rejection, infection and immune responses that are currently available through NanoString Technologies. The GeoMx DSP is limited by the ability to examine only one analyte type at a time (protein or RNA). However, a key advantage of DSP is that it is a non-destructive technique; tissues can be reused for further experimental analyses.<sup>269</sup> Indeed, reusing these tissues for spatial transcriptomic profiling using the B-HOT panel can provide further information and might allow for a better understanding of the major molecular changes that occur in the grafts after Treg therapy or rejection. Additionally, finding a way to identify the *in vivo* molecular data over time will improve our ability to understand the effect of cellular therapies or to detect early signs of rejection.

The COVID-19 outbreak has affected the TWO Study trial and the induction immunosuppression was modified as discussed in Chapter 4. While this change in the immunosuppressive protocol limits the number of enrolled patients who received alemtuzumab and Treg therapy, it will provide an opportunity for a potential subgroup analysis comparing alemtuzumab versus no induction immunosuppression. The COVID-19 pandemic has affected my research activities and some of the experiments could not be validated. For example, TCR repertoire analysis of arTregs (Figure 3.8A and B) was tested from one donor only, and it was a challenge to validate the finding during the lockdown.

This thesis explored Treg cellular therapy as a natural way to regulate transplant alloresponses with the ultimate goal of reducing the level of immunosuppressive drugs along with their toxic side effects in transplant patients. The minimisation of immunosuppressive drugs will have a crucial impact on graft survival and quality of life for transplant patients. Whilst later phase trials of polyclonal Tregs are now ongoing, more directed alloantigen-reactive Treg therapy is likely to be preferable to enhance the immunological effect and reduce off-target effects. In this study, arTregs were isolated, expanded and assessed for their function, and they demonstrated enhanced suppressive properties compared to polyTregs. A method to investigate the *in vivo* development of arTregs in patients receiving Treg therapy was also developed. Extensive immune monitoring through immunophenotyping of the peripheral immune cell compartment provided valuable insight about the immune status of patients receiving Treg therapy, as it revealed details about the cellular phenotypes post-transplantation and post-Treg infusion. Furthermore, the high spatial resolution of GeoMx DSP, which was utilised in this project, permitted a detailed molecular analysis of leukocyte infiltrates and deeper insight into the biological process that occurs in the transplanted tissue after cellular therapy compared to rejection.

## References

1. Transplant, Organ Donation and Transplantation Activity Report 2019-2020; 2020.
2. Grinyó, J.M. Why is organ transplantation clinically important? *Cold Spring Harb Perspect Med* **3**, a014985 (2013).
3. Niederkorn, J.Y. Corneal transplantation and immune privilege. *Int Rev Immunol* **32**, 57-67 (2013).
4. Dutkowski, P., de Rougemont, O. & Clavien, P.A. Alexis Carrel: genius, innovator and ideologist. *American journal of transplantation : official journal of the American Society of Transplantation and the American Society of Transplant Surgeons* **8**, 1998-2003 (2008).
5. Guild, W.R., Harrison, J.H., Merrill, J.P. & Murray, J. Successful homotransplantation of the kidney in an identical twin. *Transactions of the American Clinical and Climatological Association* **67**, 167-173 (1955).
6. Gibson, T. & Medawar, P.B. The fate of skin homografts in man. *J Anat* **77**, 299-310.294 (1943).
7. Medawar, P.B. The behaviour and fate of skin autografts and skin homografts in rabbits: A report to the War Wounds Committee of the Medical Research Council. *J Anat* **78**, 176-199 (1944).
8. Billingham, R.E., Brent, L. & Medawar, P.B. Actively acquired tolerance of foreign cells. *Nature* **172**, 603-606 (1953).
9. Owen, R.D. IMMUNOGENETIC CONSEQUENCES OF VASCULAR ANASTOMOSES BETWEEN BOVINE TWINS. *Science (New York, N. Y.)* **102**, 400-401 (1945).
10. Burnet, F.M.J.T.P.o.A.A.R. & Discussion., a.T. The Production of Antibodies. A Review and a Theoretical Discussion. (1941).
11. Main, J.M. & Prehn, R.T. Successful Skin Homografts After the Administration of High Dosage X Radiation and Homologous Bone Marrow. *JNCI: Journal of the National Cancer Institute* **15**, 1023-1029 (1955).
12. Kuss, R., Legrain, M., Mathe, G., Nedey, R. & Camey, M. Homologous human kidney transplantation. Experience with six patients. *Postgraduate medical journal* **38**, 528-531 (1962).

13. Snell, G.D.J.J.o.g. Methods for the study of histocompatibility genes. **49**, 87-108 (1948).
14. Dausset, J.J.A.h. Iso-leuco-anticorps. **20**, 156-166 (1958).
15. Morris, P.J. Transplantation--a medical miracle of the 20th century. *The New England journal of medicine* **351**, 2678-2680 (2004).
16. Bamoulid, J. *et al.* The need for minimization strategies: current problems of immunosuppression. *Transpl Int* **28**, 891-900 (2015).
17. Miller, L.W. Cardiovascular Toxicities of Immunosuppressive Agents. **2**, 807-818 (2002).
18. Gershon, R.K. & Kondo, K. Infectious immunological tolerance. *Immunology* **21**, 903-914 (1971).
19. Hall, B.M., Jelbart, M.E., Gurley, K.E. & Dorsch, S.E. Specific unresponsiveness in rats with prolonged cardiac allograft survival after treatment with cyclosporine. Mediation of specific suppression by T helper/inducer cells. *J Exp Med* **162**, 1683-1694 (1985).
20. Sakaguchi, S., Sakaguchi, N., Asano, M., Itoh, M. & Toda, M. Immunologic self-tolerance maintained by activated T cells expressing IL-2 receptor alpha-chains (CD25). Breakdown of a single mechanism of self-tolerance causes various autoimmune diseases. *J Immunol* **155**, 1151-1164 (1995).
21. Zecher, D., van Rooijen, N., Rothstein, D.M., Shlomchik, W.D. & Lakkis, F.G. An innate response to allogeneic nonself mediated by monocytes. *Journal of immunology (Baltimore, Md. : 1950)* **183**, 7810-7816 (2009).
22. Liu, W., Xiao, X., Demirci, G., Madsen, J. & Li, X.C. Innate NK cells and macrophages recognize and reject allogeneic nonself in vivo via different mechanisms. *Journal of immunology (Baltimore, Md. : 1950)* **188**, 2703-2711 (2012).
23. Oberbarnscheidt, M.H. *et al.* Non-self recognition by monocytes initiates allograft rejection. *The Journal of clinical investigation* **124**, 3579-3589 (2014).
24. Spierings, E. Minor histocompatibility antigens: past, present, and future. *Tissue antigens* **84**, 374-360 (2014).
25. Summers, C., Sheth, V.S. & Bleakley, M. Minor Histocompatibility Antigen-Specific T Cells. **8** (2020).

26. Zhang, Q. & Reed, E.F. The importance of non-HLA antibodies in transplantation. *Nature reviews. Nephrology* **12**, 484-495 (2016).
27. Wood, K.J. & Goto, R. Mechanisms of Rejection: Current Perspectives. **93**, 1-10 (2012).
28. Kabelitz, D. Expression and function of Toll-like receptors in T lymphocytes. *Curr Opin Immunol* **19**, 39-45 (2007).
29. Andonegui, G. *et al.* Endothelium-derived Toll-like receptor-4 is the key molecule in LPS-induced neutrophil sequestration into lungs. *J Clin Invest* **111**, 1011-1020 (2003).
30. Nieuwenhuijs-Moeke, G.J. *et al.* Ischemia and Reperfusion Injury in Kidney Transplantation: Relevant Mechanisms in Injury and Repair. *J Clin Med* **9**, 253 (2020).
31. Asgari, E. *et al.* Mannan-binding lectin-associated serine protease 2 is critical for the development of renal ischemia reperfusion injury and mediates tissue injury in the absence of complement C4. *FASEB journal : official publication of the Federation of American Societies for Experimental Biology* **28**, 3996-4003 (2014).
32. Schwaeble, W.J. *et al.* Targeting of mannan-binding lectin-associated serine protease-2 confers protection from myocardial and gastrointestinal ischemia/reperfusion injury. **108**, 7523-7528 (2011).
33. Nauser, C.L., Farrar, C.A. & Sacks, S.H. Complement Recognition Pathways in Renal Transplantation. **28**, 2571-2578 (2017).
34. Nauser, C.L., Farrar, C.A. & Sacks, S.H. Complement Recognition Pathways in Renal Transplantation. *Journal of the American Society of Nephrology : JASN* **28**, 2571-2578 (2017).
35. Nasralla, D. *et al.* A randomized trial of normothermic preservation in liver transplantation. *Nature* **557**, 50-56 (2018).
36. Lathan, R., Ghita, R. & Clancy, M.J. Stem Cells to Modulate IR: a Regenerative Medicine-Based Approach to Organ Preservation. *Current Transplantation Reports* **6**, 146-154 (2019).
37. Legendre, C., Sberro-Soussan, R., Zuber, J. & Frémeaux-Bacchi, V. The role of complement inhibition in kidney transplantation. *British Medical Bulletin* **124**, 5-17 (2017).

38. van der Touw, W. & Bromberg, J.S. Natural killer cells and the immune response in solid organ transplantation. *American journal of transplantation : official journal of the American Society of Transplantation and the American Society of Transplant Surgeons* **10**, 1354-1358 (2010).
39. Castro-Dopico, T. & Clatworthy, M.R. Fcγ Receptors in Solid Organ Transplantation. *Curr Transplant Rep* **3**, 284-293 (2016).
40. Jukes, J.P., Wood, K.J. & Jones, N.D. Natural killer T cells: a bridge to tolerance or a pathway to rejection? *Transplantation* **84**, 679-681 (2007).
41. Godfrey, D.I. & Kronenberg, M. Going both ways: immune regulation via CD1d-dependent NKT cells. *The Journal of clinical investigation* **114**, 1379-1388 (2004).
42. Diefenbach, A., Colonna, M. & Koyasu, S. Development, differentiation, and diversity of innate lymphoid cells. *Immunity* **41**, 354-365 (2014).
43. Spits, H. *et al.* Innate lymphoid cells — a proposal for uniform nomenclature. *Nature Reviews Immunology* **13**, 145-149 (2013).
44. Artis, D. & Spits, H. The biology of innate lymphoid cells. *Nature* **517**, 293-301 (2015).
45. Monticelli, L.A. *et al.* Lung Innate Lymphoid Cell Composition Is Altered in Primary Graft Dysfunction. *American journal of respiratory and critical care medicine* **201**, 63-72 (2020).
46. Tanaka, S. *et al.* IL-22 is required for the induction of bronchus-associated lymphoid tissue in tolerant lung allografts. *American journal of transplantation : official journal of the American Society of Transplantation and the American Society of Transplant Surgeons* **20**, 1251-1261 (2020).
47. Kang, J. *et al.* Type 3 innate lymphoid cells are associated with a successful intestinal transplant. *American journal of transplantation : official journal of the American Society of Transplantation and the American Society of Transplant Surgeons* **21**, 787-797 (2021).
48. McCallion, O., Hester, J. & Issa, F. Deciphering the Contribution of  $\gamma\delta$  T Cells to Outcomes in Transplantation. *Transplantation* **102**, 1983-1993 (2018).
49. Martínez-Llordella, M. *et al.* Multiparameter immune profiling of operational tolerance in liver transplantation. *American journal of transplantation : official journal of the American Society of Transplantation and the American Society of Transplant Surgeons* **7**, 309-319 (2007).

50. Yu, X. *et al.* Characteristics of V $\delta$ 1(+) and V $\delta$ 2(+)  $\gamma\delta$  T cell subsets in acute liver allograft rejection. *Transplant immunology* **29**, 118-122 (2013).
51. Bolte, F.J. *et al.* Intra-Hepatic Depletion of Mucosal-Associated Invariant T Cells in Hepatitis C Virus-Induced Liver Inflammation. *Gastroenterology* **153**, 1392-1403.e1392 (2017).
52. Juno, J.A. *et al.* Mucosal-Associated Invariant T Cells Are Depleted and Exhibit Altered Chemokine Receptor Expression and Elevated Granulocyte Macrophage-Colony Stimulating Factor Production During End-Stage Renal Disease. *Front Immunol* **9**, 1076 (2018).
53. Wood, K.J. & Goto, R. Mechanisms of rejection: current perspectives. *Transplantation* **93**, 1-10 (2012).
54. Afzali, B., Lombardi, G. & Lechler, R.I. Pathways of major histocompatibility complex allorecognition. *Curr Opin Organ Transplant* **13**, 438-444 (2008).
55. Boardman, D.A., Jacob, J., Smyth, L.A., Lombardi, G. & Lechler, R.I. What Is Direct Allorecognition? *Current Transplantation Reports* **3**, 275-283 (2016).
56. Herrera, O.B. *et al.* A Novel Pathway of Alloantigen Presentation by Dendritic Cells. **173**, 4828-4837 (2004).
57. Hornick, P. *et al.* Significant Frequencies of T Cells With Indirect Anti-Donor Specificity in Heart Graft Recipients With Chronic Rejection. *Circulation* **101**, 2405-2410 (2000).
58. Gökmen, M.R., Lombardi, G. & Lechler, R.I. The importance of the indirect pathway of allorecognition in clinical transplantation. *Current Opinion in Immunology* **20**, 568-574 (2008).
59. Ochando, J. *et al.* The Mononuclear Phagocyte System in Organ Transplantation. *American journal of transplantation : official journal of the American Society of Transplantation and the American Society of Transplant Surgeons* **16**, 1053-1069 (2016).
60. Morelli, A.E., Bracamonte-Baran, W. & Burlingham, W.J. Donor-derived exosomes: the trick behind the semidirect pathway of allorecognition. *Curr Opin Organ Transplant* **22**, 46-54 (2017).
61. Hughes, A.D. *et al.* Cross-dressed dendritic cells sustain effector T cell responses in islet and kidney allografts. *The Journal of clinical investigation* **130**, 287-294 (2020).

62. Liu, Z., Fan, H. & Jiang, S.J.I.r. CD4+ T - cell subsets in transplantation. **252**, 183-191 (2013).
63. Xu, A. *et al.* TGF- $\beta$ -Induced Regulatory T Cells Directly Suppress B Cell Responses through a Noncytotoxic Mechanism. **196**, 3631-3641 (2016).
64. Bevington, S.L., Cauchy, P., Withers, D.R., Lane, P.J.L. & Cockerill, P.N. T Cell Receptor and Cytokine Signaling Can Function at Different Stages to Establish and Maintain Transcriptional Memory and Enable T Helper Cell Differentiation. **8** (2017).
65. Murphy, K.M. *et al.* Signaling and transcription in T helper development. **18**, 451-494 (2000).
66. Wherry, E.J. & Kurachi, M. Molecular and cellular insights into T cell exhaustion. *Nature Reviews Immunology* **15**, 486-499 (2015).
67. Sabzevary-Ghahfarokhi, M., Shirzad, H., Rafieian-Kopaei, M., Ghatreh-Samani, M. & Shohan, M. The Role of Inflammatory Cytokines in Creating T Cell Exhaustion in Cancer. *Cancer biotherapy & radiopharmaceuticals* **33**, 267-273 (2018).
68. Karahan, G.E., Claas, F.H. & Heidt, S.J.F.i.i. B cell immunity in solid organ transplantation. **7**, 686 (2017).
69. Cross, A.R., Glotz, D. & Mooney, N. The Role of the Endothelium during Antibody-Mediated Rejection: From Victim to Accomplice. **9** (2018).
70. Colvin, R.B. Antibody-Mediated Renal Allograft Rejection: Diagnosis and Pathogenesis. **18**, 1046-1056 (2007).
71. Saadi, S., Takahashi, T., Holzknicht, R.A. & Platt, J.L. Pathways to acute humoral rejection. *Am J Pathol* **164**, 1073-1080 (2004).
72. Loupy, A. & Lefaucheur, C. Antibody-Mediated Rejection of Solid-Organ Allografts. *The New England journal of medicine* **379**, 1150-1160 (2018).
73. Valenzuela, N.M. & Reed, E.F. Antibody-mediated rejection across solid organ transplants: manifestations, mechanisms, and therapies. *The Journal of clinical investigation* **127**, 2492-2504 (2017).
74. Peng, B., Ming, Y. & Yang, C. Regulatory B cells: the cutting edge of immune tolerance in kidney transplantation. *Cell Death & Disease* **9**, 109 (2018).
75. Moore, D.K. & Loxton, A.G. Regulatory B lymphocytes: development and modulation of the host immune response during disease. *Immunotherapy* **11**, 691-704 (2019).

76. Beckett, J., Hester, J., Issa, F. & Shankar, S. Regulatory B cells in transplantation: roadmaps to clinic. **33**, 1353-1368 (2020).
77. Trzonkowski, P. *et al.* Homeostatic Repopulation by CD28-CD8+ T Cells in Alemtuzumab-Depleted Kidney Transplant Recipients Treated With Reduced Immunosuppression. **8**, 338-347 (2008).
78. Heidt, S., Hester, J., Shankar, S., Friend, P.J. & Wood, K.J. B Cell Repopulation After Alemtuzumab Induction—Transient Increase in Transitional B Cells and Long-Term Dominance of Naïve B Cells. **12**, 1784-1792 (2012).
79. Wood, K.J., Bushell, A. & Hester, J. Regulatory immune cells in transplantation. *Nature Reviews Immunology* **12**, 417-430 (2012).
80. Luft, F.C. How calcineurin inhibitors cause hypertension. *Nephrology Dialysis Transplantation* **27**, 473-475 (2011).
81. Sharif, A. & Baboolal, K. Risk factors for new-onset diabetes after kidney transplantation. *Nature Reviews Nephrology* **6**, 415-423 (2010).
82. Kawai, T. *et al.* HLA-Mismatched Renal Transplantation without Maintenance Immunosuppression. **358**, 353-361 (2008).
83. Scandling, J.D. *et al.* Tolerance and chimerism after renal and hematopoietic-cell transplantation. *The New England journal of medicine* **358**, 362-368 (2008).
84. Sykes, M. & Sachs, D.H. Mixed allogeneic chimerism as an approach to transplantation tolerance. *Immunology today* **9**, 23-27 (1988).
85. Tomita, Y., Khan, A. & Sykes, M. Role of intrathymic clonal deletion and peripheral anergy in transplantation tolerance induced by bone marrow transplantation in mice conditioned with a nonmyeloablative regimen. *J Immunol* **153**, 1087-1098 (1994).
86. Jones, N.D., Fluck, N.C., Mellor, A.L., Morris, P.J. & Wood, K.J. The induction of transplantation tolerance by intrathymic (i.t.) delivery of alloantigen: a critical relationship between i.t. deletion, thymic export of new T cells and the timing of transplantation. *International immunology* **10**, 1637-1646 (1998).
87. Turvey, S.E., Hara, M., Morris, P.J. & Wood, K.J.J.T. MECHANISMS OF TOLERANCE INDUCTION AFTER INTRATHYMIC ISLET INJECTION: Determination of the Fate of Alloreactive Thymocytes1. **68**, 30-39 (1999).
88. Kingsley, C.I., Nadig, S.N. & Wood, K.J. Transplantation tolerance: lessons from experimental rodent models. *Transpl Int* **20**, 828-841 (2007).

89. Durrbach, A. *et al.* A phase III study of belatacept versus cyclosporine in kidney transplants from extended criteria donors (BENEFIT - EXT study). **10**, 547-557 (2010).
90. Archdeacon, P., Dixon, C., Belen, O., Albrecht, R. & Meyer, J. Summary of the US FDA Approval of Belatacept. **12**, 554-562 (2012).
91. Ferrer, I.R. *et al.* Antigen-specific induced Foxp3+ regulatory T cells are generated following CD40/CD154 blockade. *Proc Natl Acad Sci U S A* **108**, 20701-20706 (2011).
92. Zhang, T., Pierson, R.N., 3rd & Azimzadeh, A.M. Update on CD40 and CD154 blockade in transplant models. *Immunotherapy* **7**, 899-911 (2015).
93. Schroder, P.M. *et al.* The past, present, and future of costimulation blockade in organ transplantation. *Curr Opin Organ Transplant* **24**, 391-401 (2019).
94. Lo, D.J. *et al.* A pilot trial targeting the ICOS-ICOS-L pathway in nonhuman primate kidney transplantation. *American journal of transplantation : official journal of the American Society of Transplantation and the American Society of Transplant Surgeons* **15**, 984-992 (2015).
95. Kitchens, W.H. *et al.* Interruption of OX40L signaling prevents costimulation blockade-resistant allograft rejection. *JCI insight* **2**, e90317 (2017).
96. Gauvreau, G.M. *et al.* OX40L blockade and allergen-induced airway responses in subjects with mild asthma. *Clinical and experimental allergy : journal of the British Society for Allergy and Clinical Immunology* **44**, 29-37 (2014).
97. Wood, K.J., Bushell, A. & Hester, J. Regulatory immune cells in transplantation. *Nature reviews. Immunology* **12**, 417-430 (2012).
98. Papp, G., Boros, P., Nakken, B., Szodoray, P. & Zeher, M. Regulatory immune cells and functions in autoimmunity and transplantation immunology. *Autoimmunity Reviews* **16**, 435-444 (2017).
99. Hoogduijn, M.J., Issa, F., Casiraghi, F. & Reinders, M.E.J. Cellular therapies in organ transplantation. *Transpl Int* (2020).
100. Sawitzki, B. *et al.* Regulatory cell therapy in kidney transplantation (The ONE Study): a harmonised design and analysis of seven non-randomised, single-arm, phase 1/2A trials. **395**, 1627-1639 (2020).

101. Trzonkowski, P. *et al.* First-in-man clinical results of the treatment of patients with graft versus host disease with human ex vivo expanded CD4+ CD25+ CD127- T regulatory cells. *Clinical immunology* **133**, 22-26 (2009).
102. Brunstein, C.G. *et al.* Infusion of ex vivo expanded T regulatory cells in adults transplanted with umbilical cord blood: safety profile and detection kinetics. *Blood* **117**, 1061-1070 (2011).
103. Theil, A. *et al.* Adoptive transfer of allogeneic regulatory T cells into patients with chronic graft-versus-host disease. *Cytotherapy* **17**, 473-486 (2015).
104. Mathew, J.M. *et al.* A Phase I Clinical Trial with Ex Vivo Expanded Recipient Regulatory T cells in Living Donor Kidney Transplants. *Scientific reports* **8**, 7428-7428 (2018).
105. Sawitzki, B. *et al.* Regulatory cell therapy in kidney transplantation (The ONE Study): a harmonised design and analysis of seven non-randomised, single-arm, phase 1/2A trials. *Lancet (London, England)* **395**, 1627-1639 (2020).
106. Marek-Trzonkowska, N. *et al.* Administration of CD4+CD25highCD127- regulatory T cells preserves  $\beta$ -cell function in type 1 diabetes in children. *Diabetes Care* **35**, 1817-1820 (2012).
107. Marek-Trzonkowska, N. *et al.* Therapy of type 1 diabetes with CD4(+)/CD25(high)/CD127-regulatory T cells prolongs survival of pancreatic islets - results of one year follow-up. *Clinical immunology (Orlando, Fla.)* **153**, 23-30 (2014).
108. Desreumaux, P. *et al.* Safety and efficacy of antigen-specific regulatory T-cell therapy for patients with refractory Crohn's disease. *Gastroenterology* **143**, 1207-1217.e1202 (2012).
109. Bluestone, J.A. *et al.* Type 1 diabetes immunotherapy using polyclonal regulatory T cells. *Sci Transl Med* **7**, 315ra189-315ra189 (2015).
110. Bacchetta, R. *et al.* Immunological outcome in haploidentical-HSC transplanted patients treated with IL-10-energized donor T cells. **5**, 16 (2014).
111. Kim, H.-J. & Cantor, H. Regulation of self-tolerance by Qa-1-restricted CD8+ regulatory T cells. *Seminars in immunology*; 2011: Elsevier; 2011. p. 446-452.
112. Zhang, Z.-X., Yang, L., Young, K.J., DuTemple, B. & Zhang, L.J.N.m. Identification of a previously unknown antigen-specific regulatory T cell and its mechanism of suppression. **6**, 782-789 (2000).

113. Xie, M.M. *et al.* Follicular regulatory T cells inhibit the development of granzyme B–expressing follicular helper T cells. *JCI Insight* **4** (2019).
114. Palathumpat, V., Dejbakhsh-Jones, S., Holm, B. & Strober, S.J.T.J.o.I. Different subsets of T cells in the adult mouse bone marrow and spleen induce or suppress acute graft-versus-host disease. **149**, 808-817 (1992).
115. Pillai, A.B., George, T.I., Dutt, S. & Strober, S.J.B., The Journal of the American Society of Hematology. Host natural killer T cells induce an interleukin-4–dependent expansion of donor CD4+ CD25+ Foxp3+ T regulatory cells that protects against graft-versus-host disease. **113**, 4458-4467 (2009).
116. Li, Y. *et al.* Analyses of peripheral blood mononuclear cells in operational tolerance after pediatric living donor liver transplantation. **4**, 2118-2125 (2004).
117. Mauri, C. & Blair, P.A.J.N.r.R. Regulatory B cells in autoimmunity: developments and controversies. **6**, 636 (2010).
118. Fillatreau, S., Sweenie, C.H., McGeachy, M.J., Gray, D. & Anderton, S.M.J.N.i. B cells regulate autoimmunity by provision of IL-10. **3**, 944-950 (2002).
119. Fleming, B.D. & Mosser, D.M.J.E.j.o.i. Regulatory macrophages: setting the threshold for therapy. **41**, 2498-2502 (2011).
120. Tiemessen, M.M. *et al.* CD4+ CD25+ Foxp3+ regulatory T cells induce alternative activation of human monocytes/macrophages. **104**, 19446-19451 (2007).
121. Marín, E., Cuturi, M.C. & Moreau, A. Tolerogenic Dendritic Cells in Solid Organ Transplantation: Where Do We Stand? *Front Immunol* **9**, 274-274 (2018).
122. Giannoukakis, N., Phillips, B., Finegold, D., Harnaha, J. & Trucco, M. Phase I (safety) study of autologous tolerogenic dendritic cells in type 1 diabetic patients. *Diabetes Care* **34**, 2026-2032 (2011).
123. Benham, H. *et al.* Citrullinated peptide dendritic cell immunotherapy in HLA risk genotype-positive rheumatoid arthritis patients. *Science translational medicine* **7**, 290ra287 (2015).
124. Bell, G.M. *et al.* Autologous tolerogenic dendritic cells for rheumatoid and inflammatory arthritis. **76**, 227-234 (2017).
125. Jauregui-Amezaga, A. *et al.* Intraperitoneal Administration of Autologous Tolerogenic Dendritic Cells for Refractory Crohn's Disease: A Phase I Study. *Journal of Crohn's & colitis* **9**, 1071-1078 (2015).

126. Willekens, B. *et al.* Tolerogenic dendritic cell-based treatment for multiple sclerosis (MS): a harmonised study protocol for two phase I clinical trials comparing intradermal and intranodal cell administration. *BMJ open* **9**, e030309 (2019).
127. Franquesa, M. *et al.* Mesenchymal Stem Cells in Solid Organ Transplantation (MiSOT) Fourth Meeting: lessons learned from first clinical trials. *Transplantation* **96**, 234-238 (2013).
128. Perico, N. *et al.* Mesenchymal stromal cells and kidney transplantation: pretransplant infusion protects from graft dysfunction while fostering immunoregulation. *Transpl Int* **26**, 867-878 (2013).
129. Perico, N. *et al.* Autologous mesenchymal stromal cells and kidney transplantation: a pilot study of safety and clinical feasibility. *Clinical journal of the American Society of Nephrology : CJASN* **6**, 412-422 (2011).
130. Reinders, M.E. *et al.* Autologous bone marrow-derived mesenchymal stromal cells for the treatment of allograft rejection after renal transplantation: results of a phase I study. *Stem cells translational medicine* **2**, 107-111 (2013).
131. Mudrabetu, C. *et al.* Safety and efficacy of autologous mesenchymal stromal cells transplantation in patients undergoing living donor kidney transplantation: a pilot study. *Nephrology (Carlton, Vic.)* **20**, 25-33 (2015).
132. Álvaro-Gracia, J.M. *et al.* Intravenous administration of expanded allogeneic adipose-derived mesenchymal stem cells in refractory rheumatoid arthritis (Cx611): results of a multicentre, dose escalation, randomised, single-blind, placebo-controlled phase Ib/IIa clinical trial. **76**, 196-202 (2017).
133. Bloor, A.J. *et al.* Production, safety and efficacy of iPSC-derived mesenchymal stromal cells in acute steroid-resistant graft versus host disease: A phase I, multicenter, open-label, dose-escalation study. 1-6 (2020).
134. Doğan, S.M. *et al.* Mesenchymal stem cell therapy in patients with small bowel transplantation: single center experience. *World journal of gastroenterology* **20**, 8215-8220 (2014).
135. Ceresa, C.D.L., Ramcharan, R.N., Friend, P.J. & Vaidya, A. Mesenchymal stromal cells promote bowel regeneration after intestinal transplantation: myth to mucosa. **26**, e91-e93 (2013).
136. Chambers, D.C. *et al.* Mesenchymal Stromal Cell Therapy for Chronic Lung Allograft Dysfunction: Results of a First-in-Man Study. *Stem cells translational medicine* **6**, 1152-1157 (2017).

137. Keller, C.A. *et al.* Feasibility, Safety, and Tolerance of Mesenchymal Stem Cell Therapy for Obstructive Chronic Lung Allograft Dysfunction. *Stem cells translational medicine* **7**, 161-167 (2018).
138. Boros, P., Ochando, J. & Zeher, M. Myeloid derived suppressor cells and autoimmunity. *Human Immunology* **77**, 631-636 (2016).
139. Cao, P. *et al.* Myeloid-derived suppressor cells in transplantation tolerance induction. *International immunopharmacology* **83**, 106421 (2020).
140. Zhang, W. *et al.* Myeloid-derived suppressor cells in transplantation: the dawn of cell therapy. *Journal of Translational Medicine* **16**, 19 (2018).
141. Sakaguchi, S. Naturally arising Foxp3-expressing CD25+CD4+ regulatory T cells in immunological tolerance to self and non-self. *Nature immunology* **6**, 345-352 (2005).
142. Jordan, M.S. *et al.* Thymic selection of CD4+ CD25+ regulatory T cells induced by an agonist self-peptide. **2**, 301-306 (2001).
143. Moran, A.E. *et al.* T cell receptor signal strength in Treg and iNKT cell development demonstrated by a novel fluorescent reporter mouse. **208**, 1279-1289 (2011).
144. Li, M.O. & Rudensky, A.Y. T cell receptor signalling in the control of regulatory T cell differentiation and function. *Nature Reviews Immunology* **16**, 220-233 (2016).
145. Tai, X., Cowan, M., Feigenbaum, L. & Singer, A. CD28 costimulation of developing thymocytes induces Foxp3 expression and regulatory T cell differentiation independently of interleukin 2. *Nature immunology* **6**, 152-162 (2005).
146. Xiao, S. *et al.* Retinoic acid increases Foxp3+ regulatory T cells and inhibits development of Th17 cells by enhancing TGF-beta-driven Smad3 signaling and inhibiting IL-6 and IL-23 receptor expression. *J Immunol* **181**, 2277-2284 (2008).
147. Fantini, M.C., Dominitzki, S., Rizzo, A., Neurath, M.F. & Becker, C.J.N.p. In vitro generation of CD4+ CD25+ regulatory cells from murine naive T cells. **2**, 1789-1794 (2007).
148. Schmitt, E. & Williams, C. Generation and Function of Induced Regulatory T Cells. **4** (2013).
149. Mikami, N. *et al.* Epigenetic conversion of conventional T cells into regulatory T cells by CD28 signal deprivation. **117**, 12258-12268 (2020).

150. Thornton, A.M. *et al.* Expression of Helios, an Ikaros transcription factor family member, differentiates thymic-derived from peripherally induced Foxp3<sup>+</sup> T regulatory cells. *J Immunol* **184**, 3433-3441 (2010).
151. Akimova, T., Beier, U.H., Wang, L., Levine, M.H. & Hancock, W.W. Helios expression is a marker of T cell activation and proliferation. *PloS one* **6**, e24226 (2011).
152. Szurek, E. *et al.* Differences in Expression Level of Helios and Neuropilin-1 Do Not Distinguish Thymus-Derived from Extrathymically-Induced CD4<sup>+</sup>Foxp3<sup>+</sup> Regulatory T Cells. *PloS one* **10**, e0141161 (2015).
153. Hori, S., Nomura, T. & Sakaguchi, S. Control of Regulatory T Cell Development by the Transcription Factor *Foxp3*. *Science* **299**, 1057-1061 (2003).
154. Brunkow, M.E. *et al.* Disruption of a new forkhead/winged-helix protein, scurfin, results in the fatal lymphoproliferative disorder of the scurfy mouse. *Nature genetics* **27**, 68-73 (2001).
155. Bennett, C.L. *et al.* The immune dysregulation, polyendocrinopathy, enteropathy, X-linked syndrome (IPEX) is caused by mutations of FOXP3. *Nature genetics* **27**, 20-21 (2001).
156. Wildin, R.S. *et al.* X-linked neonatal diabetes mellitus, enteropathy and endocrinopathy syndrome is the human equivalent of mouse scurfy. *Nature genetics* **27**, 18-20 (2001).
157. Khattri, R. *et al.* The amount of scurfin protein determines peripheral T cell number and responsiveness. *J Immunol* **167**, 6312-6320 (2001).
158. Rudensky, A.Y. Regulatory T cells and Foxp3. *Immunological Reviews* **241**, 260-268 (2011).
159. Khattri, R., Cox, T., Yasayko, S.A. & Ramsdell, F. An essential role for Scurfin in CD4<sup>+</sup>CD25<sup>+</sup> T regulatory cells. *Nature immunology* **4**, 337-342 (2003).
160. Fontenot, J.D., Gavin, M.A. & Rudensky, A.Y. Foxp3 programs the development and function of CD4<sup>+</sup>CD25<sup>+</sup> regulatory T cells. *Nature immunology* **4**, 330-336 (2003).
161. Hori, S., Nomura, T. & Sakaguchi, S. Control of Regulatory T Cell Development by the Transcription Factor *Foxp3*. **299**, 1057-1061 (2003).
162. Lee, W. & Lee, G.R. Transcriptional regulation and development of regulatory T cells. *Experimental & molecular medicine* **50**, e456 (2018).

163. Polansky, J.K. *et al.* DNA methylation controls Foxp3 gene expression. *European journal of immunology* **38**, 1654-1663 (2008).
164. Floess, S. *et al.* Epigenetic control of the foxp3 locus in regulatory T cells. *PLoS biology* **5**, e38-e38 (2007).
165. Baron, U. *et al.* DNA demethylation in the human FOXP3 locus discriminates regulatory T cells from activated FOXP3+ conventional T cells. *European journal of immunology* **37**, 2378-2389 (2007).
166. Seddiki, N. *et al.* Expression of interleukin (IL)-2 and IL-7 receptors discriminates between human regulatory and activated T cells. *J Exp Med* **203**, 1693-1700 (2006).
167. Liu, W. *et al.* CD127 expression inversely correlates with FoxP3 and suppressive function of human CD4+ T reg cells. *The Journal of experimental medicine* **203**, 1701-1711 (2006).
168. Peters, J.H. *et al.* Clinical grade Treg: GMP isolation, improvement of purity by CD127 Depletion, Treg expansion, and Treg cryopreservation. *PloS one* **3**, e3161-e3161 (2008).
169. Arroyo Hornero, R. *et al.* CD45RA Distinguishes CD4+CD25+CD127-/low TSDR Demethylated Regulatory T Cell Subpopulations With Differential Stability and Susceptibility to Tacrolimus-Mediated Inhibition of Suppression. *Transplantation* **101**, 302-309 (2017).
170. Hoffmann, P. *et al.* Only the CD45RA+ subpopulation of CD4+ CD25high T cells gives rise to homogeneous regulatory T-cell lines upon in vitro expansion. **108**, 4260-4267 (2006).
171. Peters, J.H., Hilbrands, L.B., Koenen, H.J.P.M. & Joosten, I. Ex Vivo Generation of Human Alloantigen-Specific Regulatory T Cells from CD4posCD25high T Cells for Immunotherapy. *PloS one* **3**, e2233 (2008).
172. Mathew, J.M. *et al.* Generation and Characterization of Alloantigen-Specific Regulatory T Cells For Clinical Transplant Tolerance. *Scientific Reports* **8**, 1136 (2018).
173. Chera, M. *et al.* Generation of Human Alloantigen-Specific Regulatory T Cells under Good Manufacturing Practice-Compliant Conditions for Cell Therapy. *Cell Transplantation* **24**, 2527-2540 (2015).
174. Di Ianni, M. *et al.* T regulatory cell separation for clinical application. *Transfusion and Apheresis Science* **47**, 213-216 (2012).

175. Vignali, D.A.A., Collison, L.W. & Workman, C.J. How regulatory T cells work. *Nature Reviews Immunology* **8**, 523-532 (2008).
176. Schmidt, A., Oberle, N. & Krammer, P.H. Molecular mechanisms of treg-mediated T cell suppression. *Front Immunol* **3**, 51-51 (2012).
177. Chen, W. *et al.* Conversion of peripheral CD4+CD25- naive T cells to CD4+CD25+ regulatory T cells by TGF-beta induction of transcription factor Foxp3. *J Exp Med* **198**, 1875-1886 (2003).
178. Romano, M. *et al.* Expanded Regulatory T Cells Induce Alternatively Activated Monocytes With a Reduced Capacity to Expand T Helper-17 Cells. **9** (2018).
179. Allard, B., Longhi, M.S., Robson, S.C. & Stagg, J. The ectonucleotidases CD39 and CD73: Novel checkpoint inhibitor targets. **276**, 121-144 (2017).
180. Okeke, E.B. & Uzonna, J.E. The Pivotal Role of Regulatory T Cells in the Regulation of Innate Immune Cells. **10** (2019).
181. Gondek, D.C. *et al.* Transplantation survival is maintained by granzyme B+ regulatory cells and adaptive regulatory T cells. *J Immunol* **181**, 4752-4760 (2008).
182. Grossman, W.J. *et al.* Human T regulatory cells can use the perforin pathway to cause autologous target cell death. *Immunity* **21**, 589-601 (2004).
183. Tung, S.L. *et al.* Regulatory T cell-derived extracellular vesicles modify dendritic cell function. *Scientific Reports* **8**, 6065 (2018).
184. Battaglia, M. *et al.* Rapamycin promotes expansion of functional CD4+CD25+FOXP3+ regulatory T cells of both healthy subjects and type 1 diabetic patients. *J Immunol* **177**, 8338-8347 (2006).
185. Hester, J., Schiopu, A., Nadig, S.N. & Wood, K.J. Low-Dose Rapamycin Treatment Increases the Ability of Human Regulatory T Cells to Inhibit Transplant Arteriosclerosis In Vivo. **12**, 2008-2016 (2012).
186. Matsuoka, K.-i. *et al.* Low-dose interleukin-2 therapy restores regulatory T cell homeostasis in patients with chronic graft-versus-host disease. *Sci Transl Med* **5**, 179ra143-179ra143 (2013).
187. Koreth, J. *et al.* Interleukin-2 and Regulatory T Cells in Graft-versus-Host Disease. **365**, 2055-2066 (2011).

188. Pilat, N. *et al.* Treg-mediated prolonged survival of skin allografts without immunosuppression. **116**, 13508-13516 (2019).
189. Ballesteros-Tato, A.J.I. Beyond regulatory T cells: the potential role for IL-2 to deplete T-follicular helper cells and treat autoimmune diseases. **6**, 1207-1220 (2014).
190. Bell, C.J. *et al.* Sustained in vivo signaling by long-lived IL-2 induces prolonged increases of regulatory T cells. **56**, 66-80 (2015).
191. Kawai, K., Uchiyama, M., Hester, J. & Issa, F. IL-33 drives the production of mouse regulatory T cells with enhanced in vivo suppressive activity in skin transplantation. **21**, 978-992 (2021).
192. Arroyo Hornero, R. *et al.* CD70 expression determines the therapeutic efficacy of expanded human regulatory T cells. *Communications Biology* **3**, 375 (2020).
193. Hoffmann, P. *et al.* Isolation of CD4+CD25+ regulatory T cells for clinical trials. *Biology of blood and marrow transplantation : journal of the American Society for Blood and Marrow Transplantation* **12**, 267-274 (2006).
194. Wichlan, D.G., Roddam, P.L., Eldridge, P., Handgretinger, R. & Riberdy, J.M. Efficient and reproducible large-scale isolation of human CD4+ CD25+ regulatory T cells with potent suppressor activity. *Journal of immunological methods* **315**, 27-36 (2006).
195. Fraser, H. *et al.* A Rapamycin-Based GMP-Compatible Process for the Isolation and Expansion of Regulatory T Cells for Clinical Trials. *Molecular therapy. Methods & clinical development* **8**, 198-209 (2018).
196. Peters, J.H. *et al.* Clinical grade Treg: GMP isolation, improvement of purity by CD127 Depletion, Treg expansion, and Treg cryopreservation. *PloS one* **3**, e3161 (2008).
197. Mucida, D. *et al.* Retinoic acid can directly promote TGF-beta-mediated Foxp3(+) Treg cell conversion of naive T cells. *Immunity* **30**, 471-472; author reply 472-473 (2009).
198. Urry, Z. *et al.* The role of 1 $\alpha$ ,25-dihydroxyvitamin D3 and cytokines in the promotion of distinct Foxp3+ and IL-10+ CD4+ T cells. *European journal of immunology* **42**, 2697-2708 (2012).
199. Eskandari, S.K. *et al.* Regulatory T cells engineered with TCR signaling–responsive IL-2 nanogels suppress alloimmunity in sites of antigen encounter. **12**, eaaw4744 (2020).

200. Fraser, H. *et al.* A Rapamycin-Based GMP-Compatible Process for the Isolation and Expansion of Regulatory T Cells for Clinical Trials. *Molecular therapy. Methods & clinical development* **8**, 198-209 (2018).
201. Issa, F., Hester, J., Milward, K. & Wood, K.J. Homing of regulatory T cells to human skin is important for the prevention of alloimmune-mediated pathology in an in vivo cellular therapy model. *PloS one* **7**, e53331 (2012).
202. Putnam, A.L. *et al.* Clinical grade manufacturing of human alloantigen-reactive regulatory T cells for use in transplantation. *American journal of transplantation : official journal of the American Society of Transplantation and the American Society of Transplant Surgeons* **13**, 3010-3020 (2013).
203. Sagoo, P. *et al.* Human regulatory T cells with alloantigen specificity are more potent inhibitors of alloimmune skin graft damage than polyclonal regulatory T cells. *Sci Transl Med* **3**, 83ra42 (2011).
204. Issa, F. *et al.* Ex vivo-expanded human regulatory T cells prevent the rejection of skin allografts in a humanized mouse model. *Transplantation* **90**, 1321-1327 (2010).
205. Nadig, S.N. *et al.* In vivo prevention of transplant arteriosclerosis by ex vivo-expanded human regulatory T cells. *Nature medicine* **16**, 809-813 (2010).
206. Wu, D.C. *et al.* Ex vivo expanded human regulatory T cells can prolong survival of a human islet allograft in a humanized mouse model. *Transplantation* **96**, 707-716 (2013).
207. Issa, F., Hester, J., Milward, K. & Wood, K.J. Homing of regulatory T cells to human skin is important for the prevention of alloimmune-mediated pathology in an in vivo cellular therapy model. *PloS one* **7**, e53331-e53331 (2012).
208. Peters, J.H., Hilbrands, L.B., Koenen, H.J.P.M. & Joosten, I. Ex vivo generation of human alloantigen-specific regulatory T cells from CD4(pos)CD25(high) T cells for immunotherapy. *PloS one* **3**, e2233-e2233 (2008).
209. Putnam, A.L. *et al.* Clinical grade manufacturing of human alloantigen-reactive regulatory T cells for use in transplantation. *American journal of transplantation : official journal of the American Society of Transplantation and the American Society of Transplant Surgeons* **13**, 3010-3020 (2013).
210. Sagoo, P. *et al.* Human Regulatory T Cells with Alloantigen Specificity Are More Potent Inhibitors of Alloimmune Skin Graft Damage than Polyclonal Regulatory T Cells. **3**, 83ra42-83ra42 (2011).
211. Landwehr-Kenzel, S. *et al.* Novel GMP-compatible protocol employing an allogeneic B cell bank for clonal expansion of allospecific natural regulatory T cells. *American*

- journal of transplantation : official journal of the American Society of Transplantation and the American Society of Transplant Surgeons* **14**, 594-606 (2014).
212. Sakaguchi, S. Naturally arising Foxp3-expressing CD25+CD4+ regulatory T cells in immunological tolerance to self and non-self. *Nature Immunology* **6**, 345-352 (2005).
  213. Jonuleit, H. *et al.* Identification and functional characterization of human CD4(+)CD25(+) T cells with regulatory properties isolated from peripheral blood. *The Journal of experimental medicine* **193**, 1285-1294 (2001).
  214. Ng, W.F. *et al.* Human CD4+CD25+ cells: a naturally occurring population of regulatory T cells. *Blood* **98**, 2736-2744 (2001).
  215. Veerapathran, A., Pidala, J., Beato, F., Yu, X.-Z. & Anasetti, C. Ex vivo expansion of human Tregs specific for alloantigens presented. *Blood* **118**, 5671-5680 (2011).
  216. Lin, Y.J. *et al.* Suppressive efficacy and proliferative capacity of human regulatory T cells in allogeneic and xenogeneic responses. *Transplantation* **86**, 1452 (2008).
  217. Banerjee, D.K., Dhodapkar, M.V., Matayeva, E., Steinman, R.M. & Dhodapkar, K.M. Expansion of FOXP3<sup>high</sup> regulatory T cells by human dendritic cells (DCs) in vitro and after injection of cytokine-matured DCs in myeloma patients. *Blood* **108**, 2655-2661 (2006).
  218. Putnam, A.L. *et al.* Clinical Grade Manufacturing of Human Alloantigen-Reactive Regulatory T Cells for Use in Transplantation. *American Journal of Transplantation* **13**, 3010-3020 (2013).
  219. Tu, W. *et al.* Efficient generation of human alloantigen-specific CD4+ regulatory T cells from naive precursors by CD40-activated B cells. *Blood* **112**, 2554-2562 (2008).
  220. Landwehr-Kenzel, S. *et al.* Novel GMP-Compatible Protocol Employing an Allogeneic B Cell Bank for Clonal Expansion of Allospecific Natural Regulatory T Cells. *American Journal of Transplantation* **14**, 594-606 (2014).
  221. Gupta, S., Termini, J.M., Kanagavelu, S. & Stone, G.W. Design of vaccine adjuvants incorporating TNF superfamily ligands and TNF superfamily molecular mimics. *Immunol Res* **57**, 303-310 (2013).
  222. Mathew, J.M. *et al.* Generation and Characterization of Alloantigen-Specific Regulatory T Cells For Clinical Transplant Tolerance. *Sci Rep* **8**, 1136 (2018).
  223. Sagoo, P. *et al.* Human Regulatory T Cells with Alloantigen Specificity Are More Potent Inhibitors of Alloimmune Skin Graft Damage than Polyclonal Regulatory T Cells. *Science translational medicine* **3**, 83ra42-83ra42 (2011).

224. Veerapathran, A., Pidala, J., Beato, F., Yu, X.-Z. & Anasetti, C. Ex vivo expansion of human Tregs specific for alloantigens presented directly or indirectly. *Blood* **118**, 5671-5680 (2011).
225. Brusko, T.M. *et al.* Human antigen-specific regulatory T cells generated by T cell receptor gene transfer. *PLoS one* **5**, e11726-e11726 (2010).
226. Kim, Y.C. *et al.* Engineered antigen-specific human regulatory T cells: immunosuppression of FVIII-specific T- and B-cell responses. *Blood* **125**, 1107-1115 (2015).
227. Jethwa, H., Adami, A.A. & Maher, J. Use of gene-modified regulatory T-cells to control autoimmune and alloimmune pathology: Is now the right time? *Clinical Immunology* **150**, 51-63 (2014).
228. McGovern, J.L., Wright, G.P. & Stauss, H.J. Engineering Specificity and Function of Therapeutic Regulatory T Cells. *Front Immunol* **8** (2017).
229. MacDonald, K.G. *et al.* Alloantigen-specific regulatory T cells generated with a chimeric antigen receptor. *J Clin Invest* **126**, 1413-1424 (2016).
230. Boardman, D.A. *et al.* Expression of a chimeric antigen receptor specific for donor HLA class I enhances the potency of human regulatory T cells in preventing human skin transplant rejection. *American Journal of Transplantation* **17**, 931-943 (2017).
231. Noyan, F. *et al.* Prevention of Allograft Rejection by Use of Regulatory T Cells With an MHC-Specific Chimeric Antigen Receptor. *American Journal of Transplantation* **17**, 917-930 (2017).
232. Elinav, E., Waks, T. & Eshhar, Z. Redirection of Regulatory T Cells With Predetermined Specificity for the Treatment of Experimental Colitis in Mice. *Gastroenterology* **134**, 2014-2024 (2008).
233. Tenspolde, M. *et al.* Regulatory T cells engineered with a novel insulin-specific chimeric antigen receptor as a candidate immunotherapy for type 1 diabetes. *J Autoimmun* **103**, 102289 (2019).
234. Davila, M.L. *et al.* Efficacy and toxicity management of 19-28z CAR T cell therapy in B cell acute lymphoblastic leukemia. *Science translational medicine* **6**, 224ra225-224ra225 (2014).
235. Maus, M.V. *et al.* T Cells Expressing Chimeric Antigen Receptors Can Cause Anaphylaxis in Humans. *Cancer Immunology Research* **1**, 26-31 (2013).

236. Sicard, A. *et al.* Donor-specific chimeric antigen receptor Tregs limit rejection in naive but not sensitized allograft recipients. **20**, 1562-1573 (2020).
237. Long, A.H. *et al.* 4-1BB costimulation ameliorates T cell exhaustion induced by tonic signaling of chimeric antigen receptors. *Nature medicine* **21**, 581-590 (2015).
238. Boroughs, A.C. *et al.* Chimeric antigen receptor costimulation domains modulate human regulatory T cell function. *JCI Insight* **4** (2019).
239. Dawson, N.A.J. *et al.* Functional effects of chimeric antigen receptor co-receptor signaling domains in human regulatory T cells. **12**, eaaz3866 (2020).
240. Dawson, N.A. *et al.* Systematic testing and specificity mapping of alloantigen-specific chimeric antigen receptors in regulatory T cells. *JCI Insight* **4** (2019).
241. Dawson, N.A. *et al.* Systematic testing and specificity mapping of alloantigen-specific chimeric antigen receptors in regulatory T cells. *JCI insight* **4** (2019).
242. Fritsche, E., Volk, H.D., Reinke, P. & Abou-El-Enein, M. Toward an Optimized Process for Clinical Manufacturing of CAR-Treg Cell Therapy. *Trends Biotechnol* (2020).
243. Jiang, S., Camara, N., Lombardi, G. & Lechler, R.I. Induction of allopeptide-specific human CD4+CD25+ regulatory T cells ex vivo. *Blood* **102**, 2180-2186 (2003).
244. Sagoo, P. *et al.* Alloantigen-specific regulatory T cells prevent experimental chronic graft-versus-host disease by simultaneous control of allo- and autoreactivity. *European journal of immunology* **42**, 3322-3333 (2012).
245. Tsang, J.Y.-S. *et al.* Conferring indirect allospecificity on CD4+CD25+ Tregs by TCR gene transfer favors transplantation tolerance in mice. *J Clin Invest* **118**, 3619-3628 (2008).
246. Todo, S. *et al.* A pilot study of operational tolerance with a regulatory T-cell-based cell therapy in living donor liver transplantation. *Hepatology* **64**, 632-643 (2016).
247. Harden, P. *et al.* Feasibility, Long-term Safety and Immune Monitoring of Regulatory T Cell Therapy in Living Donor Kidney Transplant Recipients. **n/a**.
248. Mathew, J.M. *et al.* A Phase I Clinical Trial with Ex Vivo Expanded Recipient Regulatory T cells in Living Donor Kidney Transplants. *Scientific Reports* **8**, 7428 (2018).

249. Roemhild, A. *et al.* Regulatory T cells for minimising immune suppression in kidney transplantation: phase I/IIa clinical trial. **371**, m3734 (2020).
250. Fribourg, M. *et al.* T-cell exhaustion correlates with improved outcomes in kidney transplant recipients. *Kidney Int* **96**, 436-449 (2019).
251. Kowli, S., Martinez, O.M., Lebrec, H., Minocherhomji, S. & Maecker, H.T. Characterization of Immune Phenotypes in Peripheral Blood of Adult Renal Transplant Recipients using Mass Cytometry (CyTOF). *Am Assoc Immunol*; 2020.
252. Hartmann, F.J. & Bendall, S.C. Immune monitoring using mass cytometry and related high-dimensional imaging approaches. *Nature reviews. Rheumatology* **16**, 87-99 (2020).
253. Gadalla, R. *et al.* Validation of CyTOF Against Flow Cytometry for Immunological Studies and Monitoring of Human Cancer Clinical Trials. **9** (2019).
254. Perfetto, S.P., Chattopadhyay, P.K. & Roederer, M. Seventeen-colour flow cytometry: unravelling the immune system. *Nature Reviews Immunology* **4**, 648-655 (2004).
255. Wolf, M. *et al.* Activation-induced expression of CD137 permits detection, isolation, and expansion of the full repertoire of CD8+ T cells responding to antigen without requiring knowledge of epitope specificities. *Blood* **110**, 201-210 (2007).
256. Yan, Z.H. *et al.* CD137 is a Useful Marker for Identifying CD4(+) T Cell Responses to Mycobacterium tuberculosis. *Scandinavian journal of immunology* **85**, 372-380 (2017).
257. Schoenbrunn, A. *et al.* A converse 4-1BB and CD40 ligand expression pattern delineates activated regulatory T cells (Treg) and conventional T cells enabling direct isolation of alloantigen-reactive natural Foxp3+ Treg. *J Immunol* **189**, 5985-5994 (2012).
258. Hermann, P., Van-Kooten, C., Gaillard, C., Banchereau, J. & Blanchard, D. CD40 ligand-positive CD8+ T cell clones allow B cell growth and differentiation. *European journal of immunology* **25**, 2972-2977 (1995).
259. Chattopadhyay, P.K., Yu, J. & Roederer, M. A live-cell assay to detect antigen-specific CD4+ T cells with diverse cytokine profiles. *Nature medicine* **11**, 1113-1117 (2005).
260. Frentsch, M. *et al.* Direct access to CD4+ T cells specific for defined antigens according to CD154 expression. *Nature medicine* **11**, 1118-1124 (2005).

261. Kirchhoff, D. *et al.* Identification and isolation of murine antigen-reactive T cells according to CD154 expression. *European journal of immunology* **37**, 2370-2377 (2007).
262. Sánchez-Fueyo, A. *et al.* Applicability, safety, and biological activity of regulatory T cell therapy in liver transplantation. *American journal of transplantation : official journal of the American Society of Transplantation and the American Society of Transplant Surgeons* **20**, 1125-1136 (2020).
263. Kanzaki, G. & Shimizu, A. Currently available useful immunohistochemical markers of renal pathology for the diagnosis of renal allograft rejection. **20**, 9-15 (2015).
264. Divella, C. *et al.* Immunohistochemical characterization of glomerular and tubulointerstitial infiltrates in renal transplant patients with chronic allograft dysfunction. *Nephrology Dialysis Transplantation* **25**, 4071-4077 (2010).
265. Van, T.M. & Blank, C.U.J.I.-O.T. A user's perspective on GeoMx™ digital spatial profiling. **1**, 11-18 (2019).
266. Decalf, J., Albert, M.L. & Ziai, J.J.T.J.o.p. New tools for pathology: a user's review of a highly multiplexed method for in situ analysis of protein and RNA expression in tissue. **247**, 650-661 (2019).
267. Jeyasekharan, A.D. *et al.* DIGITAL SPATIAL PROFILING OF IMMUNE MARKERS IN R-CHOP TREATED DIFFUSE LARGE B-CELL LYMPHOMA REVEALS A DOMINANT PROGNOSTIC SIGNIFICANCE OF M2 MACROPHAGE INFILTRATION. **37**, 356-357 (2019).
268. Toki, M.I. *et al.* High-Plex Predictive Marker Discovery for Melanoma Immunotherapy-Treated Patients Using Digital Spatial Profiling. *Clin Cancer Res* **25**, 5503-5512 (2019).
269. Merritt, C.R. *et al.* Multiplex digital spatial profiling of proteins and RNA in fixed tissue. *Nature biotechnology* **38**, 586-599 (2020).
270. Biomarkers and surrogate endpoints: preferred definitions and conceptual framework. *Clinical pharmacology and therapeutics* **69**, 89-95 (2001).
271. Califf, R.M. Biomarker definitions and their applications. *Exp Biol Med (Maywood)* **243**, 213-221 (2018).
272. Gaitonde, D.Y., Cook, D.L. & Rivera, I.M. Chronic Kidney Disease: Detection and Evaluation. *American family physician* **96**, 776-783 (2017).

273. Solez, K. *et al.* Banff 07 classification of renal allograft pathology: updates and future directions. *American journal of transplantation : official journal of the American Society of Transplantation and the American Society of Transplant Surgeons* **8**, 753-760 (2008).
274. Hariharan, S. *et al.* Post-transplant renal function in the first year predicts long-term kidney transplant survival. *Kidney Int* **62**, 311-318 (2002).
275. Salvadori, M. & Tsalouchos, A. Biomarkers in renal transplantation: An updated review. *World J Transplant* **7**, 161-178 (2017).
276. Flechner, S.M. *et al.* Kidney transplant rejection and tissue injury by gene profiling of biopsies and peripheral blood lymphocytes. **4**, 1475-1489 (2004).
277. Goerlich, N. *et al.* Kidney transplant monitoring by urinary flow cytometry: Biomarker combination of T cells, renal tubular epithelial cells, and podocalyxin-positive cells detects rejection. *Scientific Reports* **10**, 796 (2020).
278. Brouard, S. *et al.* Identification of a peripheral blood transcriptional biomarker panel associated with operational renal allograft tolerance. **104**, 15448-15453 (2007).
279. Louis, S. *et al.* Contrasting CD25<sup>hi</sup>CD4<sup>+</sup>T cells/FOXP3 patterns in chronic rejection and operational drug-free tolerance. *Transplantation* **81**, 398-407 (2006).
280. Sagoo, P. *et al.* Development of a cross-platform biomarker signature to detect renal transplant tolerance in humans. *The Journal of clinical investigation* **120**, 1848-1861 (2010).
281. Newell, K.A. *et al.* Identification of a B cell signature associated with renal transplant tolerance in humans. *The Journal of clinical investigation* **120**, 1836-1847 (2010).
282. Christians, U., Klawitter, J. & Klawitter, J. Biomarkers in Transplantation--Proteomics and Metabolomics. *Ther Drug Monit* **38 Suppl 1**, S70-S74 (2016).
283. Panzer, U. *et al.* Compartment-specific expression and function of the chemokine IP-10/CXCL10 in a model of renal endothelial microvascular injury. *Journal of the American Society of Nephrology : JASN* **17**, 454-464 (2006).
284. Rabant, M. *et al.* Early Low Urinary CXCL9 and CXCL10 Might Predict Immunological Quiescence in Clinically and Histologically Stable Kidney Recipients. *American journal of transplantation : official journal of the American Society of Transplantation and the American Society of Transplant Surgeons* **16**, 1868-1881 (2016).

285. Vasconcellos, L.M. *et al.* Cytotoxic lymphocyte gene expression in peripheral blood leukocytes correlates with rejecting renal allografts. *Transplantation* **66**, 562-566 (1998).
286. Li, B. *et al.* Noninvasive diagnosis of renal-allograft rejection by measurement of messenger RNA for perforin and granzyme B in urine. *The New England journal of medicine* **344**, 947-954 (2001).
287. Muthukumar, T. *et al.* Messenger RNA for FOXP3 in the urine of renal-allograft recipients. *The New England journal of medicine* **353**, 2342-2351 (2005).
288. Roedder, S. *et al.* The kSORT assay to detect renal transplant patients at high risk for acute rejection: results of the multicenter AART study. **11**, e1001759 (2014).
289. Christakoudi, S. *et al.* Development of a multivariable gene-expression signature targeting T-cell-mediated rejection in peripheral blood of kidney transplant recipients validated in cross-sectional and longitudinal samples. **41**, 571-583 (2019).
290. Levings, M.K., Sangregorio, R. & Roncarolo, M.-G.J.T.J.o.e.m. Human CD25+ CD4+ T regulatory cells suppress naive and memory T cell proliferation and can be expanded in vitro without loss of function. **193**, 1295-1302 (2001).
291. Putnam, A.L. *et al.* Expansion of human regulatory T-cells from patients with type 1 diabetes. **58**, 652-662 (2009).
292. Kendal, A.R. & Waldmann, H. Infectious tolerance: therapeutic potential. *Current opinion in immunology* **22**, 560-565 (2010).
293. Wood, K.J. & Sakaguchi, S. Regulatory T cells in transplantation tolerance. *Nature reviews. Immunology* **3**, 199-210 (2003).
294. Sagoo, P. *et al.* Human regulatory T cells with alloantigen specificity are more potent inhibitors of alloimmune skin graft damage than polyclonal regulatory T cells. **3**, 83ra42-83ra42 (2011).
295. Putnam, A. *et al.* Clinical grade manufacturing of human alloantigen - reactive regulatory T cells for use in transplantation. **13**, 3010-3020 (2013).
296. Peters, J.H., Hilbrands, L.B., Koenen, H.J. & Joosten, I.J.P.o. Ex vivo generation of human alloantigen-specific regulatory T cells from CD4 pos CD25 high T cells for immunotherapy. **3**, e2233 (2008).
297. Tu, W. *et al.* Efficient generation of human alloantigen-specific CD4+ regulatory T cells from naive precursors by CD40-activated B cells. **112**, 2554-2562 (2008).

298. Thomson, A.W. & Tevar, A.D. Kidney transplantation: a safe step forward for regulatory immune cell therapy. *Lancet (London, England)* **395**, 1589-1591 (2020).
299. Hester, J., Schiopu, A., Nadig, S. & Wood, K.J.A.J.o.T. Low - dose rapamycin treatment increases the ability of human regulatory T cells to inhibit transplant arteriosclerosis in vivo. **12**, 2008-2016 (2012).
300. Harden, P.N. *et al.* Feasibility, long-term safety, and immune monitoring of regulatory T cell therapy in living donor kidney transplant recipients. **21**, 1603-1611 (2021).
301. Alzhrani, A. Calculations and volcano plot 2021 [cited]Available from: [https://github.com/Alaa-web-codes/VolcanoPlots-/blob/main/VolcanoPlot%20\(4\).R](https://github.com/Alaa-web-codes/VolcanoPlots-/blob/main/VolcanoPlot%20(4).R)
302. Tran, D.Q. *et al.* Selective expression of latency-associated peptide (LAP) and IL-1 receptor type I/II (CD121a/CD121b) on activated human FOXP3+ regulatory T cells allows for their purification from expansion cultures. *Blood* **113**, 5125-5133 (2009).
303. Tran, D.Q. *et al.* GARP (LRRC32) is essential for the surface expression of latent TGF- $\beta$  on platelets and activated FOXP3<sup>+</sup> regulatory T cells. **106**, 13445-13450 (2009).
304. Stockis, J., Colau, D., Coulie, P.G. & Lucas, S. Membrane protein GARP is a receptor for latent TGF-beta on the surface of activated human Treg. *European journal of immunology* **39**, 3315-3322 (2009).
305. Koenen, H.J.P.M., Fasse, E. & Joosten, I. CD27/CFSE-Based Ex Vivo Selection of Highly Suppressive Alloantigen-Specific Human Regulatory T Cells. **174**, 7573-7583 (2005).
306. Schoenbrunn, A. *et al.* A Converse 4-1BB and CD40 Ligand Expression Pattern Delineates Activated Regulatory T Cells (Treg) and Conventional T Cells Enabling Direct Isolation of Alloantigen-Reactive Natural Foxp3<sup>+</sup> Treg. **189**, 5985-5994 (2012).
307. Sánchez-Fueyo, A. *et al.* Applicability, safety, and biological activity of regulatory T cell therapy in liver transplantation. *American journal of transplantation : official journal of the American Society of Transplantation and the American Society of Transplant Surgeons* **20**, 1125-1136 (2020).
308. Banerjee, D.K., Dhodapkar, M.V., Matayeva, E., Steinman, R.M. & Dhodapkar, K.M. Expansion of FOXP3<sup>high</sup> regulatory T cells by human dendritic cells (DCs) in vitro and after injection of cytokine-matured DCs in myeloma patients. *Blood* **108**, 2655-2661 (2006).

309. Alzhrani, A., Bottomley, M., Wood, K., Hester, J. & Issa, F. Identification, selection, and expansion of non-gene modified alloantigen-reactive Tregs for clinical therapeutic use. *Cellular immunology* **357**, 104214 (2020).
310. Thornton, A.M. *et al.* Expression of Helios, an Ikaros transcription factor family member, differentiates thymic-derived from peripherally induced Foxp3+ T regulatory cells. **184**, 3433-3441 (2010).
311. Himmel, M.E., MacDonald, K.G., Garcia, R.V., Steiner, T.S. & Levings, M.K.J.T.J.o.I. Helios+ and Helios- cells coexist within the natural FOXP3+ T regulatory cell subset in humans. **190**, 2001-2008 (2013).
312. Akimova, T., Beier, U.H., Wang, L., Levine, M.H. & Hancock, W.W.J.P.o. Helios expression is a marker of T cell activation and proliferation. **6**, e24226 (2011).
313. Baine, I., Basu, S., Ames, R., Sellers, R.S. & Macian, F. Helios induces epigenetic silencing of IL2 gene expression in regulatory T cells. *J Immunol* **190**, 1008-1016 (2013).
314. Kim, H.-J. *et al.* Stable inhibitory activity of regulatory T cells requires the transcription factor Helios. *Science (New York, N. Y.)* **350**, 334-339 (2015).
315. Chougnet, C. & Hildeman, D. Helios-controller of Treg stability and function. *Transl Cancer Res* **5**, S338-S341 (2016).
316. Takahashi, T. *et al.* Immunologic self-tolerance maintained by CD25(+)CD4(+) regulatory T cells constitutively expressing cytotoxic T lymphocyte-associated antigen 4. *J Exp Med* **192**, 303-310 (2000).
317. Thompson, C.B. & Allison, J.P. The emerging role of CTLA-4 as an immune attenuator. *Immunity* **7**, 445-450 (1997).
318. Bluestone, J.A.J.T.J.o.I. Is CTLA-4 a master switch for peripheral T cell tolerance? **158**, 1989-1993 (1997).
319. Read, S., Malmström, V. & Powrie, F.J.T.J.o.e.m. Cytotoxic T lymphocyte-associated antigen 4 plays an essential role in the function of CD25+ CD4+ regulatory cells that control intestinal inflammation. **192**, 295-302 (2000).
320. Joller, N. *et al.* Treg cells expressing the coinhibitory molecule TIGIT selectively inhibit proinflammatory Th1 and Th17 cell responses. *Immunity* **40**, 569-581 (2014).
321. Schatz, D.G. & Ji, Y. Recombination centres and the orchestration of V(D)J recombination. *Nature Reviews Immunology* **11**, 251-263 (2011).

322. Hughes, M.M. *et al.* T cell receptor CDR3 loop length repertoire is determined primarily by features of the V(D)J recombination reaction. *European journal of immunology* **33**, 1568-1575 (2003).
323. Savage, T.M. *et al.* Early expansion of donor-specific Tregs in tolerant kidney transplant recipients. *JCI insight* **3** (2018).
324. Harden, P.N. *et al.* Feasibility, long-term safety, and immune monitoring of regulatory T cell therapy in living donor kidney transplant recipients. **n/a**.
325. Amir, E.-a.D. *et al.* viSNE enables visualization of high dimensional single-cell data and reveals phenotypic heterogeneity of leukemia. *Nature biotechnology* **31**, 545-552 (2013).
326. Levine, J.H. *et al.* Data-Driven Phenotypic Dissection of AML Reveals Progenitor-like Cells that Correlate with Prognosis. *Cell* **162**, 184-197 (2015).
327. Van Gassen, S. *et al.* FlowSOM: Using self-organizing maps for visualization and interpretation of cytometry data. *Cytometry. Part A : the journal of the International Society for Analytical Cytology* **87**, 636-645 (2015).
328. Qiu, P. *et al.* Extracting a cellular hierarchy from high-dimensional cytometry data with SPADE. *Nature biotechnology* **29**, 886-891 (2011).
329. Bruggner, R.V., Bodenmiller, B., Dill, D.L., Tibshirani, R.J. & Nolan, G.P. Automated identification of stratifying signatures in cellular subpopulations. **111**, E2770-E2777 (2014).
330. Diggins, K.E., Greenplate, A.R., Leelatian, N., Wogsland, C.E. & Irish, J.M. Characterizing cell subsets using marker enrichment modeling. *Nature Methods* **14**, 275-278 (2017).
331. Liu, P. *et al.* Recent Advances in Computer-Assisted Algorithms for Cell Subtype Identification of Cytometry Data. *Front Cell Dev Biol* **8**, 234-234 (2020).
332. Ratzinger, G., Reagan, J.L., Heller, G., Busam, K.J. & Young, J.W. Differential CD52 expression by distinct myeloid dendritic cell subsets: implications for alemtuzumab activity at the level of antigen presentation in allogeneic graft-host interactions in transplantation. *Blood* **101**, 1422-1429 (2003).
333. Buggins, A.G. *et al.* Peripheral blood but not tissue dendritic cells express CD52 and are depleted by treatment with alemtuzumab. *Blood* **100**, 1715-1720 (2002).

334. Rao, S.P. *et al.* Human peripheral blood mononuclear cells exhibit heterogeneous CD52 expression levels and show differential sensitivity to alemtuzumab mediated cytotoxicity. *PLoS one* **7**, e39416-e39416 (2012).
335. Hu, Y. *et al.* Investigation of the mechanism of action of alemtuzumab in a human CD52 transgenic mouse model. *Immunology* **128**, 260-270 (2009).
336. Marino, J., Paster, J. & Benichou, G. Allorecognition by T Lymphocytes and Allograft Rejection. **7** (2016).
337. Benichou, G., Gonzalez, B., Marino, J., Ayasoufi, K. & Valujskikh, A. Role of Memory T Cells in Allograft Rejection and Tolerance. *Front Immunol* **8**, 170-170 (2017).
338. Xia, G., He, J. & Leventhal, J.R. Ex Vivo-Expanded Natural CD4+CD25+ Regulatory T Cells Synergize With Host T-Cell Depletion to Promote Long-Term Survival of Allografts. **8**, 298-306 (2008).
339. Benichou, G., Gonzalez, B., Marino, J., Ayasoufi, K. & Valujskikh, A. Role of Memory T Cells in Allograft Rejection and Tolerance. **8** (2017).
340. Adams, A.B. *et al.* Heterologous immunity provides a potent barrier to transplantation tolerance. *The Journal of clinical investigation* **111**, 1887-1895 (2003).
341. Krupnick, A.S. *et al.* Central memory CD8+ T lymphocytes mediate lung allograft acceptance. *The Journal of clinical investigation* **124**, 1130-1143 (2014).
342. Fife, B.T. & Bluestone, J.A. Control of peripheral T-cell tolerance and autoimmunity via the CTLA-4 and PD-1 pathways. *Immunological reviews* **224**, 166-182 (2008).
343. Keir, M.E., Butte, M.J., Freeman, G.J. & Sharpe, A.H. PD-1 and its ligands in tolerance and immunity. *Annual review of immunology* **26**, 677-704 (2008).
344. Barber, D.L. *et al.* Restoring function in exhausted CD8 T cells during chronic viral infection. *Nature* **439**, 682-687 (2006).
345. Morita, M. *et al.* PD-1/B7-H1 interaction contribute to the spontaneous acceptance of mouse liver allograft. *American journal of transplantation : official journal of the American Society of Transplantation and the American Society of Transplant Surgeons* **10**, 40-46 (2010).
346. Murakami, N. & Riella, L.V. Co-inhibitory pathways and their importance in immune regulation. *Transplantation* **98**, 3-14 (2014).

347. Sarraj, B. *et al.* Impaired selectin-dependent leukocyte recruitment induces T-cell exhaustion and prevents chronic allograft vasculopathy and rejection. *Proc Natl Acad Sci U S A* **111**, 12145-12150 (2014).
348. Brenchley, J.M. *et al.* Expression of CD57 defines replicative senescence and antigen-induced apoptotic death of CD8<sup>+</sup>T cells. *Blood* **101**, 2711-2720 (2003).
349. Palmer, B.E., Blyveis, N., Fontenot, A.P. & Wilson, C.C.J.T.J.o.I. Functional and phenotypic characterization of CD57<sup>+</sup> CD4<sup>+</sup> T cells and their association with HIV-1-induced T cell dysfunction. **175**, 8415-8423 (2005).
350. Hoffmann, J. *et al.* High-throughput 13-parameter immunophenotyping identifies shifts in the circulating T-cell compartment following reperfusion in patients with acute myocardial infarction. **7**, e47155 (2012).
351. Sabnani, I., Zucker, M.J., Tsang, P. & Palekar, S. Clonal T-large granular lymphocyte proliferation in solid organ transplant recipients. *Transplantation proceedings* **38**, 3437-3440 (2006).
352. Oertel, M. *et al.* Induction therapy including antithymocyte globulin induces marked alterations in T lymphocyte subpopulations after liver transplantation: results of a long-term study. *Transpl Int* **15**, 463-471 (2002).
353. Klaus, G., Mostert, K., Reckzeh, B. & Mueller, T.F. Phenotypic changes in lymphocyte subpopulations in pediatric renal-transplant patients after T-cell depletion. **76**, 1719-1724 (2003).
354. Kirk, A.D., Turgeon, N.A. & Iwakoshi, N.N. B cells and transplantation tolerance. *Nature reviews. Nephrology* **6**, 584-593 (2010).
355. Klein, U., Rajewsky, K. & Küppers, R. Human immunoglobulin (Ig)M<sup>+</sup>IgD<sup>+</sup> peripheral blood B cells expressing the CD27 cell surface antigen carry somatically mutated variable region genes: CD27 as a general marker for somatically mutated (memory) B cells. *J Exp Med* **188**, 1679-1689 (1998).
356. Spits, H. *et al.* Innate lymphoid cells--a proposal for uniform nomenclature. *Nature reviews. Immunology* **13**, 145-149 (2013).
357. Björkström, N.K., Kekäläinen, E. & Mjösberg, J. Tissue-specific effector functions of innate lymphoid cells. *Immunology* **139**, 416-427 (2013).
358. Cooper, M.A. *et al.* Human natural killer cells: a unique innate immunoregulatory role for the CD56(bright) subset. *Blood* **97**, 3146-3151 (2001).

359. Ferlazzo, G. & Morandi, B. Cross-Talks between Natural Killer Cells and Distinct Subsets of Dendritic Cells. **5** (2014).
360. Turner, J.-E., Rickassel, C., Healy, H. & Kassianos, A.J. Natural Killer Cells in Kidney Health and Disease. **10** (2019).
361. Pontrelli, P. *et al.* The Role of Natural Killer Cells in the Immune Response in Kidney Transplantation. **11** (2020).
362. Farkash, E.A. & Colvin, R.B. Diagnostic challenges in chronic antibody-mediated rejection. *Nature reviews. Nephrology* **8**, 255-257 (2012).
363. Hidalgo, L.G. *et al.* NK cell transcripts and NK cells in kidney biopsies from patients with donor-specific antibodies: evidence for NK cell involvement in antibody-mediated rejection. *American journal of transplantation : official journal of the American Society of Transplantation and the American Society of Transplant Surgeons* **10**, 1812-1822 (2010).
364. Brouard, S. *et al.* Comparative transcriptional and phenotypic peripheral blood analysis of kidney recipients under cyclosporin A or sirolimus monotherapy. *American journal of transplantation : official journal of the American Society of Transplantation and the American Society of Transplant Surgeons* **10**, 2604-2614 (2010).
365. Zhu, L. *et al.* Decreased NK cell immunity in kidney transplant recipients late post-transplant and increased NK-cell immunity in patients with recurrent miscarriage. *PloS one* **12**, e0186349-e0186349 (2017).
366. Kumar, A. *et al.* Natural Killer T Cells: An Ecological Evolutionary Developmental Biology Perspective. **8** (2017).
367. Brennan, P.J., Brigl, M. & Brenner, M.B. Invariant natural killer T cells: an innate activation scheme linked to diverse effector functions. *Nature Reviews Immunology* **13**, 101-117 (2013).
368. Brigl, M. & Brenner, M.B. How invariant natural killer T cells respond to infection by recognizing microbial or endogenous lipid antigens. *Seminars in immunology*; 2010: Elsevier; 2010. p. 79-86.
369. Novak, J. & Lehen, A.J.C. Mechanism of regulation of autoimmunity by iNKT cells. **53**, 263-270 (2011).
370. Vivier, E., Ugolini, S., Blaise, D., Chabannon, C. & Brossay, L.J.N.R.I. Targeting natural killer cells and natural killer T cells in cancer. **12**, 239-252 (2012).

371. Levine, J.H. *et al.* Data-Driven Phenotypic Dissection of AML Reveals Progenitor-like Cells that Correlate with Prognosis. *Cell* **162**, 184-197 (2015).
372. Solstad, T. *et al.* CD147 (Basigin/Emmprin) identifies FoxP3+CD45RO+CTLA4+-activated human regulatory T cells. *Blood* **118**, 5141-5151 (2011).
373. Sugiyama, D. *et al.* Anti-CCR4 mAb selectively depletes effector-type FoxP3+CD4+ regulatory T cells, evoking antitumor immune responses in humans. *Proc Natl Acad Sci U S A* **110**, 17945-17950 (2013).
374. Himmel, M.E., MacDonald, K.G., Garcia, R.V., Steiner, T.S. & Levings, M.K. Helios+ and Helios- cells coexist within the natural FOXP3+ T regulatory cell subset in humans. *J Immunol* **190**, 2001-2008 (2013).
375. Sugita, K. *et al.* Generation of Helios reporter mice and an evaluation of the suppressive capacity of Helios(+) regulatory T cells in vitro. *Experimental dermatology* **24**, 554-556 (2015).
376. Duggleby, R.C., Shaw, T.N., Jarvis, L.B., Kaur, G. & Gaston, J.S. CD27 expression discriminates between regulatory and non-regulatory cells after expansion of human peripheral blood CD4+ CD25+ cells. *Immunology* **121**, 129-139 (2007).
377. Schneider, M.A., Meingassner, J.G., Lipp, M., Moore, H.D. & Rot, A. CCR7 is required for the in vivo function of CD4+ CD25+ regulatory T cells. *J Exp Med* **204**, 735-745 (2007).
378. Macedo, C. *et al.* Long-term effects of alemtuzumab on regulatory and memory T-cell subsets in kidney transplantation. *Transplantation* **93**, 813-821 (2012).
379. Horowitz, A. *et al.* Genetic and environmental determinants of human NK cell diversity revealed by mass cytometry. **5**, 208ra145-208ra145 (2013).
380. Fu, B., Tian, Z. & Wei, H. Subsets of human natural killer cells and their regulatory effects. *Immunology* **141**, 483-489 (2014).
381. Brouard, S. *et al.* Comparative Transcriptional and Phenotypic Peripheral Blood Analysis of Kidney Recipients Under Cyclosporin A or Sirolimus Monotherapy. **10**, 2604-2614 (2010).
382. Bloom, D.D. *et al.* CD4+ CD25+ FOXP3+ regulatory T cells increase de novo in kidney transplant patients after immunodepletion with Campath-1H. *American journal of transplantation : official journal of the American Society of Transplantation and the American Society of Transplant Surgeons* **8**, 793-802 (2008).

383. Haynes, R. *et al.* Alemtuzumab-based induction treatment versus basiliximab-based induction treatment in kidney transplantation (the 3C Study): a randomised trial. **384**, 1684-1690 (2014).
384. Wang, Z. *et al.* Low-dose of tacrolimus favors the induction of functional CD4+CD25+FoxP3+ regulatory T cells in solid-organ transplantation. *International immunopharmacology* **9**, 564-569 (2009).
385. Heidt, S., Hester, J., Shankar, S., Friend, P.J. & Wood, K.J.A.J.o.T. B cell repopulation after alemtuzumab induction—transient increase in transitional B cells and long - term dominance of naïve B cells. **12**, 1784-1792 (2012).
386. Legler, D.F. *et al.* B cell-attracting chemokine 1, a human CXC chemokine expressed in lymphoid tissues, selectively attracts B lymphocytes via BLR1/CXCR5. *J Exp Med* **187**, 655-660 (1998).
387. Förster, R. *et al.* A putative chemokine receptor, BLR1, directs B cell migration to defined lymphoid organs and specific anatomic compartments of the spleen. *Cell* **87**, 1037-1047 (1996).
388. Kanzaki, G. & Shimizu, A. Currently available useful immunohistochemical markers of renal pathology for the diagnosis of renal allograft rejection. *Nephrology (Carlton, Vic.)* **20 Suppl 2**, 9-15 (2015).
389. Decalf, J., Albert, M.L. & Ziai, J. New tools for pathology: a user's review of a highly multiplexed method for in situ analysis of protein and RNA expression in tissue. *The Journal of pathology* **247**, 650-661 (2019).
390. Van, T.M. & Blank, C.U. A user's perspective on GeoMx™ digital spatial profiling. *Immuno-Oncology Technology* **1**, 11-18 (2019).
391. Beechem, J.M. High-Plex Spatially Resolved RNA and Protein Detection Using Digital Spatial Profiling: A Technology Designed for Immuno-oncology Biomarker Discovery and Translational Research. *Methods in molecular biology (Clifton, N.J.)* **2055**, 563-583 (2020).
392. Chandran, S. *et al.* Polyclonal Regulatory T Cell Therapy for Control of Inflammation in Kidney Transplants. *American journal of transplantation : official journal of the American Society of Transplantation and the American Society of Transplant Surgeons* **17**, 2945-2954 (2017).
393. Dijke, I.E., Weimar, W. & Baan, C.C. Regulatory T cells after organ transplantation: where does their action take place? *Human immunology* **69**, 389-398 (2008).
394. Kollins, D. *et al.* FOXP3+ regulatory T-cells in renal allografts: correlation with long-term graft function and acute rejection. *Clinical nephrology* **75**, 91-100 (2011).

395. Veronese, F. *et al.* Pathological and clinical correlates of FOXP3+ cells in renal allografts during acute rejection. *American journal of transplantation : official journal of the American Society of Transplantation and the American Society of Transplant Surgeons* **7**, 914-922 (2007).
396. Yapici, U. *et al.* Intragraft FOXP3 protein or mRNA during acute renal allograft rejection correlates with inflammation, fibrosis, and poor renal outcome. *Transplantation* **87**, 1377-1380 (2009).
397. Zuber, J. *et al.* Prognostic significance of graft Foxp3 expression in renal transplant recipients: a critical review and attempt to reconcile discrepancies. *Nephrology Dialysis Transplantation* **28**, 1100-1111 (2012).
398. Fontenot, J.D., Gavin, M.A. & Rudensky, A.Y.J.N.i. Foxp3 programs the development and function of CD4+ CD25+ regulatory T cells. **4**, 330-336 (2003).
399. Hori, S., Nomura, T. & Sakaguchi, S.J.S. Control of regulatory T cell development by the transcription factor Foxp3. **299**, 1057-1061 (2003).
400. Komatsu, N. *et al.* Pathogenic conversion of Foxp3+ T cells into TH17 cells in autoimmune arthritis. *Nature medicine* **20**, 62-68 (2014).
401. Hua, J. *et al.* Pathological conversion of regulatory T cells is associated with loss of allotolerance. *Scientific reports* **8**, 7059-7059 (2018).
402. Issa, F. *et al.* Transiently Activated Human Regulatory T Cells Upregulate BCL-XL Expression and Acquire a Functional Advantage in vivo. **10** (2019).
403. Zarkhin, V. *et al.* Characterization of intra-graft B cells during renal allograft rejection. *Kidney Int* **74**, 664-673 (2008).
404. Burke, J.D. & Young, H.A. IFN- $\gamma$ : A cytokine at the right time, is in the right place. *Semin Immunol* **43**, 101280-101280 (2019).
405. Ricardo, S.D., van Goor, H. & Eddy, A.A. Macrophage diversity in renal injury and repair. *The Journal of clinical investigation* **118**, 3522-3530 (2008).
406. Kassianos, A.J. *et al.* Fractalkine-CX3CR1-dependent recruitment and retention of human CD1c+ myeloid dendritic cells by in vitro-activated proximal tubular epithelial cells. *Kidney Int* **87**, 1153-1163 (2015).
407. Wang, Z. *et al.* Role of IFN-gamma in induction of Foxp3 and conversion of CD4+ CD25- T cells to CD4+ Tregs. *The Journal of clinical investigation* **116**, 2434-2441 (2006).

408. Nishibori, T., Tanabe, Y., Su, L. & David, M. Impaired development of CD4<sup>+</sup> CD25<sup>+</sup> regulatory T cells in the absence of STAT1: increased susceptibility to autoimmune disease. *J Exp Med* **199**, 25-34 (2004).
409. Wood, K.J. & Sawitzki, B. Interferon gamma: a crucial role in the function of induced regulatory T cells in vivo. *Trends in immunology* **27**, 183-187 (2006).
410. Greifenberg, V., Ribechini, E., Rössner, S. & Lutz, M.B. Myeloid-derived suppressor cell activation by combined LPS and IFN-gamma treatment impairs DC development. *European journal of immunology* **39**, 2865-2876 (2009).
411. Sawitzki, B. *et al.* IFN-gamma production by alloantigen-reactive regulatory T cells is important for their regulatory function in vivo. *J Exp Med* **201**, 1925-1935 (2005).
412. Halloran, P.F. *et al.* Interferon-gamma acts directly on rejecting renal allografts to prevent graft necrosis. *Am J Pathol* **158**, 215-226 (2001).
413. Venner, J.M. *et al.* Molecular landscape of T cell-mediated rejection in human kidney transplants: prominence of CTLA4 and PD ligands. *American journal of transplantation : official journal of the American Society of Transplantation and the American Society of Transplant Surgeons* **14**, 2565-2576 (2014).
414. Hancock, W.W., Thomson, N.M. & Atkins, R.C. Composition of interstitial cellular infiltrate identified by monoclonal antibodies in renal biopsies of rejecting human renal allografts. *Transplantation* **35**, 458-463 (1983).
415. Wyburn, K.R., Jose, M.D., Wu, H., Atkins, R.C. & Chadban, S.J. The Role of Macrophages in Allograft Rejection. **80**, 1641-1647 (2005).
416. Ikezumi, Y. *et al.* Alternatively activated macrophages in the pathogenesis of chronic kidney allograft injury. *Pediatric nephrology (Berlin, Germany)* **30**, 1007-1017 (2015).
417. van den Bosch, T.P.P. *et al.* CD16<sup>+</sup> Monocytes and Skewed Macrophage Polarization toward M2 Type Hallmark Heart Transplant Acute Cellular Rejection. **8** (2017).
418. Mellor, A.L., Lemos, H. & Huang, L. Indoleamine 2,3-Dioxygenase and Tolerance: Where Are We Now? **8** (2017).
419. Pallotta, M.T. *et al.* Indoleamine 2,3-dioxygenase is a signaling protein in long-term tolerance by dendritic cells. *Nature immunology* **12**, 870-878 (2011).
420. Jürgens, B., Hainz, U., Fuchs, D., Felzmann, T. & Heitger, A. Interferon-gamma-triggered indoleamine 2,3-dioxygenase competence in human monocyte-derived

- dendritic cells induces regulatory activity in allogeneic T cells. *Blood* **114**, 3235-3243 (2009).
421. Pallandre, J.-R. *et al.* Role of STAT3 in CD4<sup>+</sup>CD25<sup>+</sup>FOXP3<sup>+</sup> Regulatory Lymphocyte Generation: Implications in Graft-versus-Host Disease and Antitumor Immunity. **179**, 7593-7604 (2007).
422. Wang, J. *et al.* VSIG-3 as a ligand of VISTA inhibits human T-cell function. **156**, 74-85 (2019).
423. Huynh, A. *et al.* Control of PI(3) kinase in Treg cells maintains homeostasis and lineage stability. *Nature immunology* **16**, 188-196 (2015).
424. Bensinger, S.J. *et al.* Distinct IL-2 Receptor Signaling Pattern in CD4<sup>+</sup>CD25<sup>+</sup> Regulatory T Cells. **172**, 5287-5296 (2004).
425. Zeiser, R. *et al.* Differential impact of mammalian target of rapamycin inhibition on CD4<sup>+</sup>CD25<sup>+</sup>Foxp3<sup>+</sup> regulatory T cells compared with conventional CD4<sup>+</sup> T cells. *Blood* **111**, 453-462 (2008).
426. Chera, M. *et al.* Generation of Human Alloantigen-Specific Regulatory T Cells under Good Manufacturing Practice-Compliant Conditions for Cell Therapy. **24**, 2527-2540 (2015).
427. Landwehr-Kenzel, S. *et al.* Novel GMP-Compatible Protocol Employing an Allogeneic B Cell Bank for Clonal Expansion of Allospecific Natural Regulatory T Cells. **14**, 594-606 (2014).
428. Lee, L.M. *et al.* A Comparison of Ex Vivo Expanded Human Regulatory T Cells Using Allogeneic Stimulated B Cells or Monocyte-Derived Dendritic Cells. **12** (2021).
429. Huehn, J., Polansky, J.K. & Hamann, A. Epigenetic control of FOXP3 expression: the key to a stable regulatory T-cell lineage? *Nature Reviews Immunology* **9**, 83-89 (2009).
430. Floess, S. *et al.* Epigenetic control of the foxp3 locus in regulatory T cells. *PLoS biology* **5**, e38 (2007).
431. Zheng, Y. *et al.* Role of conserved non-coding DNA elements in the Foxp3 gene in regulatory T-cell fate. *Nature* **463**, 808-812 (2010).
432. Morikawa, H. & Sakaguchi, S. Genetic and epigenetic basis of Treg cell development and function: from a FoxP3-centered view to an epigenome-defined view of natural Treg cells. *Immunological reviews* **259**, 192-205 (2014).

433. Cristiano, S. *et al.* Impact of immunosuppressive drugs on the therapeutic efficacy of ex vivo expanded human regulatory T cells. *Haematologica* **101**, 91-100 (2016).
434. Group, C.S.C. Campath, calcineurin inhibitor reduction, and chronic allograft nephropathy (the 3C Study) - results of a randomized controlled clinical trial. *American journal of transplantation : official journal of the American Society of Transplantation and the American Society of Transplant Surgeons* **18**, 1424-1434 (2018).
435. Mair, F. *et al.* A targeted multi-omic analysis approach measures protein expression and low-abundance transcripts on the single-cell level. **31**, 107499 (2020).
436. Todo, S. *et al.* A pilot study of operational tolerance with a regulatory T-cell-based cell therapy in living donor liver transplantation. *Hepatology (Baltimore, Md.)* **64**, 632-643 (2016).
437. Niemann, N. & Sawitzki, B. Treg Therapy in Transplantation: How and When Will We Do It? *Curr Transplant Rep* **2**, 233-241 (2015).
438. Casiraghi, F. *et al.* Kidney transplant tolerance associated with remote autologous mesenchymal stromal cell administration. *Stem cells translational medicine* **9**, 427-432 (2020).
439. Blair, P.A. *et al.* CD19(+)CD24(hi)CD38(hi) B cells exhibit regulatory capacity in healthy individuals but are functionally impaired in systemic Lupus Erythematosus patients. *Immunity* **32**, 129-140 (2010).
440. Bouaziz, J.D., Yanaba, K. & Tedder, T.F. Regulatory B cells as inhibitors of immune responses and inflammation. *Immunological reviews* **224**, 201-214 (2008).
441. Yanaba, K. *et al.* B-lymphocyte contributions to human autoimmune disease. *Immunological reviews* **223**, 284-299 (2008).
442. Thauvat, O. *et al.* Chronic rejection triggers the development of an aggressive intragraft immune response through recapitulation of lymphoid organogenesis. *J Immunol* **185**, 717-728 (2010).
443. Ferdman, J. *et al.* Expansion and somatic hypermutation of B-cell clones in rejected human kidney grafts. *Transplantation* **98**, 766-772 (2014).
444. Sarwal, M. *et al.* Molecular heterogeneity in acute renal allograft rejection identified by DNA microarray profiling. *The New England journal of medicine* **349**, 125-138 (2003).

445. Henneken, M., Dörner, T., Burmester, G.-R. & Berek, C. Differential expression of chemokine receptors on peripheral blood B cells from patients with rheumatoid arthritis and systemic lupus erythematosus. *Arthritis Res Ther* **7**, R1001-R1013 (2005).
446. Marx, V.J.N.M. Method of the Year: spatially resolved transcriptomics. **18**, 9-14 (2021).
447. Mengel, M. *et al.* Banff 2019 Meeting Report: Molecular diagnostics in solid organ transplantation-Consensus for the Banff Human Organ Transplant (B-HOT) gene panel and open source multicenter validation. *American journal of transplantation : official journal of the American Society of Transplantation and the American Society of Transplant Surgeons* **20**, 2305-2317 (2020).

## Publications

### Papers

Alzhrani, A., Bottomley, M., Wood, K.J., Hester, J. and Issa, F. Identification, selection, and expansion of non-gene modified alloantigen-reactive Tregs for clinical therapeutic use. *Cellular Immunology*, 2020.

Harden, P.N., Game, D.S., Sawitzki, B., Van der Net, J.B., Hester, J., Bushell, A., Issa, F., Brook, M.O., Alzhrani, A., Schlickeiser, S., Scotta, C., Petchey, W., Streitz, M., Blancho, G., Tang, Q., Markmann, J., Lechler, R.I., Roberts, I.S.D., Friend, P.J., Hilton, R., Geissler, E.K., Wood, K.J. and Lombardi, G. Feasibility, long-term safety, and immune monitoring of regulatory T cell therapy in living donor kidney transplant recipients. *Am J Transplant*, 2021.

Helen L. Stark, Hayson C. Wang, Jasmina Kuburic, Alaa Alzhrani, Joanna Hester and Fadi Issa. Immune monitoring for advanced cell therapy trials in transplantation: which assays and when? *Frontiers in Immunology*, 2021.

### Abstracts

Alaa Alzhrani, Joanna Hester and Fadi Issa. An exploration of alloantigen reactive regulatory T cells in transplantation: Therapies and biomarkers. Oxford Immunology Symposium, Oxford, 2018. Poster.

Alaa Alzhrani, David Ahern, Joanna Hester and Fadi Issa. Mass cytometry analysis of the peripheral regulatory T cell compartment after cellular therapy in renal transplantation. Italian Society of Immunology SIICA, Milan, 2019. Poster.

Alaa Alzhrani, Joanna Hester and Fadi Issa. Development of a Methodology for the Production of Alloantigen-reactive Human Tregs. European Society of Organ Transplantation ESOT, Copenhagen, 2019. Poster.

Alaa Alzhrani, David Ahern, Joanna Hester and Fadi Issa. Mass cytometry analysis of the peripheral regulatory T cell compartment after cellular therapy in renal transplantation. 28<sup>th</sup> International Congress of the Transplantation Society, TTS, 2020. Poster.